POLITECNICO DI MILANO
Master degree in Space engineering
Department of Aerospace Science and Technology

Reissner Mixed Variational Theorem for Ritz Sublaminate Generalized Unified Formulation

Supervisor: Prof. Riccardo Vescovini
Co-supervisor: Prof. Michele D'Ottavio
Co-supervisor: Prof. Stefan Hallström

Student:
Pier Antonio Esposito, 919800

Academic Year 2019 - 2020

Acknowledgements

My sincere gratitude to my supervisors, Prof. Vescovini and Prof. D'Ottavio, who guided me throughout this work. They have been always available to offer me their help and knowledge in better understanding the problem and in leading me towards the solution. Especially considering that the thesis was performed remotely, they still managed to teach me a lot, both on how to perform scientific research and on how to create a positive working environment.

I would also like to thank Politecnico di Milano, KTH, and the EU for giving me the fantastic possibility of pursuing a double degree in two different European universities. It was a great opportunity that changed both my personal and work life. Thanks to Prof. Stefan Hallström for being my co-supervisor at KTH.

Thanks to my friends who have been with me along this journey, Alberto and Andrea, my friends from high school, my friends from my double degree in Sweden, and my friends from Politecnico di Milano. A particular thanks to Andrea Morelli and Niccolò Martello with whom I shared many of the feelings related to being an aerospace engineering student at Politecnico di Milano for five years. Last but not least, thanks to my family. In particolare, grazie ai miei fratelli, Lorenzo e Federico, e ai miei genitori, Nicoletta e Giuseppe. Senza il loro sostegno personale ed economico nulla di tutto ciò sarebbe stato possibile. Grazie.

Contents

List of Figures

List of Tables

Acronyms

CFHL Classical Form of Hooke's Law. 9, 44, 89, 92

CUF Carrera's Unified Formulation. 13

DOF Degrees of Freedom. 11–13, 18, 28, 29, 32, 42, 54, 59, 74, 79

ESL Equivalent Single Layer. 11–16, 19, 20, 30–32, 56, 58

FEM Finite Element Method. 23, 51, 52, 59, 72

GUF Generalized Unified Formulation. X, XI, 13–15, 81

HSDT Higher-order Shear Deformation Theories. 12

HSNDT Higher-Order Shear and Normal Deformation Theories. 12

LW LayerWise. 11–16, 19, 20, 30–32, 35, 63, 64, 69, 80, 81

MFHL Mixed Form of Hooke's Law. 9, 10, 21, 22, 44, 45

MZZF Murakami Zig-Zag Function. 12, 15, 19, 20

PVD Principle of Virtual Displacements. 3, 6, 7, 15, 19, 20, 42, 46, 69–72, 74

RMVT Reissner Mixed Variational Theorem. X, XI, 2, 3, 6, 7, 9, 15, 19–21, 28, 41–43, 46, 47, 49, 51, 52, 59, 70–72, 74, 76, 86, 93

S-GUF Sublaminate Generalized Unified Formulation. X, XI, 2, 3, 11, 13, 15, 19, 21, 22, 25, 27, 69, 86, 93

SCT Static Condensation Technique. 42, 47

Abstract

This thesis is about the development of a new numerical method for the analysis of composite shells. The present work is based on *Reissner Mixed Variational Theorem* (RMVT), the *Sublaminate Generalized Unified Formulation* (S-GUF), and the *Ritz approximation*.

The present work, in order to investigate a more efficient way to compute transverse stresses (σ_{xz}, σ_{yz}, σ_{zz}), is based upon RMVT, which allows imposing their continuity *a priori*. This is a great advantage compared to the results that would be obtained using a conventional displacement-based approach.

In order to enable computing both a global and local response, depending on the user's needs, the S-GUF framework was adopted. The *Generalized Unified Formulation* (GUF) enables to develop within a single code the possibility to use a potentially infinite number of orders of approximation, which can also be different for each variable. In addition to the GUF, the concept of *Sublaminate* was utilized: it allows to divide the domain along the thickness in sub-regions (sublaminates), and it is then possible to apply different formulations in each of these domains. Since the curvature effects of shells depend strictly on the radius-over-thickness ratio, the flexibility of S-GUF is helpful in order to correctly represent these effects only when the particular case requires it.

The governing equations obtained applying S-GUF to RMVT were solved in a weak form using the *Ritz approximation*. This choice was made to allow a quicker computational time typical of this method.

Comparing the results obtainable through the present formulation and solutions available in the literature it was possible to validate the results and therefore the formulation itself.

Finally, numerical and analytical considerations about the method here developed were drawn, such as its numerical stability, how to tune its parameters and which models result more correct from an analytical standpoint.

Sommario

Questa tesi tratta lo sviluppo di un nuovo metodo numerico per l'analisi di strutture a guscio costituite da materiali compositi. Il presente lavoro si basa sul *teorema variazionale misto di Reissner* (RMVT), i concetti di *sublaminato e formulazione generale unificata* (S-GUF), e l'*approssimazione di Ritz*.

Il presente lavoro, al fine di investigare un modo più efficiente di calcolare gli sforzi trasversali (σ_{xz}, σ_{yz}, σ_{zz}), è basata sul RMVT, che permette di imporre *a priori* la loro continuità. Ciò è un grande vantaggio rispetto ai risultati che sarebbero ottenuti usando un approccio convenzionale basato sugli spostamenti.

Per permettere il calcolo sia di una risposta globale che locale, a seconda delle necessità dell'utente, è stato utilizzato l'approccio S-GUF. La *formulazione unificata generalizzata* (GUF) permette di sviluppare all'interno di un singolo codice la possibilità di utilizzare un numero potenzialmente infinito di ordini di approssimazione, che possono differire anche per ciascuna variabile. In aggiunta a GUF, anche il concetto di *sublaminato* è stato adottato: permette di definire sublaminati all'interno della piastra o guscio, nei quali è poi possibile utilizzare differenti formulazioni. Dato che gli effetti di curvatura dipendono strettamente dal rapporto raggio di curvatura su spessore, la flessibilità di S-GUF è utile nel presente contesto per permettere di rappresentare correttamente tali effetti solo quando necessario.

Le equazioni di governo ottenute attraverso l'applicazione di S-GUF al RMVT sono state risolte in forma debole utilizzando l'*approssimazione di Ritz*. Questa scelta è stata fatta in modo da consentire un minore costo computazionale, tipico di tale approssimazione.

In seguito, confrontando i risultati ottenuti tramite la presente formulazione e le soluzioni disponibili in letteratura è stato possibile validare i risultati, e quindi la formulazione stessa.

Infine, considerazioni numeriche ed analitiche riguardo al metodo sono state tratte: la sua stabilità numerica, come fissarne i parametri e quali modelli risultino corretti da un punto di vista analitico.

Chapter 1

Introduction

1.1 Overview

The use of composite materials in the aerospace field has increased in the past decades and they are being adopted for load-bearing parts of the structures. The interest in these materials by the aerospace industry is driven by their incredible physical properties such as their stiffness-over-weight ratio, their fatigue and corrosion resistance, and so on. Furthermore, in addition to their intrinsic peculiarities, these materials can be easily tailored since they are composed of different laminae sequences. By designing properly the stacking sequence different results can be obtained. The properties that can be modified in this way are not only the mechanical ones but also the thermal and electrical. This is an advantage for all those applications in which high performances are leading the design process and costs are not limiting the exploitation of the above-mentioned features.

As a consequence, deriving from the increased usage of composite materials for safety-related functions, it is necessary to develop appropriate instruments for the analysis of their response and behavior. Therefore, these tools have to take into account the high degree of anisotropy, the high shear deformability and all additional complexities such as the fact that often aerospace structures are curved.

Due to the reasons and needs outlined above, in time a vast literature was developed about theories and numerical methods particularly suitable for the analysis of composite materials. In prospective of the present work, relevant examples are a series of works based upon the *sublaminate generalized unified formulation* and the *Ritz approximation*. In the work by D'Ottavio et al. [1], a *variable-kinematic model* in combination with the concept of *sublaminate* was applied to the *principle of virtual displacements*. Particularly, this work is based upon the variable-kinematic theory devised by Carrera, later generalized by Demasi, and the Ritz approximation, utilized to solve in a weak form the governing equations. This method was firstly applied to the *bending analysis* of composite structures [1] - even to non-uniform thickness-wise boundary conditions problems [2] -, and later used to study the *free-vibration* and *buckling analysis* of highly anisotropic plates [3, 4], and the dynamic response of viscoelastic structures [5]. The formulation was also adopted to study thermal loads, especially the thermal buckling response of composite structures by Vescovini et al. [6, 7], and piezoelectric composite plates [8]. The *sublaminate generalized unified formulation* and the *Ritz approximation* formulation was later extended to *cylindrical*

geometries by Gorgeri et al. [9, 10].

It is also worth mentioning that important developments were achieved in the application of *Carrera's unified formulation* to meshless techniques. Relevant studies based on these frameworks are the work by A.J.M. Ferreira et al. [11, 12, 13] where a radial basis functions was used in the context of Carrera's unified formulation for bending, free-vibration and buckling analysis, and the work by M. Cinefra [14] where a Mixed Interpolation of Tensorial Components (MITC) approach was used. The MITC technique was also extended to the *FEM* approach [15].

Significant work about the adoption of variable-kinematics models was also made by Demasi, who applied a *variable-kinematic model* to the *Reissner mixed variational theorem* [16], and then used a *Navier solution* to solve the equations in a strong form. Studies about *Reissner mixed variational theorem* were also conducted by D'Ottavio, who applied to it the *sublaminate generalized unified formulation* [17]; even in this latter work the *Navier solution* was adopted.

For further reference, it is reported that the *sublaminate generalized unified formulation* was also applied within the *FEM* approach. The interested reader is invited to read the works by D'Ottavio et al. [18, 19, 20].

1.2 Objective of the thesis

The present work has the objective of developing the *Reissner Mixed Variational Theorem* (RMVT) in the framework of the *Sublaminate Generalized Unified Formulation* (S-GUF) and adopting the *Ritz approximation* to solve the governing equations. Subsequently the derivation of the equations, a code for the analysis and the study of the response of composite shell structures was developed.

One of the main features of the numerical tool here presented is its capability of being flexible and adaptable to the structures to study thanks to the *variable-kinematic model* implemented. This theoretical framework allows implementing within one single code the possibility to use any kinematic theory, according to what is requested by the user. By utilizing the *Sublaminate* concept, it is possible to adopt different kinematic theories along the thickness of the structure.

Another feature of the present formulation that makes it particularly adapted for the analysis of composite materials is the possibility to impose *a priori* the continuity of transverse stresses between two different plies, enabling to draw considerations about the delamination issue. This characteristic of the program is enabled by the fact that the governing equations are based upon RMVT.

The code here developed was validated by comparing its results with these available in the literature.

Finally, the work aims at investigating the stability of the numerical method and the correct choice of the parameters involved.

1.3 Structure of the thesis

The thesis is structured as follows:

- In Chapter 2 the theoretical framework is presented. The three main pillars are: *shells*, RMVT and the S-GUF.
- In Chapter 3 the Ritz S-GUF RMVT governing equations are derived for doubly-curved geometries with constant radii of curvature.
- In Chapter 4 the numerical method is validated by comparing the results with those available in the literature. Static bending and free-vibration analysis are considered for plate, open cylinder and closed cylinder geometries. Furthermore, one challenging test case is reported were the present theory based on RMVT is compared with a similar formulation based on the PVD.
- In Chapter 5 considerations about the numerical method are drawn. In particular, a study is conducted to provide guidelines regarding the definition of a correct model in terms of Ritz approximation and orders of the model.
- In Chapter 6 the main achievements of the thesis are summarized and suggestions for future research directions in this field are given.

Chapter 2

Theoretical framework

The theoretical framework is presented is this Chapter. Firstly, a brief overview on fundamental equations of shell kinematics is provided. Then the Reissner Mixed Variational Principle is presented. Finally, the underlying features of the variable-kinematic formulation, the Sublaminate-Generalized Unified Formulation, are introduced.

2.1 Fundamental equations of shell kinematics

This Section summarizes the basic equations of shell theory. Specifically, the case of doubly-curved shells with constant radii of curvature is presented. Starting from this general framework, the case of cylindrical geometries and plates is also briefly discussed, given the importance of these structures in the context of space applications.

The main features of a doubly-curved shell geometry with constant radii of curvature are reported in Figure 2.1.

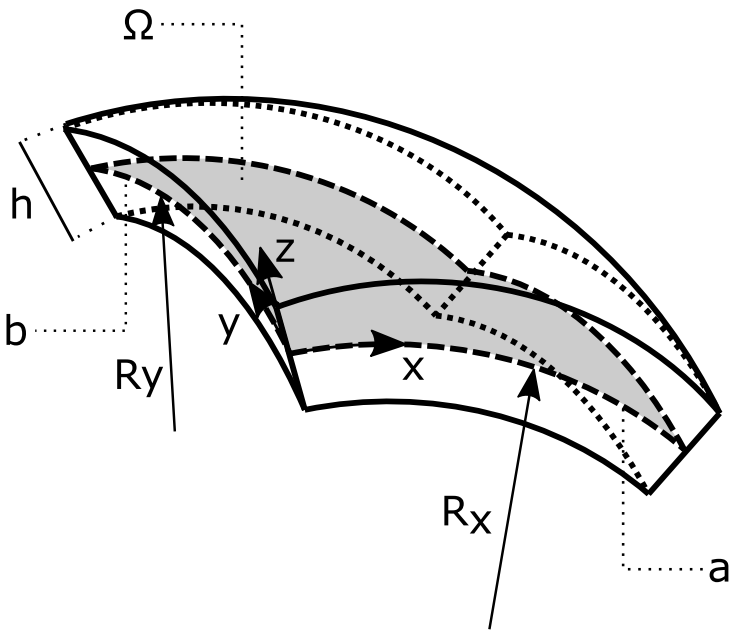

Figure 2.1: Doubly-curved shell geometry.

Referring to Figure 2.1, x and y are two curvilinear orthogonal coordinates on the reference surface Ω; the axis z denotes the thickness coordinate in the direction normal to Ω; a and b are the arc length in the x and y directions, respectively, while h is the total thickness. R_x and R_y are the radii of curvature in the x and y directions, respectively.

The following relations hold for an infinitesimal area ($\mathrm{d}\Omega$) and an infinitesimal volume ($\mathrm{d}V$):

$$\begin{aligned} \mathrm{d}\Omega &= H_x H_y \mathrm{d}x\mathrm{d}y \\ \mathrm{d}V &= H_x H_y \mathrm{d}x\mathrm{d}y\mathrm{d}z \end{aligned} \tag{2.1}$$

where $H_x = A(1 + \frac{z}{R_x})$ and $H_y = B(1 + \frac{z}{R_y})$ take into account the curvature effects. The parameters A and B are the Lamé parameters, whose values are different from one whenever the curvature is not constant. In the case of constant shells, which are focus of the present investigation, $A = 1$ and $B = 1$.

The strain-displacement relation can be written in matrix form as:

$$\boldsymbol{\varepsilon}_\Omega = (\mathbf{D}_\Omega + \mathbf{A}_\Omega)\mathbf{u} \tag{2.2}$$

$$\boldsymbol{\varepsilon}_n = (\mathbf{D}_n + \mathbf{D}_z + \lambda_D \mathbf{A}_n)\mathbf{u} \tag{2.3}$$

where

$$\mathbf{D}_\Omega = \begin{bmatrix} \frac{\partial}{H_x\,\partial x} & 0 & 0 \\ 0 & \frac{\partial}{H_y\,\partial y} & 0 \\ \frac{\partial}{H_y\,\partial y} & \frac{\partial}{H_x\,\partial x} & 0 \end{bmatrix} \qquad \mathbf{D}_n = \begin{bmatrix} 0 & 0 & \frac{\partial}{H_y\,\partial y} \\ 0 & 0 & \frac{\partial}{H_x\,\partial x} \\ 0 & 0 & 0 \end{bmatrix} \qquad \mathbf{D}_z = \begin{bmatrix} 0 & \frac{\partial}{\partial z} & 0 \\ \frac{\partial}{\partial z} & 0 & 0 \\ 0 & 0 & \frac{\partial}{\partial z} \end{bmatrix} \tag{2.4}$$

$$\mathbf{A}_\Omega = \begin{bmatrix} 0 & 0 & \frac{1}{H_x R_x} \\ 0 & 0 & \frac{1}{H_y R_y} \\ 0 & 0 & 0 \end{bmatrix} \qquad \mathbf{A}_n = \begin{bmatrix} 0 & -\frac{1}{H_y R_y} & 0 \\ -\frac{1}{H_x R_x} & 0 & 0 \\ 0 & 0 & 0 \end{bmatrix} \tag{2.5}$$

The trace λ_D can be set to 0 or 1, depending on the shell theory to be considered. When $\lambda_D = 0$, an approximation similar to the *Donnell-type shallow shell theory* is introduced [21]; when $\lambda_D = 1$ the curvature effects are entirely retained. In this work, λ_D is always taken equal to 1 unless otherwise stated.

The stain-displacement relation for cylindrical and plate geometries can be easily obtained starting from the one for doubly-curved geometries. For cylindrical geometries it suffices to impose one of the two radii of curvature equal to infinity. This also implies that either $H_x = 1$ or $H_y = 1$. For plate geometries both radii or curvature have to be imposed equal to infinite, and, therefore, $H_x = 1$ or $H_y = 1$.

Finally, the shell can be considered thin or thick depending on the ratios R/h and a/h (and b/h). Usually if either the radius or the length are one order of magnitude larger than the thickness it is acceptable to define the shell thin.

2.2 Reissner Mixed Variational Principle

The solution of the structural problem involves the ability to determine the displacement field as well as the strain and the stress fields. For this purpose, different variational strategies have been proposed in the years, involving one-, two- or three-field variational principles. For instance, the well-know *Principle of Virtual Displacements* (PVD) considers the displacement field as unknown of the problem. Strains are derived via strain-displacement relations and stresses via constitutive relations. Other principles involve the introduction of two fields (Hellinger-Reissner) or three fields (Hu-Washizu) as unknowns. In this thesis, focus is given to the mixed variational principle proposed by Reissner in 1984 [22], which is of particular interest for the study of composite structures: the so-called *Reissner Mixed Variational Theorem* (RMVT). The unknowns are the displacement field the *transverse stress* field. Strains are derived via strain-displacement relations and in-plane stresses via constitutive relations. The main advantage of this principle consists in the possibility of introducing assumptions about the transverse stress field. In particular, it allows imposing *a priori* their continuity at the interface of plies, fulfilling the interlayer equilibrium. RMVT allows thus to satisfy all the so-called C_z^0 *requirements a priori*: compatibility of the in-plane and out-of-plane displacements at each interface, and equilibrium conditions at each interface for the transverse shear stress components and the transverse normal stress component. RMVT is particularly interesting when dealing with composite structures, where accurate predictions of the interlaminar stresses are crucial to predict the onset of the delamination phenomena. A consideration that justifies the choice to introduce this approximation only for transverse stresses and not for every stress variable is the difference in the order of magnitude between the primary bending and stretching stresses and the transverse stresses. Transverse stresses have a lower order of magnitude with respect to primary bending and stretching stresses, therefore it is allowable to make "relatively crude approximative assumptions [22]" about them. Furthermore, one important benefit deriving from RMVT is that it automatically yields the correct *shear correction factors*.

A first possible derivation of RMVT consists in rephrasing the PVD by introducing the transverse stresses $(\sigma_{xz}, \sigma_{yz}, \sigma_{zz})$ as *Lagrange multipliers*. For clarity, the PVD is reported below:

$$\delta \int\int\int u(\varepsilon_{xx}, \varepsilon_{yy}, \gamma_{xy}, \gamma_{xz}, \gamma_{yz}, \varepsilon_{zz}) \mathrm{d}x_1 \mathrm{d}x_2 \mathrm{d}x_3 = 0 \tag{2.6}$$

where u is the *specific strain energy*, and $\varepsilon_{xx}, \varepsilon_{yy}, \gamma_{xy}, \gamma_{xz}, \gamma_{yz}, \varepsilon_{zz}$ are the strains. It is recalled here that, under the assumption of *infinitesimal displacements*, the geometric relations between strains and displacements are:

$$\begin{aligned} \varepsilon_{xx} &= \frac{\partial u_x}{\partial x} \quad \varepsilon_{yy} = \frac{\partial u_y}{\partial y} \quad \varepsilon_{zz} = \frac{\partial u_z}{\partial z} \\ \gamma_{xy} &= \frac{\partial u_x}{\partial y} + \frac{\partial u_y}{\partial x} \quad \gamma_{xz} = \frac{\partial u_x}{\partial z} + \frac{\partial u_z}{\partial x} \quad \gamma_{yz} = \frac{\partial u_y}{\partial z} + \frac{\partial u_z}{\partial y} \end{aligned} \tag{2.7}$$

After introducing the Lagrange multipliers, Eq.(2.6) becomes:

$$\begin{aligned} \delta \int\int\int u(\varepsilon_{xx}, \varepsilon_{yy}, \gamma_{xy}, \gamma_{xz}, \gamma_{yz}, \varepsilon_{zz}) + \sigma_{xz}\left(\frac{\partial u_x}{\partial z} + \frac{\partial u_z}{\partial x} - \gamma_{xz}\right) \\ + \sigma_{yz}\left(\frac{\partial u_y}{\partial z} + \frac{\partial u_z}{\partial y} - \gamma_{yz}\right) + \sigma_{zz}\left(\frac{\partial u_z}{\partial z} - \varepsilon_{zz}\right) \mathrm{d}x_1 \mathrm{d}x_2 \mathrm{d}x_3 = 0 \end{aligned} \tag{2.8}$$

Splitting then the energy function u into two parts:

$$u(\varepsilon_{xx}, \varepsilon_{yy}, \gamma_{xy}, \gamma_{xz}, \gamma_{yz}, \varepsilon_{zz}) = u_0(\varepsilon_{xx}, \varepsilon_{yy}, \gamma_{xy}) + u_1(\varepsilon_{xx}, \varepsilon_{yy}, \gamma_{xy}, \gamma_{xz}, \gamma_{yz}, \varepsilon_{zz}) \tag{2.9}$$

where: $u_0(\varepsilon_{xx}, \varepsilon_{yy}, \gamma_{xy}) = u(\varepsilon_{xx}, \varepsilon_{yy}, \gamma_{xy}, 0, 0, 0)$ is the energy when only in-plane strains are present. Since the material is assumed to be hyperelastic, it is possible to compute the transverse stresses as:

$$\begin{aligned} \sigma_{xz} &= \frac{\partial u}{\partial \gamma_{xz}} = \frac{\partial u_1}{\partial \gamma_{xz}} \\ \sigma_{yz} &= \frac{\partial u}{\partial \gamma_{yz}} = \frac{\partial u_1}{\partial \gamma_{yz}} \\ \sigma_{zz} &= \frac{\partial u}{\partial \gamma_{zz}} = \frac{\partial u_1}{\partial \gamma_{zz}} \end{aligned} \tag{2.10}$$

Using these three equations it is possible to determine the transverse strains as function of the transverse stresses ($\boldsymbol{\sigma}_n = \{\sigma_{xz}, \sigma_{yz}, \sigma_{zz}\}^T$) and of the in-plane strains ($\boldsymbol{\varepsilon}_\Omega = \{\varepsilon_{xx}, \varepsilon_{yy}, \gamma_{xy}\}^T$):

$$\begin{aligned} \gamma_{xz} &= \gamma_{xz}(\boldsymbol{\sigma}_n, \boldsymbol{\varepsilon}_\Omega) \\ \gamma_{yz} &= \gamma_{yz}(\boldsymbol{\sigma}_n, \boldsymbol{\varepsilon}_\Omega) \\ \varepsilon_{zz} &= \varepsilon_{zz}(\boldsymbol{\sigma}_n, \boldsymbol{\varepsilon}_\Omega) \end{aligned} \tag{2.11}$$

where the subscript Ω refers to in-plane quantities and n to out-of-plane quantities.

Through a partial Legendre transformation it is possible to define a complementary energy function w as a function only of $\boldsymbol{\sigma}_n$ and $\boldsymbol{\varepsilon}_\Omega$. Specifically:

$$w(\boldsymbol{\sigma}_n, \boldsymbol{\varepsilon}_\Omega) = \sigma_{zz}\varepsilon_{zz} + \sigma_{xz}\gamma_{xz} + \sigma_{yz}\gamma_{yz} - u_1(\varepsilon_{xx}, \varepsilon_{yy}, \gamma_{xy}, \gamma_{xz}(\boldsymbol{\sigma}_n, \boldsymbol{\varepsilon}_\Omega), \gamma_{yz}(\boldsymbol{\sigma}_n, \boldsymbol{\varepsilon}_\Omega), \varepsilon_{zz}(\boldsymbol{\sigma}_n, \boldsymbol{\varepsilon}_\Omega)) \tag{2.12}$$

It follows as usual: $\varepsilon_{zz} = \frac{\partial w}{\partial \sigma_{zz}}$, $\gamma_{xz} = \frac{\partial w}{\partial \sigma_{xz}}$, $\gamma_{yz} = \frac{\partial w}{\partial \sigma_{yz}}$.
Substituting then u_1 from Eq.(2.12) into Eq.(2.9) it leads to:

$$u(\boldsymbol{\sigma}_n, \boldsymbol{\varepsilon}_\Omega) = u_0(\boldsymbol{\varepsilon}_\Omega) + \sigma_{zz}\varepsilon_{zz}(\boldsymbol{\sigma}_n, \boldsymbol{\varepsilon}_\Omega) + \sigma_{xz}\gamma_{xz}(\boldsymbol{\sigma}_n, \boldsymbol{\varepsilon}_\Omega) + \sigma_{yz}\gamma_{yz}(\boldsymbol{\sigma}_n, \boldsymbol{\varepsilon}_\Omega) - w(\boldsymbol{\sigma}_n, \boldsymbol{\varepsilon}_\Omega) \tag{2.13}$$

Using then this new expression of the *specific strain energy*, which is function only of in-plane strains and of transverse stresses, in Eq.(2.8) the mixed variational theorem is obtained as:

$$\delta \int\int\int u_0(\boldsymbol{\varepsilon}_\Omega) + \frac{\partial u_z}{\partial z}\sigma_{zz} + \left(\frac{\partial u_x}{\partial z} + \frac{\partial u_z}{\partial x}\right)\sigma_{xz} + \left(\frac{\partial u_y}{\partial z} + \frac{\partial u_z}{\partial y}\right)\sigma_{yz} - w(\boldsymbol{\sigma}_n, \boldsymbol{\varepsilon}_\Omega)\, \mathrm{d}x_1 \mathrm{d}x_2 \mathrm{d}x_3 = 0 \tag{2.14}$$

with arbitrary $\delta u_x, \delta u_y, \delta u_z, \delta\sigma_{xz}, \delta\sigma_{yz}, \delta\sigma_{zz}$.
This derivation of RMVT, since builds upon the PVD, highlights the fact that this principle is indeed an augmentation of the PVD. Therefore, considering the two unknown fields, the main conditions to be fulfilled are the *essential conditions* of the displacement field and not the *natural conditions* of the transverse stress field.

To further clarify the variational principle, it is useful to present its derivation under a different perspective. In particular, a second possible derivation of RMVT was proposed by Reissner in 1986 [23]. This derivation starts from the *mixed variational principle of*

Hellinger-Reissner which considers all displacements and all stresses as independent variables. Hellinger-Reissner variational principle for a general volume in absence of body forces and free boundaries:

$$\delta \int\int\int w(\sigma_{xx},\sigma_{yy},\sigma_{zz},\sigma_{xy},\sigma_{xz},\sigma_{yz}) - \sigma_{xx}\varepsilon_{xx} - \sigma_{yy}\varepsilon_{yy} - \sigma_{xy}\gamma_{xy} - \sigma_{xz}\gamma_{xz} - \sigma_{yz}\gamma_{yz} - \sigma_{zz}\varepsilon_{zz}\,\mathrm{d}x_1\mathrm{d}x_2\mathrm{d}x_3 = 0 \quad (2.15)$$

where w is a given function and the variations of $\delta\sigma_{xx}$, $\delta\sigma_{yy}$, $\delta\sigma_{xy}$, $\delta\sigma_{xz}$, $\delta\sigma_{yz}$, $\delta\sigma_{zz}$, δu_x, δu_y, δu_z are arbitrary.

Considering now the three constitutive equations coming from the hyperelasticity of the material:

$$\varepsilon_{xx} = \frac{\partial w}{\partial \sigma_{xx}} \quad \varepsilon_{yy} = \frac{\partial w}{\partial \sigma_{yy}} \quad \gamma_{xy} = \frac{\partial w}{\partial \sigma_{xy}} \quad (2.16)$$

it is possible to use them to determine σ_{xx}, σ_{yy} and σ_{xy} as:

$$\sigma_{xx} = \sigma_{xx}(\boldsymbol{\sigma}_n, \boldsymbol{\varepsilon}_\Omega) \quad \sigma_{yy} = \sigma_{yy}(\boldsymbol{\sigma}_n, \boldsymbol{\varepsilon}_\Omega) \quad \sigma_{xy} = \sigma_{xy}(\boldsymbol{\sigma}_n, \boldsymbol{\varepsilon}_\Omega) \quad (2.17)$$

Using then the new expressions of σ_{xx}, σ_{yy} and σ_{xy} it is possible to define a *semi-complementary energy density* v which depends only on $\boldsymbol{\sigma}_n$ and $\boldsymbol{\varepsilon}_\Omega$:

$$v(\boldsymbol{\sigma}_n, \boldsymbol{\varepsilon}_\Omega) = \varepsilon_{xx}\sigma_{xx}(\boldsymbol{\sigma}_n, \boldsymbol{\varepsilon}_\Omega) + \varepsilon_{yy}\sigma_{yy}(\boldsymbol{\sigma}_n, \boldsymbol{\varepsilon}_\Omega) + \gamma_{xy}\sigma_{xy}(\boldsymbol{\sigma}_n, \boldsymbol{\varepsilon}_\Omega) - w(\boldsymbol{\sigma}_n, \sigma_{xx}(\boldsymbol{\sigma}_n, \boldsymbol{\varepsilon}_\Omega), \sigma_{yy}(\boldsymbol{\sigma}_n, \boldsymbol{\varepsilon}_\Omega), \sigma_{xy}(\boldsymbol{\sigma}_n, \boldsymbol{\varepsilon}_\Omega)) \quad (2.18)$$

The expression of Eq.(2.18) implies the following subset of constitutive equations:

$$\sigma_{xx} = \frac{\partial v}{\partial \varepsilon_{xx}} \quad \sigma_{yy} = \frac{\partial v}{\partial \varepsilon_{yy}} \quad \sigma_{xy} = \frac{\partial v}{\partial \gamma_{xy}} \quad (2.19)$$

Then substituting the expression of w from Eq.(2.18) into Eq.(2.15) the desired variational equation is obtained:

$$\delta \int\int\int v(\boldsymbol{\sigma}_n, \boldsymbol{\varepsilon}_\Omega) + \sigma_{xz}\gamma_{xz} + \sigma_{yz}\gamma_{yz} + \sigma_{zz}\varepsilon_{zz}\,\mathrm{d}x_1\mathrm{d}x_2\mathrm{d}x_3 = 0 \quad (2.20)$$

Finally, to confirm the correctness of Eq.(2.20), it must be verified that through the introduction of the constraint equations (2.19) and the geometric relations (2.7), it indeed gives three equations of equilibrium and three constitutive equations. The three constitutive equations give the transverse stains as function of the in-plane strains and the transverse stresses. We can deduce this beginning from Eq.(2.20):

$$\int\int\int \frac{\partial v}{\partial \varepsilon_{xx}}\delta\varepsilon_{xx} + \frac{\partial v}{\partial \varepsilon_{yy}}\delta\varepsilon_{yy} + \frac{\partial v}{\partial \gamma_{xy}}\delta\gamma_{xy} + \frac{\partial v}{\partial \sigma_{xz}}\delta\sigma_{xz} + \frac{\partial v}{\partial \sigma_{yz}}\delta\sigma_{yz} + \frac{\partial v}{\partial \sigma_{zz}}\delta\sigma_{zz} + \sigma_{xz}\delta\gamma_{xz} + \sigma_{yz}\delta\gamma_{yz} + \sigma_{zz}\delta\varepsilon_{zz} + \gamma_{xz}\delta\sigma_{xz} + \gamma_{yz}\delta\sigma_{yz} + \varepsilon_{zz}\delta\sigma_{zz}\,\mathrm{d}x_1\mathrm{d}x_2\mathrm{d}x_3 = 0 \quad (2.21)$$

Using Eq.(2.19) it follows that:

$$\int\int\int \sigma_{xx}\delta\varepsilon_{xx} + \sigma_{yy}\delta\varepsilon_{yy} + \sigma_{xy}\delta\varepsilon_{xy} + \sigma_{xz}\delta\gamma_{xz} + \sigma_{yz}\delta\gamma_{yz} + \sigma_{zz}\delta\varepsilon_{zz} + \left(\frac{\partial v}{\partial \sigma_{xz}} + \gamma_{xz}\right)\delta\sigma_{xz} + \left(\frac{\partial v}{\partial \sigma_{yz}} + \gamma_{yz}\right)\delta\sigma_{yz} + \left(\frac{\partial v}{\partial \sigma_{zz}} + \varepsilon_{zz}\right)\delta\sigma_{zz}\,\mathrm{d}x_1\mathrm{d}x_2\mathrm{d}x_3 = 0 \quad (2.22)$$

Using then the arbitrariness of the virtual variations it follows that the three constitutive equations are:

$$\gamma_{xz} = -\frac{\partial v(\boldsymbol{\sigma}_n, \boldsymbol{\varepsilon}_\Omega)}{\partial \sigma_{xz}} \quad \gamma_{yz} = -\frac{\partial v(\boldsymbol{\sigma}_n, \boldsymbol{\varepsilon}_\Omega)}{\partial \sigma_{yz}} \quad \varepsilon_{zz} = -\frac{\partial v(\boldsymbol{\sigma}_n, \boldsymbol{\varepsilon}_\Omega)}{\partial \sigma_{zz}} \tag{2.23}$$

while the three equilibrium equations can be obtained upon expressing ε_{xx}, ε_{yy}, γ_{xy}, γ_{xz}, γ_{yz} and ε_{zz} through their geometric relations, and by collecting the virtual quantities δu_x, δu_y and δu_z.

RMVT can be rewritten in a more practical form by specifying the volume as $V = \Omega \times [-\frac{h}{2} \leq z \leq \frac{h}{2}]$ and by making explicit the energy functions in terms of strains and stresses; loads of inertia and general volume forces are considered:

$$\int_\Omega \int_{-\frac{h}{2}}^{\frac{h}{2}} \delta\boldsymbol{\varepsilon}_{\Omega G}^T \boldsymbol{\sigma}_{\Omega H} + \delta\boldsymbol{\varepsilon}_{nG}^T \boldsymbol{\sigma}_{nM} + \delta\boldsymbol{\sigma}_{nM}^T (\boldsymbol{\varepsilon}_{nG} - \boldsymbol{\varepsilon}_{nH}) \, \mathrm{d}z\mathrm{d}\Omega = - \int_\Omega \int_{-\frac{h}{2}}^{\frac{h}{2}} \delta\mathbf{u}^T \rho\ddot{\mathbf{u}} \, \mathrm{d}z\mathrm{d}\Omega + \int_\Omega \int_{-\frac{h}{2}}^{\frac{h}{2}} \delta\mathbf{u}^T \mathbf{f} \, \mathrm{d}z\mathrm{d}\Omega \tag{2.24}$$

where: subscript G identifies the strains evaluated referring to the strain-displacement relations; subscript H denotes strains and stresses obtained via the *mixed form of Hooke's law* (see Subsection 2.2.1); subscript M denotes the transverse stresses modeled with an *axiomatic approach*. Subscript Ω stands for in-plane quantities, subscript n for out-of-plane quantities. In particular, the vectors above collect the following quantities:

$$\boldsymbol{\varepsilon}_\Omega = \begin{Bmatrix} \varepsilon_{xx} \\ \varepsilon_{yy} \\ \varepsilon_{xy} \end{Bmatrix} \quad \boldsymbol{\varepsilon}_n = \begin{Bmatrix} \gamma_{yz} \\ \gamma_{xz} \\ \varepsilon_{zz} \end{Bmatrix} \quad \boldsymbol{\sigma}_\Omega = \begin{Bmatrix} \sigma_{xx} \\ \sigma_{yy} \\ \sigma_{xy} \end{Bmatrix} \quad \boldsymbol{\sigma}_n = \begin{Bmatrix} \sigma_{yz} \\ \sigma_{xz} \\ \sigma_{zz} \end{Bmatrix} \tag{2.25}$$

and

$$\mathbf{u} = \begin{Bmatrix} u_x \\ u_y \\ u_z \end{Bmatrix} \quad \mathbf{f} = \begin{Bmatrix} f_x \\ f_y \\ f_z \end{Bmatrix} \tag{2.26}$$

2.2.1 Mixed form of Hooke's law

When employing RMVT a constitutive relation expressing *in-plane stresses* and *transverse strains* as a function of *in-plane strains* and of *transverse stresses* is needed (see Eqs.(2.11), (2.17) and (2.23)). For this purpose, the *Mixed Form of Hooke's Law* (MFHL) [16] is introduced. The derivation of the MFHL is straightforward, as outlined next, starting from a compact form of the *Classical Form of Hooke's Law* (CFHL).

Beginning from the CFHL expressed in a laminate frame of reference (further considerations can be found in Appendix A) let's split the in-plane and out-of-plane components:

$$\begin{Bmatrix} \boldsymbol{\sigma}_\Omega \\ \boldsymbol{\sigma}_n \end{Bmatrix} = \begin{bmatrix} \widetilde{\mathbf{C}}_{\Omega\Omega} & \widetilde{\mathbf{C}}_{\Omega n} \\ \widetilde{\mathbf{C}}_{n\Omega} & \widetilde{\mathbf{C}}_{nn} \end{bmatrix} \begin{Bmatrix} \boldsymbol{\varepsilon}_\Omega \\ \boldsymbol{\varepsilon}_n \end{Bmatrix} \tag{2.27}$$

where the stress and strain components have been collected as follows:

$$\boldsymbol{\sigma}_\Omega = [\sigma_{xx} \quad \sigma_{yy} \quad \tau_{xy}]^T \quad \boldsymbol{\sigma}_n = [\tau_{yz} \quad \tau_{xz} \quad \sigma_{zz}]^T \tag{2.28}$$

$$\boldsymbol{\varepsilon}_\Omega = [\varepsilon_{xx} \quad \varepsilon_{yy} \quad \gamma_{xy}]^T \quad \boldsymbol{\varepsilon}_n = [\gamma_{yz} \quad \gamma_{xz} \quad \varepsilon_{zz}]^T \tag{2.29}$$

From the second relationship of Eq.(2.27), it is possible to derive $\boldsymbol{\varepsilon}_n$ in terms of $\boldsymbol{\sigma}_n$ and $\boldsymbol{\varepsilon}_\Omega$:

$$\boldsymbol{\varepsilon}_n = (\widetilde{\mathbf{C}}_{nn})^{-1}\boldsymbol{\sigma}_n - (\widetilde{\mathbf{C}}_{nn})^{-1}\widetilde{\mathbf{C}}_{n\Omega}\boldsymbol{\varepsilon}_\Omega \tag{2.30}$$

Substituting back this expression of $\boldsymbol{\varepsilon}_n$ into the first one of Eq.(2.27), it is obtained:

$$\boldsymbol{\sigma}_\Omega = [\widetilde{\mathbf{C}}_{\Omega\Omega} - \widetilde{\mathbf{C}}_{\Omega n}(\widetilde{\mathbf{C}}_{nn})^{-1}\widetilde{\mathbf{C}}_{n\Omega}]\boldsymbol{\varepsilon}_\Omega + \widetilde{\mathbf{C}}_{\Omega n}(\widetilde{\mathbf{C}}_{nn})^{-1}\boldsymbol{\sigma}_n \tag{2.31}$$

Therefore, from Eq.(2.31) and Eq.(2.30), the MFHL is obtained as:

$$\left\{ \begin{array}{c} \boldsymbol{\sigma}_\Omega \\ \boldsymbol{\varepsilon}_n \end{array} \right\} = \begin{bmatrix} \mathbf{C}_{\Omega\Omega} & \mathbf{C}_{\Omega n} \\ \mathbf{C}_{n\Omega} & \mathbf{C}_{nn} \end{bmatrix} \left\{ \begin{array}{c} \boldsymbol{\varepsilon}_\Omega \\ \boldsymbol{\sigma}_n \end{array} \right\} \tag{2.32}$$

where:

$$\mathbf{C}_{\Omega\Omega} = \widetilde{\mathbf{C}}_{\Omega\Omega} - \widetilde{\mathbf{C}}_{\Omega n}(\widetilde{\mathbf{C}}_{nn})^{-1}\widetilde{\mathbf{C}}_{n\Omega} \tag{2.33}$$

$$\mathbf{C}_{\Omega n} = \widetilde{\mathbf{C}}_{\Omega n}(\widetilde{\mathbf{C}}_{nn})^{-1} \tag{2.34}$$

$$\mathbf{C}_{n\Omega} = -(\widetilde{\mathbf{C}}_{nn})^{-1}\widetilde{\mathbf{C}}_{n\Omega} \tag{2.35}$$

$$\mathbf{C}_{nn} = (\widetilde{\mathbf{C}}_{\Omega n})^{-1} \tag{2.36}$$

or explicitly:

$$\mathbf{C}_{\Omega\Omega} = \begin{bmatrix} \widetilde{C}_{11} - \dfrac{(\widetilde{C}_{13})^2}{\widetilde{C}_{33}} & \widetilde{C}_{12} - \dfrac{\widetilde{C}_{13}}{\widetilde{C}_{33}}\widetilde{C}_{23} & \widetilde{C}_{16} - \dfrac{\widetilde{C}_{13}}{\widetilde{C}_{33}}\widetilde{C}_{36} \\ \widetilde{C}_{12} - \dfrac{\widetilde{C}_{13}}{\widetilde{C}_{33}}\widetilde{C}_{23} & \widetilde{C}_{22} - \dfrac{(\widetilde{C}_{23})^2}{\widetilde{C}_{33}} & \widetilde{C}_{26} - \dfrac{\widetilde{C}_{23}}{\widetilde{C}_{33}}\widetilde{C}_{36} \\ \widetilde{C}_{16} - \dfrac{\widetilde{C}_{13}}{\widetilde{C}_{33}}\widetilde{C}_{36} & \widetilde{C}_{26} - \dfrac{\widetilde{C}_{23}}{\widetilde{C}_{33}}\widetilde{C}_{36} & \widetilde{C}_{66} - \dfrac{(\widetilde{C}_{36})^2}{\widetilde{C}_{33}} \end{bmatrix} \quad \mathbf{C}_{\Omega n} = \begin{bmatrix} 0 & 0 & \dfrac{\widetilde{C}_{13}}{\widetilde{C}_{33}} \\ 0 & 0 & \dfrac{\widetilde{C}_{23}}{\widetilde{C}_{33}} \\ 0 & 0 & \dfrac{\widetilde{C}_{36}}{\widetilde{C}_{33}} \end{bmatrix}$$

$$\mathbf{C}_{n\Omega} = \begin{bmatrix} 0 & 0 & 0 \\ 0 & 0 & 0 \\ -\dfrac{\widetilde{C}_{13}}{\widetilde{C}_{33}} & -\dfrac{\widetilde{C}_{23}}{\widetilde{C}_{33}} & -\dfrac{\widetilde{C}_{36}}{\widetilde{C}_{33}} \end{bmatrix} \quad \mathbf{C}_{nn} = \begin{bmatrix} \dfrac{\widetilde{C}_{55}}{\widetilde{C}_{55}\widetilde{C}_{44} - (\widetilde{C}_{45})^2} & -\dfrac{\widetilde{C}_{45}}{\widetilde{C}_{55}\widetilde{C}_{44} - (\widetilde{C}_{45})^2} & 0 \\ -\dfrac{\widetilde{C}_{45}}{\widetilde{C}_{55}\widetilde{C}_{44} - (\widetilde{C}_{45})^2} & \dfrac{\widetilde{C}_{44}}{\widetilde{C}_{55}\widetilde{C}_{44} - (\widetilde{C}_{45})^2} & 0 \\ 0 & 0 & \dfrac{1}{\widetilde{C}_{33}} \end{bmatrix} \tag{2.37}$$

The constitutive law of Eq.(2.32) can be rewritten in extended from as:

$$\left\{ \begin{array}{c} \sigma_{xx} \\ \sigma_{yy} \\ \sigma_{xy} \\ \gamma_{yz} \\ \gamma_{xz} \\ \varepsilon_{zz} \end{array} \right\} = \begin{bmatrix} C_{11} & C_{12} & C_{16} & 0 & 0 & C_{13} \\ C_{12} & C_{22} & C_{26} & 0 & 0 & C_{23} \\ C_{16} & C_{26} & C_{66} & 0 & 0 & C_{36} \\ 0 & 0 & 0 & C_{44} & C_{45} & 0 \\ 0 & 0 & 0 & C_{54} & C_{55} & 0 \\ -C_{13} & -C_{23} & -C_{36} & 0 & 0 & C_{33} \end{bmatrix} \left\{ \begin{array}{c} \varepsilon_{xx} \\ \varepsilon_{yy} \\ \gamma_{xy} \\ \sigma_{yz} \\ \sigma_{xz} \\ \sigma_{zz} \end{array} \right\} \tag{2.38}$$

where the elastic coefficients C_{ik} are non-homogeneous quantities given the semi-inverse nature of the constitutive law (they are not to be confused with the coefficients in the ply frame of reference adopted in Appendix A).

2.3 Variable-kinematic formulation

The present work has the objective of deriving a numerical tool that enables to study a broad class of structures: thin or thick shells, any kind of lamination sequence, sandwich materials with one or more cores, and so on. The idea is to allow the study of these structures while minimizing the DOF, and thus the computational cost.

In order to achieve this goal, the adoption of a variable-kinematic model is proposed. This formulation allows the user to specify the kinematic formulation to be used in the analysis. For instance, if a thick shell is to be studied, a high-order model is required. On the other hand, if a thin plate is the object of the study and a global response is sufficient, a low-order model would suffice, allowing the problem to be solved with less kinematic-related degrees of freedom.

Furthermore, the inherent heterogeneity of many composite structures along the thickness direction - this is particularly true in the case of sandwich configurations - requires more refined models only in particular areas, while the implementation of these same models in other regions would entail a waste of DOF. The *sublaminate* technique was therefore implemented. It allows to divide the structure into sub-regions along the thickness and to use for each one of them the proper model.

The present section introduces the classical *Equivalent Single Layer* (ESL) and *Layer-Wise* (LW) formulations, and the *sublaminate* technique. Then the S-GUF formulation, which is capable of embedding both ESL and LW theories at sublaminate level, is presented.

2.3.1 Equivalent single-layer models

The majority of approaches developed in the past decades are based on the reduction of the 3-D problem to an equivalent 2-D problem. This simplification is made possible by introducing a reference 2-D surface of the structure and adopting *ad-hoc* kinematic assumptions. This approach is known as *axiomatic displacement-based approach*. Early examples of these theories are the *Kirchhoff plate theory* [24] and *Mindlin plate theory* [25], for plate geometries, and *Kirchhoff-Love theory* [26, 27], for shell geometries. These theories were first applied to single-layer structures and subsequently to multi-layer plates, where they describe the behavior of the structure as an equivalent single-ply (from here the name ESL).

One important remark about 2-D models is that their effectiveness is strictly related to the thickness-to-length ratio (h/a) and the shear deformability. Thin plates ($h/a \ll 1$) have lower 3-D effects and, therefore, even if a low-order 2-D model is employed for their description only minor errors are introduced. For a given geometry, the effects of shear deformability - or, to a more general extent, 3-D effects - become larger for decreasing values of the shear moduli. This aspect is important when considering composite materials, which are commonly characterized by a lower shear moduli with respect to isotropic materials. Another aspect to be considered is the radius-over-thickness ratio (R/h). If the ratio R/h is high then some 3-D effects can be discarded, introducing the Donnell approximation for shallow shells [28], while if the ratio R/h is low a more rich description is required in order to deal with a so-called deep shell.

When 3-D effects must be taken into account, due to one of the reasons stated above, a finer kinematic description must be adopted. This has the consequence of expanding

the variables through DOF not associated to physical quantities. Theories of this kind are the *Higher-order Shear Deformation Theories* (HSDT) and *Higher-order Shear and Normal Deformation Theories* (HSNDT). An example of HSNDT is given by:

$$\begin{cases} u_x(x,y,z,t) &= u_{x0} + zu_{x1} + z^2u_{x2} + z^3u_{x3} \\ u_y(x,y,z,t) &= u_{y0} + zu_{y1} + z^2u_{y2} + z^3u_{y3} \\ u_z(x,y,z,t) &= u_{z0} + zu_{z1} + z^2u_{z2} \end{cases} \tag{2.39}$$

The idea of modelling the kinematic variables as an expansion of terms allows to derive a potentially infinite number of theories. A formal expression valid for different HSNDT can be obtained using Einstein notation for repeated indexes:

$$\begin{cases} u_x(x,y,z,t) &= F^x_{\alpha_{u_x}}(z)u_{x\alpha_{u_x}}(x,y,t) & \alpha_{u_x} = 0,1,...,N_{\alpha_{u_x}} \\ u_y(x,y,z,t) &= F^y_{\alpha_{u_y}}(z)u_{y\alpha_{u_y}}(x,y,t) & \alpha_{u_y} = 0,1,...,N_{\alpha_{u_y}} \\ u_z(x,y,z,t) &= F^z_{\alpha_{u_z}}(z)u_{z\alpha_{u_z}}(x,y,t) & \alpha_{u_z} = 0,1,...,N_{\alpha_{u_z}} \end{cases} \tag{2.40}$$

where $N_{\alpha_{u_x}}$, $N_{\alpha_{u_y}}$, $N_{\alpha_{u_z}}$ are the orders of expansion for u_x, u_y and u_z respectively, and the functions along z are named F for *thickness functions*. In general, there is no need to use different kinds of thickness functions depending on the variable, therefore: $F^x_{\alpha_{u_x}} = F_{\alpha_{u_x}}$, $F^y_{\alpha_{u_y}} = F_{\alpha_{u_y}}$, $F^z_{\alpha_{u_z}} = F_{\alpha_{u_z}}$.

One important modification of ESL theories came from Murakami [29]. Aiming at describing the piece-wise continuous displacement field typical of composite materials, Murakami proposed to augment the ESL theories with the *Murakami Zig-Zag Function* (MZZF). These functions can be effective to improve the accuracy of the ESL model by requiring one single additional DOF. The MZZF can be expressed as:

$$F_{ZZ} = (-1)^p \xi_p \tag{2.41}$$

where p is a generic ply and z_p is the thickness coordinate of a ply respect to its own frame of reference (Figure 2.5). $\xi_p = \frac{z_p}{h_p}$ is the nondimensional thickness coordinate of the pth ply.

A general formulation of a model including these functions is:

$$\begin{cases} u_x(x,y,z,t) &= F_{\alpha_{u_x}}(z)u_{x\alpha_{u_x}}(x,y,t) + F_{ZZ}(z)u_{xZZ}(x,y,t) & \alpha_{u_x} = 0,1,...,N_{\alpha_{u_x}} \\ u_y(x,y,z,t) &= F_{\alpha_{u_y}}(z)u_{y\alpha_{u_y}}(x,y,t) + F_{ZZ}(z)u_{yZZ}(x,y,t) & \alpha_{u_y} = 0,1,...,N_{\alpha_{u_y}} \\ u_z(x,y,z,t) &= F_{\alpha_{u_z}}(z)u_{z\alpha_{u_z}}(x,y,t) + F_{ZZ}(z)u_{zZZ}(x,y,t) & \alpha_{u_z} = 0,1,...,N_{\alpha_{u_z}} \end{cases} \tag{2.42}$$

It is important to notice that the MZZF can also be added to an arbitrary sub-set of variables and not necessarily to all of them.

One final remark about the MZZF is the fact that its employment is mainly justified in periodic laminates where indeed a peculiar zig-zag path occurs for displacements [30].

2.3.2 Layerwise models

The ESL theories presented earlier are particularly convenient when the structure is thin or moderately thick because they allow a good global description with low numerical effort. On the other hand, *LayerWise* models (LW) assume a variable field satisfying only C^0-continuity through the thickness and apply to every single ply in the layer the specified

kinematic description. This latter model has a number of unknowns that depends on the number of plies. It allows an improved description of the structure compared to an ESL model since the kinematic model is defined ply-by-ply. However, the number of theory-related DOF becomes larger with respect to an ESL model. Furthermore, the number of DOF depends on the number of plies.

A general expression for a LW theory is:

$$\begin{cases} u_x^p(x,y,z_p,t) &= F^p_{\alpha_{u_x}}(z_p)u^p_{x\alpha_{u_x}}(x,y,t) \qquad \alpha_{u_x} = 0,1,...,N_{\alpha_{u_x}} \\ u_y^p(x,y,z_p,t) &= F^p_{\alpha_{u_y}}(z_p)u^p_{y\alpha_{u_y}}(x,y,t) \qquad \alpha_{u_y} = 0,1,...,N_{\alpha_{u_y}} \\ u_z^p(x,y,z_p,t) &= F^p_{\alpha_{u_z}}(z_p)u^p_{z\alpha_{u_z}}(x,y,t) \qquad \alpha_{u_z} = 0,1,...,N_{\alpha_{u_z}} \end{cases} \tag{2.43}$$

Since in general there is no need to select different kinds of thickness functions for different plies: $F^p_{\alpha_{u_x}} = F^p_{\alpha_{u_y}} = F^p_{\alpha_{u_z}} = F_{\alpha_{u_z}}$.

Figure 2.2 shows a comparison between two hypothetical descriptions, obtainable through the two different models.

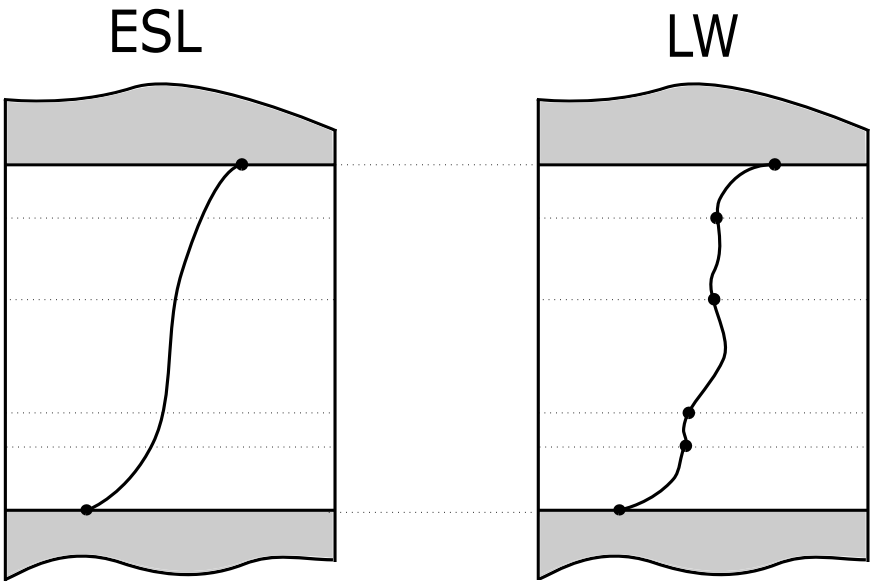

Figure 2.2: Comparison between ESL and LW models.

2.3.3 Sublaminate Generalized Unified Formulation

The current work is based on a variable-kinematic formulation, meaning that the orders of expansion can be set by the user depending on the structure to study. In particular, the approach used is the *Sublaminate Generalized Unified Formulation* (S-GUF). This approach inherits the features of the unified formulation due to Carrera [31] - *Carrera's Unified Formulation* (CUF) - and its successive extension by Demasi [32] - *Generalized Unified Formulation* (GUF). A peculiar aspect regards the introduction of the so-called *sublaminates*, i.e. arbitrary clusters of plies, leading to the *Sublaminate Generalized Unified Formulation* (S-GUF).

CUF introduced a compact notation that allows to express 2-D ESL and LW theories within the same framework. Using Einstein notation for repeated indexes:

$$\begin{cases} u_x(x,y,z,t) & = F_{\alpha_{u_x}}(z) u_{x\alpha_{u_x}}(x,y,t) & \alpha_{u_x} = 0,1,...,N \\ u_y(x,y,z,t) & = F_{\alpha_{u_y}}(z) u_{y\alpha_{u_y}}(x,y,t) & \alpha_{u_y} = 0,1,...,N \\ u_z(x,y,z,t) & = F_{\alpha_{u_z}}(z) u_{z\alpha_{u_z}}(x,y,t) & \alpha_{u_z} = 0,1,...,N \end{cases} \tag{2.44}$$

where N is the order of expansion, which is taken equal for all the displacement components. Furthermore, the unified formulation allows to write the governing equations in function of kernels whose form is independent of the theory adopted.

Demasi introduced the GUF [32], the main features being the possibility of selecting different orders of expansions for each variable and also to adopt different descriptions for each one of them (ESL or LW).

$$\begin{cases} u_x^{(p)}(x,y,z_{(p)},t) & = F_{\alpha_{u_x}}(z_{(p)}) u_{x\alpha_{u_x}}^{(p)}(x,y,t) & \alpha_{u_x} = 0,1,...,N_{\alpha_{u_x}} \\ u_y^{(p)}(x,y,z_{(p)},t) & = F_{\alpha_{u_y}}(z_{(p)}) u_{y\alpha_{u_y}}^{(p)}(x,y,t) & \alpha_{u_y} = 0,1,...,N_{\alpha_{u_y}} \\ u_z^{(p)}(x,y,z_{(p)},t) & = F_{\alpha_{u_z}}(z_{(p)}) u_{z\alpha_{u_z}}^{(p)}(x,y,t) & \alpha_{u_z} = 0,1,...,N_{\alpha_{u_z}} \end{cases} \tag{2.45}$$

where $N_{\alpha_{u_x}}$, $N_{\alpha_{u_y}}$ and $N_{\alpha_{u_z}}$ are the orders of expansion of each variable, and the superscript (p) indicates the possibility to adopt an ESL model or a LW model independently for each variable.

A sublaminate is defined as a group of adjacent plies sharing the same kinematic description. Each sublaminate is identified by the plies, and the local kinematic description. Collecting physical plies into sublaminates is a particularly effective practice when it is used to separate portions characterized by highly different mechanical properties. In this manner, an appropriate model based on the GUF can be applied to each sub-portion of the structure, taking into consideration the local properties. For instance, a sandwich panel could be modeled using a high-order theory for the core and lower-order theories for the facesheets. Employing the sublaminate concept, it is possible to partition the structure and adopt the appropriate model for each part of it, obtaining both an accurate and cost-efficient solution. A visualization of sublaminates defined as the collection of physical plies is given in Figure 2.3.

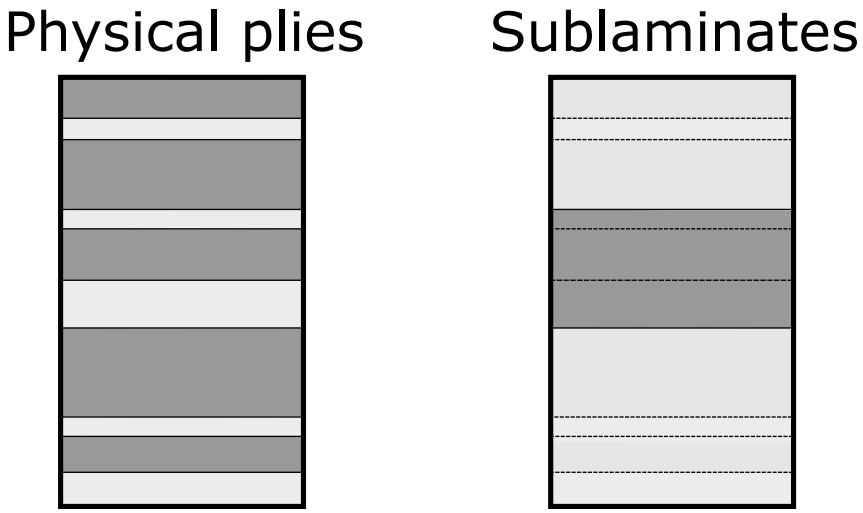

Figure 2.3: Collection of physical plies into three different sublaminates.

In the general case, after defining the sublaminates within the structure, different GUF models can be adopted for each sublaminate, being either an equivalent single-layer theory or a layerwise theory. This process results in a truly *multiple-kinematic model*. Within the proposed framework, the classical ESL theory can be interpreted as a special case of the S-GUF where the sublaminate coincides with the whole laminate, and an ESL theory is adopted. Similarly, the classical LW theory can be obtained when a sublaminate is defined for each physical ply, or when a single sublaminate with a LW theory is chosen. A second possible use of the sublaminate concept is the division of one physical ply into two or more numerical plies. This choice allows to further increase the accuracy of the solution. For instance, since the radius of curvature is assumed constant within each sublaminate (or ply for a LW theory) when performing the computations, partitioning a ply into two numerical sublaminates allows the geometric description to be improved. Figure 2.4 shows the advantages of using combinations of the GUF and *sublaminate* techniques.

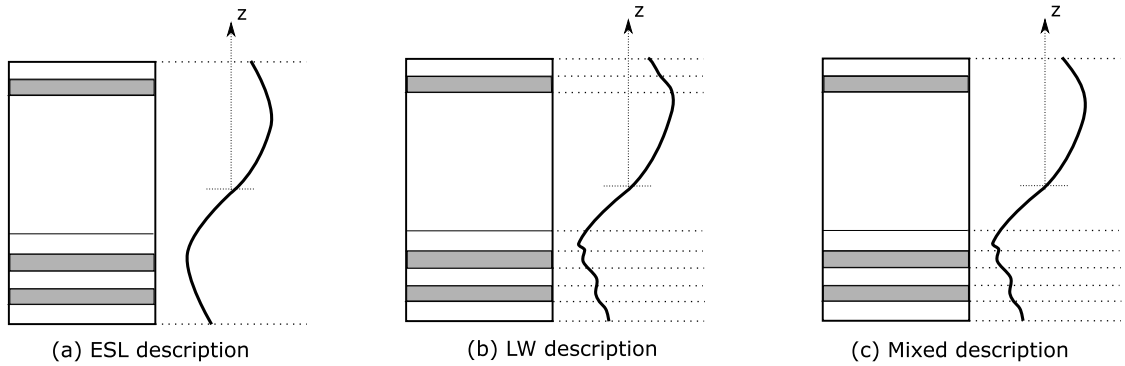

Figure 2.4: (a) ESL: low accuracy, low computational cost; (b) LW: high accuracy, high computational cost; (c) Mixed: local accuracy, medium computational cost.

Thus the S-GUF framework, previously applied to the PVD by D'Ottavio et al. [1], and here extended to RMVT, allowed to program within one single code a potentially infinite number of kinematic theories. This enables the user to freely select the kind of description to adopt, either for the whole structure or for each sub-portion of the domain along the thickness.

It is convenient to notice that the ESL model can be considered as a particular case of the LW model, where all the variables of different plies are forced to be the same within the same sublaminate. This translates in taking $z_p = z_k$ (z_k is the thickness coordinate of a sublaminate respect to its own frame of reference, Figure 2.5) and:

$$\begin{aligned} v_r^{p,k} &= v_r^k \\ v_{r\alpha_{v_r}}^{p,k} &= v_{r\alpha_{v_r}}^k \end{aligned} \qquad \forall p \in [1, N_p^k] \qquad (v = u, \sigma;\ r = x, y, z) \tag{2.46}$$

Therefore, in the subsequent developments, the 2-D kinematic approximation will be used with the notation of Eq.(2.47) in both ESL and LW cases.

Finally, as stated in Section 2.2, the present work is based upon RMVT, hence the S-GUF approach was applied not only to the displacements variables but extended to all the independent variables: displacements and transverse stresses [16]. A formal writing of S-GUF in a LW approximation through Einstein notation for repeated indexes is (the MZZF is formally included into the generic function F_{α_v}):

$$\begin{cases} u_x^{p,k}(x,y,z_p,t) &= F_{\alpha_{u_x}}(z_p)u_{x\alpha_{u_x}}^{p,k}(x,y,t) & \alpha_{u_x}=0,1,...,N_{u_x}^k \\ u_y^{p,k}(x,y,z_p,t) &= F_{\alpha_{u_y}}(z_p)u_{y\alpha_{u_y}}^{p,k}(x,y,t) & \alpha_{u_y}=0,1,...,N_{u_y}^k \\ u_z^{p,k}(x,y,z_p,t) &= F_{\alpha_{u_z}}(z_p)u_{z\alpha_{u_z}}^{p,k}(x,y,t) & \alpha_{u_z}=0,1,...,N_{u_z}^k \\ \sigma_{xz}^{p,k}(x,y,z_p,t) &= \mathcal{F}_{\alpha_{\sigma_{xz}}}(z_p)\sigma_{xz\alpha_{\sigma_{xz}}}^{p,k}(x,y,t) & \alpha_{\sigma_{xz}}=0,1,...,N_{\sigma_{xz}}^k \\ \sigma_{yz}^{p,k}(x,y,z_p,t) &= \mathcal{F}_{\alpha_{\sigma_{yz}}}(z_p)\sigma_{yz\alpha_{\sigma_{yz}}}^{p,k}(x,y,t) & \alpha_{\sigma_{yz}}=0,1,...,N_{\sigma_{yz}}^k \\ \sigma_{zz}^{p,k}(x,y,z_p,t) &= \mathcal{F}_{\alpha_{\sigma_{zz}}}(z_p)\sigma_{zz\alpha_{\sigma_{zz}}}^{p,k}(x,y,t) & \alpha_{\sigma_{zz}}=0,1,...,N_{\sigma_{zz}}^k \end{cases} \tag{2.47}$$

where the superscript k refers to the kth sublaminate, the superscript p refers to the pth ply and $N_{u_x}^k, N_{u_y}^k, N_{u_z}^k, N_{\sigma_{xz}}^k, N_{\sigma_{yz}}^k, N_{\sigma_{zz}}^k$ are the orders of expansion of $u_x^k, u_y^k, u_z^k, \sigma_{xz}^k, \sigma_{yz}^k$, σ_{zz}^k, respectively. For transverse stresses the functions of the thickness coordinate are formally indicated with the symbol $\mathcal{F}$, instead of the symbol F used for displacements, to distinguish the cases in which the two type of variables are considered. However, the set of functions used will be the same for practical purposes.

2.3.4 Thickness functions

The thickness functions used to expand the model are *a combination of Legendre orthogonal polynomials* which, for sake of convenience, are the same whether an ESL or a LW description is adopted.

A non-dimensional coordinate ξ is introduced for the thickness. It will be specified as ξ_k in case an ESL model is adopted or as ξ_p for a LW model. They are defined as follows:

$$\xi_p = \frac{z_p}{h_p/2} \qquad \xi_k = \frac{z_k}{h_k/2} \tag{2.48}$$

and are related through:

$$\xi_p = \frac{h_k}{h_p}\xi_k + \frac{2}{h_p}(z_{0k} - z_{0p}) \tag{2.49}$$

where: h_p is the thickness of the ply, h_k is the thickness of the sublaminate, z_p is the thickness coordinate in the ply reference system, z_k is the thickness coordinate in the sublaminate reference system, z_{0p} is the ply middle plane coordinate in the laminate reference system, and z_{0k} is the sublaminate middle plane coordinate in the laminate reference system. Graphic visualization of these frames of reference is given in Figure 2.5.

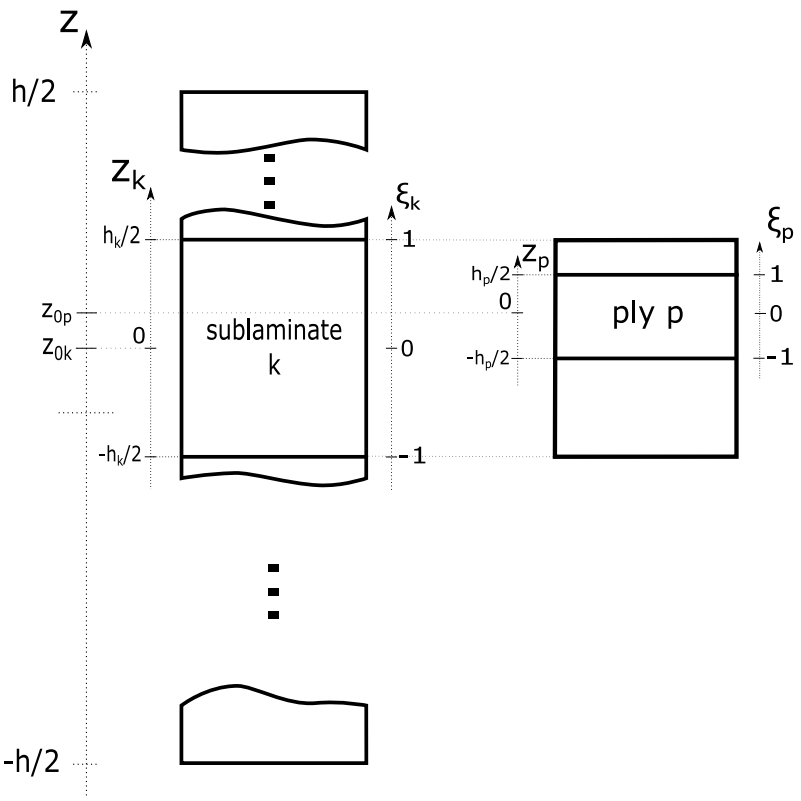

Figure 2.5: Representation of frames of reference in the thickness direction and of non-dimensional coordinates ξ_k, ξ_p.

Then, using a non-dimensional coordinate, the thickness functions are given by:

$$if \quad N_{v_r}^k = 0 : \; F_0(\xi) = 1 \tag{2.50}$$

$$\begin{aligned} if \quad N_{v_r^k} > 0 : \; F_0(\xi) &= \frac{1+\xi}{2} \\ F_1(\xi) &= \frac{1-\xi}{2} \\ F_l(\xi) &= P_l(\xi) - P_{l-2}(\xi) \qquad l = 2, 3, ..., N_{v_r}^k \end{aligned} \tag{2.51}$$

where $v = u$, σ and $r = x, y, z$; and P_l is the Legendre polynomial of order l which can be defined recursively as follows:

$$P_0 = 1; \quad P_1 = \xi; \quad P_{l+1} = \frac{(2l+1)\xi P_l - l P_{l-1}}{l+1} \tag{2.52}$$

This set of functions has one peculiarity which makes it notably adapted for being used in this context: at $\xi = 1$, all the thickness functions F_α are equal to zero except for F_0:

$$\begin{cases} F_0(1) &= 1 \\ F_\alpha(1) &= 0 \qquad \alpha = 1, ..., N \end{cases} \tag{2.53}$$

at $\xi = -1$, all the thickness functions F_α are equal to zero except for F_1:

$$\begin{cases} F_1(-1) &= 1 \\ F_\alpha(-1) &= 0 \qquad \alpha = 0, 2, ..., N \end{cases} \tag{2.54}$$

A representation of the first five thickness functions is reported in Figure 2.6.

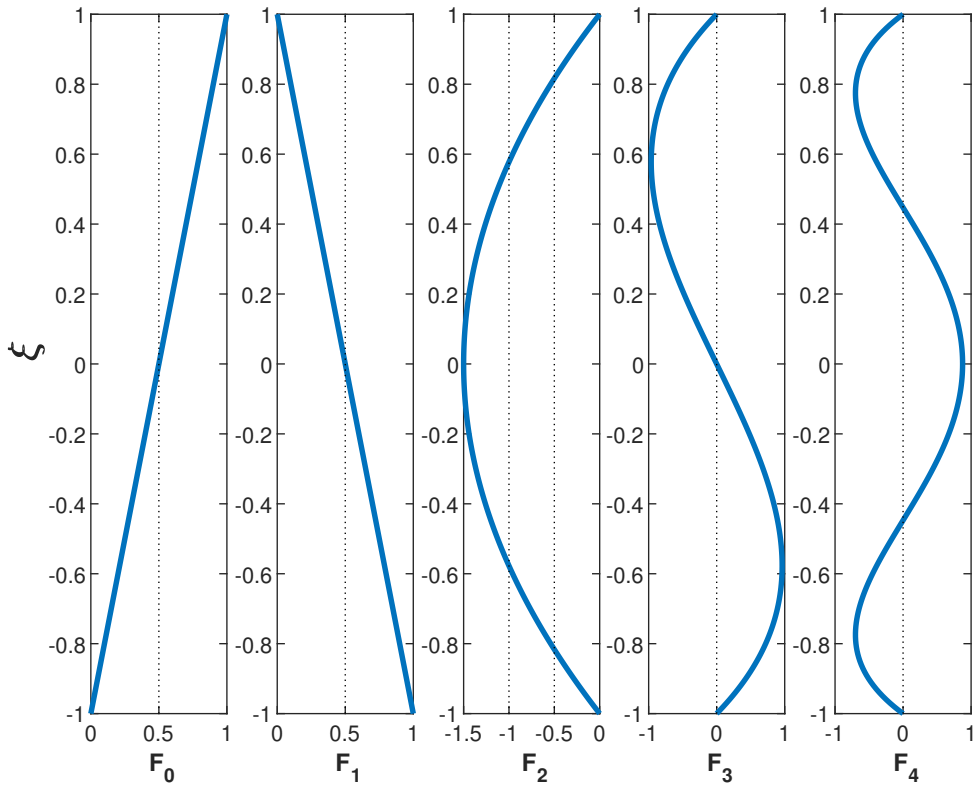

Figure 2.6: Representation of the first 5 thickness functions in a non-dimensional coordinate ξ.

The above features imply that the values of the variables at the top of the layer (either ply or sublaminate) are determined only by the value of F_0, corresponding to the DOF v_{r_0} ($v = u, \sigma$ and $r = x, y, z$), while the values at the bottom of the layer are determined by the value of F_1, corresponding to the DOF v_{r_1}.

This property is a great advantage when assembling the various ply and sublaminate contributions. For this reason, the DOF of the model are organized in a vector in the the following manner:

$$v_r^{p,k} = \left\{ \begin{array}{c} v_{r_0}^{p,k} \\ v_{r_2}^{p,k} \\ v_{r_3}^{p,k} \\ \vdots \\ v_{r_{N_{v_r}^k}}^{p,k} \\ v_{r_1}^{p,k} \end{array} \right\} \tag{2.55}$$

Collecting the terms in this way, the value at the top of the ply/sublaminate is determined by the variable occupying the first position in the vector, while the value at the bottom is determined by the variable in the last position. In Subsection 3.4.2 and Subsection 3.4.3,

the advantage of this choice is clearly shown in the assembly phase, since to complete this process a simple "superposition" of matrices is required.

2.3.5 Models nomenclature

As shown in the previous section, a vast number of models can be generated due to the S-GUF approach. It is necessary, therefore, for clarity purposes, to introduce a well-defined nomenclature for the models adopted.

A generic nomenclature for the models here adopted is:

$$XY^{(N^k_{\sigma_{xz}}(C4),N^k_{\sigma_{yz}}(C5),N^k_{\sigma_{zz}}(C6))}_{N^k_{u_x}(C1),N^k_{u_y}(C2),N^k_{u_z}(C3)}$$

where:

$$\begin{aligned} X &= \{E, L\} \\ Y &= \{D, M\} \\ C1, C2, C3 &= \{-, E, Z, EZ\} \\ C4, C5, C6 &= \{-, E\} \end{aligned}$$

- X: it denotes the model adopted. If $X = E$ an ESL model is adopted, if $X = L$ a LW model is adopted.
- Y: it denotes the theory upon which the model is built.
  If $Y = D$ the PVD is adopted, and therefore the variables $\sigma_{xz}, \sigma_{yz}, \sigma_{zz}$ are discarded and not reported in the model acronym.
  If $Y = M$ RMVT is adopted, and therefore all six variables are retained.
- $C1, C2, C3$: specify additional characteristics of the model for the displacement variables. $C1, C2, C3 = E$ denotes that an ESL description is adopted for that specific variable (such specification of course makes sense only if $X = L$). $C1, C2, C3 = Z$ denotes that this specific variable has been augmented with the MZZF (this specification makes sense only if $X = E$). If $C1, C2, C3 = EZ$ then that specific variable is described by an ESL model and employs also the MZZF (this specification makes sense only if $X = L$). $C1, C2, C3$ may also be completely absent ($C1, C2, C3 = -$), and they are all independent from one another.
- $C4, C5, C6$: specify additional characteristics of the model relative to stress variables. $C4, C5, C6 = E$ denotes that an ESL description is adopted for that specific variable (such specification of course makes sense only if $X = L$). It is not possible to add the MZZF to stress variables inasmuch it was not reputed to bring additional value to the model in terms of accuracy. $C4, C5, C6$ may also be completely absent ($C4, C5, C6 = -$), and they are all independent from one another.
- $N_{u_x}, N_{u_y}, N_{u_z}, N_{\sigma_{xz}}, N_{\sigma_{yz}}, N_{\sigma_{zz}}$: are the orders of expansion of each variable. When $Y = D$, it follows that $N_{\sigma_{xz}}, N_{\sigma_{yz}}, N_{\sigma_{zz}}$ do not appear.

Any of the above models can be used in each sublaminate. The only constraint is that they all have to be based upon the same variational principle, i.e., they all need to have either $Y = D$ or $Y = M$.

For clarity, three examples are reported below (they are not meant to have any practical purpose):

- $ED_{3Z,4,3Z}$: the PVD is used. An ESL theory is applied to all variables. The orders of expansion are: $N_{u_x} = 3$, $N_{u_y} = 4$ and $N_{u_z} = 3$. Both u_x and u_z are augmented with the MZZF.
- $LD_{3E,5,2}$: the PVD is used. A LW theory is applied. The orders of expansion are: $N_{u_x} = 3$, $N_{u_y} = 5$ and $N_{u_z} = 2$. The variable u_x is the only one described through an ESL theory.
- $LM^{3,4E,4}_{3,4EZ,3}$: RMVT is used. A LW theory is applied. The orders of expansion for the displacement variables are: $N_{u_x} = 3$, $N_{u_y} = 4$ and $N_{u_z} = 3$. The orders of expansion for the stress variables are: $N_{\sigma_{xz}} = 3$, $N_{\sigma_{yz}} = 4$ and $N_{\sigma_{zz}} = 4$. Both u_y and σ_{yz} are described through an ESL theory. The variable u_y is augmented with the MZZF.

Chapter 3

Ritz S-GUF RMVT governing equations

In the present chapter the governing equations for a doubly-curved shell are derived by applying the S-GUF formalism and the Ritz approximation to RMVT.

The main steps in the derivation of the Ritz S-GUF RMVT governing equations are:

- Expansion of stress and strain matrices through the geometric relations and the MFHL.
- Application of the S-GUF: the displacements and transverse stresses are written according to the S-GUF formalism.
- Introduction of the Ritz approximation: the in-plane approximation is applied to all the independent variables.
- Theory expansion: all independent variables are expanded according to the selected model.
- Assembly procedure of plies contributions: matrices relative to single plies are assembled at sublaminate level.
- Assembly procedure of sublaminates contributions: matrices relative to single sublaminates are assembled to obtain the mass and stiffness matrices relative to the whole structure.

3.1 RMVT according to S-GUF formalism

The derivation of the governing equations begins from RMVT. Recalling Eq.(2.24):

$$\int_\Omega \int_{-\frac{h}{2}}^{\frac{h}{2}} \delta\boldsymbol{\varepsilon}_{\Omega G}^T \boldsymbol{\sigma}_{\Omega H} + \delta\boldsymbol{\varepsilon}_{nG}^T \boldsymbol{\sigma}_{nM} + \delta\boldsymbol{\sigma}_{nM}^T (\boldsymbol{\varepsilon}_{nG} - \boldsymbol{\varepsilon}_{nH}) \, \mathrm{d}z\mathrm{d}\Omega = - \int_\Omega \int_{-\frac{h}{2}}^{\frac{h}{2}} \delta\mathbf{u}^T \rho \ddot{\mathbf{u}} \, \mathrm{d}z\mathrm{d}\Omega + \int_\Omega \int_{-\frac{h}{2}}^{\frac{h}{2}} \delta\mathbf{u}^T \mathbf{f} \, \mathrm{d}z\mathrm{d}\Omega \quad (3.1)$$

Dividing the shell thickness in k sublaminates and p plies, and considering only the case of normal forces applied on top and bottom surfaces, it is possible to express the functional of Eq.(3.1) as:

$$\sum_{k=1}^{N_k}\sum_{p=1}^{N_p^k}\int_\Omega\int_{z_p^{bot}}^{z_p^{top}} \delta\boldsymbol{\varepsilon}_{\Omega G}^{p,k^T}\boldsymbol{\sigma}_{\Omega H}^{p,k}+\delta\boldsymbol{\varepsilon}_{nG}^{p,k^T}\boldsymbol{\sigma}_{nM}^{p,k}+\delta\boldsymbol{\sigma}_{nM}^{p,k^T}(\boldsymbol{\varepsilon}_{nG}^{p,k}-\boldsymbol{\varepsilon}_{nH}^{p,k})\,\mathrm{d}z\mathrm{d}\Omega =$$
$$\sum_{k=1}^{N_k}\sum_{p=1}^{N_p^k}\left[-\int_\Omega\int_{z_p^{bot}}^{z_p^{top}}\delta\mathbf{u}^{p,k^T}\rho^{p,k}\ddot{\mathbf{u}}^{p,k}\,\mathrm{d}z\mathrm{d}\Omega\right]+\int_{\Omega_{top}}\delta u_z^{top}f_z^{top}\,\mathrm{d}\Omega_{top}+\int_{\Omega_{bot}}\delta u_z^{bot}f_z^{bot}\,\mathrm{d}\Omega_{bot} \tag{3.2}$$

where N_k is the number of sublaminates, N_k^p the number of plies into sublaminate k, and:

$$\mathrm{d}\Omega_{top}=\left(1+\frac{h}{2R_x}\right)\left(1+\frac{h}{2R_y}\right)\mathrm{d}x\mathrm{d}y\quad \mathrm{d}\Omega_{bot}=\left(1-\frac{h}{2R_x}\right)\left(1-\frac{h}{2R_y}\right)\mathrm{d}x\mathrm{d}y \tag{3.3}$$

The four terms on the left-hand side of Eq.(3.2) can be elaborated by using the geometric relationships given by Eqs.(2.2), (2.3) and the MFHL of Eq.(2.32):

$$\begin{aligned}\delta\boldsymbol{\varepsilon}_{\Omega G}^{p,k^T}\boldsymbol{\sigma}_{\Omega H}^{p,k} &= \delta(\mathbf{D}_\Omega\mathbf{u}^{p,k}+\mathbf{A}_\Omega\mathbf{u}^{p,k})^T(\mathbf{C}_{\Omega\Omega}^{p,k}\boldsymbol{\varepsilon}_{\Omega G}^{p,k}+\mathbf{C}_{\Omega n}^{p,k}\boldsymbol{\sigma}_{nM}^{p,k})\\ &= \delta(\mathbf{D}_\Omega\mathbf{u}^{p,k})^T\mathbf{C}_{\Omega\Omega}^{p,k}\mathbf{D}_\Omega\mathbf{u}^{p,k}+\delta(\mathbf{D}_\Omega\mathbf{u}^{p,k})^T\mathbf{C}_{\Omega n}^{p,k}\boldsymbol{\sigma}_{nM}^{p,k}\\ &\quad+\delta(\mathbf{D}_\Omega\mathbf{u}^{p,k})^T\mathbf{C}_{\Omega\Omega}^{p,k}\mathbf{A}_\Omega\mathbf{u}^{p,k}+\delta(\mathbf{A}_\Omega\mathbf{u}^{p,k})^T\mathbf{C}_{\Omega\Omega}^{p,k}\mathbf{D}_\Omega\mathbf{u}^{p,k}\\ &\quad+\delta(\mathbf{A}_\Omega\mathbf{u}^{p,k})^T\mathbf{C}_{\Omega n}^{p,k}\boldsymbol{\sigma}_{nM}^{p,k}+\delta(\mathbf{A}_\Omega\mathbf{u}^{p,k})^T\mathbf{C}_{\Omega\Omega}^{p,k}\mathbf{A}_\Omega\mathbf{u}^{p,k}\end{aligned} \tag{3.4}$$

$$\begin{aligned}\delta\boldsymbol{\varepsilon}_{nG}^{p,k^T}\boldsymbol{\sigma}_{nM}^{p,k} &= \delta(\mathbf{D}_n\mathbf{u}^{p,k}+\lambda_D\mathbf{A}_n\mathbf{u}^{p,k}+\mathbf{D}_z\mathbf{u}^{p,k})^T\boldsymbol{\sigma}_{nM}^{p,k}\\ &= \delta(\mathbf{D}_n\mathbf{u}^{p,k})^T\boldsymbol{\sigma}_{nM}^{p,k}+\delta(\lambda_D\mathbf{A}_n\mathbf{u}^{p,k})^T\boldsymbol{\sigma}_{nM}^{p,k}+\delta(\mathbf{D}_z\mathbf{u}^{p,k})^T\boldsymbol{\sigma}_{nM}^{p,k}\end{aligned} \tag{3.5}$$

$$\begin{aligned}\delta\boldsymbol{\sigma}_{nM}^{p,k^T}\boldsymbol{\varepsilon}_{nG}^{p,k} &= \delta\boldsymbol{\sigma}_{nM}^{p,k^T}(\mathbf{D}_n\mathbf{u}^{p,k}+\lambda_D\mathbf{A}_n\mathbf{u}^{p,k}+\mathbf{D}_z\mathbf{u}^{p,k})\\ &= \delta\boldsymbol{\sigma}_{nM}^{p,k^T}\mathbf{D}_n\mathbf{u}^{p,k}+\delta\boldsymbol{\sigma}_{nM}^{p,k^T}\lambda_D\mathbf{A}_n\mathbf{u}^{p,k}+\delta\boldsymbol{\sigma}_{nM}^{p,k^T}\mathbf{D}_z\mathbf{u}^{p,k}\end{aligned} \tag{3.6}$$

$$\begin{aligned}\delta\boldsymbol{\sigma}_{nM}^{p,k^T}\boldsymbol{\varepsilon}_{nH}^{p,k} &= \delta\boldsymbol{\sigma}_{nM}^{p,k^T}(\mathbf{C}_{n\Omega}^{p,k}\boldsymbol{\varepsilon}_{\Omega G}^{p,k}+\mathbf{C}_{nn}^{p,k}\boldsymbol{\sigma}_{nM}^{p,k})\\ &= \delta\boldsymbol{\sigma}_{nM}^{p,k^T}\mathbf{C}_{n\Omega}^{p,k}\mathbf{D}_\Omega\mathbf{u}^{p,k}+\delta\boldsymbol{\sigma}_{nM}^{p,k^T}\mathbf{C}_{n\Omega}^{p,k}\mathbf{A}_\Omega\mathbf{u}^{p,k}+\delta\boldsymbol{\sigma}_{nM}^{p,k^T}\mathbf{C}_{nn}^{p,k}\boldsymbol{\sigma}_{nM}^{p,k}\end{aligned} \tag{3.7}$$

In order to simplify the notation from here on, transverse stresses will be represented by the following notation:

$$\begin{aligned}\sigma_{xz} &\rightarrow s_x\\ \sigma_{yz} &\rightarrow s_y\\ \sigma_{zz} &\rightarrow s_z\end{aligned} \tag{3.8}$$

Expanding vectors and matrices according to their definitions at (2.25), (2.4), (2.5), (2.38), and using the S-GUF 2-D approximation as expressed in Eq.(2.47), component-wise expressions of the four terms on the left-hand side of Eq.(3.2) are obtained. These equations are not reported here for brevity but their full expressions can be found in Appendix B (Eqs. (B.1), (B.2), (B.3), (B.4)).

3.2 Thickness integrals

Thickness integrals can be introduced to have a more compact writing of the equations according to the following notation:

$$ {}^{(R_xR_yH_xH_y)}_{(R_xR_yH_xH_y)}Z^{p,k\alpha_{v_r}\beta_{v_s}}_{RS(\partial)v_r(\partial)v_s} = \int_{z_p^{bot}}^{z_p^{top}} \frac{(R_xR_yH_xH_y)}{(R_xR_yH_xH_y)} C^{p,k}_{ij} F_{\alpha_{v_r}(,z)} F_{\beta_{v_s}(,z)} \, \mathrm{d}z \quad R,S = -,1,...,6 \tag{3.9} $$

$$ {}^{H_xH_y}Z^{p,k\alpha_{u_r}\beta_{u_s}}_{\rho u_r u_s} = \int_{z_p^{bot}}^{z_p^{top}} \rho^{p,k} F_{\alpha_{u_r}} F_{\beta_{u_s}} H_xH_y \, \mathrm{d}z \tag{3.10} $$

where top and bottom prescripts indicate the presence of R_x, R_y, H_x, H_y in the integral, at the numerator and denominator, respectively.

Therefore, after substituting Eqs.(B.1), (B.2), (B.3), (B.4) into Eq.(3.1), it is possible to introduce the definitions of the *thickness integrals* (Eq.(3.9), Eq.(3.10)). The equation obtained as a result of these steps is not reported here for brevity but its full expression can be found in Appendix B (Eq.(B.5)).

3.3 Ritz method

Due to the expansions operated in Section 3.1, the volume integrals of the variational statement can be transformed into surface integrals. It is now possible to proceed to solve it through an exact solution like the *Navier* or *Levy-type* kind or through a numerical method.

Exact solutions offer in terms of accuracy the best results possible, however they are obtainable only in few cases: for proper boundary conditions, certain stacking sequences, and simple geometries. On the other hand, fully numerical methods such as the *Finite Element Method* (FEM) can be applied to a wide variety of problems and can be used to obtain solutions as accurate as required, but, in general, at a high computational cost.

In the present work, a trade-off between a fully analytical method and a fully numerical one (e.g. FEM) is achieved by referring to the Ritz method. The unknowns are expanded with polynomial expansions whose orders are generally higher than the orders adopted in a FEM framework. The method converges quickly to the correct solution for smooth problems and can be adopted even if discontinuities in the material properties are present. Worth of mentioning is the possibility - not exploited in the context of this work - of accounting for planar shapes other than square or rectangular by introducing mapping functions. The Ritz approximation is therefore expressed as:

$$ \begin{cases} u_x(x,y,t) &= N_{u_xj}(x,y)u_{xj}(t) \\ u_y(x,y,t) &= N_{u_yj}(x,y)u_{yj}(t) \\ u_z(x,y,t) &= N_{u_zj}(x,y)u_{zj}(t) \\ \sigma_{xz}(x,y,t) &= N_{\sigma_{xzj}}(x,y)\sigma_{xzj}(t) \\ \sigma_{yz}(x,y,t) &= N_{\sigma_{yzj}}(x,y)\sigma_{yzj}(t) \\ \sigma_{zz}(x,y,t) &= N_{\sigma_{zzj}}(x,y)\sigma_{zzj}(t) \end{cases} \qquad j = 1,2,...,M \tag{3.11} $$

The Ritz functions N_j are subjected to the following requirements:

- N_j must satisfy the essential conditions.
- N_j have to be at least C^{n-1}-continuous where n is the higher order of derivation in the variational principle with respect to the variables x or y.
- N_j have to form a complete and linearly independent set of functions.
- N_j have to satisfy complementary conditions: the approximation of the general stresses should be different than zero when general displacements are prescribed and vice-versa.

In addition to the above-listed mathematical requirements of the Ritz functions, also some numerical aspects need to be taken into account. In particular, in order to have a numerically stable method it is important to use an orthogonal basis of functions so not to have ill-conditioned matrices [3]. Examples of bases that are commonly used are: Legendre polynomials, Chebyshev polynomials, and trigonometric functions. Furthermore, these kinds of bases generate matrices with a high degree of sparsity, a highly beneficial feature from a numerical standpoint.

Finally, a powerful way of building complete and compliant sets of Ritz functions is to compose them as the product of two functions: one being part of a mathematically complete base and the other one assuring that essential boundary conditions are satisfied.

A nondimensional domain ξ, η is defined as:

$$\xi = \frac{x}{a/2} \qquad \eta = \frac{y}{b/2} \tag{3.12}$$

where a and b are the sizes of the structure along the physical coordinates of the reference surface (x, y) respectively. The Ritz functions $N_{v_r i}$ $(v_r = u_x, u_y, u_z, \sigma_{xz}, \sigma_{yz}, \sigma_{zz})$ can be expressed by assuming separation of variables as:

$$N_{v_r i}(\xi, \eta) = \Phi_{v_r,m}(\xi)\Psi_{v_r,n}(\eta) \qquad \begin{matrix} m = 1, 2, ..., R \\ n = 1, 2, ..., S \end{matrix} \tag{3.13}$$

where the Ritz order of approximation M is:

$$M = R \times S \tag{3.14}$$

and the index i can be expressed as:

$$i = S(m-1) + n \tag{3.15}$$

The two components of the Ritz function, along ξ and η respectively, can be written as:

$$\Phi_{v_r,m}(\xi) = f_{v_r}(\xi)\phi_{v_r,m}(\xi) \tag{3.16}$$

$$\Psi_{v_r,n}(\eta) = g_{v_r}(\eta)\psi_{v_r,n}(\eta) \tag{3.17}$$

and the boundary functions f_{v_r} and g_{v_r} are defined as:

$$\begin{aligned} f_{v_r}(\xi) &= (1+\xi)^{e_{1r}}(1-\xi)^{e_{3r}} \\ g_{v_r}(\eta) &= (1+\eta)^{e_{2r}}(1-\eta)^{e_{4r}} \end{aligned} \tag{3.18}$$

In the above, the functions $\phi_{v,m}(\xi)$ and $\psi_{v,n}(\eta)$ provide the completeness to the set, while $f_v(\xi)$ and $g_v(\eta)$ ensure that boundary conditions are respected. Depending on the type of boundary condition along the edge (*free* (F), *simply-supported* (S), *clamped* (C)) each exponent $e_{\gamma r}$ ($\gamma = 1, ..., 4$) can be either 0 or 1.

Referring to the Ritz functions used for the displacement variables:

- Free edge (F): there are no particular restrictions to be imposed, therefore $e_{\gamma r} = 0$ ($r = x, y, z$).
- Simply-supported (S): if the edge is simply-supported and parallel to the Cartesian axis, transverse and tangential displacements are locked, considering the function f_{u_r} it follows that $e_{\gamma x} = 0$, $e_{\gamma y} = 1$ and $e_{\gamma z} = 1$, while for g_{u_r} accordingly, $e_{\gamma x} = 1$, $e_{\gamma y} = 0$ and $e_{\gamma z} = 1$. In case the simply-supported edge is inclined with respect to the Cartesian axis only the transverse displacement vanishes: $e_{\gamma z} = 1$.
- Clamped (C): if the edge is clamped, no displacement is possible on the edge, therefore, $e_{\gamma r} = 1$ ($r = x, y, z$).

While each variable, in principle, can be expanded with a different order, it is of practical interest to distinguish between displacements and stresses. This choice - as shown in Chapter 5 - enabled to draw considerations about the correct tuning of these parameters. In particular:

$$\begin{cases} u_x(x,y,t) &= N_{u_x j_1}(x,y) u_{x j_1}(t) \\ u_y(x,y,t) &= N_{u_y j_1}(x,y) u_{y j_1}(t) \\ u_z(x,y,t) &= N_{u_z j_1}(x,y) u_{z j_1}(t) \\ \sigma_{xz}(x,y,t) &= N_{\sigma_{xz} j_2}(x,y) \sigma_{xz j_2}(t) \\ \sigma_{yz}(x,y,t) &= N_{\sigma_{yz} j_2}(x,y) \sigma_{yz j_2}(t) \\ \sigma_{zz}(x,y,t) &= N_{\sigma_{zz} j_2}(x,y) \sigma_{zz j_2}(t) \end{cases} \qquad \begin{aligned} j_1 &= 1, 2, ..., M_u \\ j_2 &= 1, 2, ..., M_s \end{aligned} \tag{3.19}$$

where M_u is the Ritz order of approximation adopted for displacement variables and M_s is the Ritz order of approximation adopted for transverse stress variables.

Considering the current S-GUF framework the Ritz approximation is expressed as:

$$\begin{cases} u^{p,k}_{x\beta_{u_x}}(x,y,t) &= N_{u_x j_1}(x,y) u^{p,k}_{x\beta_{u_x} j_1}(t) \\ u^{p,k}_{y\beta_{u_y}}(x,y,t) &= N_{u_y j_1}(x,y) u^{p,k}_{y\beta_{u_y} j_1}(t) \\ u^{p,k}_{z\beta_{u_z}}(x,y,t) &= N_{u_z j_1}(x,y) u^{p,k}_{z\beta_{u_z} j_1}(t) \\ s^{p,k}_{x\beta_{s_x}}(x,y,t) &= N_{s_x j_2}(x,y) s^{p,k}_{x\beta_{s_x} j_2}(t) \\ s^{p,k}_{y\beta_{s_y}}(x,y,t) &= N_{s_y j_2}(x,y) s^{p,k}_{y\beta_{s_y} j_2}(t) \\ s^{p,k}_{z\beta_{s_z}}(x,y,t) &= N_{s_z j_2}(x,y) s^{p,k}_{z\beta_{s_z} j_2}(t) \end{cases} \qquad \begin{aligned} j_1 &= 1, 2, ..., M_u \\ j_2 &= 1, 2, ..., M_s \end{aligned} \tag{3.20}$$

The same approximation is carried out for virtual quantities.

It is important to observe that the Ritz functions have no dependency on the ply nor on the sublaminate under the assumptions that the boundary conditions are homogeneous throughout the thickness on each side.

The following compact notation is introduced for the integrals of the Ritz functions (*Ritz integrals*) (when referring to general Ritz approximations the subscripts 1 and 2 are omitted):

$$I^{defg}_{v_r v_s ij} = \int_x \int_y \frac{\partial^{d+e} N_{v_r i}}{\partial x^d \partial y^e} \frac{\partial^{f+g} N_{v_s j}}{\partial x^f \partial y^g} \mathrm{d}x\mathrm{d}y \qquad (d,e,f,g = 0,1) \tag{3.21}$$

Hence, using the approximations at (3.20), and notation (3.21), Eq.(B.5) is re-written as:

$$\begin{aligned}
&\sum_{k=1}^{N_k}\sum_{p=1}^{N_p^k}\Big[\delta u^{p,k^T}_{x\alpha_{u_x}i_1} Z^{p,k\alpha_{u_x}\beta_{u_x}}_{\rho u_x u_x} I^{0000}_{u_x u_x i_1 j_1} \ddot{u}^{p,k}_{x\beta_{u_x}j_1} + \delta u^{p,k^T}_{y\alpha_{u_y}i_1} Z^{p,k\alpha_{u_y}\beta_{u_y}}_{\rho u_y u_y} I^{0000}_{u_y u_y i_1 j_1} \ddot{u}^{p,k}_{y\beta_{u_y}j_1} \\
&\quad + \delta u^{p,k^T}_{z\alpha_{u_z}i_1} Z^{p,k\alpha_{u_z}\beta_{u_z}}_{\rho u_z u_z} I^{0000}_{u_z u_z i_1 j_1} \ddot{u}^{p,k}_{z\beta_{u_z}j_1}\Big] + \\
&\sum_{k=1}^{N_k}\sum_{p=1}^{N_p^k}\Big[\delta u^{p,k}_{x\alpha_{u_x}i_1} {}^{H_y}_{H_x}Z^{p,k\alpha_{u_x}\beta_{u_x}}_{11u_x u_x} I^{1010}_{u_x u_x i_1 j_1} u^{p,k}_{x\beta_{u_x}j_1} + \delta u^{p,k}_{x\alpha_{u_x}i_1} Z^{p,k\alpha_{u_x}\beta_{u_y}}_{12u_x u_y} I^{1001}_{u_x u_y i_1 j_1} u^{p,k}_{y\beta_{u_y}j_1} \\
&\quad + \delta u^{p,k}_{x\alpha_{u_x}i_1} Z^{p,k\alpha_{u_x}\beta_{u_x}}_{16u_x u_x} I^{1001}_{u_x u_x i_1 j_1} u^{p,k}_{x\beta_{u_x}j_1} + \delta u^{p,k}_{x\alpha_{u_x}i_1} {}^{H_y}_{H_x}Z^{p,k\alpha_{u_x}\beta_{u_y}}_{16u_x u_y} I^{1010}_{u_x u_y i_1 j_1} u^{p,k}_{y\beta_{u_y}j_1} \\
&\quad + \delta u^{p,k}_{y\alpha_{u_y}i_1} Z^{p,k\alpha_{u_y}\beta_{u_x}}_{12u_y u_x} I^{0110}_{u_y u_x i_1 j_1} u^{p,k}_{x\beta_{u_x}j_1} + \delta u^{p,k}_{y\alpha_{u_y}i_1} {}^{H_x}_{H_y}Z^{p,k\alpha_{u_y}\beta_{u_y}}_{22u_y u_y} I^{0101}_{u_y u_y i_1 j_1} u^{p,k}_{y\beta_{u_y}j_1} \\
&\quad + \delta u^{p,k}_{y\alpha_{u_y}i_1} {}^{H_x}_{H_y}Z^{p,k\alpha_{u_y}\beta_{u_x}}_{26u_y u_x} I^{0101}_{u_y u_x i_1 j_1} u^{p,k}_{x\beta_{u_x}j_1} + \delta u^{p,k}_{y\alpha_{u_y}i_1} Z^{p,k\alpha_{u_y}\beta_{u_y}}_{26u_y u_y} I^{0110}_{u_y u_y i_1 j_1} u^{p,k}_{y\beta_{u_y}j_1} \\
&\quad + \delta u^{p,k}_{x\alpha_{u_x}i_1} Z^{p,k\alpha_{u_x}\beta_{u_x}}_{16u_x u_x} I^{0110}_{u_x u_x i_1 j_1} u^{p,k}_{x\beta_{u_x}j_1} + \delta u^{p,k}_{x\alpha_{u_x}i_1} {}^{H_x}_{H_y}Z^{p,k\alpha_{u_x}\beta_{u_y}}_{26u_x u_y} I^{0101}_{u_x u_y i_1 j_1} u^{p,k}_{y\beta_{u_y}j_1} \\
&\quad + \delta u^{p,k}_{x\alpha_{u_x}i_1} {}^{H_x}_{H_y}Z^{p,k\alpha_{u_x}\beta_{u_x}}_{66u_x u_x} I^{0101}_{u_x u_x i_1 j_1} u^{p,k}_{x\beta_{u_x}j_1} + \delta u^{p,k}_{x\alpha_{u_x}i_1} Z^{p,k\alpha_{u_x}\beta_{u_y}}_{66u_x u_y} I^{0110}_{u_x u_y i_1 j_1} u^{p,k}_{y\beta_{u_y}j_1} \\
&\quad + \delta u^{p,k}_{y\alpha_{u_y}i_1} {}^{H_y}_{H_x}Z^{p,k\alpha_{u_y}\beta_{u_x}}_{16u_y u_x} I^{1010}_{u_y u_x i_1 j_1} u^{p,k}_{x\beta_{u_x}j_1} + \delta u^{p,k}_{y\alpha_{u_y}i_1} Z^{p,k\alpha_{u_y}\beta_{u_y}}_{26u_y u_y} I^{1001}_{u_y u_y i_1 j_1} u^{p,k}_{y\beta_{u_y}j_1} \\
&\quad + \delta u^{p,k}_{y\alpha_{u_y}i_1} Z^{p,k\alpha_{u_y}\beta_{u_x}}_{66u_y u_x} I^{1001}_{u_y u_x i_1 j_1} u^{p,k}_{x\beta_{u_x}j_1} + \delta u^{p,k}_{y\alpha_{u_y}i_1} {}^{H_y}_{H_x}Z^{p,k\alpha_{u_y}\beta_{u_y}}_{66u_y u_y} I^{1010}_{u_y u_y i_1 j_1} u^{p,k}_{y\beta_{u_y}j_1} \\
&\quad + \delta u^{p,k}_{x\alpha_{u_x}i_1} {}^{H_y}Z^{p,k\alpha_{u_x}\beta_{s_z}}_{13u_x s_z} I^{1000}_{u_x s_z i_1 j_2} s^{p,k}_{z\beta_{s_z}j_2} + \delta u^{p,k}_{y\alpha_{u_y}i_1} {}^{H_x}Z^{p,k\alpha_{u_x}\beta_{s_z}}_{23u_y s_z} I^{0100}_{u_y s_z i_1 j_2} s^{p,k}_{z\beta_{s_z}j_2} \\
&\quad + \delta u^{p,k}_{x\alpha_{u_x}i_1} {}^{H_x}Z^{p,k\alpha_{u_x}\beta_{sz}}_{36u_x s_z} I^{0100}_{u_x s_z i_1 j_2} s^{p,k}_{z\beta_{s_z}j_2} + \delta u^{p,k}_{y\alpha_{u_y}i_1} {}^{H_y}Z^{p,k\alpha_{u_y}\beta_{sz}}_{36u_y s_z} I^{1000}_{u_y s_z i_1 j_2} s^{p,k}_{z\beta_{s_z}j_2} \\
&\quad + \delta u^{p,k}_{x\alpha_{u_x}i_1} {}^{H_y}_{H_x R_x}Z^{p,k\alpha_{u_x}\beta_{u_z}}_{11u_x u_z} I^{1000}_{u_x u_z i_1 j_1} u^{p,k}_{z\beta_{u_z}j_1} + \delta u^{p,k}_{x\alpha_{u_x}i_1} {}_{R_y}Z^{p,k\alpha_{u_x}\beta_{u_z}}_{12u_x u_z} I^{1000}_{u_x u_z i_1 j_1} u^{p,k}_{z\beta_{u_z}j_1} \\
&\quad + \delta u^{p,k}_{y\alpha_{u_y}i_1} {}_{R_x}Z^{p,k\alpha_{u_y}\beta_{u_z}}_{12u_y u_z} I^{0100}_{u_y u_z i_1 j_1} u^{p,k}_{z\beta_{u_z}j_1} + \delta u^{p,k}_{y\alpha_{u_y}i_1} {}^{H_x}_{H_y R_y}Z^{p,k\alpha_{u_y}\beta_{u_z}}_{22u_y u_z} I^{0100}_{u_y u_z i_1 j_1} u^{p,k}_{z\beta_{u_z}j_1} \\
&\quad + \delta u^{p,k}_{x\alpha_{u_x}i_1} {}_{R_x}Z^{p,k\alpha_{u_x}\beta_{u_z}}_{16u_x u_z} I^{0100}_{u_x u_z i_1 j_1} u^{p,k}_{z\beta_{u_z}j_1} + \delta u^{p,k}_{x\alpha_{u_x}i_1} {}^{H_x}_{H_y R_y}Z^{p,k\alpha_{u_x}\beta_{u_z}}_{26u_x u_z} I^{0100}_{u_x u_z i_1 j_1} u^{p,k}_{z\beta_{u_z}j_1} \\
&\quad + \delta u^{p,k}_{y\alpha_{u_y}i_1} {}^{H_y}_{H_x R_x}Z^{p,k\alpha_{u_y}\beta_{u_z}}_{16u_y u_z} I^{1000}_{u_y u_z i_1 j_1} u^{p,k}_{z\beta_{u_z}j_1} + \delta u^{p,k}_{y\alpha_{u_y}i_1} {}_{R_y}Z^{p,k\alpha_{u_y}\beta_{u_z}}_{26u_y u_z} I^{1000}_{u_y u_z i_1 j_1} u^{p,k}_{z\beta_{u_z}j_1} \\
&\quad + \delta u^{p,k}_{z\alpha_{u_z}i_1} {}^{H_y}_{H_x R_x}Z^{p,k\alpha_{u_z}\beta_{ux}}_{11u_z u_x} I^{0010}_{u_z u_x i_1 j_1} u^{p,k}_{x\beta_{u_x}j_1} + \delta u^{p,k}_{z\alpha_{u_z}i_1} {}_{R_x}Z^{p,k\alpha_{u_z}\beta_{uy}}_{12u_z u_y} I^{0001}_{u_z u_y i_1 j_1} u^{p,k}_{y\beta_{u_y}j_1} \\
&\quad + \delta u^{p,k}_{z\alpha_{u_z}i_1} {}_{R_x}Z^{p,k\alpha_{u_z}\beta_{ux}}_{16u_z u_x} I^{0001}_{u_z u_x i_1 j_1} u^{p,k}_{x\beta_{u_x}j_1} + \delta u^{p,k}_{z\alpha_{u_z}i_1} {}^{H_y}_{H_x R_x}Z^{p,k\alpha_{u_z}\beta_{uy}}_{16u_z u_y} I^{0010}_{u_z u_y i_1 j_1} u^{p,k}_{y\beta_{u_y}j_1} \\
&\quad + \delta u^{p,k}_{z\alpha_{u_z}i_1} {}_{R_y}Z^{p,k\alpha_{u_z}\beta_{ux}}_{12u_z u_x} I^{0010}_{u_z u_x i_1 j_1} u^{p,k}_{x\beta_{u_x}j_1} + \delta u^{p,k}_{z\alpha_{u_z}i_1} {}^{H_x}_{H_y R_y}Z^{p,k\alpha_{u_z}\beta_{uy}}_{22u_z u_y} I^{0001}_{u_z u_y i_1 j_1} u^{p,k}_{y\beta_{u_y}j_1} \\
&\quad + \delta u^{p,k}_{z\alpha_{u_z}i_1} {}^{H_x}_{H_y R_y}Z^{p,k\alpha_{u_z}\beta_{ux}}_{26u_z u_x} I^{0001}_{u_z u_x i_1 j_1} u^{p,k}_{x\beta_{u_x}j_1} + \delta u^{p,k}_{z\alpha_{u_z}i_1} {}_{R_y}Z^{p,k\alpha_{u_z}\beta_{uy}}_{26u_z u_y} I^{0010}_{u_z u_y i_1 j_1} u^{p,k}_{y\beta_{u_y}j_1} \\
&\quad + \delta u^{p,k}_{z\alpha_{u_z}i_1} {}^{H_y}_{R_x}Z^{p,k\alpha_{u_z}\beta_{sz}}_{13u_z s_z} I^{0000}_{u_z s_z i_1 j_2} s^{p,k}_{z\beta_{s_z}j_2} + \delta u^{p,k}_{z\alpha_{u_z}i_1} {}^{H_x}_{R_y}Z^{p,k\alpha_{u_z}\beta_{sz}}_{23u_x s_z} I^{0000}_{u_z s_z i_1 j_2} s^{p,k}_{z\beta_{s_z}j_2} \\
&\quad + \delta u^{p,k}_{z\alpha_{u_z}i_1} {}^{H_y}_{H_x R_x^2}Z^{p,k\alpha_{u_z}\beta_{uz}}_{11u_z u_z} I^{0000}_{u_z u_z i_1 j_1} u^{p,k}_{z\beta_{u_z}j_1} + \delta u^{p,k}_{z\alpha_{u_z}i_1} {}_{R_x R_y}Z^{p,k\alpha_{u_z}\beta_{uz}}_{12u_z u_z} I^{0000}_{u_z u_z i_1 j_1} u^{p,k}_{z\beta_{u_z}j_1} \\
&\quad + \delta u^{p,k}_{z\alpha_{u_z}i_1} {}_{R_x R_y}Z^{p,k\alpha_{u_z}\beta_{uz}}_{12u_z u_z} I^{0000}_{u_z u_z i_1 j_1} u^{p,k}_{z\beta_{u_z}j_1} + \delta u^{p,k}_{z\alpha_{u_z}i_1} {}^{H_x}_{H_y R_y^2}Z^{p,k\alpha_{u_z}\beta_{uz}}_{22u_z u_z} I^{0000}_{u_z u_z i_1 j_1} u^{p,k}_{z\beta_{u_z}j_1} \\
&\quad + \delta u^{p,k}_{z\alpha_{u_z}i_1} {}^{H_x}Z^{p,k\alpha_{u_z}\beta_{sy}}_{u_z s_y} I^{0100}_{u_z s_z i_1 j_2} s^{p,k}_{y\beta_{s_y}j_2} + \delta u^{p,k}_{z\alpha_{u_z}i_1} {}^{H_y}Z^{p,k\alpha_{u_z}\beta_{sx}}_{u_z s_x} I^{1000}_{u_z s_x i_1 j_2} s^{p,k}_{x\beta_{s_x}j_2} \\
&\quad - \delta u^{p,k}_{y\alpha_{u_y}i_1} \lambda_D {}^{H_x}_{R_y}Z^{p,k\alpha_{uy}\beta_{sy}}_{u_y s_y} I^{0000}_{u_y s_y i_1 j_2} s^{p,k}_{y\beta_{s_y}j_2} - \delta u^{p,k}_{x\alpha_{ux}i_1} \lambda_D {}^{H_y}_{R_x}Z^{p,k\alpha_{ux}\beta_{sx}}_{u_x s_x} I^{0000}_{u_x s_x i_1 j_2} s^{p,k}_{x\beta_{s_x}j_2}
\end{aligned}$$

$$
\begin{aligned}
&+\delta u^{p,k}_{y\alpha_{u_y}i_1}\,{}^{H_xH_y}Z^{p,k\alpha_{u_y}\beta_{s_y}}_{\partial u_y s_y}I^{0000}_{u_y s_y i_1 j_2}s^{p,k}_{y\beta_{s_y}j_2}+\delta u^{p,k}_{x\alpha_{u_x}i_1}\,{}^{H_xH_y}Z^{p,k\alpha_{u_x}\beta_{s_x}}_{\partial u_x s_x}I^{0000}_{u_x s_x i_1 j_2}s^{p,k}_{x\beta_{s_x}j_2}\\
&+\delta u^{p,k}_{z\alpha_{u_z}i_1}\,{}^{H_xH_y}Z^{p,k\alpha_{u_z}\beta_{s_z}}_{\partial u_z s_z}I^{0000}_{u_z s_z i_1 j_2}s^{p,k}_{z\beta_{s_z}j_2}+\delta s^{p,k}_{y\alpha_{s_y}i_2}\,{}^{H_x}Z^{p,k\alpha_{s_y}\beta_{u_z}}_{s_y u_z}I^{0001}_{s_y u_z i_2 j_1}u^{p,k}_{z\beta_{u_z}j_1}\\
&+\delta s^{p,k}_{x\alpha_{s_x}i_2}\,{}^{H_y}Z^{p,k\alpha_{s_x}\beta_{u_z}}_{s_x u_z}I^{0010}_{s_x u_z i_2 j_1}u^{p,k}_{z\beta_{u_z}j_1}-\delta s^{p,k}_{y\alpha_{s_y}i_2}\lambda_D\,{}^{H_x}_{R_y}Z^{p,k\alpha_{s_y}\beta_{u_y}}_{s_y u_y}I^{0000}_{s_y u_y i_2 j_1}u^{p,k}_{y\beta_{u_y}j_1}\\
&-\delta s^{p,k}_{x\alpha_{s_x}i_2}\lambda_D\,{}^{H_y}_{R_x}Z^{p,k\alpha_{s_x}\beta_{u_x}}_{s_x u_x}I^{0000}_{s_x u_x i_2 j_1}u^{p,k}_{x\beta_{u_x}j_1}+\delta s^{p,k}_{y\alpha_{s_y}i_2}\,{}^{H_xH_y}Z^{p,k\alpha_{s_y}\beta_{u_y}}_{s_y\partial u_y}I^{0000}_{s_y u_y i_2 j_1}u^{p,k}_{y\beta_{u_y}j_1}\\
&+\delta s^{p,k}_{x\alpha_{s_x}i_2}\,{}^{H_xH_y}Z^{p,k\alpha_{s_x}\beta_{u_x}}_{s_x\partial u_x}I^{0000}_{s_x u_x i_2 j_1}u^{p,k}_{x\beta_{u_x}j_1}+\delta s^{p,k}_{z\alpha_{s_z}i_2}\,{}^{H_xH_y}Z^{p,k\alpha_{s_z}\beta_{u_z}}_{s_z\partial u_z}I^{0000}_{s_z u_z i_2 j_1}u^{p,k}_{z\beta_{u_z}j_1}\\
&+\delta s^{p,k}_{z\alpha_{s_z}i_2}\,{}^{H_y}Z^{p,k\alpha_{s_z}\beta_{u_x}}_{13 s_z u_x}I^{0010}_{s_z u_x i_2 j_1}u^{p,k}_{x\beta_{u_x}j_1}+\delta s^{p,k}_{z\alpha_{s_z}i_2}\,{}^{H_x}Z^{p,k\alpha_{s_z}\beta_{u_y}}_{23 s_z u_y}I^{0001}_{s_z u_y i_2 j_1}u^{p,k}_{y\beta_{u_y}j_1}\\
&+\delta s^{p,k}_{z\alpha_{s_z}i_2}\,{}^{H_x}Z^{p,k\alpha_{s_z}\beta_{u_x}}_{36 s_z u_x}I^{0001}_{s_z u_x i_2 j_1}u^{p,k}_{x\beta_{u_x}j_1}+\delta s^{p,k}_{z\alpha_{s_z}i_2}\,{}^{H_y}Z^{p,k\alpha_{s_z}\beta_{u_y}}_{36 s_z u_y}I^{0010}_{s_z u_y i_2 j_1}u^{p,k}_{y\beta_{u_y}j_1}\\
&+\delta s^{p,k}_{z\alpha_{s_z}i_2}\,{}^{H_y}_{R_x}Z^{p,k\alpha_{s_z}\beta_{u_z}}_{13 s_z u_z}I^{0000}_{s_z u_z i_2 j_1}u^{p,k}_{z\beta_{u_z}j_1}+\delta s^{p,k}_{z\alpha_{s_z}i_2}\,{}^{H_x}_{R_y}Z^{p,k\alpha_{s_z}\beta_{u_z}}_{23 s_z u_z}I^{0000}_{s_z u_z i_2 j_1}u^{p,k}_{z\beta_{u_z}j_1}\\
&-\delta s^{p,k}_{y\alpha_{s_y}i_2}\,{}^{H_xH_y}Z^{p,k\alpha_{s_y}\beta_{s_y}}_{44 s_y s_y}I^{0000}_{s_y s_y i_2 j_2}s^{p,k}_{y\beta_{s_y}j_2}-\delta s^{p,k}_{y\alpha_{s_y}i_2}\,{}^{H_xH_y}Z^{p,k\alpha_{s_y}\beta_{s_x}}_{45 s_y s_x}I^{0000}_{s_y s_x i_2 j_2}s^{p,k}_{x\beta_{s_x}j_2}\\
&-\delta s^{p,k}_{x\alpha_{s_x}i_2}\,{}^{H_xH_y}Z^{p,k\alpha_{s_x}\beta_{s_y}}_{45 s_x s_y}I^{0000}_{s_x s_y i_2 j_2}s^{p,k}_{y\beta_{s_y}j_2}-\delta s^{p,k}_{x\alpha_{s_x}i_2}\,{}^{H_xH_y}Z^{p,k\alpha_{s_x}\beta_{s_x}}_{55 s_x s_x}I^{0000}_{s_x s_x i_2 j_2}s^{p,k}_{x\beta_{s_x}j_2}\\
&-\delta s^{p,k}_{z\alpha_{s_z}i_2}\,{}^{H_xH_y}Z^{p,k\alpha_{s_z}\beta_{s_z}}_{33 s_z s_z}I^{0000}_{s_z s_z i_2 j_2}s^{p,k}_{z\beta_{s_z}j_2}\Bigg]\\
&=\delta u^{N^k_p,N_k}_{z0i}\int_x\int_y f^{top}_z N_{uzi_1}\left(1+\frac{h}{2R_x}\right)\left(1+\frac{h}{2R_y}\right)\mathrm{d}x\mathrm{d}y\\
&\quad+\delta u^{1,1}_{z1i}\int_x\int_y f^{bot}_z N_{uzi_1}\left(1-\frac{h}{2R_x}\right)\left(1-\frac{h}{2R_y}\right)\mathrm{d}x\mathrm{d}y
\end{aligned}
\tag{3.22}
$$

The mathematical description represented by Eq.(3.22) is independent of the model adopted and of the Ritz approximation orders, therefore it is completely general, regardless of the number of sublaminates.

It is here highlighted that the present formulation is based upon fundamental blocks called *kernels*. The fundamental blocks constituting the S-GUF framework are:

$$
{}^{(R_xR_yH_xH_y)}_{(R_xR_yH_xH_y)}Z^{p,k\alpha_{v_r}\beta_{v_s}}_{RS(\partial)v_r(\partial)v_s}I^{defg}_{v_r v_s ij}
\qquad
\begin{aligned}R,S &= -,1,...,6\\ r,s &= x,y,z\end{aligned}
\tag{3.23}
$$

$$
{}^{H_xH_y}Z^{p,k\alpha_{u_r}\beta_{u_s}}_{\rho u_r u_s}I^{defg}_{u_r u_s ij}
\qquad r,s = x,y,z
\tag{3.24}
$$

3.4 Expansion and assembly

According to the selected model - among the potentially infinite number available - it is then required to expand and assembly the fundamental *kernels* of the formulation (Eq.(3.23, Eq.(3.24)). Expanding these kernels in accordance with the chosen kinematic model and assembling them, the *stiffness matrix* and the *mass matrix* are obtained.

In the following subsections the processes of theory expansion, ply contributions assembly and sublaminate contributions assembly are illustrated.

3.4.1 Theory expansion

The first indexes to be expanded are those related to the model: α_{v_r} and β_{v_s}. The explicit expansion of one of the terms, for two generic variables v_r and v_s, has the following expression (top and bottom prescripts (R_x, R_y, H_x, H_y) and possible derivations in the thickness integral are omitted for brevity):

$$\delta v^{p,k}_{r\alpha_{v_r}i} Z^{p,k\alpha_{v_r}\beta_{v_s}}_{RSv_rv_s} I^{defg}_{v_rv_sij} v^{p,k}_{s\alpha_{v_s}j} =$$
$$\delta v^{p,k}_{r0i} Z^{p,k00}_{RSv_rv_s} I^{defg}_{v_rv_sij} v^{p,k}_{s0j} + \delta v^{p,k}_{r0i} Z^{p,k01}_{RSv_rv_s} I^{defg}_{v_rv_sij} v^{p,k}_{s1j} + ... + \delta v^{p,k}_{r0i} Z^{p,k0N^k_{v_s}}_{RSv_rv_s} I^{defg}_{v_rv_sij} v^{p,k}_{sN^k_{v_s}j}$$
$$+ \delta v^{p,k}_{r1i} Z^{p,k10}_{RSv_rv_s} I^{defg}_{v_rv_sij} v^{p,k}_{s0j} + \delta v^{p,k}_{r1i} Z^{p,k11}_{RSu_ru_s} I^{defg}_{u_ru_sij} v^{p,k}_{s1j} + ... + \delta v^{p,k}_{r1i} Z^{p,k1N^k_{v_s}}_{RSv_rv_s} I^{defg}_{v_rv_sij} v^{p,k}_{sN^k_{v_s}j}$$
$$+\delta v^{p,k}_{rN^k_{v_s}i} Z^{p,kN^k_{v_s}0}_{RSv_rv_s} I^{defg}_{v_rv_sij} v^{p,k}_{s0j} + \delta v^{p,k}_{rN^k_{v_s}i} Z^{p,kN^k_{v_s}1}_{RSv_rv_s} I^{defg}_{v_rv_sij} v^{p,k}_{s1j} + ... + \delta v^{p,k}_{rN^k_{v_s}i} Z^{p,kN^k_{v_s}N^k_{v_s}}_{RSv_rv_s} I^{defg}_{v_rv_sij} v^{p,k}_{sN^k_{v_s}j} \tag{3.25}$$

where $N_{v^k_r}$ and $N_{v^k_s}$ are the orders of expansion of the generic variables v_r and v_s, respectively. A similar expression can be obtained for the terms composing the inertial virtual work by formally substituting the subscript RS with ρ.

A graphical representation is presented in Figure 3.1 to clarify the expansion at theory level.

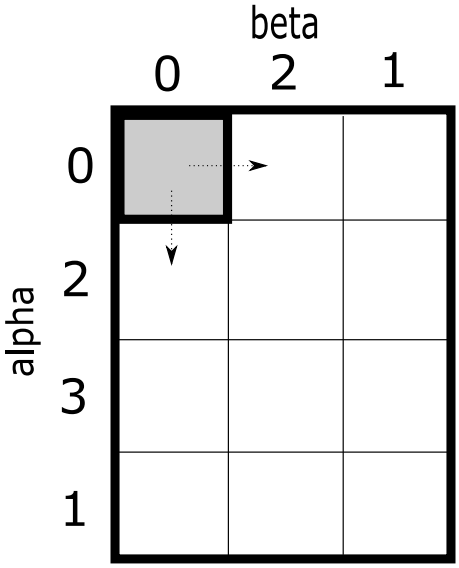

Figure 3.1: Thickness integral matrix size depending of the orders of α_v and β_v. Example with $N_{\alpha_v} = 3$ and $N_{\beta_v} = 2$.

Regrouping the DOF of a generic ply p in a generic sublaminate k, it follows:

$$\delta \mathbf{v}^{p,k}_{ri} = \begin{Bmatrix} \delta v^{p,k}_{r0i} \\ \delta v^{p,k}_{r2i} \\ \vdots \\ \delta v^{p,k}_{rN^k_{v_r}i} \\ \delta v^{p,k}_{r1i} \end{Bmatrix} \qquad \mathbf{v}^{p,k}_{sj} = \begin{Bmatrix} v^{p,k}_{s0j} \\ v^{p,k}_{s2j} \\ \vdots \\ v^{p,k}_{sN^k_{v_s}j} \\ v^{p,k}_{s1j} \end{Bmatrix} \tag{3.26}$$

By means of the definitions introduced in Eq.(3.26), the generic terms of RMVT become:

$$\delta v^{p,k}_{r\alpha_{v_r}i} {}^{(R_xR_yH_xH_y)}_{(R_xR_yH_xH_y)} Z^{p,k\alpha_{v_r}\beta_{v_s}}_{RS(\partial)v_r(\partial)v_s} I^{defg}_{v_rv_sij} v^{p,k}_{s\beta_{v_s}j} \Rightarrow \delta \mathbf{v}^{p,k}_{ri} {}^{(R_xR_yH_xH_y)}_{(R_xR_yH_xH_y)} \mathbf{Z}^{p,k}_{RS(\partial)v_r(\partial)v_s} I^{defg}_{v_rv_sij} \mathbf{v}^{p,k}_{sj} \tag{3.27}$$

$$\delta u^{p,k}_{r\alpha_{u_r}i} {}^{H_xH_y} Z^{p,k\alpha_{u_r}\beta_{u_s}}_{\rho u_r u_s} I^{defg}_{u_ru_sij} u^{p,k}_{s\beta_{u_s}j} \Rightarrow \delta \mathbf{u}^{p,k}_{ri} {}^{H_xH_y} \mathbf{Z}^{p,k}_{\rho u_r u_s} I^{defg}_{u_ru_sij} \mathbf{u}^{p,k}_{sj} \tag{3.28}$$

Therefore, the grouping of variables into vectors of DOF belonging to the same theory expansion implies the expansion of the thickness integrals of each ply p with respect to the order of the theory selected for the sublaminate k. This is symbolically expressed as follows:

$$\begin{matrix}(R_xR_yH_xH_y)\\(R_xR_yH_xH_y)\end{matrix} Z^{p,k\alpha_{v_r}\beta_{v_s}}_{RS(\partial)v_r(\partial)v_s} \xrightarrow[(\alpha_{v_r},\beta_{v_s})\text{ cycling}]{\text{theory expansion}} \begin{matrix}(R_xR_yH_xH_y)\\(R_xR_yH_xH_y)\end{matrix} \mathbf{Z}^{p,k}_{RS(\partial)v_r(\partial)v_s}$$
$$H_xH_y\, Z^{p,k\alpha_{u_r}\beta_{u_s}}_{\rho u_r u_s} \xrightarrow[(\alpha_{u_r},\beta_{u_s})\text{ cycling}]{\text{theory expansion}} H_xH_y\, \mathbf{Z}^{p,k}_{\rho u_r u_s} \qquad r,s = x,y,z \quad (3.29)$$

where the matrices $\begin{matrix}(...)\\(...)\end{matrix}\mathbf{Z}^{p,k}_{(...)}$ have size $(N^k_{v_r}+1, N^k_{v_s}+1)$.

3.4.2 Assembly of plies at sublaminate level

The sublaminates are numbered from bottom to top, and the same holds for the plies within each sublaminate. An example is given in Figure 3.2, where the following notation is introduced: N^k is the number of sublaminates, N^k_p is the number of plies in sublaminate k.

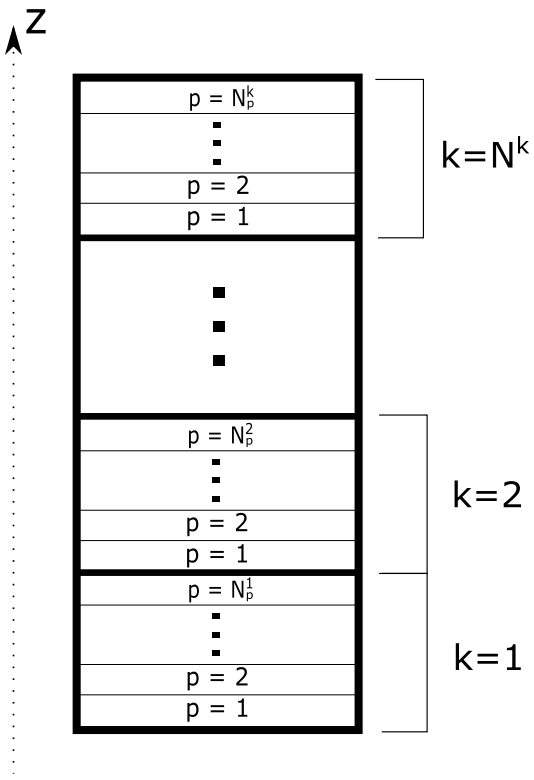

Figure 3.2: Notation adopted to number sublaminates and plies.

To clarify the expansion and assembly procedures, an example is presented next. A sandwich shell is considered, as illustrated in Figure 3.3, which is composed of three sublaminates. The first sublaminate corresponds to the bottom skin and comprises three plies. The second sublaminate includes the core. The third sublaminate corresponds to the top skin and comprises three plies. The three models adopted are:

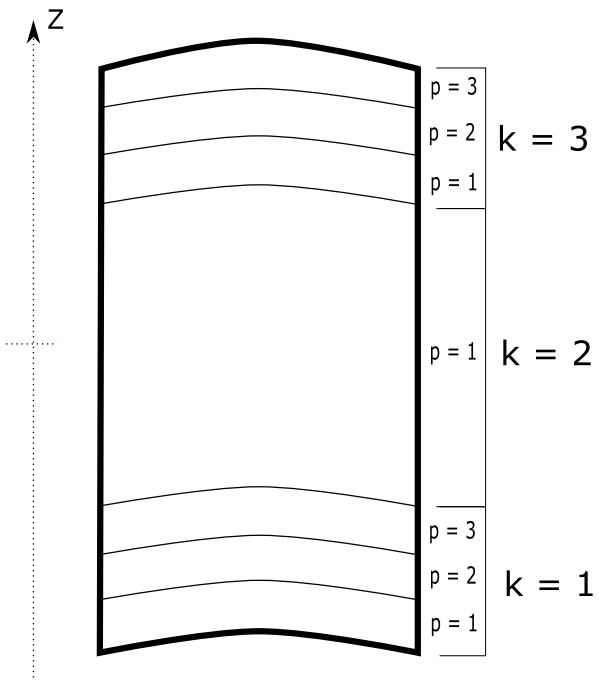

Figure 3.3: Shell case composed of three sublaminates.

The following models and descriptions are considered for the shell case.

$k = 3$: LW model, with ESL description for u_z and s_z. All variables are expanded to the second order.

$$LM^{2,2,2E}_{2,2,2E} \begin{cases} \alpha_{u_x}, \beta_{u_x} = 0, 2, 1 \\ \alpha_{u_y}, \beta_{u_y} = 0, 2, 1 \\ \alpha_{u_z}, \beta_{u_z} = 0, 2, 1 \\ \alpha_{s_x}, \beta_{s_x} = 0, 2, 1 \\ \alpha_{s_y}, \beta_{s_y} = 0, 2, 1 \\ \alpha_{s_z}, \beta_{s_z} = 0, 2, 1 \end{cases}$$

$k = 2$: ESL model. u_x, u_y, s_x and s_y are expanded to the third order; u_z and s_z are expanded to the second order.

$$EM^{3,3,2}_{3,3,2} \begin{cases} \alpha_{u_x}, \beta_{u_x} = 0, 2, 3, 1 \\ \alpha_{u_y}, \beta_{u_y} = 0, 2, 3, 1 \\ \alpha_{u_z}, \beta_{u_z} = 0, 2, 1 \\ \alpha_{s_x}, \beta_{s_x} = 0, 2, 3, 1 \\ \alpha_{s_y}, \beta_{s_y} = 0, 2, 3, 1 \\ \alpha_{s_z}, \beta_{s_z} = 0, 2, 1 \end{cases}$$

$k = 1$: ESL model. u_x, u_y, s_x and s_y are expanded to the first order; u_z and s_z are expanded to the zeroth order.

$$EM^{1,1,0}_{1,1,0} \quad \begin{cases} \alpha_{u_x}, \beta_{u_x} = 0, 1 \\ \alpha_{u_y}, \beta_{u_y} = 0, 1 \\ \alpha_{u_z}, \beta_{u_z} = 0 \\ \alpha_{s_x}, \beta_{s_x} = 0, 1 \\ \alpha_{s_y}, \beta_{s_y} = 0, 1 \\ \alpha_{s_z}, \beta_{s_z} = 0 \end{cases}$$

This case will be referred to in the upcoming schematic depictions of the assembly procedure.

To proceed with the assembly procedure the plies contributions within each sublaminate k must be summed. Similarly to what was done for the theory expansion, the expansion of subscript p is formally done by:

$$\begin{matrix} {}^{(R_xR_yH_xH_y)}_{(R_xR_yH_xH_y)}\mathbf{Z}^{p,k}_{RS(\partial)v_r(\partial)v_s} & \xrightarrow[\text{p cycling}]{\text{ply assembly}} & {}^{(R_xR_yH_xH_y)}_{(R_xR_yH_xH_y)}\mathbf{Z}^{k}_{RS(\partial)v_r(\partial)v_s} \\ {}^{H_xH_y}\mathbf{Z}^{p,k}_{\rho u_r u_s} & \xrightarrow[\text{p cycling}]{\text{ply assembly}} & {}^{H_xH_y}\mathbf{Z}^{k}_{\rho u_r u_s} \end{matrix} \qquad r, s = x, y, z \tag{3.30}$$

The assembly procedure of matrices ${}^{(\dots)}_{(\dots)}\mathbf{Z}^{p,k}_{(\dots)}$ depends on the kinematic model applied within each sublaminate k. The size of the resulting matrix will depend also on whether the variables involved in the thickness integral are described through an ESL or a LW theory.

If both variables involved in the thickness integral are described in an ESL manner, then: $\partial \mathbf{v}^{p,k}_{ri} = \partial \mathbf{v}^{p+1,k}_{ri} = \partial \mathbf{v}^{k}_{ri}$ and $\mathbf{v}^{p,k}_{sj} = \mathbf{v}^{p+1,k}_{sj} = \mathbf{v}^{k}_{sj}$.

The assembly procedure consists in the simple superposition of all the matrices relative to each ply, i.e.: ${}^{(\dots)}_{(\dots)}\mathbf{Z}^{k}_{RS(\partial)v_r(\partial)v_s} = \sum_{p=1}^{N^k_p} {}^{(\dots)}_{(\dots)}\mathbf{Z}^{p,k}_{RS(\partial)v_r(\partial)v_s}$. In this specific case ${}^{(\dots)}_{(\dots)}\mathbf{Z}^{k}_{RS(\partial)v_r(\partial)v_s}$ has the same size of ${}^{(\dots)}_{(\dots)}\mathbf{Z}^{p,k}_{RS(\partial)v_r(\partial)v_s}$, which is $(N^k_{v_r} + 1, N^k_{v_s} + 1)$. The process is illustrated in Figure 3.4.

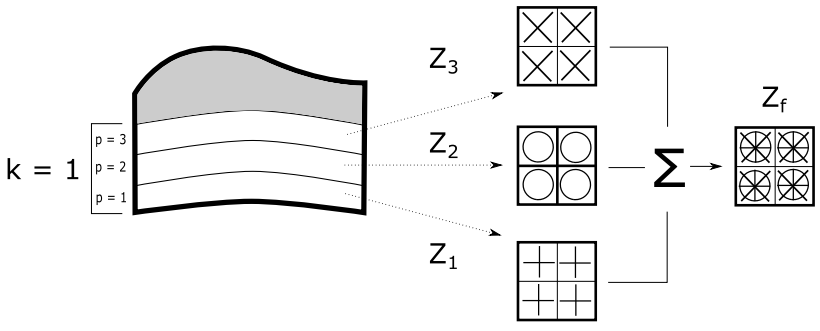

Figure 3.4: Assembly procedure with an ESL description. In particular the assembly of the thickness kernels of ${}^{H_y}_{H_x}Z_{11u_xu_x}$ is shown, with reference to the case in Figure 3.3.

If both variables involved in the thickness integral are described in a LW manner then the interply continuity is imposed as $\partial v^{p,k}_{r0i} = \partial v^{p+1,k}_{r1i}$ and $v^{p,k}_{s0j} = v^{p+1,k}_{s1j}$ due to the choice

operated for the thickness functions, see Eq.(2.51), and the way the DOF are collected, see Eq.(2.55). This continuity condition is easily imposed thanks to the way the terms were collected. In this case the size of matrix ${}^{(...)}_{(...)}\mathbf{Z}^k_{RS(\partial)v_r(\partial)v_s}$ is $[(N^k_{v_r}+1)N^k_p-(N^k_p-1),(N^k_{v_s}+1)N^k_p-(N^k_p-1)]$ its size depending on the number of plies.

The resulting vectors collecting the kinematic parameters after the assembly has been operated are:

$$\delta\mathbf{v}^k_{ri}=\left\{\begin{array}{c}\delta v^{N^k_p,k}_{r0i}\\ \vdots\\ \delta v^{p,k}_{r0i}=\delta v^{p+1,k}_{r1i}\\ \vdots\\ \delta v^{1,k}_{r0i}=\delta v^{2,k}_{r1i}\\ \vdots\\ \delta v^{1,k}_{r1i}\end{array}\right\}\qquad \mathbf{v}^k_{sj}=\left\{\begin{array}{c} v^{N^k_p,k}_{s0j}\\ \vdots\\ v^{p,k}_{s0j}=v^{p+1,k}_{s1j}\\ \vdots\\ v^{1,k}_{s0j}=v^{2,k}_{s1j}\\ \vdots\\ v^{1,k}_{s1j}\end{array}\right\} \tag{3.31}$$

For clarity, the assembly procedure for a LW sublaminate is graphically presented in Figure 3.5.

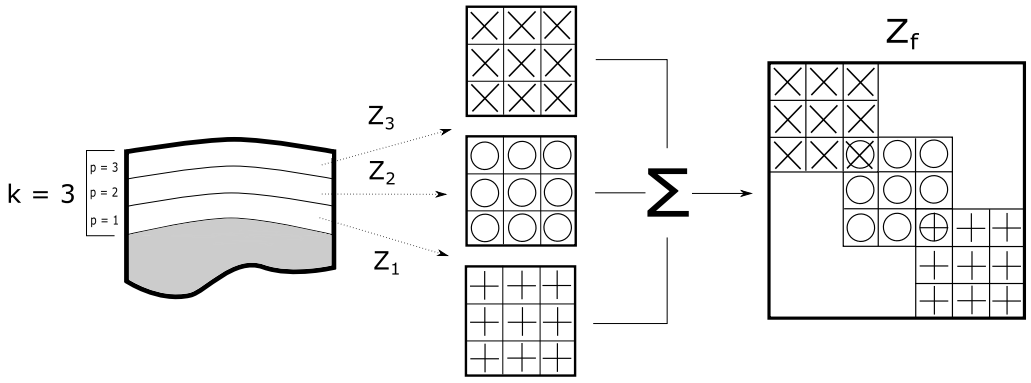

Figure 3.5: Assembly procedure with a LW description. The assembly of the thickness kernels of $Z_{12u_yu_x}$ is shown, with reference to the case in Figure 3.3.

If the two variables involved in the thickness integral have two different descriptions (one ESL and the other one LW) then it follows that the process of assembly is a combination of the two methods described above. For instance, in case the virtual variation variable has a LW description and the real variable has an ESL description: $v^{p,k}_{s0i}=v^{p+1,k}_{s1i}$ and $\mathbf{v}^{p,k}_{rj}=\mathbf{v}^{p+1,k}_{rj}=\mathbf{v}^k_{rj}$. Therefore, the size of matrix ${}^{(...)}_{(...)}\mathbf{Z}^k_{RS(\partial)v_r(\partial)v_s}$ is $[(N^k_{v_s}+1)N^k_p-(N^k_p-1),N^k_{v_r}+1]$. The process is illustrated in Figure 3.6.

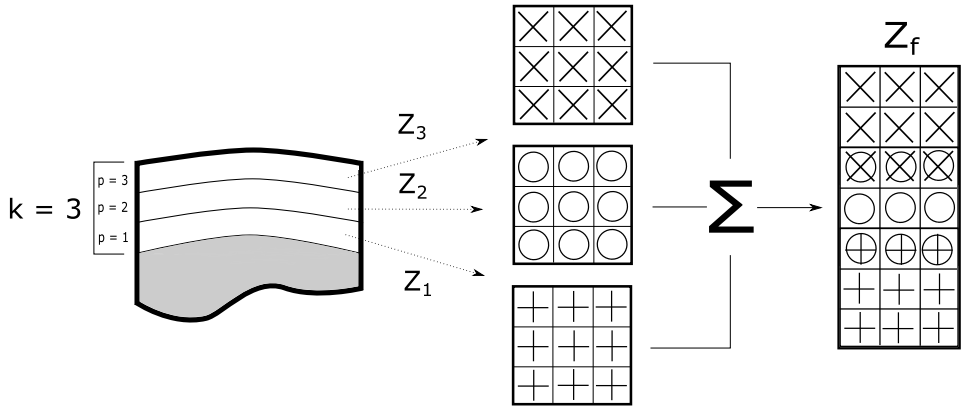

Figure 3.6: Assembly procedure with a LW description. In particular the assembly of the thickness kernels of ${}^{H_x}Z_{36u_xs_z}$ is shown, with reference to the case in Figure 3.3.

After the kernels are expanded over the theory-related indices and the ply contributions are assembled, the variational statement of Eq.(3.22) is rewritten as:

$$
\begin{aligned}
&\sum_{k=1}^{N_k}\Big[\delta\mathbf{u}^{k^T}_{xi_1}\,{}^{H_xH_y}\mathbf{Z}^k_{\rho u_x u_x} I^{0000}_{u_x u_x i_1 j_1}\ddot{\mathbf{u}}^k_{xj_1} + \delta\mathbf{u}^{k^T}_{yi_1}\,{}^{H_xH_y}\mathbf{Z}^k_{\rho u_y u_y} I^{0000}_{u_y u_y i_1 j_1}\ddot{\mathbf{u}}^k_{yj_1} \\
&\quad + \delta\mathbf{u}^{k^T}_{zi_1}\,{}^{H_xH_y}\mathbf{Z}^k_{\rho u_z u_z} I^{0000}_{u_z u_z i_1 j_1}\ddot{\mathbf{u}}^k_{zj_1}\Big] + \\
&\sum_{k=1}^{N_k}\Big[\delta\mathbf{u}^{k^T}_{xi_1}\,{}^{H_y}_{H_x}\mathbf{Z}^k_{11u_x u_x} I^{1010}_{u_x u_x i_1 j_1}\mathbf{u}^k_{xj_1} + \delta\mathbf{u}^{k^T}_{xi_1}\mathbf{Z}^k_{12u_x u_y} I^{1001}_{u_x u_y i_1 j_1}\mathbf{u}^k_{yj_1} \\
&\quad + \delta\mathbf{u}^{k^T}_{xi_1}\mathbf{Z}^k_{16u_x u_x} I^{1001}_{u_x u_x i_1 j_1}\mathbf{u}^k_{xj_1} + \delta\mathbf{u}^{k^T}_{xi_1}\,{}^{H_y}_{H_x}\mathbf{Z}^k_{16u_x u_y} I^{1010}_{u_x u_y i_1 j_1}\mathbf{u}^k_{yj_1} \\
&\quad + \delta\mathbf{u}^{k^T}_{yi_1}\mathbf{Z}^k_{12u_y u_x} I^{0110}_{u_y u_x i_1 j_1}\mathbf{u}^k_{xj_1} + \delta\mathbf{u}^{k^T}_{yi_1}\,{}^{H_x}_{H_y}\mathbf{Z}^k_{22u_y u_y} I^{0101}_{u_y u_y i_1 j_1}\mathbf{u}^k_{yj_1} \\
&\quad + \delta\mathbf{u}^{k^T}_{yi_1}\,{}^{H_x}_{H_y}\mathbf{Z}^k_{26u_y u_x} I^{0101}_{u_y u_x i_1 j_1}\mathbf{u}^k_{xj_1} + \delta\mathbf{u}^{k^T}_{yi_1}\mathbf{Z}^k_{26u_y u_y} I^{0110}_{u_y u_y i_1 j_1}\mathbf{u}^k_{yj_1} \\
&\quad + \delta\mathbf{u}^{k^T}_{xi_1}\mathbf{Z}^k_{16u_x u_x} I^{0110}_{u_x u_x i_1 j_1}\mathbf{u}^k_{xj_1} + \delta\mathbf{u}^{k^T}_{xi_1}\,{}^{H_x}_{H_y}\mathbf{Z}^k_{26u_x u_y} I^{0101}_{u_x u_y i_1 j_1}\mathbf{u}^k_{yj_1} \\
&\quad + \delta\mathbf{u}^{k^T}_{xi_1}\,{}^{H_x}_{H_y}\mathbf{Z}^k_{66u_x u_x} I^{0101}_{u_x u_x i_1 j_1}\mathbf{u}^k_{xj_1} + \delta\mathbf{u}^{k^T}_{xi_1}\mathbf{Z}^k_{66u_x u_y} I^{0110}_{u_x u_y i_1 j_1}\mathbf{u}^k_{yj_1} \\
&\quad + \delta\mathbf{u}^{k^T}_{yi_1}\,{}^{H_y}_{H_x}\mathbf{Z}^k_{16u_y u_x} I^{1010}_{u_y u_x i_1 j_1}\mathbf{u}^k_{xj_1} + \delta\mathbf{u}^{k^T}_{yi_1}\mathbf{Z}^k_{26u_y u_y} I^{1001}_{u_y u_y i_1 j_1}\mathbf{u}^k_{yj_1} \\
&\quad + \delta\mathbf{u}^{k^T}_{yi_1}\mathbf{Z}^k_{66u_y u_x} I^{1001}_{u_y u_x i_1 j_1}\mathbf{u}^k_{xj_1} + \delta\mathbf{u}^{k^T}_{yi_1}\,{}^{H_y}_{H_x}\mathbf{Z}^k_{66u_y u_y} I^{1010}_{u_y u_y i_1 j_1}\mathbf{u}^k_{yj_1} \\
&\quad + \delta\mathbf{u}^{k^T}_{xi_1}\,{}^{H_y}\mathbf{Z}^k_{13u_x s_z} I^{1000}_{u_x s_z i_1 j_2}\mathbf{s}^k_{zj_2} + \delta\mathbf{u}^{k^T}_{yi_1}\,{}^{H_x}\mathbf{Z}^k_{23u_y s_z} I^{0100}_{u_y s_z i_1 j_2}\mathbf{s}^k_{zj_2} \\
&\quad + \delta\mathbf{u}^{k^T}_{xi_1}\,{}^{H_x}\mathbf{Z}^k_{36u_x s_z} I^{0100}_{u_x s_z i_1 j_2}\mathbf{s}^k_{z\beta_{s_z} j_2} + \delta\mathbf{u}^{k^T}_{yi_1}\,{}^{H_y}\mathbf{Z}^k_{36u_y s_z} I^{1000}_{u_y s_z i_1 j_2}\mathbf{s}^k_{zj_2} \\
&\quad + \delta\mathbf{u}^{k^T}_{xi_1}\,{}^{H_y}_{H_x R_x}\mathbf{Z}^k_{11u_x u_z} I^{1000}_{u_x u_z i_1 j_1}\mathbf{u}^k_{zj_1} + \delta\mathbf{u}^{k^T}_{xi_1}\,{}_{R_y}\mathbf{Z}^k_{12u_x u_z} I^{1000}_{u_x u_z i_1 j_1}\mathbf{u}^k_{zj_1} \\
&\quad + \delta\mathbf{u}^{k^T}_{yi_1}\,{}_{R_x}\mathbf{Z}^k_{12u_y u_z} I^{0100}_{u_y u_z i_1 j_1}\mathbf{u}^k_{zj_1} + \delta\mathbf{u}^{k^T}_{yi_1}\,{}^{H_x}_{H_y R_y}\mathbf{Z}^k_{22u_y u_z} I^{0100}_{u_y u_z i_1 j_1}\mathbf{u}^k_{zj_1} \\
&\quad + \delta\mathbf{u}^{k^T}_{xi_1}\,{}_{R_x}\mathbf{Z}^k_{16u_x u_z} I^{0100}_{u_x u_z i_1 j_1}\mathbf{u}^k_{zj_1} + \delta\mathbf{u}^{k^T}_{xi_1}\,{}^{H_x}_{H_y R_y}\mathbf{Z}^k_{26u_x u_z} I^{0100}_{u_x u_z i_1 j_1}\mathbf{u}^k_{zj_1} \\
&\quad + \delta\mathbf{u}^{k^T}_{yi_1}\,{}^{H_y}_{H_x R_x}\mathbf{Z}^k_{16u_y u_z} I^{1000}_{u_y u_z i_1 j_1}\mathbf{u}^k_{zj_1} + \delta\mathbf{u}^{k^T}_{yi_1}\,{}_{R_y}\mathbf{Z}^k_{26u_y u_z} I^{1000}_{u_y u_z i_1 j_1}\mathbf{u}^k_{zj_1}
\end{aligned}
\tag{3.32}
$$

$$
\begin{aligned}
&+\delta\mathbf{u}_{zi_1}^{k^T}\,{}^{H_y}_{H_xR_x}\mathbf{Z}^k_{11u_zu_x}I^{0010}_{u_zu_xi_1j_1}\mathbf{u}^k_{xj_1}+\delta\mathbf{u}_{zi_1}^{k^T}\,{}^{}_{R_x}\mathbf{Z}^k_{12u_zu_y}I^{0001}_{u_zu_yi_1j_1}\mathbf{u}^k_{yj_1}\\
&+\delta\mathbf{u}_{zi_1}^{k^T}\,{}^{}_{R_x}\mathbf{Z}^k_{16u_zu_x}I^{0001}_{u_zu_xi_1j_1}\mathbf{u}^k_{xj_1}+\delta\mathbf{u}_{zi_1}^{k^T}\,{}^{H_y}_{H_xR_x}\mathbf{Z}^k_{16u_zu_y}I^{0010}_{u_zu_yi_1j_1}\mathbf{u}^k_{yj_1}\\
&+\delta\mathbf{u}_{zi_1}^{k^T}\,{}^{}_{R_y}\mathbf{Z}^k_{12u_zu_x}I^{0010}_{u_zu_xi_1j_1}\mathbf{u}^k_{xj_1}+\delta\mathbf{u}_{zi_1}^{k^T}\,{}^{H_x}_{H_yR_y}\mathbf{Z}^k_{22u_zu_y}I^{0001}_{u_zu_yi_1j_1}\mathbf{u}^k_{yj_1}\\
&+\delta\mathbf{u}_{zi_1}^{k^T}\,{}^{H_x}_{H_yR_y}\mathbf{Z}^k_{26u_zu_x}I^{0001}_{u_zu_xi_1j_1}\mathbf{u}^k_{xj_1}+\delta\mathbf{u}_{zi_1}^{k^T}\,{}^{}_{R_y}\mathbf{Z}^k_{26u_zu_y}I^{0010}_{u_zu_yi_1j_1}\mathbf{u}^k_{yj_1}\\
&+\delta\mathbf{u}_{zi_1}^{k^T}\,{}^{H_y}_{R_x}\mathbf{Z}^k_{13u_zs_z}I^{0000}_{u_zs_zi_1j_2}\mathbf{s}^k_{zj_2}+\delta\mathbf{u}_{zi_1}^{k^T}\,{}^{H_x}_{R_y}\mathbf{Z}^k_{23u_zs_z}I^{0000}_{u_zs_zi_1j_2}\mathbf{s}^k_{zj_2}\\
&+\delta\mathbf{u}_{zi_1}^{k^T}\,{}^{H_y}_{H_xR_x^2}\mathbf{Z}^k_{11u_zu_z}I^{0000}_{u_zu_zi_1j_1}\mathbf{u}^k_{zj_1}+\delta\mathbf{u}_{zi_1}^{k^T}\,{}^{}_{R_xR_y}\mathbf{Z}^k_{12u_zu_z}I^{0000}_{u_zu_zi_1j_1}\mathbf{u}^k_{zj_1}\\
&+\delta\mathbf{u}_{zi_1}^{k^T}\,{}^{}_{R_xR_y}\mathbf{Z}^k_{12u_zu_z}I^{0000}_{u_zu_zi_1j_1}\mathbf{u}^k_{zj_1}+\delta\mathbf{u}_{zi_1}^{k^T}\,{}^{H_x}_{H_yR_y^2}\mathbf{Z}^k_{22u_zu_z}I^{0000}_{u_zu_zi_1j_1}\mathbf{u}^k_{zj_1}\\
&+\delta\mathbf{u}_{zi_1}^{k^T}\,{}^{H_x}\mathbf{Z}^k_{u_zs_y}I^{0100}_{u_zs_yi_1j_2}\mathbf{s}^k_{yj_2}+\delta\mathbf{u}_{zi_1}^{k^T}\,{}^{H_y}\mathbf{Z}^k_{u_zs_x}I^{1000}_{u_zs_xi_1j_2}\mathbf{s}^k_{xj_2}\\
&-\delta\mathbf{u}_{yi_1}^{k^T}\lambda_D\,{}^{H_x}_{R_y}\mathbf{Z}^k_{u_ys_y}I^{0000}_{u_ys_yi_1j_2}\mathbf{s}^k_{yj_2}-\delta\mathbf{u}_{xi_1}^{k^T}\lambda_D\,{}^{H_y}_{R_x}\mathbf{Z}^k_{u_xs_x}I^{0000}_{u_xs_xi_1j_2}\mathbf{s}^k_{xj_2}\\
&+\delta\mathbf{u}_{yi_1}^{k^T}\,{}^{H_xH_y}\mathbf{Z}^k_{\partial u_ys_y}I^{0000}_{u_ys_yi_1j_2}\mathbf{s}^k_{yj_2}+\delta\mathbf{u}_{xi_1}^{k^T}\,{}^{H_xH_y}\mathbf{Z}^k_{\partial u_xs_x}I^{0000}_{u_xs_xi_1j_2}\mathbf{s}^k_{xj_2}\\
&+\delta\mathbf{u}_{zi_1}^{k^T}\,{}^{H_xH_y}\mathbf{Z}^k_{\partial u_zs_z}I^{0000}_{u_zs_zi_1j_2}\mathbf{s}^k_{zj_2}+\delta\mathbf{s}_{yi_2}^{k^T}\,{}^{H_x}\mathbf{Z}^k_{s_yu_z}I^{0001}_{s_yu_zi_2j_1}\mathbf{u}^k_{zj_1}\\
&+\delta\mathbf{s}_{xi_2}^{k^T}\,{}^{H_y}\mathbf{Z}^k_{s_xu_z}I^{0010}_{s_xu_zi_2j_1}\mathbf{u}^k_{zj_1}-\delta\mathbf{s}_{yi_2}^{k^T}\lambda_D\,{}^{H_x}_{R_y}\mathbf{Z}^k_{s_yu_y}I^{0000}_{s_yu_yi_2j_1}\mathbf{u}^k_{yj_1}\\
&-\delta\mathbf{s}_{xi_1}^{k^T}\lambda_D\,{}^{H_y}_{R_x}\mathbf{Z}^k_{s_xu_x}I^{0000}_{s_xu_xi_2j_1}\mathbf{u}^k_{xj_1}+\delta\mathbf{s}_{yi_2}^{k^T}\,{}^{H_xH_y}\mathbf{Z}^k_{s_y\partial u_y}I^{0000}_{s_yu_yi_2j_1}\mathbf{u}^k_{yj_1}\\
&+\delta\mathbf{s}_{xi_2}^{k^T}\,{}^{H_xH_y}\mathbf{Z}^k_{s_x\partial u_x}I^{0000}_{s_xu_xi_2j_1}\mathbf{u}^k_{xj_1}+\delta\mathbf{s}_{zi_2}^{k^T}\,{}^{H_xH_y}\mathbf{Z}^k_{s_z\partial u_z}I^{0000}_{s_zu_zi_2j_1}\mathbf{u}^k_{zj_1}\\
&+\delta\mathbf{s}_{zi_2}^{k^T}\,{}^{H_y}\mathbf{Z}^k_{13s_zu_x}I^{0010}_{s_zu_xi_2j_1}\mathbf{u}^k_{xj_1}+\delta\mathbf{s}_{zi_2}^{k^T}\,{}^{H_x}\mathbf{Z}^k_{23s_zu_y}I^{0001}_{s_zu_yi_2j_1}\mathbf{u}^k_{yj_1}\\
&+\delta\mathbf{s}_{zi_2}^{k^T}\,{}^{H_x}\mathbf{Z}^k_{36s_zu_x}I^{0001}_{s_zu_xi_2j_1}\mathbf{u}^k_{xj_1}+\delta\mathbf{s}_{zi_2}^{k^T}\,{}^{H_y}\mathbf{Z}^k_{36s_zu_y}I^{0010}_{s_zu_yi_2j_1}\mathbf{u}^k_{yj_1}\\
&+\delta\mathbf{s}_{zi_2}^{k^T}\,{}^{H_y}_{R_x}\mathbf{Z}^k_{13s_zu_z}I^{0000}_{s_zu_zi_2j_1}\mathbf{u}^k_{zj_1}+\delta\mathbf{s}_{zi_2}^{k^T}\,{}^{H_x}_{R_y}\mathbf{Z}^k_{23s_zu_z}I^{0000}_{s_zu_zi_2j_1}\mathbf{u}^k_{zj_1}\\
&-\delta\mathbf{s}_{yi_2}^{k^T}\,{}^{H_xH_y}\mathbf{Z}^k_{44s_ys_y}I^{0000}_{s_ys_yi_2j_2}\mathbf{s}^k_{yj_2}-\delta\mathbf{s}_{yi_2}^{k^T}\,{}^{H_xH_y}\mathbf{Z}^k_{45s_ys_x}I^{0000}_{s_ys_xi_2j_2}\mathbf{s}^k_{xj_2}\\
&-\delta\mathbf{s}_{xi}^{k^T}\,{}^{H_xH_y}\mathbf{Z}^k_{45s_xs_y}I^{0000}_{s_xs_yi_2j_2}\mathbf{s}^k_{yj_2}-\delta\mathbf{s}_{xi_2}^{k^T}\,{}^{H_xH_y}\mathbf{Z}^k_{55s_xs_x}I^{0000}_{s_xs_xi_2j_2}\mathbf{s}^k_{xj_2}\\
&-\delta\mathbf{s}_{zi_2}^{k^T}\,{}^{H_xH_y}\mathbf{Z}^k_{33s_zs_z}I^{0000}_{s_zs_zi_2j_2}\mathbf{s}^k_{zj_2}\Big]\\
&=\delta u_{z0i}^{N_p^k,N_k}\int_x\int_y f_z^{top}N_{u_zi_1}\left(1+\frac{h}{2R_x}\right)\left(1+\frac{h}{2R_y}\right)\mathrm{d}x\mathrm{d}y\\
&\quad+\delta u_{z1i}^{1,1}\int_x\int_y f_z^{bot}N_{u_zi_1}\left(1-\frac{h}{2R_x}\right)\left(1-\frac{h}{2R_y}\right)\mathrm{d}x\mathrm{d}y
\end{aligned}
$$

3.4.3 Assembly of sublaminates

The final assembly procedure is the summation of the sublaminate contributions in order to take into account the continuity of the generic variables at the interfaces. The assembly is formally expressed as:

$$\begin{array}{l} {}^{(R_xR_yH_xH_y)}_{(R_xR_yH_xH_y)}\mathbf{Z}^k_{RS(\partial)v_r(\partial)v_s} \xrightarrow[\text{k cycling}]{\text{sublaminate assembly}} {}^{(R_xR_yH_xH_y)}_{(R_xR_yH_xH_y)}\mathbf{Z}_{RS(\partial)v_r(\partial)v_s} \\ {}^{H_xH_y}\mathbf{Z}^k_{\rho u_r u_s} \xrightarrow[\text{k cycling}]{\text{sublaminate assembly}} {}^{H_xH_y}\mathbf{Z}_{\rho u_r u_s} \end{array} \qquad r,s = x,y,z \tag{3.33}$$

matrices ${}^{(R_xR_yH_xH_y)}_{(R_xR_yH_xH_y)}\mathbf{Z}_{RS(\partial)v_r(\partial)v_s}$ and ${}^{H_xH_y}\mathbf{Z}_{\rho u_r u_s}$ have size $(N_{DOF_{v_r}}, N_{DOF_{v_s}})$, where

$$N_{DOF_{v_r}} = \sum_{k=1}^{N_k} N^k_{DOF_{v_r}} - (N_k - 1) \qquad N_{DOF_{v_s}} = \sum_{k=1}^{N_k} N^k_{DOF_{v_s}} - (N_k - 1) \tag{3.34}$$

The sublaminate assembly procedure is always carried out as the LW ply assembly procedure. Therefore, the degrees of freedom of the laminate are grouped as:

$$\delta\mathbf{v}_{ri} = \begin{Bmatrix} \delta v^{N_k}_{ri} \\ \vdots \\ \delta v^1_{ri} \end{Bmatrix} \qquad \mathbf{v}_{sj} = \begin{Bmatrix} v^{N_k}_{sj} \\ \vdots \\ v^1_{sj} \end{Bmatrix} \tag{3.35}$$

Graphically, the process can be represented as in Figure 3.7.

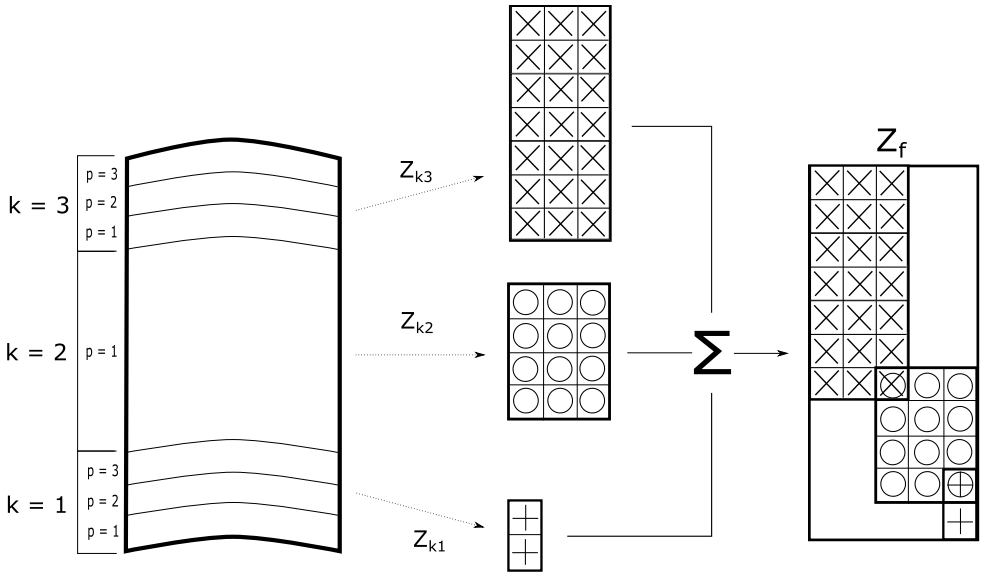

Figure 3.7: Assembly procedure with a LW description. In particular the assembly of the thickness kernels of ${}^{H_x}Z_{23u_ys_z}$ is shown, with reference to the case in Figure 3.3.

After the sublaminate assembly procedure is performed and the virtual variables are collected, the variational statement of Eq.(3.32) is re-written as:

$$
\begin{aligned}
&\delta\mathbf{u}^T_{xi_1}\Big[{}^{H_xH_y}\mathbf{Z}_{\rho u_x u_x} I^{0000}_{u_x u_x i_1 j_1}\ddot{\mathbf{u}}^k_{xj_1} + {}^{H_y}_{H_x}\mathbf{Z}_{11 u_x u_x} I^{1010}_{u_x u_x i_1 j_1}\mathbf{u}_{xj_1} + \mathbf{Z}_{12 u_x u_y} I^{1001}_{u_x u_y i_1 j_1}\mathbf{u}_{yj_1} \\
&\quad + \mathbf{Z}_{16 u_x u_x} I^{1001}_{u_x u_x i_1 j_1}\mathbf{u}^k_{xj_1} + {}^{H_y}_{H_x}\mathbf{Z}_{16 u_x u_y} I^{1010}_{u_x u_y i_1 j_1}\mathbf{u}_{yj_1} + \mathbf{Z}_{16 u_x u_x} I^{0110}_{u_x u_x i_1 j_1}\mathbf{u}_{xj_1} \\
&\quad + {}^{H_x}_{H_y}\mathbf{Z}_{26 u_x u_y} I^{0101}_{u_x u_y i_1 j_1}\mathbf{u}_{yj_1} + {}^{H_x}_{H_y}\mathbf{Z}_{66 u_x u_x} I^{0101}_{u_x u_x i_1 j_1}\mathbf{u}_{xj_1} + \mathbf{Z}_{66 u_x u_y} I^{0110}_{u_x u_y i_1 j_1}\mathbf{u}_{yj_1} \\
&\quad + {}^{H_y}\mathbf{Z}_{13 u_x s_z} I^{1000}_{u_x s_z i_1 j_2}\mathbf{s}_{zj_2} + {}^{H_x}\mathbf{Z}_{36 u_x s_z} I^{0100}_{u_x s_z i_1 j_2}\mathbf{s}_{z\beta_s z j_2} + {}^{H_y}_{H_x R_x}\mathbf{Z}_{11 u_x u_z} I^{1000}_{u_x u_z i_1 j_1}\mathbf{u}_{zj_1} \\
&\quad + {}_{R_y}\mathbf{Z}_{12 u_x u_z} I^{1000}_{u_x u_z i_1 j_1}\mathbf{u}_{zj_1} + {}_{R_x}\mathbf{Z}_{16 u_x u_z} I^{0100}_{u_x u_z i_1 j_1}\mathbf{u}_{zj_1} + {}^{H_x}_{H_y R_y}\mathbf{Z}_{26 u_x u_z} I^{0100}_{u_x u_z i_1 j_1}\mathbf{u}_{zj_1} \\
&\quad - \lambda_D\, {}^{H_y}_{R_x}\mathbf{Z}_{u_x s_x} I^{0000}_{u_x s_x i_1 j_2}\mathbf{s}_{xj_2} + {}^{H_xH_y}\mathbf{Z}_{\partial u_x s_x} I^{0000}_{u_x s_x i_1 j_2}\mathbf{s}_{xj_2}\Big] + \\
&\delta\mathbf{u}^T_{yi_1}\Big[{}^{H_xH_y}\mathbf{Z}_{\rho u_y u_y} I^{0000}_{u_y u_y i_1 j_1}\ddot{\mathbf{u}}_{yj_1} + \mathbf{Z}_{12 u_y u_x} I^{0110}_{u_y u_x i_1 j_1}\mathbf{u}_{xj_1} + {}^{H_x}_{H_y}\mathbf{Z}_{22 u_y u_y} I^{0101}_{u_y u_y i_1 j_1}\mathbf{u}_{yj_1} \\
&\quad + {}^{H_x}_{H_y}\mathbf{Z}_{26 u_y u_x} I^{0101}_{u_y u_x i_1 j_1}\mathbf{u}_{xj_1} + \mathbf{Z}_{26 u_y u_y} I^{0110}_{u_y u_y i_1 j_1}\mathbf{u}_{yj_1} + {}^{H_y}_{H_x}\mathbf{Z}_{16 u_y u_x} I^{1010}_{u_y u_x i_1 j_1}\mathbf{u}_{xj_1} \\
&\quad + \mathbf{Z}_{26 u_y u_y} I^{1001}_{u_y u_y i_1 j_1}\mathbf{u}_{yj_1} + \mathbf{Z}_{66 u_y u_x} I^{1001}_{u_y u_x i_1 j_1}\mathbf{u}_{xj_1} + {}^{H_y}_{H_x}\mathbf{Z}_{66 u_y u_y} I^{1010}_{u_y u_y i_1 j_1}\mathbf{u}_{yj_1} \\
&\quad + {}^{H_x}\mathbf{Z}_{23 u_y s_z} I^{0100}_{u_y s_z i_1 j_2}\mathbf{s}_{zj_2} + {}^{H_y}\mathbf{Z}_{36 u_y s_z} I^{1000}_{u_y s_z i_1 j_2}\mathbf{s}_{zj_2} + {}_{R_x}\mathbf{Z}_{12 u_y u_z} I^{0100}_{u_y u_z i_1 j_1}\mathbf{u}_{zj_1} \\
&\quad + {}^{H_x}_{H_y R_y}\mathbf{Z}_{22 u_y u_z} I^{0100}_{u_y u_z i_1 j_1}\mathbf{u}_{zj_1} + {}^{H_y}_{H_x R_x}\mathbf{Z}_{16 u_y u_z} I^{1000}_{u_y u_z i_1 j_1}\mathbf{u}_{zj_1} + {}_{R_y}\mathbf{Z}_{26 u_y u_z} I^{1000}_{u_y u_z i_1 j_1}\mathbf{u}_{zj_1} \\
&\quad - \lambda_D\, {}^{H_x}_{R_y}\mathbf{Z}_{u_y s_y} I^{0000}_{u_y s_y i_1 j_2}\mathbf{s}_{yj_2} + {}^{H_xH_y}\mathbf{Z}_{\partial u_y s_y} I^{0000}_{u_y s_y i_1 j_2}\mathbf{s}_{yj_2}\Big] + \\
&\delta\mathbf{u}^T_{zi_1}\Big[{}^{H_xH_y}\mathbf{Z}_{\rho u_z u_z} I^{0000}_{u_z u_z i_1 j_1}\ddot{\mathbf{u}}_{zj_1} + {}^{H_y}_{H_x R_x}\mathbf{Z}_{11 u_z u_x} I^{0010}_{u_z u_x i_1 j_1}\mathbf{u}_{xj_1} + {}_{R_x}\mathbf{Z}_{12 u_z u_y} I^{0001}_{u_z u_y i_1 j_1}\mathbf{u}_{yj_1} \\
&\quad + {}_{R_x}\mathbf{Z}_{16 u_z u_x} I^{0001}_{u_z u_x i_1 j_1}\mathbf{u}_{xj_1} + {}^{H_y}_{H_x R_x}\mathbf{Z}_{16 u_z u_y} I^{0010}_{u_z u_y i_1 j_1}\mathbf{u}_{yj_1} + {}_{R_y}\mathbf{Z}_{12 u_z u_x} I^{0010}_{u_z u_x i_1 j_1}\mathbf{u}_{xj_1} \\
&\quad + {}^{H_x}_{H_y R_y}\mathbf{Z}_{22 u_z u_y} I^{0001}_{u_z u_y i_1 j_1}\mathbf{u}_{yj_1} + {}^{H_x}_{H_y R_y}\mathbf{Z}_{26 u_z u_x} I^{0001}_{u_z u_x i_1 j_1}\mathbf{u}_{xj_1} + {}_{R_y}\mathbf{Z}_{26 u_z u_y} I^{0010}_{u_z u_y i_1 j_1}\mathbf{u}_{yj_1} \\
&\quad + {}^{H_y}_{R_x}\mathbf{Z}_{13 u_z s_z} I^{0000}_{u_z s_z i_1 j_2}\mathbf{s}_{zj_2} + {}^{H_x}_{R_y}\mathbf{Z}_{23 u_z s_z} I^{0000}_{u_z s_z i_1 j_2}\mathbf{s}_{zj_2} + {}^{H_y}_{H_x R_x^2}\mathbf{Z}_{11 u_z u_z} I^{0000}_{u_z u_z i_1 j_1}\mathbf{u}_{zj_1} \\
&\quad + {}_{R_x R_y}\mathbf{Z}_{12 u_z u_z} I^{0000}_{u_z u_z i_1 j_1}\mathbf{u}_{zj_1} + {}_{R_x R_y}\mathbf{Z}_{12 u_z u_z} I^{0000}_{u_z u_z i_1 j_1}\mathbf{u}_{zj_1} + {}^{H_x}_{H_y R_y^2}\mathbf{Z}_{22 u_z u_z} I^{0000}_{u_z u_z i_1 j_1}\mathbf{u}_{zj_1} \\
&\quad + {}^{H_x}\mathbf{Z}_{u_z s_y} I^{0100}_{u_z s_y i_1 j_2}\mathbf{s}_{yj_2} + {}^{H_y}\mathbf{Z}_{u_z s_x} I^{1000}_{u_z s_x i_1 j_2}\mathbf{s}_{xj_2} + {}^{H_xH_y}\mathbf{Z}_{\partial u_z s_z} I^{0000}_{u_z s_z i_1 j_2}\mathbf{s}_{zj_2}\Big] + \\
&\delta\mathbf{s}^T_{xi_2}\Big[{}^{H_y}\mathbf{Z}_{s_x u_z} I^{0010}_{s_x u_z i_2 j_1}\mathbf{u}_{zj_1} - \lambda_D\, {}^{H_y}_{R_x}\mathbf{Z}_{s_x u_x} I^{0000}_{s_x u_x i_2 j_1}\mathbf{u}_{xj_1} + {}^{H_xH_y}\mathbf{Z}^k_{s_x \partial u_x} I^{0000}_{s_x u_x i_2 j_1}\mathbf{u}_{xj_1} \\
&\quad - {}^{H_xH_y}\mathbf{Z}_{45 s_x s_y} I^{0000}_{s_x s_y i_2 j_2}\mathbf{s}_{yj_2} - {}^{H_xH_y}\mathbf{Z}_{55 s_x s_x} I^{0000}_{s_x s_x i_2 j_2}\mathbf{s}_{xj_2}\Big] + \\
&\delta\mathbf{s}^T_{yi_2}\Big[{}^{H_x}\mathbf{Z}_{s_y u_z} I^{0001}_{s_y u_z i_2 j_1}\mathbf{u}_{zj_1} - \lambda_D\, {}^{H_x}_{R_y}\mathbf{Z}_{s_y u_y} I^{0000}_{s_y u_y i_2 j_1}\mathbf{u}_{yj_1} + {}^{H_xH_y}\mathbf{Z}_{s_y \partial u_y} I^{0000}_{s_y u_y i_2 j_1}\mathbf{u}_{yj_1} \\
&\quad - {}^{H_xH_y}\mathbf{Z}_{44 s_y s_y} I^{0000}_{s_y s_y i_2 j_2}\mathbf{s}_{yj_2} - \mathbf{Z}_{45 s_y s_x} I^{0000}_{s_y s_x i_2 j_2}\mathbf{s}_{xj_2}\Big] + \\
&\delta\mathbf{s}^T_{zi_2}\Big[{}^{H_xH_y}\mathbf{Z}_{s_z \partial u_z} I^{0000}_{s_z u_z i_2 j_1}\mathbf{u}_{zj_1} + {}^{H_y}\mathbf{Z}_{13 s_z u_x} I^{0010}_{s_z u_x i_2 j_1}\mathbf{u}_{xj_1} + {}^{H_x}\mathbf{Z}_{23 s_z u_y} I^{0001}_{s_z u_y i_2 j_1}\mathbf{u}_{yj_1} \\
&\quad + {}^{H_x}\mathbf{Z}_{36 s_z u_x} I^{0001}_{s_z u_x i_2 j_1}\mathbf{u}_{xj_1} + {}^{H_y}\mathbf{Z}_{36 s_z u_y} I^{0010}_{s_z u_y i_2 j_1}\mathbf{u}_{yj_1} + {}^{H_y}_{R_x}\mathbf{Z}_{13 s_z u_z} I^{0000}_{s_z u_z i_2 j_1}\mathbf{u}_{zj_1} \\
&\quad + {}^{H_x}_{R_y}\mathbf{Z}_{23 s_z u_z} I^{0000}_{s_z u_z i_2 j_1}\mathbf{u}_{zj_1} - {}^{H_xH_y}\mathbf{Z}_{33 s_z s_z} I^{0000}_{s_z s_z i_2 j_2}\mathbf{s}_{zj_2}\Big] \\
&\quad = \delta\mathbf{u}^T_{zi_1}\mathbf{L}^{top}_{zi_1} I^{top}_{u_z f_z i_1} f^{top}_0 + \delta\mathbf{u}^T_{zi_1}\mathbf{L}^{bot}_{zi_1} I^{bot}_{u_z f_z i_1} f^{bot}_0
\end{aligned}
\tag{3.36}
$$

where the load amplitudes (f_0^{top}, f_0^{bot}) have been split from the function describing their

distribution in the (x, y) plane. Ritz load integrals are introduced:

$$\begin{aligned} I^{top}_{u_z f_z i_1} &= \int_x \int_y N_{u_z i_1} f_z^{top}(x,y)\left(1+\frac{h}{2R_x}\right)\left(1+\frac{h}{2R_y}\right)\mathrm{d}x\mathrm{d}y \\ I^{bot}_{u_z f_z i_1} &= \int_x \int_y N_{u_z i_1} f_z^{bot}(x,y)\left(1-\frac{h}{2R_x}\right)\left(1-\frac{h}{2R_y}\right)\mathrm{d}x\mathrm{d}y \end{aligned} \tag{3.37}$$

and

$$\mathbf{L}^{top}_{zi_1} = \begin{Bmatrix} 1 \\ 0 \\ \vdots \\ 0 \\ 0 \end{Bmatrix}_{(N_{DOF_{u_z}}\times 1)} \qquad \mathbf{L}^{bot}_{zi_1} = \begin{Bmatrix} 0 \\ 0 \\ \vdots \\ 0 \\ 1 \end{Bmatrix}_{(N_{DOF_{u_z}}\times 1)} \tag{3.38}$$

3.5 Mass and stiffness matrices

Finally, Eq.(3.36) can be written in a more compact manner through the introduction of the *mass matrix* ($\mathbf{M}_{ij}$) and the *stiffness matrix* ($\mathbf{K}_{ij}$):

$$\delta\mathbf{v}_i^T\mathbf{M}_{ij}\ddot{\mathbf{v}}_j + \delta\mathbf{v}_i^T\mathbf{K}_{ij}\mathbf{v}_j = \delta\mathbf{v}_i^T\mathbf{L}_i^{top}f_0^{top} + \delta\mathbf{v}_i^T\mathbf{L}_i^{bot}f_0^{bot} \tag{3.39}$$

where

$$\delta\mathbf{v}_i = \begin{Bmatrix} \delta\mathbf{u}_{xi_1} \\ \delta\mathbf{u}_{yi_1} \\ \delta\mathbf{u}_{zi_1} \\ \delta\mathbf{s}_{xi_2} \\ \delta\mathbf{s}_{yi_2} \\ \delta\mathbf{s}_{zi_2} \end{Bmatrix} \qquad \mathbf{v}_j = \begin{Bmatrix} \mathbf{u}_{xj_1} \\ \mathbf{u}_{yj_1} \\ \mathbf{u}_{zj_1} \\ \mathbf{s}_{xj_2} \\ \mathbf{s}_{yj_2} \\ \mathbf{s}_{zj_2} \end{Bmatrix} \qquad \mathbf{L}_i^{top} = \begin{Bmatrix} \mathbf{0} \\ \mathbf{0} \\ \mathbf{L}^{top}_{zi_1}I^{top}_{u_z f_z i_1} \\ \mathbf{0} \\ \mathbf{0} \\ \mathbf{0} \end{Bmatrix} \qquad \mathbf{L}_i^{bot} = \begin{Bmatrix} \mathbf{0} \\ \mathbf{0} \\ \mathbf{L}^{bot}_{zi_1}I^{bot}_{u_z f_z i_1} \\ \mathbf{0} \\ \mathbf{0} \\ \mathbf{0} \end{Bmatrix} \tag{3.40}$$

$$\mathbf{M}_{ij} = \begin{bmatrix} \mathbf{M}_{u_x u_x i_1 j_1} & \mathbf{0} & \mathbf{0} & \mathbf{0} & \mathbf{0} & \mathbf{0} \\ \mathbf{0} & \mathbf{M}_{u_y u_y i_1 j_1} & \mathbf{0} & \mathbf{0} & \mathbf{0} & \mathbf{0} \\ \mathbf{0} & \mathbf{0} & \mathbf{M}_{u_z u_z i_1 j_1} & \mathbf{0} & \mathbf{0} & \mathbf{0} \\ \mathbf{0} & \mathbf{0} & \mathbf{0} & \mathbf{0} & \mathbf{0} & \mathbf{0} \\ \mathbf{0} & \mathbf{0} & \mathbf{0} & \mathbf{0} & \mathbf{0} & \mathbf{0} \\ \mathbf{0} & \mathbf{0} & \mathbf{0} & \mathbf{0} & \mathbf{0} & \mathbf{0} \end{bmatrix} \tag{3.41}$$

$$\mathbf{K}_{ij} = \begin{bmatrix} \mathbf{K}_{u_x u_x i_1 j_1} & \mathbf{K}_{u_x u_y i_1 j_1} & \mathbf{K}_{u_x u_z i_1 j_1} & \mathbf{K}_{u_x s_x i_1 j_2} & \mathbf{0}_{u_x s_y i_1 j_2} & \mathbf{K}_{u_x s_z i_1 j_2} \\ \mathbf{K}_{u_y u_x i_1 j_1} & \mathbf{K}_{u_y u_y i_1 j_1} & \mathbf{K}_{u_y u_z i_1 j_1} & \mathbf{0}_{u_y s_x i_1 j_2} & \mathbf{K}_{u_y s_y i_1 j_2} & \mathbf{K}_{u_y s_z i_1 j_2} \\ \mathbf{K}_{u_z u_x i_1 j_1} & \mathbf{K}_{u_z u_y i_1 j_1} & \mathbf{K}_{u_z u_z i_1 j_1} & \mathbf{K}_{u_z s_x i_1 j_2} & \mathbf{K}_{u_z s_y i_1 j_2} & \mathbf{K}_{u_z s_z i_1 j_2} \\ \mathbf{K}_{s_x u_x i_2 j_1} & \mathbf{0}_{s_x u_y i_2 j_1} & \mathbf{K}_{s_x u_z i_2 j_1} & \mathbf{K}_{s_x s_x i_2 j_2} & \mathbf{K}_{s_x s_y i_2 j_2} & \mathbf{0}_{s_x s_z i_2 j_2} \\ \mathbf{0}_{s_y u_x i_2 j_1} & \mathbf{K}_{s_y u_y i_2 j_1} & \mathbf{K}_{s_y u_z i_2 j_1} & \mathbf{K}_{s_y s_x i_2 j_2} & \mathbf{K}_{s_y s_y i_2 j_2} & \mathbf{0}_{s_y s_z i_2 j_2} \\ \mathbf{K}_{s_z u_x i_2 j_1} & \mathbf{K}_{s_z u_y i_2 j_1} & \mathbf{K}_{s_z u_z i_2 j_1} & \mathbf{0}_{s_z s_x i_2 j_2} & \mathbf{0}_{s_z s_y i_2 j_2} & \mathbf{K}_{s_z s_z i_2 j_2} \end{bmatrix} \tag{3.42}$$

where:

$$
\begin{aligned}
\mathbf{M}_{u_x u_x i_1 j_1} &= {}^{H_x H_y}\mathbf{Z}_{\rho u_x u_x} I^{0000}_{u_x u_x i_1 j_1} \\
\mathbf{M}_{u_y u_y i_1 j_1} &= {}^{H_x H_y}\mathbf{Z}_{\rho u_y u_y} I^{0000}_{u_y u_y i_1 j_1} \\
\mathbf{M}_{u_z u_z i_1 j_1} &= {}^{H_x H_y}\mathbf{Z}_{\rho u_z u_z} I^{0000}_{u_z u_z i_1 j_1}
\end{aligned}
$$

$$
\begin{aligned}
\mathbf{K}_{u_x u_x i_1 j_1} &= {}^{H_y}_{H_x}\mathbf{Z}_{11 u_x u_x} I^{1010}_{u_x u_x i_1 j_1} + \mathbf{Z}_{16 u_x u_x}(I^{1001}_{u_x u_x i_1 j_1} + I^{0110}_{u_x u_x i_1 j_1}) \\
&\quad + {}^{H_x}_{H_y}\mathbf{Z}_{66 u_x u_x} I^{0101}_{u_x u_x i_1 j_1} \\
\mathbf{K}_{u_x u_y i_1 j_1} &= \mathbf{Z}_{12 u_x u_y} I^{1001}_{u_x u_y i_1 j_1} + {}^{H_y}_{H_x}\mathbf{Z}_{16 u_x u_y} I^{1010}_{u_x u_y i_1 j_1} \\
&\quad + {}^{H_x}_{H_y}\mathbf{Z}_{26 u_x u_y} I^{0101}_{u_x u_y i_1 j_1} + \mathbf{Z}_{66 u_x u_y} I^{0110}_{u_x u_y i_1 j_1} \\
\mathbf{K}_{u_x u_z i_1 j_1} &= {}^{H_y}_{H_x R_x}\mathbf{Z}_{11 u_x u_z} I^{1000}_{u_x u_z i_1 j_1} + {}_{R_y}\mathbf{Z}_{12 u_x u_z} I^{1000}_{u_x u_z i_1 j_1} + {}_{R_x}\mathbf{Z}_{16 u_x u_z} I^{0100}_{u_x u_z i_1 j_1} \\
&\quad + {}^{H_x}_{H_y R_y}\mathbf{Z}_{26 u_x u_z} I^{0100}_{u_x u_z i_1 j_1} \\
\mathbf{K}_{u_x s_x i_1 j_2} &= -\lambda_D\, {}^{H_y}_{R_x}\mathbf{Z}_{u_x s_x} I^{0000}_{u_x s_x i_1 j_2} + {}^{H_x H_y}\mathbf{Z}_{\partial u_x s_x} I^{0000}_{u_x s_x i_1 j_2} \\
\mathbf{K}_{u_x s_z i_1 j_2} &= {}^{H_x}\mathbf{Z}_{36 u_x s_z} I^{0100}_{u_x s_z i_1 j_2} + {}^{H_y}\mathbf{Z}_{13 u_x s_z} I^{1000}_{u_x s_z i_1 j_2} \\
\mathbf{K}_{u_y u_x i_1 j_1} &= \mathbf{Z}_{12 u_y u_x} I^{0110}_{u_y u_x i_1 j_1} + {}^{H_x}_{H_y}\mathbf{Z}_{26 u_y u_x} I^{0101}_{u_y u_x i_1 j_1} + {}^{H_y}_{H_x}\mathbf{Z}_{16 u_y u_x} I^{1010}_{u_y u_x i_1 j_1} \\
&\quad + \mathbf{Z}_{66 u_y u_x} I^{1001}_{u_y u_x i_1 j_1} \\
\mathbf{K}_{u_y u_y i_1 j_1} &= {}^{H_x}_{H_y}\mathbf{Z}_{22 u_y u_y} I^{0101}_{u_y u_y i_1 j_1} + \mathbf{Z}_{26 u_y u_y}(I^{0110}_{u_y u_y i_1 j_1} + I^{1001}_{u_y u_y i_1 j_1}) + {}^{H_y}_{H_x}\mathbf{Z}_{66 u_y u_y} I^{1010}_{u_y u_y i_1 j_1} \\
\mathbf{K}_{u_y u_z i_1 j_1} &= {}_{R_x}\mathbf{Z}_{12 u_y u_z} I^{0100}_{u_y u_z i_1 j_1} + {}^{H_x}_{H_y R_y}\mathbf{Z}_{22 u_y u_z} I^{0100}_{u_y u_z i_1 j_1} + {}^{H_y}_{H_x R_x}\mathbf{Z}_{16 u_y u_z} I^{1000}_{u_y u_z i_1 j_1} \\
&\quad + {}_{R_y}\mathbf{Z}_{26 u_y u_z} I^{1000}_{u_y u_z i_1 j_1} \\
\mathbf{K}_{u_y s_y i_1 j_2} &= -\lambda_D\, {}^{H_x}_{R_y}\mathbf{Z}_{u_y s_y} I^{0000}_{u_y s_y i_1 j_2} + {}^{H_x H_y}\mathbf{Z}_{\partial u_y s_y} I^{0000}_{u_y s_y i_1 j_2} \\
\mathbf{K}_{u_y s_z i_1 j_2} &= {}^{H_x}\mathbf{Z}_{23 u_y s_z} I^{0100}_{u_y s_z i_1 j_2} + {}^{H_y}\mathbf{Z}_{36 u_y s_z} I^{1000}_{u_y s_z i_1 j_2} \\
\mathbf{K}_{u_z u_x i_1 j_1} &= {}^{H_y}_{H_x R_x}\mathbf{Z}_{11 u_z u_x} I^{0010}_{u_z u_x i_1 j_1} + {}_{R_y}\mathbf{Z}_{12 u_z u_x} I^{0010}_{u_z u_x i_1 j_1} + {}^{H_x}_{H_y R_y}\mathbf{Z}_{26 u_z u_x} I^{0001}_{u_z u_x i_1 j_1} \\
&\quad + {}_{R_x}\mathbf{Z}_{16 u_z u_x} I^{0001}_{u_z u_x i_1 j_1} \\
\mathbf{K}_{u_z u_y i_1 j_1} &= {}_{R_x}\mathbf{Z}_{12 u_z u_y} I^{0001}_{u_z u_y i_1 j_1} + {}^{H_y}_{H_x R_x}\mathbf{Z}_{16 u_z u_y} I^{0010}_{u_z u_y i_1 j_1} + {}^{H_x}_{H_y R_y}\mathbf{Z}_{22 u_z u_y} I^{0001}_{u_z u_y i_1 j_1} \\
&\quad + {}_{R_y}\mathbf{Z}_{26 u_z u_y} I^{0010}_{u_z u_y i_1 j_1} \\
\mathbf{K}_{u_z u_z i_1 j_1} &= {}^{H_y}_{H_x R_x^2}\mathbf{Z}_{11 u_z u_z} I^{0000}_{u_z u_z i_1 j_1} + {}_{R_x R_y}\mathbf{Z}_{12 u_z u_z} I^{0000}_{u_z u_z i_1 j_1} + {}_{R_x R_y}\mathbf{Z}_{12 u_z u_z} I^{0000}_{u_z u_z i_1 j_1} \\
&\quad + {}^{H_x}_{H_y R_y^2}\mathbf{Z}_{22 u_z u_z} I^{0000}_{u_z u_z i_1 j_1} \\
\mathbf{K}_{u_z s_x i_1 j_2} &= {}^{H_y}\mathbf{Z}_{u_z s_x} I^{1000}_{u_z s_x i_1 j_2} \\
\mathbf{K}_{u_z s_y i_1 j_2} &= {}^{H_x}\mathbf{Z}_{u_z s_y} I^{0100}_{u_z s_y i_1 j_2} \\
\mathbf{K}_{u_z s_z i_1 j_2} &= {}^{H_x H_y}\mathbf{Z}_{\partial u_z s_z} I^{0000}_{u_z s_z i_1 j_2} + {}^{H_y}_{R_x}\mathbf{Z}_{13 u_z s_z} I^{0000}_{u_z s_z i_1 j_2} + {}^{H_x}_{R_y}\mathbf{Z}_{23 u_z s_z} I^{0000}_{u_z s_z i_1 j_2} \\
\mathbf{K}_{s_x u_x i_2 j_1} &= -\lambda_D\, {}^{H_y}_{R_x}\mathbf{Z}_{s_x u_x} I^{0000}_{s_x u_x i_2 j_1} + {}^{H_x H_y}\mathbf{Z}_{s_x \partial u_x} I^{0000}_{s_x u_x i_2 j_1} \\
\mathbf{K}_{s_x u_z i_2 j_1} &= {}^{H_y}\mathbf{Z}_{s_x u_z} I^{0010}_{s_x u_z i_2 j_1} \\
\mathbf{K}_{s_x s_x i_2 j_2} &= -\,{}^{H_x H_y}\mathbf{Z}_{55 s_x s_x} I^{0000}_{s_x s_x i_2 j_2}
\end{aligned}
$$

$$
\begin{aligned}
\mathbf{K}_{s_x s_y i_2 j_2} &= -\,{}^{H_x H_y}\mathbf{Z}_{45 s_x s_y} I^{0000}_{s_x s_y i_2 j_2} \\
\mathbf{K}_{s_y u_y i_2 j_1} &= -\lambda_D\,{}^{H_x}_{R_y}\mathbf{Z}_{s_y u_y} I^{0000}_{s_y u_y i_2 j_1} + {}^{H_x H_y}\mathbf{Z}_{s_y \partial u_y} I^{0000}_{s_y u_y i_2 j_1} \\
\mathbf{K}_{s_y u_z i_2 j_1} &= {}^{H_x}\mathbf{Z}_{s_y u_z} I^{0001}_{s_y u_z i_2 j_1} \\
\mathbf{K}_{s_y s_x i_2 j_2} &= -\mathbf{Z}_{45 s_y s_x} I^{0000}_{s_y s_x i_2 j_2} \\
\mathbf{K}_{s_y s_y i_2 j_2} &= -\,{}^{H_x H_y}\mathbf{Z}_{44 s_y s_y} I^{0000}_{s_y s_y i_2 j_2} \\
\mathbf{K}_{s_z u_x i_2 j_1} &= {}^{H_y}\mathbf{Z}_{13 s_z u_x} I^{0010}_{s_z u_x i_2 j_1} + {}^{H_x}\mathbf{Z}_{36 s_z u_x} I^{0001}_{s_z u_x i_2 j_1} \\
\mathbf{K}_{s_z u_y i_2 j_1} &= {}^{H_x}\mathbf{Z}_{23 s_z u_y} I^{0001}_{s_z u_y i_2 j_1} + {}^{H_y}\mathbf{Z}_{36 s_z u_y} I^{0010}_{s_z u_y i_2 j_1} \\
\mathbf{K}_{s_z u_z i_2 j_1} &= {}^{H_x H_y}\mathbf{Z}_{s_z \partial u_z} I^{0000}_{s_z u_z i_2 j_1} + {}^{H_y}_{R_x}\mathbf{Z}_{13 s_z u_z} I^{0000}_{s_z u_z i_2 j_1} + {}^{H_x}_{R_y}\mathbf{Z}_{23 s_z u_z} I^{0000}_{s_z u_z i_2 j_1} \\
\mathbf{K}_{s_z s_z i_2 j_2} &= -\,{}^{H_x H_y}\mathbf{Z}_{33 s_z s_z} I^{0000}_{s_z s_z i_2 j_2}
\end{aligned}
$$

General subscripts i and j range from 1 to the largest value between M_u and M_s, from here on denoted with M. The variables expanded with the lowest Ritz order will contribute only up to that specific order, while for the remaining orders their contributions will be null.

3.6 Ritz expansion

The final step deals with the summation of the Ritz expansion series represented through indexes i and j. Written explicitly, the shell equilibrium equations in a weak form are:

$$
\begin{aligned}
&\delta\mathbf{v}_1^T[\mathbf{M}_{11}\ddot{\mathbf{v}}_1 + \ldots + \mathbf{M}_{1M}\ddot{\mathbf{v}}_M + \mathbf{K}_{11}\mathbf{v}_1 + \ldots + \mathbf{K}_{1M}\mathbf{v}_M] = \delta\mathbf{v}_1^T[\mathbf{L}_1^{top} f_0^{top} + \mathbf{L}_1^{bot} f_0^{bot}] \\
&\delta\mathbf{v}_2^T[\mathbf{M}_{21}\ddot{\mathbf{v}}_1 + \ldots + \mathbf{M}_{2M}\ddot{\mathbf{v}}_M + \mathbf{K}_{21}\mathbf{v}_1 + \ldots + \mathbf{K}_{2M}\mathbf{v}_M] = \delta\mathbf{v}_2^T[\mathbf{L}_2^{top} f_0^{top} + \mathbf{L}_2^{bot} f_0^{bot}] \\
&\quad\vdots \\
&\delta\mathbf{v}_M^T[\mathbf{M}_{M1}\ddot{\mathbf{v}}_1 + \ldots + \mathbf{M}_{MM}\ddot{\mathbf{v}}_M + \mathbf{K}_{M1}\mathbf{v}_1 + \ldots + \mathbf{K}_{MM}\mathbf{v}_M] = \delta\mathbf{v}_M^T[\mathbf{L}_M^{top} f_0^{top} + \mathbf{L}_M^{bot} f_0^{bot}]
\end{aligned}
\tag{3.46}
$$

Therefore, regrouping all the variables into one vector:

$$
\mathbf{v} = \left\{ \begin{array}{c} \mathbf{u}_{x1} \\ \mathbf{u}_{y1} \\ \mathbf{u}_{z1} \\ \mathbf{s}_{x1} \\ \mathbf{s}_{y1} \\ \mathbf{s}_{z1} \\ \vdots \\ \mathbf{u}_{xi} \\ \vdots \\ \mathbf{s}_{zi} \\ \vdots \\ \mathbf{u}_{xM} \\ \vdots \\ \mathbf{s}_{zM} \end{array} \right\} = \left\{ \begin{array}{c} \mathbf{v}_1 \\ \vdots \\ \mathbf{v}_i \\ \vdots \\ \mathbf{v}_M \end{array} \right\} \tag{3.47}
$$

Assembling matrices $\mathbf{M}_{ij}$, $\mathbf{K}_{ij}$ and $\mathbf{L}_i$, symbolically expressed by:

$$\begin{aligned} \mathbf{M}_{ij} &\xrightarrow[(i,j)\text{ cycling}]{\text{Ritz expansion}} \mathbf{M} \\ \mathbf{K}_{ij} &\xrightarrow[(i,j)\text{ cycling}]{\text{Ritz expansion}} \mathbf{K} \\ \mathbf{L}_{i} &\xrightarrow[(i)\text{ cycling}]{\text{Ritz expansion}} \mathbf{L} \end{aligned} \tag{3.48}$$

and using the arbitrariness of virtual variations, the set of governing equations is obtained:

$$\mathbf{M}\ddot{\mathbf{v}} + \mathbf{K}\mathbf{v} = \mathbf{L} \tag{3.49}$$

where

$$\mathbf{L} = \mathbf{L}^{top} f_0^{top} + \mathbf{L}^{bot} f_0^{bot} \tag{3.50}$$

Even if equations for doubly-curved shells have been derived, the present work will focus on *cylindrical geometries* (both open and closed) and *plate geometries* due to their broad employment compared to general doubly-curved shells.

The governing equations for cylindrical geometries can be easily obtained starting from the equations for shells by imposing either $R_x \to \infty$ or $R_y \to \infty$ (it implies that $H_x \to 1$ or $H_y \to 1$, respectively). Additional details on the cylinder governing equations can be found in Section C.1, in Appendix C.

The governing equations for plate geometries can be easily obtained starting from the equations for shells by imposing $R_x \to \infty$ and $R_y \to \infty$ (it implies that $H_x \to 1$ and $H_y \to 1$, respectively). Additional details on the plate governing equations can be found in Section C.2, in Appendix C. It is remarked that in plate equations, compared to shell and cylinder equations, less coupling terms are present. Sub-stiffness matrices $\mathbf{K}_{u_x u_z i_1 j_1}$, $\mathbf{K}_{u_z u_x i_1 j_1}$, $\mathbf{K}_{u_y u_z i_1 j_1}$, $\mathbf{K}_{u_z u_y i_1 j_1}$ and $\mathbf{K}_{u_z u_z i_1 j_1}$ are null.

3.7 Linear static and free-vibration analysis

After computing matrices $\mathbf{M}$ and $\mathbf{K}$ it is possible to solve a broad number of problems. The focus is here posed upon the *linear static* and the *free-vibration analysis*.

Linear static analysis The cases here investigated concern normal loads applied to the top and bottom surfaces. Four distinct load cases can be taken into account in the code: localized loads, concentrated loads (over a finite portion of the structure), uniform loads, and bisinusoidal loads.

The solution of linear static problems is of interest to check the potential of the RMVT formulation in providing improved profiles for the transverse stresses, whose continuity is enforced a priori.

The problem can be formulated starting from Eq.(3.49) and neglecting time dependence, resulting in:

$$\mathbf{K}\mathbf{v} = \mathbf{L}^{top} f_0^{top} + \mathbf{L}^{bot} f_0^{bot} \tag{3.51}$$

or more compactly:

$$\mathbf{K}\mathbf{v} = \mathbf{L} \tag{3.52}$$

where:

$$\mathbf{L} = \mathbf{L}^{top} f_0^{top} + \mathbf{L}^{bot} f_0^{bot} \tag{3.53}$$

The linear system of Eq.(3.52) is then solved numerically and the unknown Ritz amplitudes are found as part of the solution. The evaluation of the displacement and stress fields can be operated during the post-processing of the results, as outlined in the next section.

Free-vibration The free-vibration analysis deals with the homogeneous problem, which is obtained when the loads are set to zero, i.e.:

$$f_0^{top} = 0 \qquad f_0^{bot} = 0 \tag{3.54}$$

The problem obtained is therefore:

$$\mathbf{M}\ddot{\mathbf{v}} + \mathbf{K}\mathbf{v} = \mathbf{0} \tag{3.55}$$

As anticipated before, Eq.(3.55) has the structure of an eigenvalue problem. A trivial solution of the problem is $\mathbf{v}(t) = \mathbf{0}$. In order to obtain non-trivial solutions the following solution is hypothesized:

$$\mathbf{v}(t) = \hat{\mathbf{v}} e^{j\omega t} \tag{3.56}$$

Substituting it into Eq.(3.55), the problem is obtained in the form:

$$[\mathbf{K} - \omega^2 \mathbf{M}]\hat{\mathbf{v}} = \mathbf{0} \tag{3.57}$$

which is a standard eigenvalue problem, whose solution allows the natural frequencies and corresponding eigenmodes to be found.

Due to the approach here adopted the size of the matrices is very high, and therefore to compute all of the eigenpairs would result in a too expensive computational effort. Therefore, usually, only a subset of these eigenpairs will be computed when solving the problem,

starting from those associated with lower frequencies. Furthermore, to compute all of the eigenpairs would result in a useless effort, since many would be associated with high frequencies, but since the loads usually have limited spectral content, these modes would be barely, if not at all, excited.

Compared to the equations obtained through the PVD, the equations based upon RMVT include both displacement and stress unknowns.

A *Static Condensation Technique* (SCT) can be operated, as illustrated below, consisting in the elimination of the stress variables. This technique will be here adopted when performing the *free-vibration analysis* to directly retrieve physical quantities.

Referring to Eq.(3.49), the vector $\mathbf{v}$ can be partitioned into $\mathbf{u}$ and $\mathbf{s}$, corresponding to displacement- and stress-related DOF, respectively. The governing equations in Eq.(3.49) can then be re-written as:

$$\begin{cases} \mathbf{M_{uu}}\ddot{\mathbf{u}} + \mathbf{K_{uu}}\mathbf{u} + \mathbf{K_{us}}\mathbf{s} = \mathbf{L} \\ \mathbf{K_{su}}\mathbf{u} + \mathbf{K_{ss}}\mathbf{s} = \mathbf{0} \end{cases} \tag{3.58}$$

where

$$\mathbf{u} = \begin{Bmatrix} \mathbf{u}_{x1} \\ \mathbf{u}_{y1} \\ \mathbf{u}_{z1} \\ \vdots \\ \mathbf{u}_{xj_1} \\ \mathbf{u}_{yj_1} \\ \mathbf{u}_{zj_1} \\ \vdots \\ \mathbf{u}_{xM_u} \\ \mathbf{u}_{yM_u} \\ \mathbf{u}_{zM_u} \end{Bmatrix} \qquad \mathbf{s} = \begin{Bmatrix} \mathbf{s}_{x1} \\ \mathbf{s}_{y1} \\ \mathbf{s}_{z1} \\ \vdots \\ \mathbf{s}_{xj_2} \\ \mathbf{s}_{yj_2} \\ \mathbf{s}_{zj_2} \\ \vdots \\ \mathbf{s}_{xM_s} \\ \mathbf{s}_{yM_s} \\ \mathbf{s}_{zM_s} \end{Bmatrix} \tag{3.59}$$

using the second equation of Eq.(3.58):

$$\mathbf{s} = -(\mathbf{K_{ss}})^{-1}\mathbf{K_{su}}\mathbf{u} \tag{3.60}$$

and then substituting into the first equation of Eq.(3.58):

$$\mathbf{M_{uu}}\ddot{\mathbf{u}} + (\mathbf{K_{uu}} - \mathbf{K_{us}}(\mathbf{K_{ss}})^{-1}\mathbf{K_{su}})\mathbf{u} = \mathbf{L} \tag{3.61}$$

redefining:

$$\mathbf{K_{mix}} = \mathbf{K_{uu}} - \mathbf{K_{us}}(\mathbf{K_{ss}})^{-1}\mathbf{K_{su}} \tag{3.62}$$

the expression of Eq.(3.61) becomes:

$$\mathbf{M_{uu}}\ddot{\mathbf{u}} + \mathbf{K_{mix}}\mathbf{u} = \mathbf{L} \tag{3.63}$$

After computing the displacements through Eq.(3.63), the stresses can be obtained *a posteriori* by means of Eq.(3.60).

Note that the SCT leads to the same results as solving the whole system. The results would differ in case it was applied at sublaminate or ply level. However, in that case, it would not be possible to enforce the continuity of transverse stresses at the interfaces.

3.8 Post-processing of the solution

After solving the problem, either it is linear static or free-vibration, the unknown Ritz amplitudes are found. From there, the displacements field can be retrieved as:

$$\left\{\begin{array}{lll} u_x^{p,k}(x,y,z,t) = F_{\beta_{u_x}}(z)u_{x\beta_{u_x}}^{p,k}(x,y,t) & = F_{\beta_{u_x}}(z)N_{u_xj_1}(x,y)u_{x\beta_{u_x}j_1}^{p,k}(t) & \\ u_y^{p,k}(x,y,z,t) = F_{\beta_{u_y}}(z)u_{y\beta_{u_y}}^{p,k}(x,y,t) & = F_{\beta_{u_y}}(z)N_{u_yj_1}(x,y)u_{y\beta_{u_y}j_1}^{p,k}(t) & j_1 = 1,2,...,M_u \\ u_z^{p,k}(x,y,z,t) = F_{\beta_{u_z}}(z)u_{z\beta_{u_z}}^{p,k}(x,y,t) & = F_{\beta_{u_z}}(z)N_{u_zj_1}(x,y)u_{z\beta_{u_z}j_1}^{p,k}(t) & \end{array}\right. \tag{3.64}$$

Regarding *transverse stresses*, it is possible to proceed in three ways to recover them: *a priori* by using the test functions used in RMVT, through the *classical form of Hooke's law* or by *integration of the indefinite equilibrium equations.*

A priori:

$$\left\{\begin{array}{lll} s_x^{p,k}(x,y,z,t) = \mathcal{F}_{\beta_{s_x}}(z)s_{x\beta_{s_x}}^{p,k}(x,y,t) & = \mathcal{F}_{\beta_{s_x}}(z)N_{s_xj_2}(x,y)s_{x\beta_{s_x}j_2}^{p,k}(t) & \\ s_y^{p,k}(x,y,z,t) = \mathcal{F}_{\beta_{s_y}}(z)s_{y\beta_{s_y}}^{p,k}(x,y,t) & = \mathcal{F}_{\beta_{s_y}}(z)N_{s_yj_2}(x,y)s_{y\beta_{s_y}j_2}^{p,k}(t) & j_2 = 1,2,...,M_s \\ s_z^{p,k}(x,y,z,t) = \mathcal{F}_{\beta_{s_z}}(z)s_{z\beta_{s_z}}^{p,k}(x,y,t) & = \mathcal{F}_{\beta_{s_z}}(z)N_{s_zj_2}(x,y)s_{z\beta_{s_z}j_2}^{p,k}(t) & \end{array}\right. \tag{3.65}$$

Classical form of Hooke's law:

For plates:

$$\begin{aligned} \sigma_{yz}^{p,k} =& C_{44}^{p,k}\frac{\partial N_{u_zj_1}}{\partial y}F_{\beta_{u_z}}u_{z\beta_{u_z}j_1}^{p,k} + C_{44}^{p,k}N_{u_zj_1}\frac{\partial F_{\beta_{u_y}}}{\partial z}u_{y\beta_{u_y}j_1}^{p,k} + C_{45}^{p,k}\frac{\partial N_{u_zj_1}}{\partial x}F_{\beta_{u_z}}u_{z\beta_{u_z}j_1}^{p,k} \\ &+ C_{45}^{p,k}N_{u_xj_1}\frac{\partial F_{\beta_{u_x}}}{\partial z}u_{x\beta_{u_x}j_1}^{p,k} \\ \sigma_{xz}^{p,k} =& C_{45}^{p,k}\frac{\partial N_{u_zj_1}}{\partial y}F_{\beta_{u_z}}u_{z\beta_{u_z}j_1}^{p,k} + C_{45}^{p,k}N_{u_zj_1}\frac{\partial F_{\beta_{u_y}}}{\partial z}u_{y\beta_{u_y}j_1}^{p,k} + C_{55}^{p,k}\frac{\partial N_{u_zj_1}}{\partial x}F_{\beta_{u_z}}u_{z\beta_{u_z}j_1}^{p,k} \\ &+ C_{55}^{p,k}N_{u_xj_1}\frac{\partial F_{\beta_{u_x}}}{\partial z}u_{x\beta_{u_x}j_1}^{p,k} \\ \sigma_{zz}^{p,k} =& C_{13}^{p,k}\frac{\partial N_{u_xj_1}}{\partial x}F_{\beta_{u_x}}u_{x\beta_{u_x}j_1}^{p,k} + C_{23}^{p,k}\frac{\partial N_{u_yj_1}}{\partial y}F_{\beta_{u_y}}u_{y\beta_{u_y}j_1}^{p,k} + C_{33}^{p,k}N_{u_zj_1}\frac{F_{\beta_{u_z}}}{\partial z}u_{z\beta_{u_z}j_1}^{p,k} \\ &+ C_{36}^{p,k}\frac{\partial N_{u_yj_1}}{\partial x}F_{\beta_{u_y}}u_{y\beta_{u_y}j_1}^{p,k} + C_{36}^{p,k}\frac{\partial N_{u_xj_1}}{\partial y}F_{\beta_{u_x}}u_{x\beta_{u_x}j_1}^{p,k} \end{aligned} \tag{3.66}$$

For cylinders:

$$
\begin{aligned}
\sigma_{yz}^{p,k} =& -\frac{1}{R_y(1+\frac{z}{R_y})} C_{44}^{p,k} N_{u_x j_1} F_{\beta_{u_y}} u_{y\beta_{u_y} j_1}^{p,k} + \frac{1}{1+\frac{z}{R_y}} C_{44}^{p,k} \frac{\partial N_{u_z j_1}}{\partial y} F_{\beta_{u_z}} u_{z\beta_{u_z} j_1}^{p,k} \\
&+ C_{44}^{p,k} N_{u_y j_1} \frac{F_{\beta_{u_y}}}{\partial z} u_{y\beta_{u_y} j_1}^{p,k} + C_{45}^{p,k} \frac{\partial N_{u_z j_1}}{\partial x} F_{\beta_{u_z}} u_{z\beta_{u_z} j_1}^{p,k} + C_{45}^{p,k} N_{u_x j_1} \frac{F_{\beta_{u_x}}}{\partial z} u_{x\beta_{u_x} j_1}^{p,k} \\
\sigma_{xz}^{p,k} =& -\frac{1}{R_y(1+\frac{z}{R_y})} C_{45}^{p,k} N_{u_x j_1} F_{\beta_{u_y}} u_{y\beta_{u_y} j_1}^{p,k} + \frac{1}{1+\frac{z}{R_y}} C_{45}^{p,k} \frac{\partial N_{u_z j_1}}{\partial y} F_{\beta_{u_z}} u_{z\beta_{u_z} j_1}^{p,k} \\
&+ C_{45}^{p,k} N_{u_y j_1} \frac{F_{\beta_{u_y}}}{\partial z} u_{y\beta_{u_y} j_1}^{p,k} + C_{55}^{p,k} \frac{\partial N_{u_z j_1}}{\partial x} F_{\beta_{u_z}} u_{z\beta_{u_z} j_1}^{p,k} + C_{55}^{p,k} N_{u_x j_1} \frac{F_{\beta_{u_x}}}{\partial z} u_{x\beta_{u_x} j_1}^{p,k} \\
\sigma_{zz}^{p,k} =& C_{13}^{p,k} \frac{\partial N_{u_x j_1}}{\partial x} F_{\beta_{u_x}} u_{x\beta_{u_x} j_1}^{p,k} + \frac{1}{1+\frac{z}{R_y}} C_{23}^{p,k} \frac{\partial N_{u_y j_1}}{\partial y} F_{\beta_{u_y}} u_{y\beta_{u_y} j_1}^{p,k} \\
&+ \frac{1}{R_y(1+\frac{z}{R_y})} C_{23}^{p,k} N_{u_z j_1} F_{\beta_{u_z}} u_{z\beta_{u_z} j_1}^{p,k} + C_{33}^{p,k} N_{u_z j_1} \frac{F_{\beta_{u_z}}}{\partial z} u_{z\beta_{u_z} j_1}^{p,k} \\
&+ C_{33}^{p,k} \frac{\partial N_{u_y j_1}}{\partial x} F_{\beta_{u_y}} u_{y\beta_{u_y} j_1}^{p,k} + \frac{1}{1+\frac{z}{R_y}} C_{36}^{p,k} \frac{\partial N_{u_x j_1}}{\partial x} F_{\beta_{u_x}} u_{x\beta_{u_x} j_1}^{p,k}
\end{aligned}
\tag{3.67}
$$

Integration of the indefinite equilibrium equations:

For plates:

$$
\begin{aligned}
&\frac{\partial \sigma_{xx}}{\partial x} + \frac{\partial \sigma_{xy}}{\partial y} + \frac{\partial \sigma_{xz}}{\partial z} = 0 \Rightarrow \frac{\partial \sigma_{xz}}{\partial z} = -\left(\frac{\partial \sigma_{xx}}{\partial x} + \frac{\partial \sigma_{xy}}{\partial y} \right) \\
&\frac{\partial \sigma_{xy}}{\partial x} + \frac{\partial \sigma_{yy}}{\partial y} + \frac{\partial \sigma_{yz}}{\partial z} = 0 \Rightarrow \frac{\partial \sigma_{yz}}{\partial z} = -\left(\frac{\partial \sigma_{xy}}{\partial x} + \frac{\partial \sigma_{yy}}{\partial y} \right) \\
&\frac{\partial \sigma_{xz}}{\partial x} + \frac{\partial \sigma_{yz}}{\partial y} + \frac{\partial \sigma_{zz}}{\partial z} = 0 \Rightarrow \frac{\partial \sigma_{zz}}{\partial z} = -\left(\frac{\partial \sigma_{xz}}{\partial x} + \frac{\partial \sigma_{yz}}{\partial y} \right)
\end{aligned}
\tag{3.68}
$$

For cylinders:

$$
\begin{aligned}
&\left(1+\frac{z}{R_y}\right) \frac{\partial \sigma_{xx}}{\partial x} + \frac{\partial \sigma_{xy}}{\partial y} + \frac{\partial}{\partial z}\left[\left(1+\frac{z}{R_y}\right) \sigma_{xz} \right] = 0 \\
&\left(1+\frac{z}{R_y}\right)^2 \frac{\partial \sigma_{xy}}{\partial x} + \left(1+\frac{z}{R_y}\right) \frac{\partial \sigma_{yy}}{\partial y} + \frac{\partial}{\partial z}\left[\left(1+\frac{z}{R_y}\right)^2 \sigma_{yz} \right] = 0 \\
&\left(1+\frac{z}{R_y}\right) \frac{\partial \sigma_{xz}}{\partial x} + \frac{\partial \sigma_{yz}}{\partial y} + \frac{\partial}{\partial z}\left[\left(1+\frac{z}{R_y}\right) \sigma_{zz} \right] - \frac{\sigma_{yy}}{R_y} = 0
\end{aligned}
\tag{3.69}
$$

It is worth specifying that in the code, σ_{xz} and σ_{yz} are calculated by integrating the derivatives of $\sigma_{xx}, \sigma_{yy}, \sigma_{xy}$ obtained through the CFHL. Although, this choice may not be consistent when a mixed approach is adopted, for a "converged" case using the CFHL or the MFHL will results in practically equal results, as stated by Demasi [33]. For the same reason, σ_{zz} is obtained by integrating the derivatives of the transverse shear stresses calculated using the CFHL.

Finally, it is important to remark that among the three possible ways to recover the transverse stresses, only computing them *a priori* or by *integration of the indefinite equilibrium equations* allows satisfying the inter-laminar equilibrium condition.

As regards with *in-plane stresses*, they can be evaluated by recalling the MFHL.

For plates:

$$\begin{aligned}
\sigma_{xx}^{p,k} =& C_{11}^{p,k}\frac{\partial N_{u_x j_1}}{\partial x}F_{\beta_{u_x}}u_{x\beta_{u_x}j_1}^{p,k} + C_{12}^{p,k}\frac{\partial N_{u_y j_1}}{\partial y}F_{\beta_{u_y}}u_{y\beta_{u_y}j_1}^{p,k} + C_{16}^{p,k}\frac{\partial N_{u_y j_1}}{\partial x}F_{\beta_{u_y}}u_{y\beta_{u_y}j_1}^{p,k} \\
&+ C_{16}^{p,k}\frac{\partial N_{u_x j_1}}{\partial y}F_{\beta_{u_x}}u_{x\beta_{u_x}j_1}^{p,k} + C_{13}^{p,k}N_{\sigma_{zz}j_2}F_{\beta_{\sigma_{zz}}}\sigma_{zz\beta_{\sigma_{zz}}j_2}^{p,k} \\
\sigma_{yy}^{p,k} =& C_{12}^{p,k}\frac{\partial N_{u_x j_1}}{\partial x}F_{\beta_{u_x}}u_{x\beta_{u_x}j_1}^{p,k} + C_{22}^{p,k}\frac{\partial N_{u_y j_1}}{\partial y}F_{\beta_{u_y}}u_{y\beta_{u_y}j_1}^{p,k} + C_{26}^{p,k}\frac{\partial N_{u_y j_1}}{\partial x}F_{\beta_{u_y}}u_{y\beta_{u_y}j_1}^{p,k} \\
&+ C_{26}^{p,k}\frac{\partial N_{u_x j_1}}{\partial y}F_{\beta_{u_x}}u_{x\beta_{u_x}j_1}^{p,k} + C_{26}^{p,k}N_{\sigma_{zz}j_2}F_{\beta_{\sigma_{zz}}}\sigma_{zz\beta_{\sigma_{zz}}j_2}^{p,k} \\
\sigma_{xy}^{p,k} =& C_{16}^{p,k}\frac{\partial N_{u_x j_1}}{\partial x}F_{\beta_{u_x}}u_{x\beta_{u_x}j_1}^{p,k} + C_{26}^{p,k}\frac{\partial N_{u_y j_1}}{\partial y}F_{\beta_{u_y}}u_{y\beta_{u_y}j_1}^{p,k} + C_{66}^{p,k}\frac{\partial N_{u_y j_1}}{\partial x}F_{\beta_{u_y}}u_{y\beta_{u_y}j_1}^{p,k} \\
&+ C_{66}^{p,k}\frac{\partial N_{u_x j_1}}{\partial y}F_{\beta_{u_x}}u_{x\beta_{u_x}j_1}^{p,k} + C_{36}^{p,k}N_{\sigma_{zz}j_2}F_{\beta_{\sigma_{zz}}}\sigma_{zz\beta_{\sigma_{zz}}j_2}^{p,k}
\end{aligned} \tag{3.70}$$

For cylinders:

$$\begin{aligned}
\sigma_{xx}^{p,k} =& C_{11}^{p,k}\frac{\partial N_{u_x j_1}}{\partial x}F_{\beta_{u_x}}u_{x\beta_{u_x}j_1}^{p,k} + \frac{1}{1+\frac{z}{R_y}}C_{12}^{p,k}\frac{\partial N_{u_y j_1}}{\partial y}F_{\beta_{u_y}}u_{y\beta_{u_y}j_1}^{p,k} \\
&+ C_{16}^{p,k}\frac{\partial N_{u_y j_1}}{\partial x}F_{\beta_{u_y}}u_{y\beta_{u_y}j_1}^{p,k} + \frac{1}{1+\frac{z}{R_y}}C_{16}^{p,k}\frac{\partial N_{u_x j_1}}{\partial y}F_{\beta_{u_x}}u_{x\beta_{u_x}j_1}^{p,k} \\
&+ \frac{1}{R_y(1+\frac{z}{R_y})}C_{12}^{p,k}N_{u_z j_1}F_{\beta_{u_z}}u_{z\beta_{u_z}j_1}^{p,k} + C_{13}^{p,k}N_{\sigma_{zz}j_2}F_{\beta_{\sigma_{zz}}}\sigma_{zz\beta_{\sigma_{zz}}j_2}^{p,k} \\
\sigma_{yy}^{p,k} =& C_{12}^{p,k}\frac{\partial N_{u_x j_1}}{\partial x}F_{\beta_{u_x}}u_{x\beta_{u_x}j_1}^{p,k} + \frac{1}{1+\frac{z}{R_y}}C_{22}^{p,k}\frac{\partial N_{u_y j_1}}{\partial y}F_{\beta_{u_y}}u_{y\beta_{u_y}j_1}^{p,k} \\
&+ C_{26}^{p,k}\frac{\partial N_{u_y j_1}}{\partial x}F_{\beta_{u_y}}u_{y\beta_{u_y}j_1}^{p,k} + \frac{1}{1+\frac{z}{R_y}}C_{26}^{p,k}\frac{\partial N_{u_x j_1}}{\partial y}F_{\beta_{u_x}}u_{x\beta_{u_x}j_1}^{p,k} \\
&+ \frac{1}{R_y(1+\frac{z}{R_y})}C_{22}^{p,k}N_{u_z j_1}F_{\beta_{u_z}}u_{z\beta_{u_z}j_1}^{p,k} + C_{23}^{p,k}N_{\sigma_{zz}j_2}F_{\beta_{\sigma_{zz}}}\sigma_{zz\beta_{\sigma_{zz}}j_2}^{p,k} \\
\sigma_{xy}^{p,k} =& C_{16}^{p,k}\frac{\partial N_{u_x j_1}}{\partial x}F_{\beta_{u_x}}u_{x\beta_{u_x}j_1}^{p,k} + \frac{1}{1+\frac{z}{R_y}}C_{26}^{p,k}\frac{\partial N_{u_y j_1}}{\partial y}F_{\beta_{u_y}}u_{y\beta_{u_y}j_1}^{p,k} \\
&+ C_{66}^{p,k}\frac{\partial N_{u_y j_1}}{\partial x}F_{\beta_{u_y}}u_{y\beta_{u_y}j_1}^{p,k} + \frac{1}{1+\frac{z}{R_y}}C_{66}^{p,k}\frac{\partial N_{u_x j_1}}{\partial y}F_{\beta_{u_x}}u_{x\beta_{u_x}j_1}^{p,k} \\
&+ \frac{1}{R_y(1+\frac{z}{R_y})}C_{26}^{p,k}N_{u_z j_1}F_{\beta_{u_z}}u_{z\beta_{u_z}j_1}^{p,k} + C_{36}^{p,k}N_{\sigma_{zz}j_2}F_{\beta_{\sigma_{zz}}}\sigma_{zz\beta_{\sigma_{zz}}j_2}^{p,k}
\end{aligned} \tag{3.71}$$

where R_y is the mid-surface curvature radius in the y direction.

Note that it is also possible to compute the *in-plane stresses* through the *classical form of Hooke's law*, but the choice of using the MFHL is more consistent with the mixed variational theorem here adopted.

Chapter 4

Model validation

In order to benchmark the mathematical model derived and the implemented code, results present in the scientific literature were used. The test cases reported have been divided depending on the geometry of the structure: plate, cylindrical panel, closed cylinder; and on the kind of analysis: linear static deflection, free-vibration. Finally, one challenging test case is reported where the present theory based on RMVT is compared with a similar formulation based on the PVD.

In all of the following test cases, a uniform notation has been adopted. a is the size in the x-direction, b is the size in the y-direction, h is the total thickness in the z-direction. R is the radius of curvature of the middle surface in the y-direction (Figure 4.1).

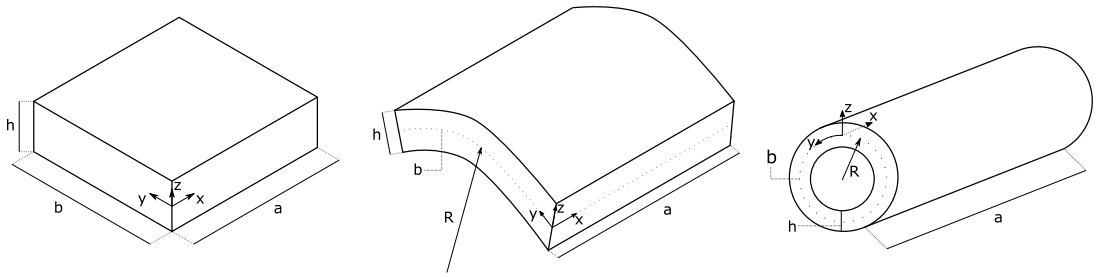

Figure 4.1: Notations adopted for plate, cylindrical panel and closed cylinder geometries.

The stacking sequence is for convenience described from top to bottom. When describing the physical properties of composite materials, the subscript 1 will indicate the direction parallel to the fibers, 2 the transverse direction, and 3 the thickness direction. θ represents the angle of each ply with respect to the laminate reference frame and it is measured from the x-axis, counter-clockwise with respect to the z-axis (Figure 4.2).

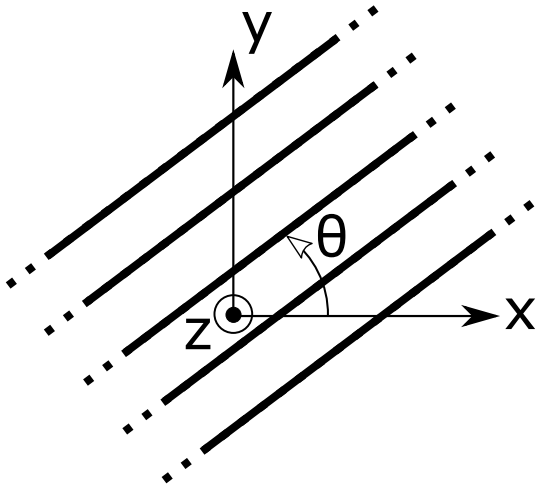

Figure 4.2: Notations adopted for the angles of each ply.

Boundary conditions are represented by a letter: F (*free*), S (*simply-supported*) and C (*clamped*). Therefore, the boundary conditions of the structure are represented by four letters, one for each side. The first letter corresponds to the left side ($x = 0$), and the others, respectively, to the following sides moving counter-clockwise with respect to the z-axis. For closed cylinders only two boundaries exist. The first letter corresponds to the side at $x = 0$, and the second to the side at $x = a$.

The *Legendre base* was utilized for the Ritz expansion in all of the test cases, except for the circumferential direction of closed cylinders where *Fourier polynomials* were used. Since the Ritz functions are built as the product of two separate functions, one in the x-direction and one in y-direction, it is possible to specify in the code the desired order for each one of them. R_u and R_s are the orders of Ritz expansion in the x-direction for displacements and stresses, respectively; S_u and S_s are the orders of Ritz expansion in the y-direction for displacements and stresses, respectively. It follows that:

$$\begin{aligned} M_u &= R_u \times S_u \\ M_s &= R_s \times S_s \end{aligned} \tag{4.1}$$

Unless otherwise specified, the employed Ritz orders of approximation are taken sufficiently high so to ensure the convergence of the results. They were always chosen so that: $R_s = R_u + 1$ and $S_s = S_u + 1$. An analysis justifying this choice can be found in Section 5.1.

The SCT was utilized for free-vibration problems, in order to retrieve directly only the significant physical quantities; while for static bending problems the whole mixed stiffness matrix has been inverted.

Since in the present RMVT formulation the transverse stress field can be freely chosen, it is possible to satisfy *a priori* the equilibrium condition on the top and bottom surfaces. Unless otherwise stated, however, no top-bottom stress boundary conditions have been imposed.

4.1 Plate - Bending

The first problem considered is the bending of a square sandwich plate, for which the exact solution was obtained by Pagano [34]. The problem is illustrated in Figure 4.3 and is defined as follows.

Geometry Square plate ($a = b$). The sandwich plate is constituted of one core and two single-ply skins, each thick one tenth of the total thickness. Different values of length-over-thickness ratio ($D = a/h$) are investigated: $D = 2, 4, 10$.

Composite stack Sandwich material: $[0/core/0]$.

Material properties

	$\mathbf{E_{11}}$ **[Pa]**	$\mathbf{E_{22}}$ **[Pa]**	$\mathbf{E_{33}}$ **[Pa]**
Skin	1.7237×10^{11}	6.8948×10^{9}	6.8948×10^{9}
Core	2.7579×10^{8}	2.7579×10^{8}	3.4474×10^{9}
	$\mathbf{G_{12}}$ **[Pa]**	$\mathbf{G_{13}}$ **[Pa]**	$\mathbf{G_{23}}$ **[Pa]**
Skin	3.4474×10^{9}	3.4474×10^{9}	1.3790×10^{9}
Core	1.1032×10^{8}	4.1369×10^{8}	4.1369×10^{8}
	$\boldsymbol{\nu_{12}}$ **[-]**	$\boldsymbol{\nu_{13}}$ **[-]**	$\boldsymbol{\nu_{23}}$ **[-]**
Skin	0.25	0.25	0.25
Core	0.25	0.25	0.25

Table 4.1: Pagano test case: skin and core material properties.

Boundary conditions Simply-supported on all four sides: *SSSS*.

Load Bisinusoidal load applied on the top surface: $P = P_0 sin(\frac{\pi}{a}x) sin(\frac{\pi}{b}y)$.

Results The results are made non-dimensional in the following manner:

$$(\bar{\sigma}_{xx}, \bar{\sigma}_{yy}, \bar{\sigma}_{xy}) = \frac{1}{P_0 D^2}(\sigma_{xx}, \sigma_{yy}, \sigma_{xy}) \qquad (\bar{\sigma}_{xz}, \bar{\sigma}_{yz}) = \frac{1}{P_0 D}(\sigma_{xz}, \sigma_{yz}) \tag{4.2}$$

The nondimensional thickness coordinate $\xi = \frac{z}{h}$ has been adopted.

Computational model Three sublaminates are used, one for each skin and one for the core, in view of minimizing the computational cost without affecting the accuracy. The models are chosen depending on the thickness ratio D, as reported in Table 4.2. For the core, which is characterized by a higher shear deformability, higher models compared to the skins were used.

D	**Top skin**	**Core**	**Bottom skin**	**Model ID**
2	$EM^{3,3,3}_{3,3,3}$	$EM^{4,4,3}_{4,4,3}$	$EM^{3,3,3}_{3,3,3}$	M1
4	$EM^{2,2,2}_{2,2,2}$	$EM^{3,3,3}_{3,3,3}$	$EM^{2,2,2}_{2,2,2}$	M2
10	$EM^{2,2,1}_{2,2,1}$	$EM^{3,3,2}_{3,3,2}$	$EM^{2,2,1}_{2,2,1}$	M3

Table 4.2: Pagano test case: models adopted depending on $D = \frac{a}{h}$.

The Ritz orders of expansion adopted are: $R_u = 8$, $R_s = 9$, $S_u = 8$, $S_s = 9$. The transverse stresses are obtained directly from the assumed field.

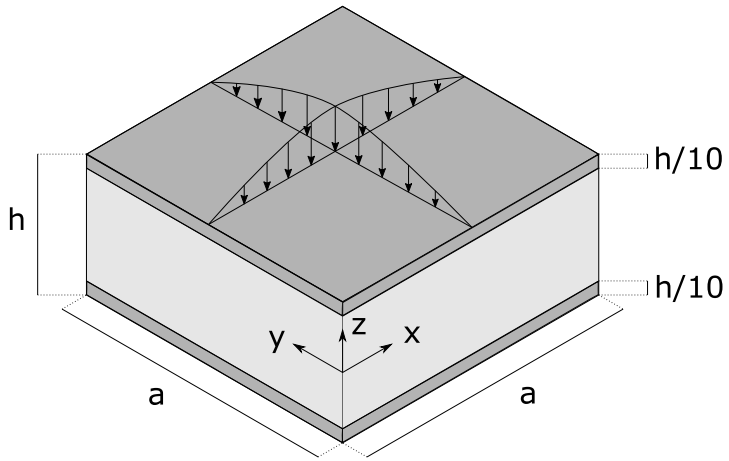

Figure 4.3: Pagano test case: simply-supported square sandwich under bi-sinusoidal pressure load.

First of all, the convergence of the Ritz approximation is addressed. Since it is an approximation of global quantities over the whole domain, a good way to determine its convergence rate is through the strain energy U, which is, indeed, a global quantity. Figure 4.4 shows the convergence of the total energy in function of the Ritz orders for model M1. As it is shown, the Ritz approximation converges monotonically and quickly to the value obtained with a high order of expansion ($R_u = S_u = 6$ and $R_s = S_s = 7$), which is taken as the reference (U_{ref}).

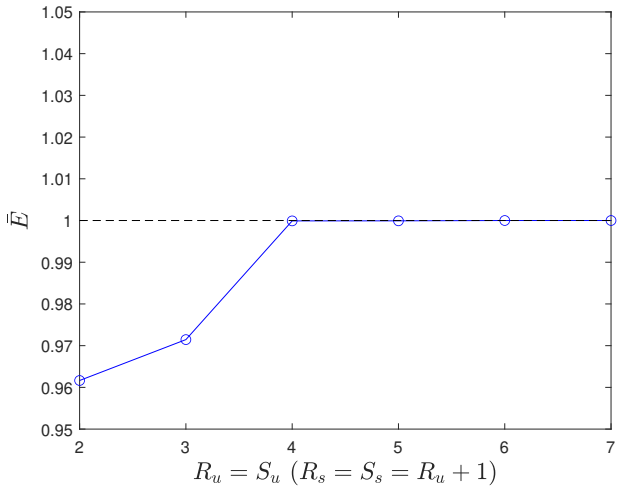

Figure 4.4: Total strain energy in function of different Ritz orders of expansion. $\bar{E} = \frac{U_{Ritz}}{U_{ex}}$ is the total strain energy normalized over the total strain energy for a converged value of the Ritz orders.

Tables 4.3, 4.4, 4.5 compare the results obtained by Pagano's exact solution and those obtained through the present theory for the thickness ratios: $D = 2, 4, 10$. The results are in excellent accordance with the exact solution. Given the variational principle here adopted, it is remarked that transverse stresses match up to the fourth digit the exact solution in all three cases. This confirms the advantageous feature of RMVT when computing the transverse stresses *a priori*.

D	Quantity	x	y	ξ	Exact [34]	Present (M1)
2	$\bar{\sigma}_{xx}$	a/2	b/2	0.5	3.278	3.278
	$\bar{\sigma}_{xx}$	a/2	b/2	-0.5	-2.653	-2.653
	$\bar{\sigma}_{xx}$	a/2	b/2	0.4	-2.22	-2.22
	$\bar{\sigma}_{xx}$	a/2	b/2	-0.4	1.668	1.668
	$\bar{\sigma}_{yy}$	a/2	b/2	0.5	0.4517	0.4517
	$\bar{\sigma}_{yy}$	a/2	b/2	-0.5	-0.3919	-0.3919
	$\bar{\sigma}_{xz}$	0	b/2	0	0.185	0.185
	$\bar{\sigma}_{yz}$	a/2	0	0	0.1399	0.1399
	$\bar{\sigma}_{xy}$	0	0	0.5	-0.2403	-0.2403
	$\bar{\sigma}_{xy}$	0	0	-0.5	0.2338	0.2338

Table 4.3: Pagano test case: results for $D = 2$. Model M1 was adopted.

D	Quantity	x	y	ξ	Exact [34]	Present (M2)
4	$\bar{\sigma}_{xx}$	a/2	b/2	0.5	1.556	1.556
	$\bar{\sigma}_{xx}$	a/2	b/2	-0.5	-1.512	-1.512
	$\bar{\sigma}_{xx}$	a/2	b/2	0.4	-0.233	-0.224
	$\bar{\sigma}_{xx}$	a/2	b/2	-0.4	0.196	0.1873
	$\bar{\sigma}_{yy}$	a/2	b/2	0.5	0.2595	0.2596
	$\bar{\sigma}_{yy}$	a/2	b/2	-0.5	-0.2533	-0.2534
	$\bar{\sigma}_{xz}$	0	b/2	0	0.239	0.239
	$\bar{\sigma}_{yz}$	a/2	0	0	0.1072	0.1072
	$\bar{\sigma}_{xy}$	0	0	0.5	-0.1437	-0.1437
	$\bar{\sigma}_{xy}$	0	0	-0.5	0.1481	0.1480

Table 4.4: Pagano test case: results for $D = 4$. Model M2 was adopted.

D	Quantity	x	y	ξ	Exact [34]	Present (M3)
10	$\bar{\sigma}_{xx}$	a/2	b/2	± 0.5	± 1.152	± 1.152
	$\bar{\sigma}_{xx}$	a/2	b/2	± 0.4	± 0.629	± 0.629
	$\bar{\sigma}_{yy}$	a/2	b/2	0.5	0.1099	0.1105
	$\bar{\sigma}_{yy}$	a/2	b/2	-0.5	-0.1099	-0.1099
	$\bar{\sigma}_{xz}$	0	b/2	0	0.300	0.300
	$\bar{\sigma}_{yz}$	a/2	0	0	0.0527	0.0527
	$\bar{\sigma}_{xy}$	0	0	0.5	-0.0717	-0.0707
	$\bar{\sigma}_{xy}$	0	0	-0.5	0.0717	0.0717

Table 4.5: Pagano test case: results for $D = 10$. Model M3 was adopted.

4.2 Plate - Free-vibration

As benchmark for the free-vibration problem of plates, the results obtained by Demasi [35] are considered. The results by Demasi are obtained through a FEM based upon RMVT. The case named "Benchmark 5" in Demasi's article [35] is here considered, which is defined as follows.

Geometry Square plate ($a = b$). Length-over-thickness ratio: $D = a/h = 4$.
Lamination Antisymmetric angle-ply: $[+30/-30]$; 2 plies of equal thickness $h_p = h/2$.
Material properties

$\mathbf{E_{11}}$ [-]	$\mathbf{E_{22}}$ [-]	$\mathbf{E_{33}}$ [-]	$\mathbf{G_{12}}$ [-]	$\mathbf{G_{13}}$ [-]	$\mathbf{G_{23}}$ [-]	$\boldsymbol{\nu_{12}}$ [-]	$\boldsymbol{\nu_{13}}$ [-]	$\boldsymbol{\nu_{23}}$ [-]	$\boldsymbol{\rho}$ $\left[\frac{kg}{m^3}\right]$
25	1	1	0.5	0.5	0.2	0.25	0.25	0.25	1500

Table 4.6: Demasi test case: ply material properties. $E_{11}, E_{22}, E_{33}, G_{12}, G_{13}, G_{23}$ are normalized over E_{22}.

Boundary conditions Three configurations are investigated: *CCCC*, *FCFC* and *FCCF*.
Results The results are normalized in the following manner:

$$\bar{\omega} = \frac{a^2}{h}\sqrt{\frac{\rho}{E_{22}}}\,\omega \tag{4.3}$$

Computational model The same RMVT model used by Demasi is employed, i.e. $LM4 = LM^{4,4,4}_{4,4,4}$. The Ritz orders of expansion adopted are: $R_u = S_u = 8$ ($R_s = S_s = R_u + 1$).

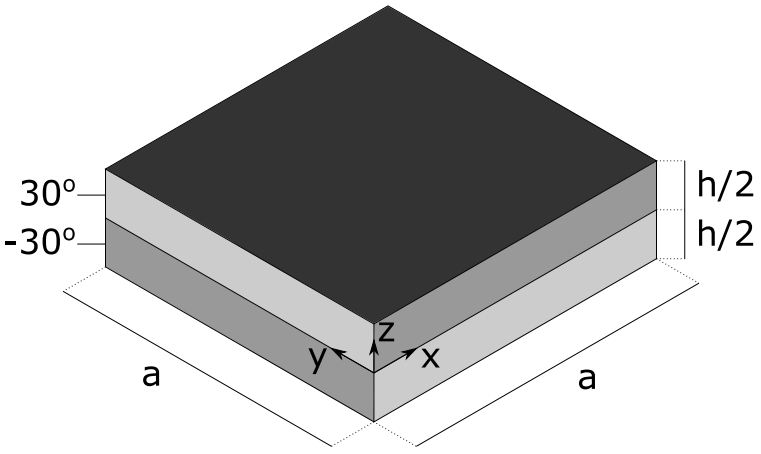

Figure 4.5: Demasi test case.

Table 4.7 compares the results obtained by Demasi's FEM and those obtained through the present model. The results by Demasi were computed with 4×4 (MESH1) and 5×5 (MESH2) quadratic isoparametric plate elements (Q9). Figures 4.6, 4.8, 4.7 compare the modal shapes of the first 4 vibration modes for the 3 sets of boundary conditions.

Frequency parameter	$\bar{\omega}_1$	$\bar{\omega}_2$	$\bar{\omega}_3$	$\bar{\omega}_4$
CCCC				
MESH 1 [35]	8.819	13.046	15.320	18.701
MESH 2 [35]	8.801	12.970	15.247	18.466
Present	8.782	12.900	15.184	18.195
FCFC				
MESH 1 [35]	4.782	6.659	10.080	12.325
MESH 2 [35]	4.759	6.632	9.970	12.228
Present	4.731	6.592	9.866	12.130
FCCF				
MESH 1 [35]	2.864	6.220	8.079	9.732
MESH 2 [35]	2.858	6.198	8.057	9.663
Present	2.848	6.171	8.029	9.549

Table 4.7: Demasi test case: comparison of the first four circular frequencies.

Table 4.7 shows a very good agreement between the FEM results of Demasi and the present Ritz-based results. This benchmark is particularly useful as it allows to compare two RMVT-based computational models that differ only in the discretization method. It can be noticed that the present Ritz method predicts lower frequencies compared to those obtained from the FEM approach: the discretization error using higher order Ritz polynomials is lower than that of the rather coarse FEM meshes employed by Demasi.

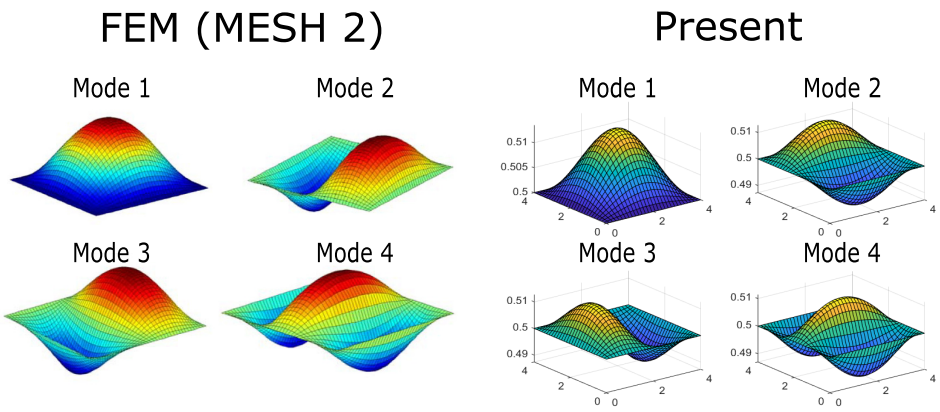

Figure 4.6: Demasi test case: first four modes corresponding to the plate with boundary conditions CCCC.

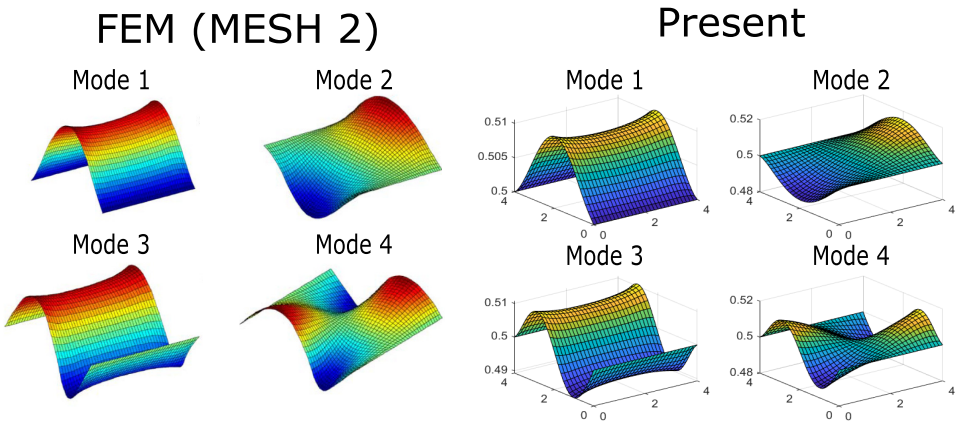

Figure 4.7: Demasi test case: first four modes corresponding to the plate with boundary conditions FCFC.

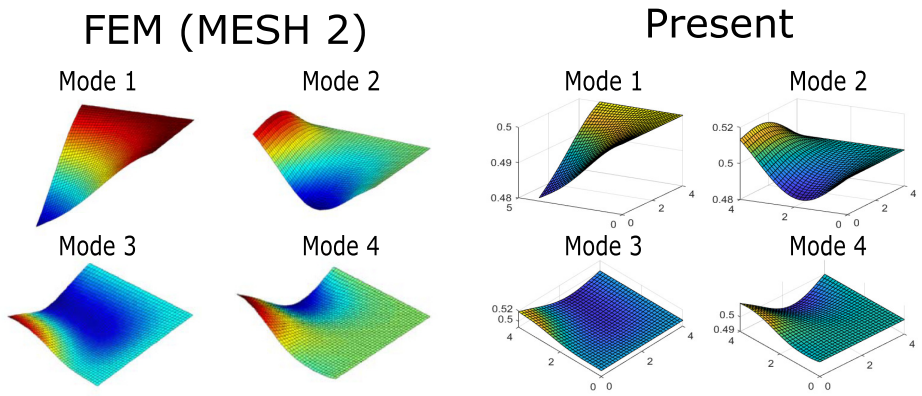

Figure 4.8: Demasi test case: first four modes corresponding to the plate with boundary conditions FCCF.

4.3 Open shell - Bending

In order to validate the results for the bending problem of an open shell, the exact solution derived by Ren [36] for the cylindrical bending problem is utilized. In the cylindrical bending problem a state of plane strain in the plane (y, z) is assumed (i.e., the panel is considered to extend indefinitely along the x axis). Among the benchmark configurations studied by Ren, the attention is restricted to the most challenging one, involving a strongly orthotropic laminate. The problem, illustrated in Figure 4.9, is defined as follows.

Geometry Semi-infinite cylindrical panel. Curvature radius: $R = 10$. The length of the middle surface in the y-direction is $b = \phi R$, where $\phi = \frac{\pi}{3}$. Different values of depth ratios ($S = R/h$) are investigated: $S = 2, 4, 10, 50, 100, 500$. For $S = 2$, the shell is thick, or deep, with $b/h = \Phi R/h = 2\Phi$; for $S = 500$, the shell is thin, or shallow, with $b/h = 500\Phi$.

Composite stack 3 plies of equal thickness: [90/0/90] (outer plies have fibers oriented in circumferential direction).

Material properties

$\mathbf{E_{11}}$ [Pa]	$\mathbf{E_{22}}$ [Pa]	$\mathbf{E_{33}}$ [Pa]
172×10^9	6.9×10^9	6.9×10^9
$\mathbf{G_{12}}$ [Pa]	$\mathbf{G_{13}}$ [Pa]	$\mathbf{G_{23}}$ [Pa]
3.4×10^9	3.4×10^9	1.4×10^9
$\boldsymbol{\nu_{12}}$ [-]	$\boldsymbol{\nu_{13}}$ [-]	$\boldsymbol{\nu_{23}}$ [-]
0.25	0.25	0.25

Table 4.8: Ren test case: ply material properties.

Boundary conditions For the sides at $y = 0$ and $y = b$: *SS*. For the sides normal to the x-direction, no boundary conditions should be specified. However, due to the way the cylindrical bending problem was implemented, all four boundary conditions have to be specified within the code. For this case *FF* conditions were used.

Load Sinusoidal load applied on the top surface: $P = P_0 sin(\frac{\pi}{b}y)$.

Results The results are made non-dimensional in the following manner:

$$\begin{gathered} \bar{u}_y = \frac{100E_{22}}{P_0 h S^3} u_y \qquad \bar{u}_z = \frac{10E_{22}}{P_0 h S^4} u_z \\ (\bar{\sigma}_{xx}, \bar{\sigma}_{yy}) = \frac{1}{P_0 S^2}(\sigma_{xx}, \sigma_{yy}) \qquad \bar{\sigma}_{zz} = \frac{1}{\sigma_{xx}(\frac{h}{2}, \frac{b}{2})}\sigma_{zz} \qquad \bar{\sigma}_{yz} = \frac{1}{P_0 S}\sigma_{yz} \end{gathered} \tag{4.4}$$

The nondimensional thickness coordinate $\xi = \frac{z}{h}$ has been adopted.

Computational model Three models were used depending on the depth ratio S, as reported in Table 4.9. Due to the cylindrical bending assumption, it is unnecessary to allocate DOF in the x-direction: in Table 4.9, the symbol "$-$" indicates that the variables u_x and σ_{xz} have been omitted from the model.

S	Model	Model ID
2, 4, 10	$LM^{-,6,5}_{-,6,5}$	M1
50, 100	$LM^{-,3,2}_{-,3,2}$	M2
500	$EM^{-,3,2}_{-,3,2}$	M3

Table 4.9: Ren test case: models adopted depending on $S = \frac{R}{h}$.

Furthermore, since the results will be independent with respect to the axial direction, this condition can be represented by imposing $R_u = R_s = 1$. Setting the Ritz orders of expansion equal to 1 conveys constant values along the x direction. The Ritz orders of expansion adopted are: $R_u = 1$, $R_s = 1$, $S_u = 10$, $S_s = 11$.

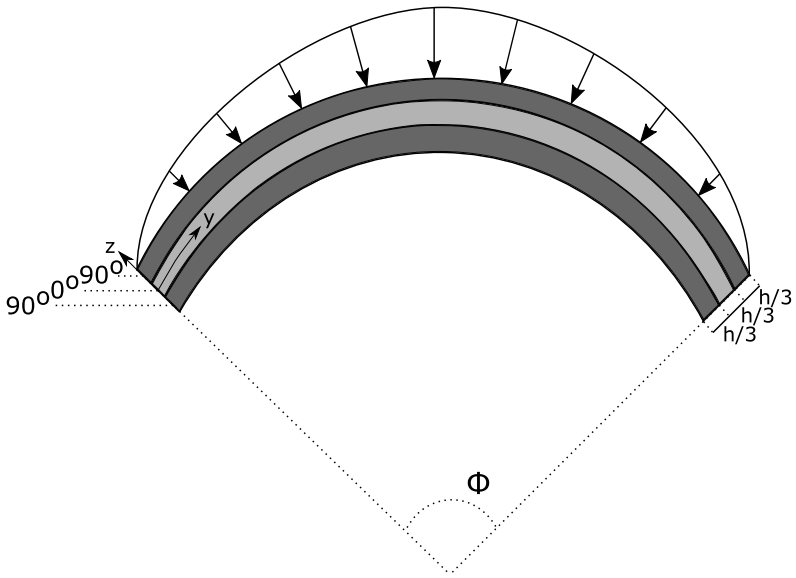

Figure 4.9: Ren test case: shell panel in cylindrical bending.

In table 4.10 results obtained by Ren's exact solution and the present theory are compared. The transverse stresses are obtained from the assumed model.

	Exact [36]				Present			
S	$\bar{u}_z$ $\left(0, \frac{b}{2}\right)$	$\bar{\sigma}_{yy}$ $\left(\mp\frac{h}{2}, \frac{b}{2}\right)$	$\bar{\sigma}_{xx}$ $\left(\mp\frac{h}{2}, \frac{b}{2}\right)$	$\bar{\sigma}_{yz}$ $(0,0)$	$\bar{u}_z$ $\left(0, \frac{b}{2}\right)$	$\bar{\sigma}_{yy}$ $\left(\mp\frac{h}{2}, \frac{b}{2}\right)$	$\bar{\sigma}_{xx}$ $\left(\mp\frac{h}{2}, \frac{b}{2}\right)$	$\bar{\sigma}_{yz}$ $(0,0)$
2	1.436	−3.467 2.463	−0.0347 0.0871	0.394	1.476	−3.122 2.801	−0.0316 0.1063	0.408
4	0.457	−1.772 1.367	−0.0177 0.0293	0.476	0.462	−1.669 1.452	−0.0176 0.0321	0.482
10	0.144	−0.995 0.897	−0.0100 0.0115	0.525	0.144	−0.976 0.912	−0.0098 0.0118	0.526
50	0.0808	−0.798 0.792	−0.0080 0.0079	0.526	0.0810	−0.796 0.785	−0.0080 0.0079	0.525
100	0.0787	−0.786 0.781	−0.0079 0.0078	0.523	0.0788	−0.786 0.780	−0.0079 0.0078	0.523
500	0.0773	−0.780 0.768	−0.0078 0.0077	0.525	0.0779	−0.779 0.778	−0.0079 0.0077	0.554

Table 4.10: Ren test case: comparison of the exact solution with the results from the present theory.

The results present good agreement with the exact solution. Discrepancies are larger for low R/h ratios, and as the ratio R/h increases, the agreement between the present theory and the exact solution improves. Furthermore, a higher ratio R/h allows obtaining good results even if less accurate models are adopted. For instance, for $S = 500$ an ESL model has been adopted, nevertheless, the results obtained are still in very good agreement with the exact solution.

For high orders of depth ratios ($S = 100, 500$), it is also possible to introduce an approximation similar to the Donnell shallow shell theory by setting $\lambda_D = 0$ in Eq.(2.3). Table 4.11 compares results obtained from model $LM^{-,3,2}_{-,3,2}$ with and without Donnell approximation. Substantial differences are found, in particular it can be noticed that both displacements and stresses are underestimated if the contribution to the transverse shear strain of the tangential displacement due to the curvature is neglected. In the present framework, imposing $\lambda_D = 0$ allows computing fewer terms, but the benefits from a numerical standpoint are almost negligible since the bottleneck is given by the solution of the linear system. Therefore, since the benefits of the Donnell approximation are minor and the results are sensibly worsened by it, it is not optimal to discard part of the curvature effects on the transverse deformations.

	$\lambda_D = 1$				$\lambda_D = 0$			
S	$\bar{u}_z$ $\left(0, \frac{b}{2}\right)$	$\bar{\sigma}_{yy}$ $\left(\mp\frac{h}{2}, \frac{b}{2}\right)$	$\bar{\sigma}_{xx}$ $\left(\mp\frac{h}{2}, \frac{b}{2}\right)$	$\bar{\sigma}_{yz}$ $(0,0)$	$\bar{u}_z$ $\left(0, \frac{b}{2}\right)$	$\bar{\sigma}_{yy}$ $\left(\mp\frac{h}{2}, \frac{b}{2}\right)$	$\bar{\sigma}_{xx}$ $\left(\mp\frac{h}{2}, \frac{b}{2}\right)$	$\bar{\sigma}_{yz}$ $(0,0)$
100	0.0788	-0.786 0.780	-0.0079 0.0078	0.523	0.0623	-0.6975 0.6942	-0.0070 0.0070	0.465
500	0.0779	-0.779 0.778	-0.0078 0.0078	0.521	0.0615	-0.6923 0.6916	-0.0069 0.0069	0.464

Table 4.11: Ren test case: Donnell's approximation effects.

Finally, it is possible to compare the distribution along the thickness obtained through the present theory of $\bar{\sigma}_{zz}$, $\bar{\sigma}_{yy}$, $\bar{\sigma}_{yz}$ and $\bar{u}_y$ for $S = 10$, with the exact solution.

As it is shown in Figure 4.10 the present theory is able to retrieve the exact solution with a high degree of accuracy. Finally, it is remarked that $\bar{\sigma}_{zz}$ and $\bar{\sigma}_{yz}$ fit very well the exact solution and have been computed *a priori*, without, therefore, the need of any post-processing computation.

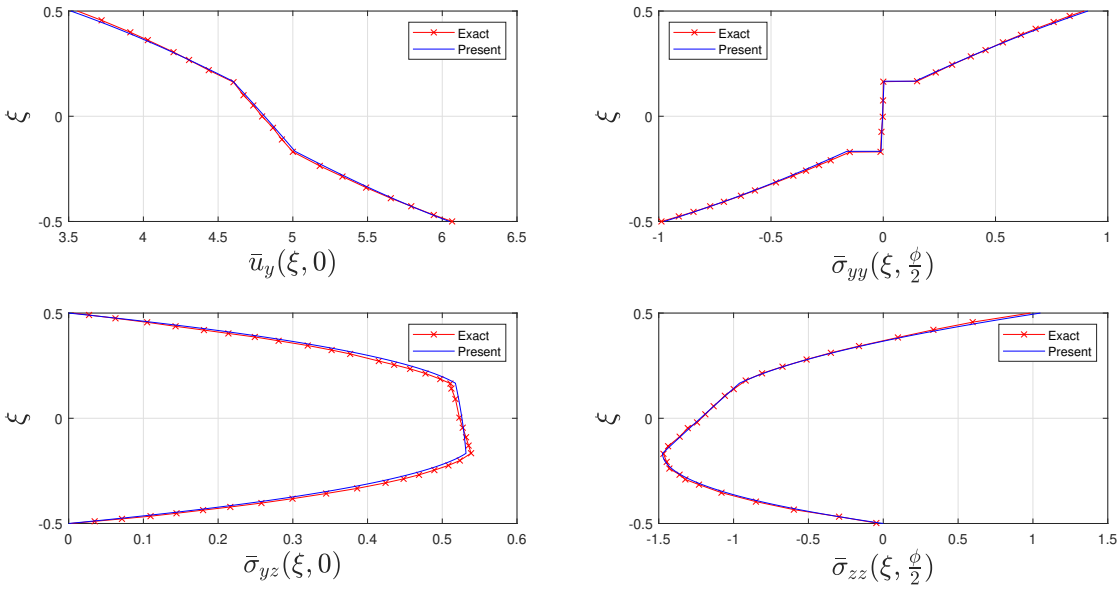

Figure 4.10: Comparison between the exact solution by Ren and the present theory of the through-the-thickness distributions of $\bar{u}_y$, $\bar{\sigma}_{yy}$, $\bar{\sigma}_{yz}$ and $\bar{\sigma}_{zz}$.

4.4 Open shell - Free-vibration

In order to validate the results for the free-vibration problem for open shells, the results obtained by Asadi and Qatu [37] are used as benchmark. In particular, among all the lay-ups investigated by Asadi and Qatu, the focus will be posed on the angle-ply lamination scheme $[-45/45]_3$, in order to present a challenging test case. The problem is illustrated in Figure 4.11 and is defined as follows.

Geometry Square cylindrical panel ($a = b$). The length-over-thickness ratio ($D = a/h$) is 10 (moderately thick), the depth ratio ($S = R/h$) is 5 (very deep).

Composite stack Antisymmetric angle-ply: $[-45/45]_3$, all plies of equal thickness.

Material properties

$\mathbf{E_{11}}$ [-]	$\mathbf{E_{22}}$ [-]	$\mathbf{E_{33}}$ [-]	$\mathbf{G_{12}}$ [-]	$\mathbf{G_{13}}$ [-]	$\mathbf{G_{23}}$ [-]	$\boldsymbol{\nu_{12}}$ [-]	$\boldsymbol{\nu_{13}}$ [-]	$\boldsymbol{\nu_{23}}$ [-]	$\boldsymbol{\rho}$ $\left[\frac{\boldsymbol{kg}}{\boldsymbol{m^3}}\right]$
25	1	1	0.5	0.5	0.2	0.25	0.25	0.572	1

Table 4.12: Asadi and Qatu test case: ply material properties. $E_{11}, E_{22}, E_{33}, G_{12}, G_{13}, G_{23}$ are normalized over E_{22}.

Boundary conditions Different BCs are investigated: *SSSS*, *CCCC*, *CSCS*, *CFCF*, *CFSF*, *FSFC*.

Results The first 5 natural circular frequencies are considered and are normalized as:

$$\bar{\omega} = \frac{a^2}{h}\sqrt{\frac{\rho}{E_{22}}}\,\omega \tag{4.5}$$

Computational model Two ESL theories are adopted for computing the free-vibration (global) response: a mixed first-order shear deformation theory and a higher-order theory. In both theories top-bottom stress boundary conditions were imposed: $\sigma_{xz}(x, y, \frac{h}{2}) = \sigma_{yz}(x, y, \frac{h}{2}) = \sigma_{zz}(x, y, \frac{h}{2}) = 0$ and $\sigma_{xz}(x, y, -\frac{h}{2}) = \sigma_{yz}(x, y, -\frac{h}{2}) = \sigma_{zz}(x, y, -\frac{h}{2}) = 0$.

Model	**Model ID**
$EM^{2,2,1}_{1,1,0}$	M1
$EM^{4,4,3}_{3,3,2}$	M2

Table 4.13: Asadi and Qatu test case: models adopted.

The Ritz orders of expansion adopted are: $R_u = S_u = 15$ ($R_s = S_s = R_u + 1$).

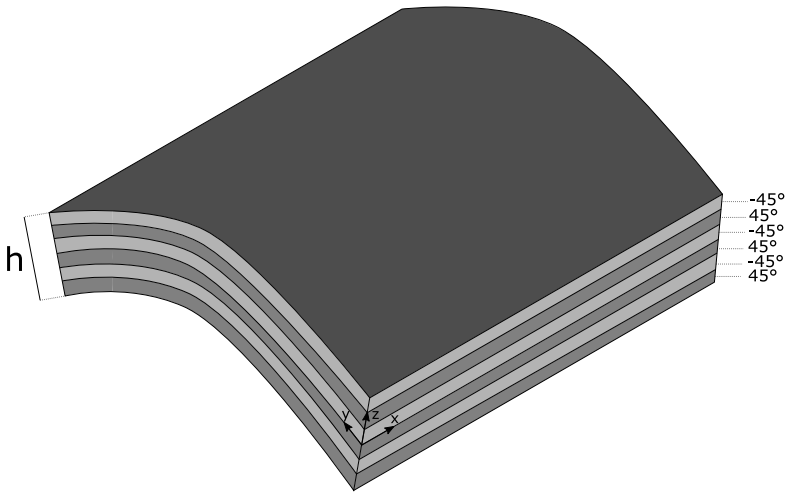

Figure 4.11: Asadi and Qatu test case.

Table 4.14 compares the results reported by Asadi and Qatu [37], with those obtained by the present model. The results reported by Asadi and Qatu are obtained through two different methods. The first one is based upon a first-order shear deformation theory (referred to as FSDT), which includes both shear deformation and rotary inertia effects, but it does not include z/R effects; the second method is a 3-D elasticity solution obtained with the FEM (referred to as 3D). The number of quadratic solid elements used in the FEM by Asadi and Qatu [37] did not exceed $[40 \times 40 \times 12]$.

As it results from Table 4.14 the present mixed first-order shear deformation theory outperforms the FSDT theory presented by Asadi and Qatu for every set of boundary conditions and for all of the first five natural frequencies. Furthermore, the present theory $EM^{4,4,3}_{3,3,2}$ conveys results in very good agreement with those of the 3-D FEM analysis. Taking the 3-D FEM solution as reference, the maximum error committed is of about 5%. These results prove the capability of the present high order theory to retain the effects due to the transverse deformability, anisotropic couplings and curvature of deep shells. As a general remark, a relative error of few percentages is still acceptable as the reference results are obtained through a 3-D FEM which is, by definition, not exact.

The choice of imposing the correct values of top and bottom transverse stresses not only has the effect of reducing the number of unknowns, and therefore the computational effort required to solve the algebraic system, but considerably improves the overall results. Table 4.15 compares the results of the present theories with and without the exact enforcement of the homogeneous stress boundary conditions at the top and bottom surfaces of the shell. As can be noticed, imposing top and bottom boundary conditions sensibly improves the results. In some of the cases here considered, the improvements make the results of the mixed FSDT (13 DOF) comparable with those of the higher-order model (25 DOF) where no boundary conditions were imposed. In fact, imposing top and bottom exact values for transverse stresses allows computing a more accurate stress field. This then enables the RMVT to estimate better *shear correction factors*. From Table 4.15, it is also clear that using correct shear correction factors is particularly important for low order theories: the improvements introduced for the mixed FSDT are larger than that for the high-order model.

Frequency parameter	$\bar{\omega}_1$	$\bar{\omega}_2$	$\bar{\omega}_3$	$\bar{\omega}_4$	$\bar{\omega}_5$
SSSS					
FSDT [37]	24.859	26.994	41.519	41.181	43.027
Present (M1)	23.701	26.830	38.557	40.634	42.733
3D [37]	22.842	26.432	37.744	38.975	41.111
Present (M2)	22.993	26.599	37.516	39.951	42.152
CCCC					
FSDT [37]	39.578	41.011	47.437	50.070	56.788
Present (M1)	38.046	39.045	46.235	48.186	54.268
3D [37]	37.562	38.711	45.369	47.324	53.543
Present (M2)	37.441	38.381	45.692	47.569	53.289
CSCS					
FSDT [37]	29.705	36.949	41.861	47.042	52.652
Present (M1)	28.357	36.466	39.188	45.833	50.179
3D [37]	27.675	35.182	38.499	44.261	48.880
Present (M2)	27.778	36.027	38.199	45.080	49.344
CFCF					
FSDT [37]	15.980	18.462	28.015	30.252	32.923
Present (M1)	15.194	17.833	27.105	29.028	31.231
3D [37]	15.344	17.798	26.640	28.518	31.178
Present (M2)	14.904	17.493	26.801	28.529	30.567
CFSF					
FSDT [37]	13.916	14.368	22.996	24.014	29.325
Present (M1)	13.150	14.204	22.047	23.510	28.070
3D [37]	13.127	14.149	21.550	23.253	27.606
Present (M2)	12.725	13.973	21.647	23.294	27.424
FSFC					
FSDT [37]	4.9792	17.060	18.186	29.258	29.487
Present (M1)	4.8114	16.068	17.170	27.835	28.551
3D [37]	4.7332	15.332	17.011	27.282	28.683
Present (M2)	4.7144	15.701	16.833	27.306	28.301

Table 4.14: Asadi and Qatu test case: comparison of the first five circular frequencies.

Frequency parameter	$\bar{\omega}_1$	$\bar{\omega}_2$	$\bar{\omega}_3$	$\bar{\omega}_4$	$\bar{\omega}_5$
SSSS					
Present (M1)	23.701	26.830	38.557	40.634	42.733
Present (M1) no b.cs.	25.189	26.996	41.652	41.875	43.202
Present (M2)	22.993	26.599	37.516	39.951	42.152
Present (M2) no b.cs.	23.246	26.667	38.057	40.166	42.314
CCCC					
Present (M1)	38.046	39.045	46.235	48.186	54.268
Present (M1) no b.cs.	39.813	41.345	47.826	50.573	57.138
Present (M2)	37.441	38.381	45.692	47.569	53.289
Present (M2) no b.cs.	37.797	38.919	45.991	48.056	53.898
CSCS					
Present (M1)	28.357	36.466	39.188	45.833	50.179
Present (M1) no b.cs.	29.914	41.345	47.826	50.573	52.911
Present (M2)	27.778	36.027	38.199	45.080	49.344
Present (M2) no b.cs.	28.106	36.230	38.771	45.415	49.988
CFCF					
Present (M1)	15.194	17.833	27.105	29.028	31.231
Present (M1) no b.cs.	15.916	18.670	27.982	30.511	32.989
Present (M2)	14.904	17.493	26.801	28.529	30.567
Present (M2) no b.cs.	15.063	17.666	26.983	28.870	30.962
CFSF					
Present (M1)	13.150	14.204	22.047	23.510	28.070
Present (M1) no b.cs.	13.716	14.624	22.766	24.116	29.356
Present (M2)	12.725	13.973	21.647	23.294	27.424
Present (M2) no b.cs.	12.881	14.070	21.845	23.387	27.713
FSFC					
Present (M1)	4.811	16.068	17.170	27.835	28.551
Present (M1) no b.cs.	5.070	16.778	18.242	28.937	29.254
Present (M2)	4.714	15.701	16.833	27.306	28.301
Present (M2) no b.cs.	4.757	15.880	17.040	27.540	28.427

Table 4.15: Top and bottom boundary conditions effects.

Finally, Figure 4.12 compares the modal shapes obtained through the present method (M2) and those reported by Asadi and Qatu. The perfect agreement between the modal shapes allows to confirm the pertinence of the comparison of the corresponding natural frequencies.

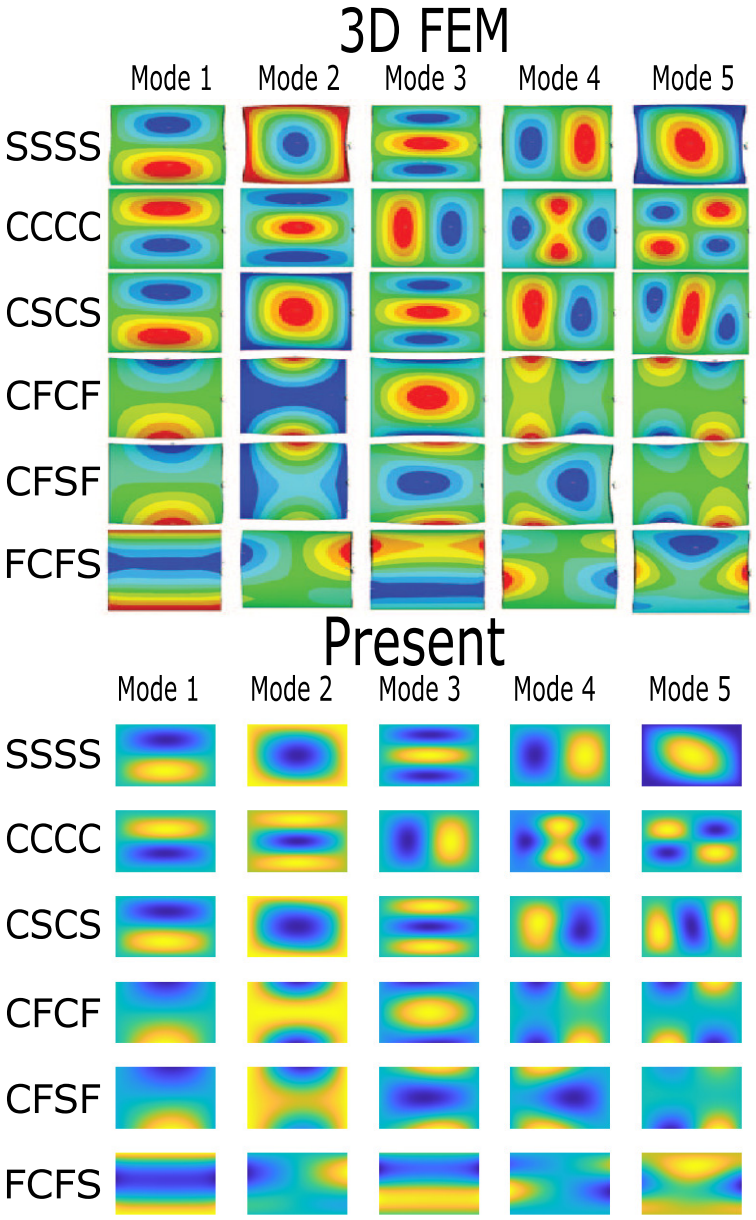

Figure 4.12: First five modes comparison between the 3-D FEM by Asadi and Qatu and the present theory.

4.5 Closed shell - Bending

In order to validate the results for the bending problem of a closed circular cylindrical shell, the exact elasticity solution reported by Chandrashekhara and Kumar [38] for a closed cylinder with a localized load is utilized. The problem is illustrated in Figure 4.13 and defined as follows.

Geometry Closed circular cylinder with mid-surface radius R, length-over-thickness ratio: $D = a/h = 5$, and radius-over-thickness ratio: $S = R/h = 5$.

Composite stack Symmetric cross-ply laminate: [90/0/90] (all plies of equal thickness).

Material properties

$\mathbf{E_{11}}$ [Pa]	$\mathbf{E_{22}}$ [Pa]	$\mathbf{E_{33}}$ [Pa]
84.4×10^9	7.32×10^9	7.32×10^9
$\mathbf{G_{12}}$ [Pa]	$\mathbf{G_{13}}$ [Pa]	$\mathbf{G_{23}}$ [Pa]
4.1×10^9	4.1×10^9	4.1×10^9
$\boldsymbol{\nu_{12}}$ [-]	$\boldsymbol{\nu_{13}}$ [-]	$\boldsymbol{\nu_{23}}$ [-]
0.3	0.3	0.32

Table 4.16: Chandrashekhara and Kumar test case: ply material properties.

Boundary conditions Simple-support (SS) at $x = 0$ and at $x = a$.

Load Localized pressure load of uniform amplitude P_0 on the outer surface. The loaded area extends from $x_1 = \frac{3}{8}a$ to $x_2 = \frac{5}{8}a$ and from $y_1 = -\theta_1(R + \frac{h}{2})$ to $y_2 = \theta_1(R + \frac{h}{2})$, where $\theta_1 = \frac{1}{8}\, rad$.

Results Through-thickness distributions of non-dimensional displacements and stresses:

$$\begin{aligned} \bar{u}_x\left(0, 0, \xi = \frac{z}{h}\right) &= \frac{100 E_{22}}{P_0 h S^4} u_x(0, 0, \xi) \\ (\bar{\sigma}_{xx}, \bar{\sigma}_{yy})\left(\frac{L}{2}, 0, \xi\right) &= \frac{1}{P_0 S^2}(\sigma_{xx}, \sigma_{yy})\left(\frac{L}{2}, 0, \xi\right) \\ (\bar{\sigma}_{xz}, \bar{\sigma}_{yz}, \bar{\sigma}_{zz})\left(\frac{L}{2}, 0, \xi\right) &= \frac{1}{P_0 S^2}(\sigma_{xz}, \sigma_{yz}, \sigma_{zz})\left(\frac{L}{2}, 0, \xi\right) \end{aligned} \tag{4.6}$$

Computational model Since we are interested in a local response, a LW model is adopted.

Model	Model ID
$LM^{3,3,2}_{3,3,2}$	M1

Table 4.17: Chandrashekhara and Kumar test case: model.

The Ritz orders of expansions adopted are: $R_u = S_u = 20$ ($R_s = S_s = R_u + 1$). It is here selected $R_u = S_u$ and $R_s = S_s$ for simplicity, however different orders could be investigated in order improve computational efficiency respect to the Ritz approximation.

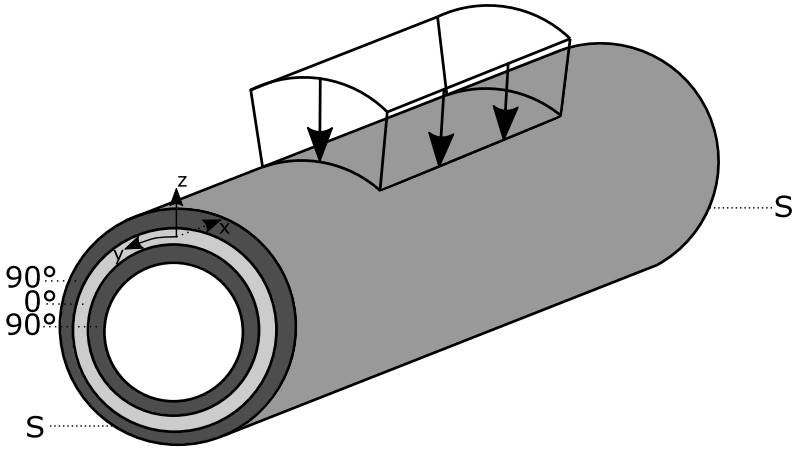

Figure 4.13: Chandrashekhara and Kumar test case.

Figure 4.14 compares the distribution along the thickness of the axial displacement $\bar{u}_x$ and of the in-plane stresses $\bar{\sigma}_{xx}$ and $\bar{\sigma}_{yy}$. The distributions predicted by the present theory fit well the exact solution with small discrepancies, in particular next to the top and bottom surfaces.

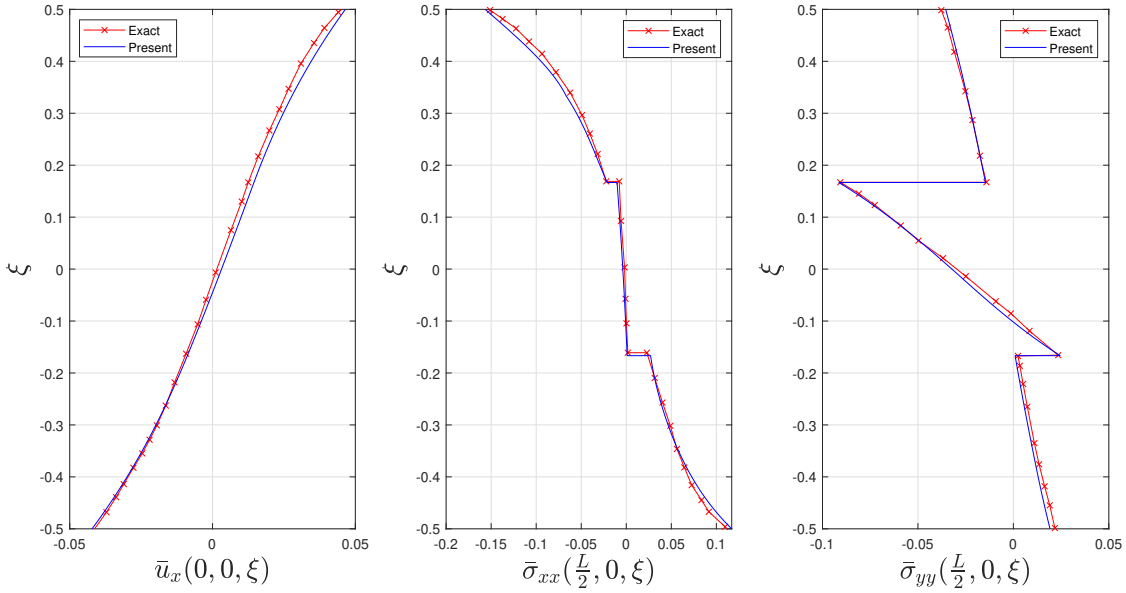

Figure 4.14: $\bar{u}_x$, $\bar{\sigma}_{xx}$, $\bar{\sigma}_{yy}$: comparison between the exact solution by Chandrashekhara and Kumar, and the present theory.

In this case, the sources of complexities are the low ratio S and the presence of a localized load condition. This latter aspect can be particularly difficult to be handled in the context of a formulation based on the use of global shape functions. However, as demonstrated by the results, a high number of shape functions can be easily considered thanks to the efficiency of the implementation, allowing to capture even local effects.

The abrupt changes of stresses justify the decision to adopt a LW theory for this test case. In fact, even if the LW model is computationally demanding, it assumes fields which are C^0-continuous along the thickness. This allows capturing sudden variations typical of

the interfaces. It is reported also that the present problem is solved in about $5.5\,s$ on a regular personal computer equipped with an *Intel Core i7* and *16 GB of RAM*. Therefore, even very high order models in the present formulation can be easily solved by nowadays computational power.

For the sake of completeness, thickness distributions of transverse stresses are also reported in Figure 4.15, however no comparison with the reference solution of Chandrashekhara and Kumar is possible since these results were not reported in [38].

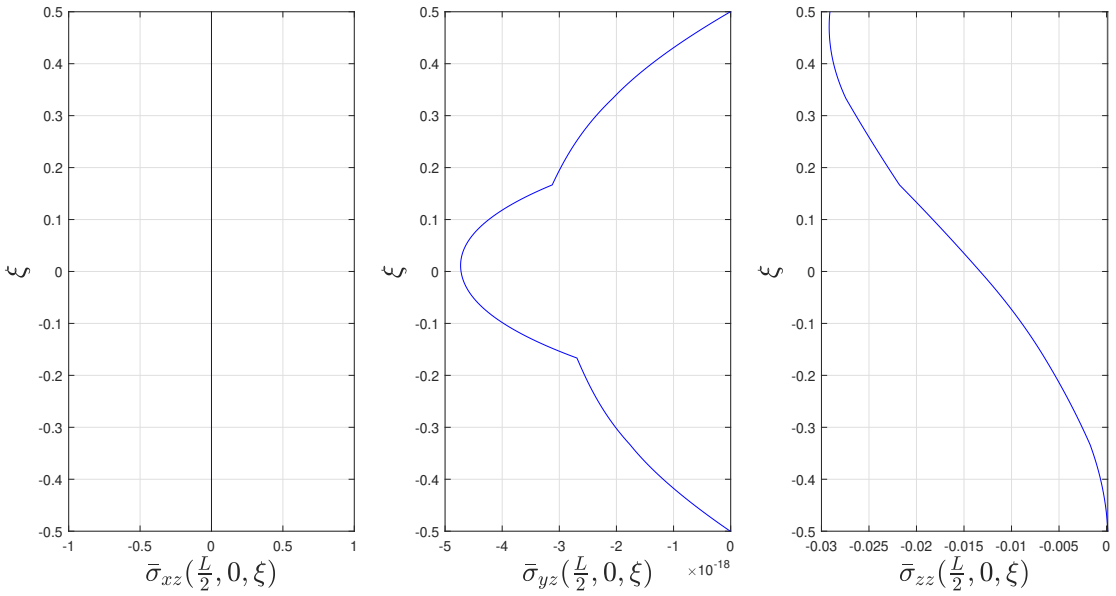

Figure 4.15: $\bar{\sigma}_{xz}$, $\bar{\sigma}_{yz}$, $\bar{\sigma}_{zz}$: computed *a priori* using the present theory.

4.6 Closed shell - Free-vibration

To validate the present implementation against the free-vibration problem of closed shells, reference is made to the results obtained by Brischetto [39] for a sandwich shell with composite skins. Brischetto computed the frequencies by adopting a 3-D analysis based on a layerwise approach. The free-vibration analysis was applied to cylinders with different radius-over-thickness ratios (R/h). The problem, illustrated in Figure 4.16, is defined as follows.

Geometry Closed circular cylinder of length $a = 100$ and mid-surface radius of curvature $R = 10$. Different radius-over-thickness ratios ($S = R/h$) are investigated : $S = 1000, 100, 10, 5$. Length-over-thickness ratio: $D = a/h = 10\,S$. The sandwich cylinder is constituted of two skins and one core. The core thickness is: $h_c = 0.7h$. The top and bottom skins have equal thickness, and it is: $h_s = 0.15h$. Furthermore, each skin is made of two plies of equal thickness.

Composite stack Sandwich material: [90/0/*core*/0/90].

Material properties The material properties of the Graphite-Epoxy plies are:

$\mathbf{E_{11}}$ [Pa]	$\mathbf{E_{22}}$ [Pa]	$\mathbf{E_{33}}$ [Pa]	$\mathbf{G_{12}}$ [Pa]	$\mathbf{G_{13}}$ [Pa]
132.38×10^9	10.756×10^9	10.756×10^9	5.6537×10^9	5.6537×10^9
$\mathbf{G_{23}}$ [Pa]	$\boldsymbol{\nu_{12}}$ [-]	$\boldsymbol{\nu_{13}}$ [-]	$\boldsymbol{\nu_{23}}$ [-]	$\boldsymbol{\rho_{GE}}$ $[\boldsymbol{kg/m^3}]$
3.603×10^9	0.24	0.24	0.49	1600

Table 4.18: Brischetto test case: Graphite-Epoxy material properties.

The material properties of the PVC core are:

$\mathbf{E_{11}}$ [Pa]	$\mathbf{E_{22}}$ [Pa]	$\mathbf{E_{33}}$ [Pa]	$\mathbf{G_{12}}$ [Pa]	$\mathbf{G_{13}}$ [Pa]
180×10^6	180×10^6	180×10^6	65.7×10^6	65.7×10^6
$\mathbf{G_{23}}$ [Pa]	$\boldsymbol{\nu_{12}}$ [-]	$\boldsymbol{\nu_{13}}$ [-]	$\boldsymbol{\nu_{23}}$ [-]	$\boldsymbol{\rho_{PVC}}$ $[\boldsymbol{kg/m^3}]$
65.7×10^6	0.37	0.37	0.37	50

Table 4.19: Brischetto test case: PVC material properties.

Boundary conditions Simple-support (SS) at $x = 0$ and at $x = a$.

Results Non-dimensional natural circular frequencies:

$$\bar{\omega} = \frac{a^2}{h}\sqrt{\frac{\rho_{GE}}{E_{22_{GE}}}}\,\omega \tag{4.7}$$

Computational model For this benchmark, three sublaminates are used, 1 for each skin and one for the core, in view of minimizing the computational cost without affecting the accuracy. Thanks to the versatility of the formulation, higher-order theories are implemented straight-forwardly as the curvature effects increase, as shown in Table 4.20. Furthermore, higher orders are adopted for the highly shear-deformable core, compared to the orders adopted for the stiff skins.

S	Top skin	Core	Bottom skin	Model ID
$10, 5$	$EM^{2,2,1}_{2,2,1}$	$EM^{4,4,3}_{4,4,3}$	$EM^{2,2,1}_{2,2,1}$	M1
$1000, 100$	$EM^{3,3,2}_{3,3,2}$	$EM^{5,5,4}_{5,5,4}$	$EM^{3,3,2}_{3,3,2}$	M2

Table 4.20: Brischetto test case: models adopted depending on $S = \frac{R}{h}$.

The Ritz orders of expansion adopted are: $R_u = 40$, $R_s = 41$, $S_u = 40$, $S_s = 41$. The high orders assure converged results for all the considered modes (convergence study is omitted for brevity).

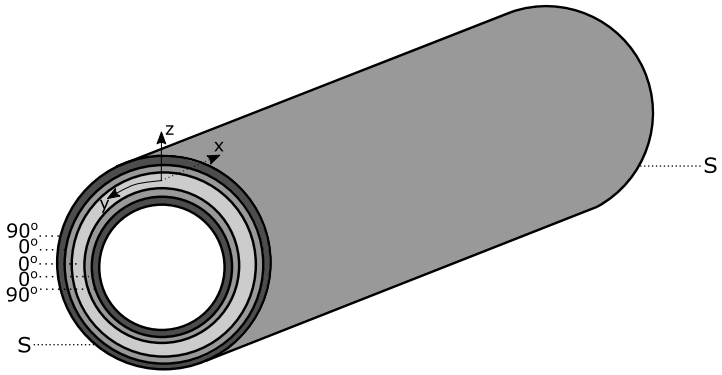

Figure 4.16: Brischetto test case.

Brischetto uses a Navier-type solution which allows computing modes corresponding to a specified pair of half-wave numbers along the axial and circumferential directions. This type of solution does not introduce any in-plane discretization errors. Since Brischetto's solution technique outputs a coarser set of natural frequencies respect to the present theory, many additional modes obtained through the present method are not reported.

In Table 4.21 the results obtained by Brischetto and the present theory are compared. In particular, the results refer to the first three frequencies for different radius-over-thickness ratios relative to different combinations of half-wave numbers (m for the circumferential direction and n for the axial direction). The results for geometries with high radius-over-thickness ratios ($R/h = 1000$ and $R/h = 100$) match almost perfectly, while results for low radius-over-thickness ratios ($R/h = 10$ and $R/h = 5$) are less accurate but with errors much lower than 1%, therefore, acceptable.

As previously discussed, high models coupled with a high in-plane discretization allow to obtain excellent results, Table 4.21 amply confirms it.

S	1000 (M1)	100 (M1)	10 (M2)	5 (M2)
I mode (m=0, n=1)				
Brischetto [39]	8797.8	879.79	87.986	44.004
Present	8797.8	879.79	87.986	44.004
II mode (m=0, n=1)				
Brischetto [39]	31038	3103.8	310.42	155.25
Present	31038	3103.8	310.46	155.27
III mode (m=0, n=1)				
Brischetto [39]	98885	9888.8	991.38	340.44
Present	98885	9888.8	991.37	340.45
I mode (m=2, n=1)				
Brischetto [39]	4597.4	459.76	46.133	23.238
Present	4597.4	459.75	46.135	23.239
II mode (m=2, n=1)				
Brischetto [39]	41954	4195.4	419.69	209.84
Present	41954	4200.0	419.72	209.85
III mode (m=2, n=1)				
Brischetto [39]	139995	13999	1376.7	395.64
Present	139995	13999	1376.8	395.65
I mode (m=2, n=2)				
Brischetto [39]	11287	1128.7	113.47	57.167
Present	11287	1138.7	113.47	57.170
II mode (m=2, n=2)				
Brischetto [39]	68111	6811.1	681.1	340.25
Present	68111	6811.1	681.18	340.29
III mode (m=2, n=2)				
Brischetto [39]	140500	14049	1382.3	473.05
Present	140499	14050	1382.4	473.09
I mode (m=2, n=3)				
Brischetto [39]	17724	1772.6	178.60	89.936
Present	17724	1772.6	178.60	89.937
II mode (m=2, n=3)				
Brischetto [39]	96930	9693.0	968.91	481.89
Present	96930	9693.0	969.05	481.81
II mode (m=2, n=3)				
Brischetto [39]	141452	14145	1392.4	500.05
Present	141452	14145	1392.5	500.10

Table 4.21: Brischetto test case: first three fundamental frequencies for different radius-to-thickness ratios and for different combinations of half-wave numbers.

4.7 RMVT comparison with PVD

Finally, one last test case is proposed in order to highlight the differences of the present method with the Ritz S-GUF PVD formulation developed by D'Ottavio et al. [1]. A *free-edge bending problem* is considered.

Geometry Square cylindrical panel ($a = b$). The length-over-thickness ratio ($D = a/h$) is 5, the depth ratio ($S = R/h$) is 10.

Composite stack Double-core sandwich: [90/0/90/*core*/90/0/90/*core*/90/0/90]. The thickness of each ply is $h_p = 0.015h$. The thickness of each core is $h_c = 0.4325h$.

Material properties

	$\mathbf{E_{11}}$ [Pa]	$\mathbf{E_{22}}$ [Pa]	$\mathbf{E_{33}}$ [Pa]
Ply	172.5×10^9	6.9×10^9	6.9×10^9
Core	0.276×10^9	0.276×10^9	3.45×10^9
	$\mathbf{G_{12}}$ [Pa]	$\mathbf{G_{13}}$ [Pa]	$\mathbf{G_{23}}$ [Pa]
Ply	3.45×10^9	3.45×10^9	2.76×10^9
Core	0.1104×10^9	0.414×10^9	0.414×10^9
	$\boldsymbol{\nu_{12}}$ [-]	$\boldsymbol{\nu_{13}}$ [-]	$\boldsymbol{\nu_{23}}$ [-]
Ply	0.25	0.25	0.25
Core	0.25	0.02	0.02

Table 4.22: RMVT comparison with PVD test case: ply and core material properties.

Boundary conditions Cantilever cylindrical panel: *CFFF*.

Load Bisinusoidal load applied on the top surface: $P = P_0 sin(\frac{\pi}{a}x) sin(\frac{\pi}{b}y)$.

Results Through-thickness distributions of non-dimensional displacements and stresses evaluated at $x = a$ and $y = b/2$:

$$
\begin{aligned}
(\bar{u}_x, \bar{u}_y) &= \frac{100 E_{22}^{ply}}{P_0 h D^3}(u_x, u_y) \quad \bar{u}_z = \frac{100 E_{22}^{ply}}{P_0 h D^4}(u_x, u_y) \\
(\bar{\sigma}_{xx}, \bar{\sigma}_{yy}) &= \frac{1}{P_0 D^2}(\sigma_{xx}, \sigma_{yy}) \quad \bar{\sigma}_{xy} = \frac{10}{P_0 D^2}\sigma_{xy} \\
(\bar{\sigma}_{xz}, \bar{\sigma}_{yz}, \bar{\sigma}_{zz}) &= \frac{1}{P_0 D}(\sigma_{xz}, \sigma_{yz}, \sigma_{zz})
\end{aligned}
\tag{4.8}
$$

The nondimensional thickness coordinate $\xi = \frac{z}{h}$ has been adopted.

Computational model Five sublaminates are used, one for each skin and one for each core, in view of minimizing the computational cost without affecting the accuracy. For the cores, which are characterized by a higher shear deformability, higher models compared to the skins were used. LW models were used in the sublaminates associated to the skins.

Variational principle	Top skin	Core 1	Middle skin	Core 2	Bottom skin
RMVT	$LM^{2,2,1}_{2,2,1}$	$EM^{3,3,2}_{3,3,2}$	$LM^{2,2,1}_{2,2,1}$	$EM^{3,3,2}_{3,3,2}$	$LM^{2,2,1}_{2,2,1}$
PVD	$LD_{2,2,1}$	$ED_{3,3,2}$	$LD_{2,2,1}$	$ED_{3,3,2}$	$LD_{2,2,1}$

Table 4.23: RMVT comparison with PVD test case: models adopted.

The Ritz orders of expansion adopted are: $R_u = S_u = 10$ ($R_s = S_s = R_u + 1$).

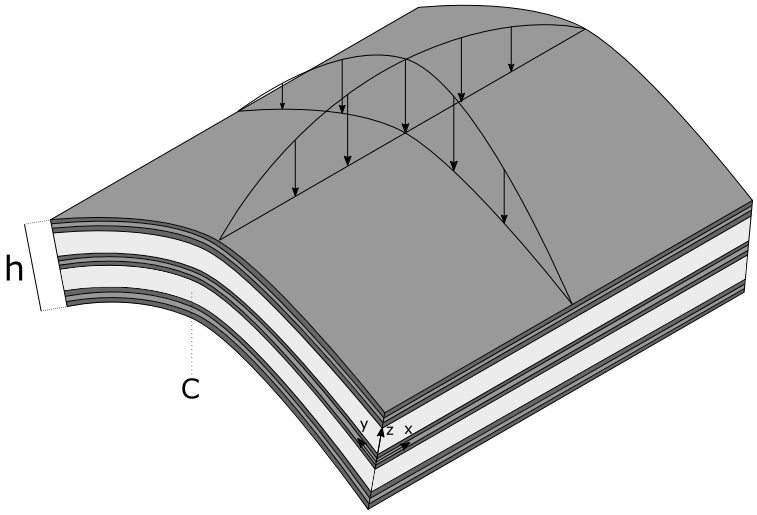

Figure 4.17: RMVT and PVD comparison test case.

Figure 4.18 compares the through-thickness distributions of displacements and stresses obtained with RMVT and PVD. The transverse stresses for RMVT are obtained *a priori* while for PVD are obtained through *integration of the equilibrium equations*.

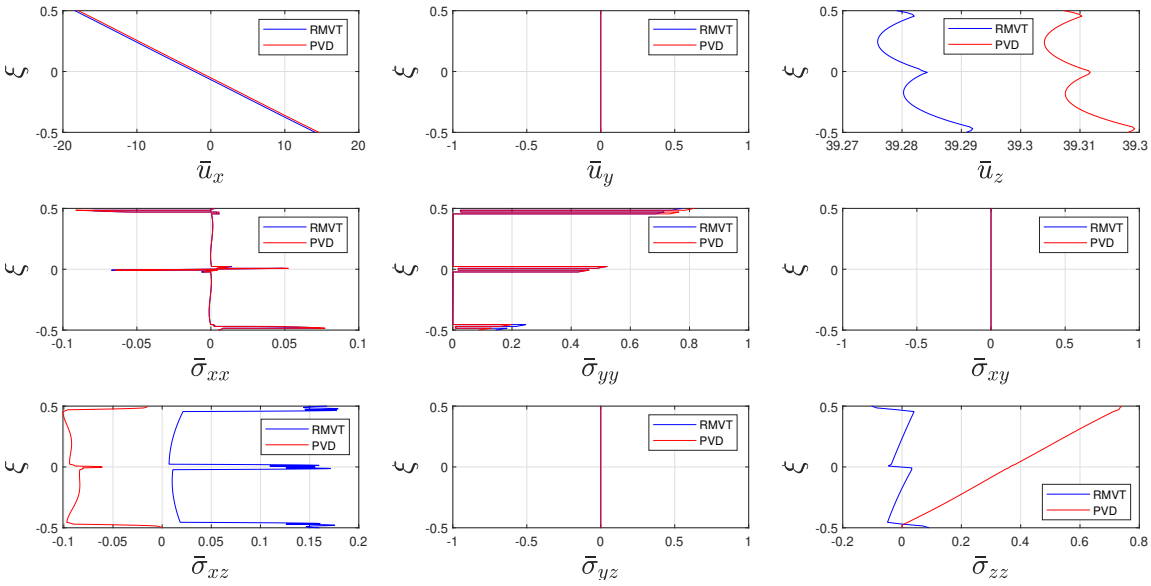

Figure 4.18: Through-thickness distributions of $\bar{u}_x$, $\bar{u}_y$, $\bar{u}_z$, $\bar{\sigma}_{xx}$, $\bar{\sigma}_{yy}$, $\bar{\sigma}_{xy}$, $\bar{\sigma}_{xz}$, $\bar{u}_{yz}$ and $\bar{\sigma}_{zz}$. Comparison between RMVT and PVD.

The test case is particularly challenging, as can be noticed from the fact that even the bending stresses $\bar{\sigma}_{xx}$ and $\bar{\sigma}_{yy}$ present some small discrepancies between the two models. As illustrated in Figure 4.19, the differences are mainly located in the bottom skin and in the top skin. Since this test case presents a difficult configuration it is suited to highlight the differences between the two similar formulations, based on two different variational principles, RMVT and PVD.

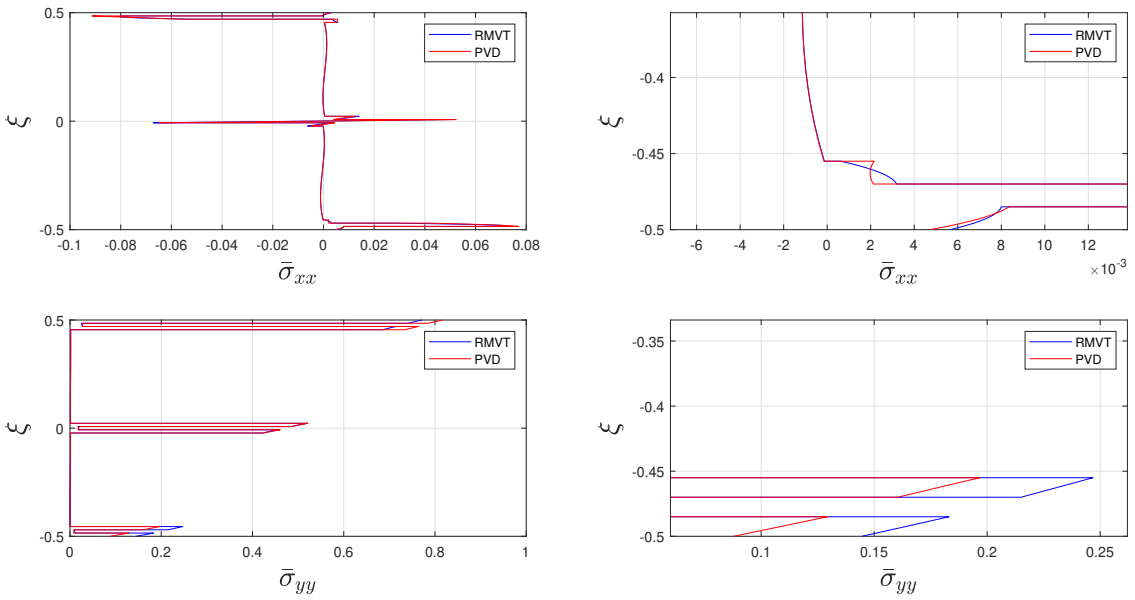

Figure 4.19: Through-thickness distributions of $\bar{\sigma}_{xx}$ and $\bar{\sigma}_{yy}$. Comparison between RMVT and PVD.

Considering $\bar{\sigma}_{xz}$ it can be noticed that the values obtained by RMVT result to be shifted towards higher values compared to the solution based on the PVD, Figure 4.20. Furthermore, the RMVT solution presents oscillations within the three skins, while the values obtained by the PVD are smoother. $\bar{\sigma}_{xz}$ computed through RMVT fails to fulfill the top-bottom equilibrium conditions $\bar{\sigma}_{xz}(h/2) = \bar{\sigma}_{xz}(-h/2) = 0$. Exploiting the characteristic of RMVT, it is possible to fulfill these conditions *a priori* by imposing the correct values of $\bar{\sigma}_{xz}(h/2) = 0$ and $\bar{\sigma}_{xz}(-h/2) = 0$, Figure 4.21.

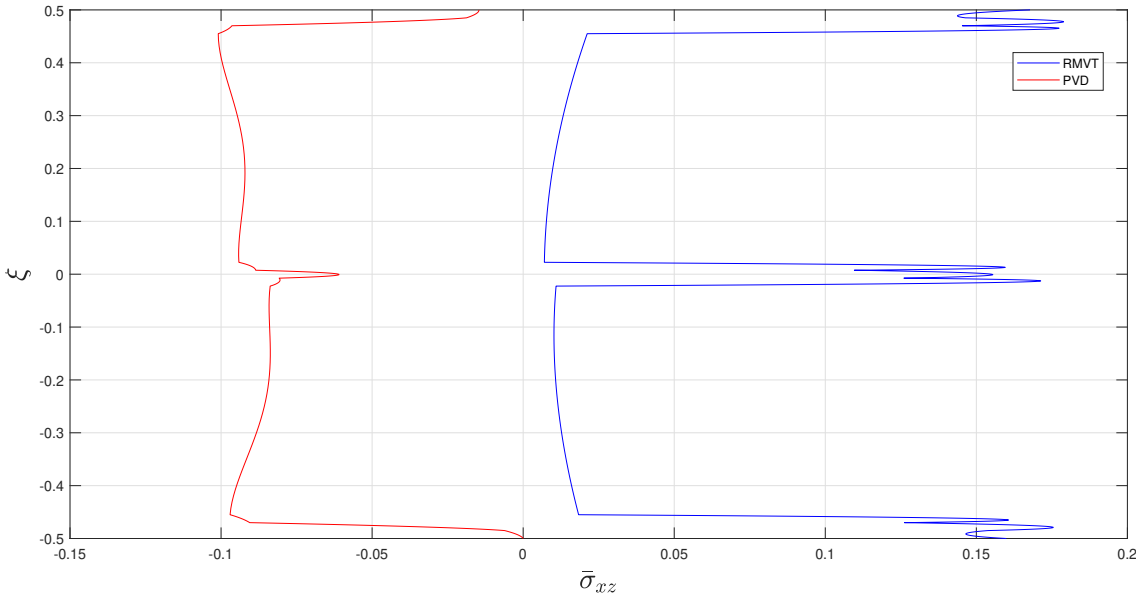

Figure 4.20: Through-thickness distribution of $\bar{\sigma}_{xz}$. Comparison between RMVT and PVD.

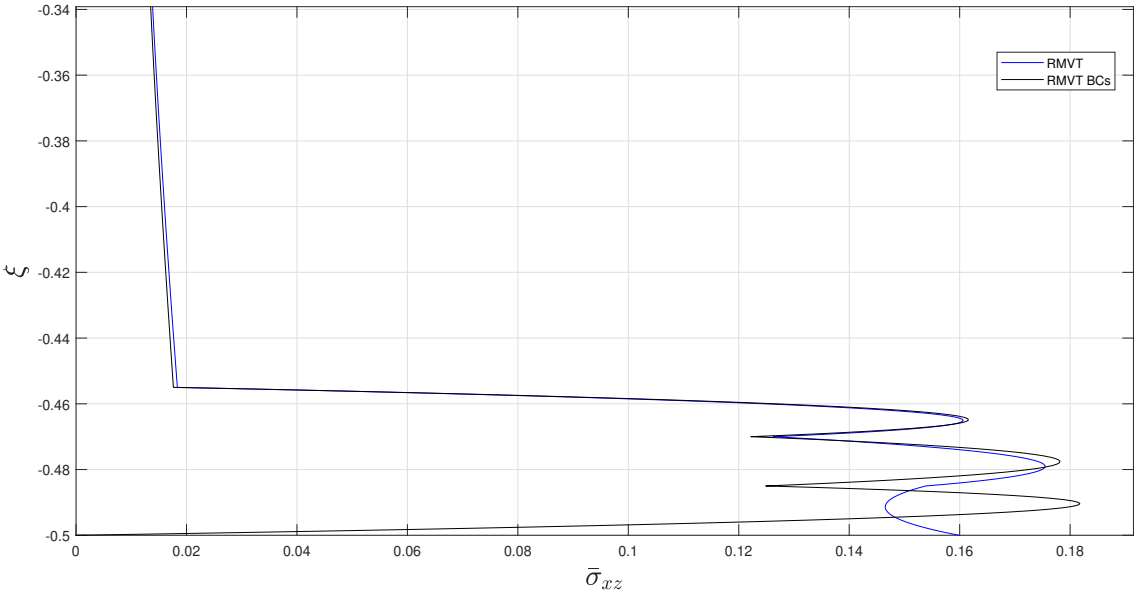

Figure 4.21: Through-thickness distribution of $\bar{\sigma}_{xz}$ with and without the imposition of top-bottom stress boundary conditions. Comparison between RMVT and PVD.

The value of $\bar{\sigma}_{zz}$ was computed at several distances from the *free-edge* as shown in Figure 4.22. $\bar{\sigma}_{zz}$ computed through RMVT presents in all cases an almost repetitive distribution between the bottom half and the top half. $\bar{\sigma}_{zz}$ computed through the PVD presents a similar distribution to the one computed through RMVT only at $x = 0.9a$, as the free-edge is approached it changes distribution and increases linearly throughout the thickness.

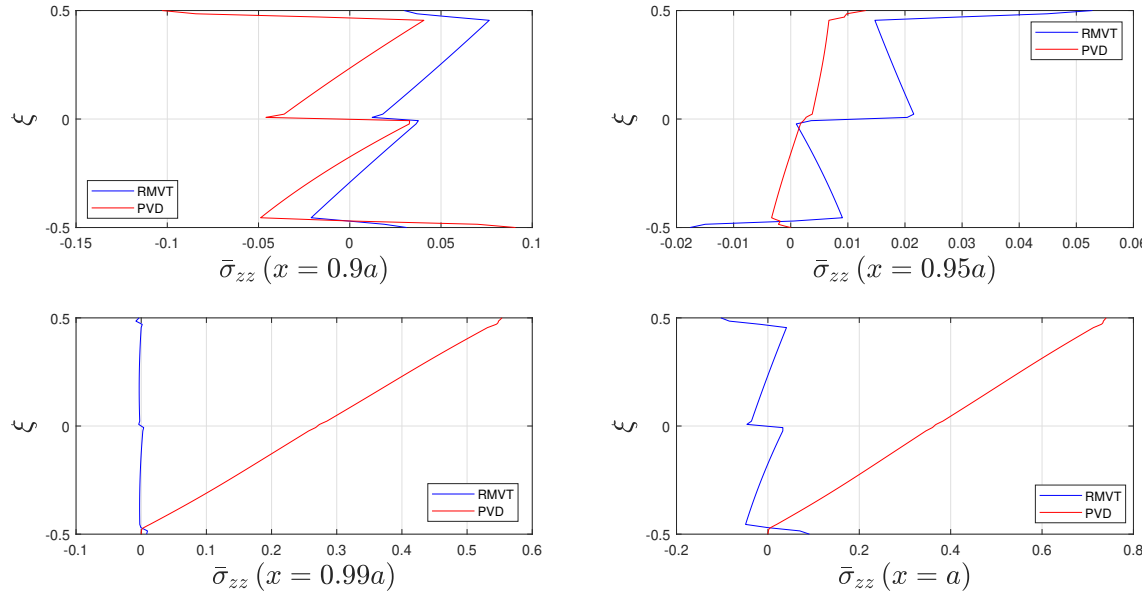

Figure 4.22: Through-thickness distributions of $\bar{\sigma}_{zz}$ computed at different distances from the free-edge. Comparison between RMVT and PVD.

In order to assess which numerical method provides the most accurate results, further studies should be conducted. For instance, this same problem should be solved using a commercial FEM software and its solution compared to those presented here.

Chapter 5

Assessment of the numerical tool

The present mixed theory assumes both kinematic variables (u_x, u_y, u_z) and static variables $(\sigma_{xz}, \sigma_{yz}, \sigma_{zz})$. These variables are described by a model (through the thickness) and the Ritz approximation (in-plane). The present chapter presents some considerations about how these energetically conjugated fields should be chosen so that a stable, and, possibly, optimal method is obtained. Different aspects play a role: the model orders, the orders of the Ritz approximation, and the top-bottom stress boundary conditions. Regarding the stress boundary conditions on the boundary of the domain in the (x, y) plane $(\partial\Omega)$, no particular conditions have to be imposed, as it derives from the variational principle.

In the present Chapter, by making the hypothesis that the in-plane approximation (Ritz) and the out-of-plane approximation (model) do not influence each other, these two aspects will be studied separately. Therefore, the first section will investigate the effect of different orders for the Ritz approximation, while the second section will present results about the model orders and the top-bottom stress boundary conditions. Both the linear static problem and the free-vibration analysis will be considered.

5.1 Ritz orders of expansion

In a classical displacement-based approach Ritz orders of expansion refer only to the displacement variables and, depending on the specific problem, they need to be set to an order high enough to reach convergence [1]. Nevertheless, when employing a mixed variational principle, in addition to convergence considerations, also the relative Ritz orders of expansions for displacement variables and stress variables have to be taken into account. It will be here shown that the Ritz order of expansion for stress variables has to be higher than the order for displacement variables: $M_s > M_u$. In particular, since in the present framework it is possible to select two independent orders of Ritz approximation, one in the x-direction (R) and one in the y-direction (S), it is shown that a correct Ritz approximation requires: $R_s > R_u$ and $S_s > S_u$. In this section, the results are compared with those obtained from the corresponding displacement-based model.

Test case In order to focus only on the effects of selecting different relative orders of Ritz approximation for displacement and stress variables, an isotropic plate is considered.

Geometry Square plate $(a = b)$, characterized by a thickness ratio (a/h) of 10.

Material properties

$\mathbf{E_{11}}$ [Pa]	$\mathbf{E_{22}}$ [Pa]	$\mathbf{E_{33}}$ [Pa]	$\mathbf{G_{12}}$ [Pa]	$\mathbf{G_{13}}$ [Pa]
68.9×10^9	68.9×10^9	68.9×10^9	26.7×10^9	26.5×10^9
$\mathbf{G_{23}}$ [Pa]	$\boldsymbol{\nu_{12}}$ [-]	$\boldsymbol{\nu_{13}}$ [-]	$\boldsymbol{\nu_{23}}$ [-]	$\boldsymbol{\rho}$ $[\boldsymbol{kg/m^3}]$
26.5×10^9	0.3	0.3	0.3	2740

Table 5.1: Aluminum material properties.

Boundary conditions Three sets are investigated: *FFFF*, *SSSS* and *CCCC*.

Computational model The model here adopted is $EM^{0,0,-}_{1,1,0}$, "-" indicates that no DOF are used for σ_{zz}. No top-bottom stress boundary conditions are imposed. Since the plate is isotropic and the dimensions in the x and y directions are the same, there is no reason to select different Ritz orders of expansion along the two directions, therefore: $R_u = S_u$ and $R_s = S_s$. Four different orders of Ritz approximation are considered (R_u and S_u are fixed at 15):

1. $R_s = R_u - 1$; $S_s = S_u - 1 \quad \rightarrow \Delta = -1$.
2. $R_s = R_u$; $S_s = S_u \quad \rightarrow \Delta = 0$.
3. $R_s = R_u + 1$; $S_s = S_u + 1 \quad \rightarrow \Delta = +1$.
4. $R_s = R_u + 5$; $S_s = S_u + 5 \quad \rightarrow \Delta = +5$.

In Figure 5.1 are compared the first twenty-five modes obtained through the RMVT model and an equivalent PVD model. The PVD equivalent model is $ED_{1,1,0}$ with Ritz orders of expansion: $R_u = 15$ and $S_u = 15$. Furthermore, the first four modes are reported in Figure 5.2 (for brevity only the case with boundary conditions *SSSS* is shown, similar results can be observed for any set of boundary conditions).

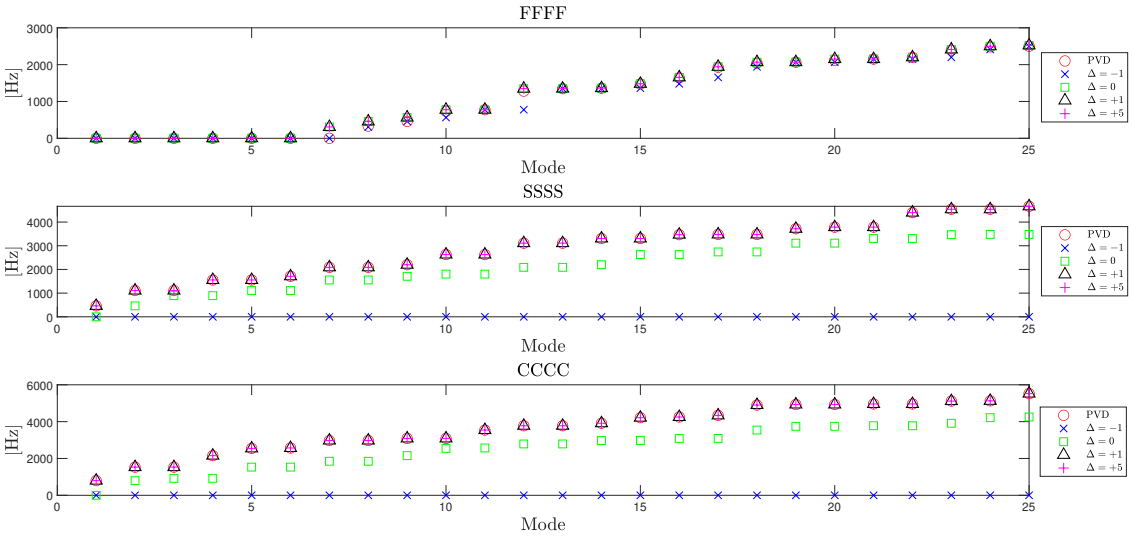

Figure 5.1: Comparison of first twenty-five modes of an isotropic square plate obtained through RMVT with different Ritz orders of expansion and an equivalent PVD model.

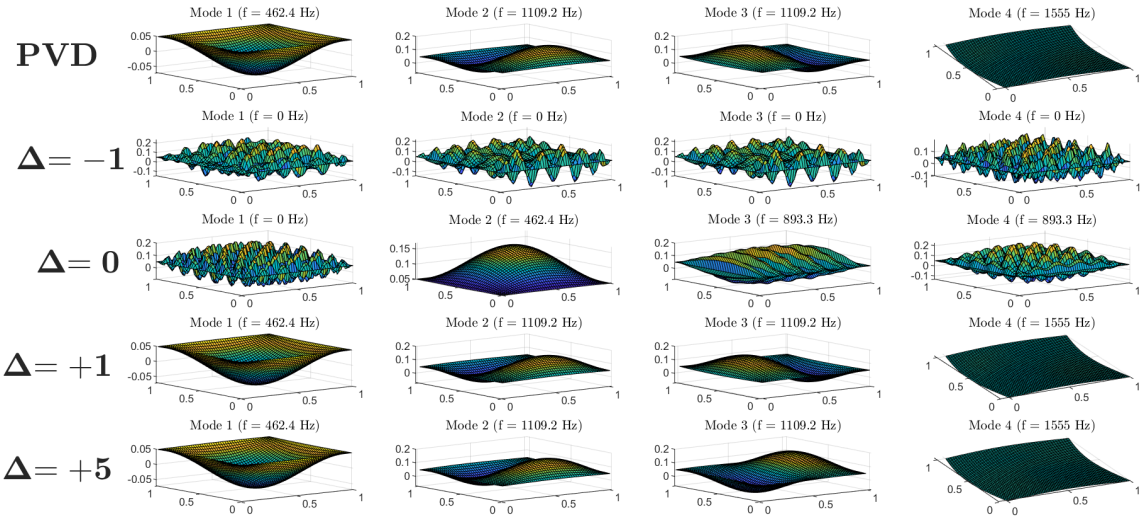

Figure 5.2: Comparison of first four modal shapes of an isotropic simply-supported square plate obtained through RMVT with different Ritz orders of expansion for displacement and stress variables, and an equivalent PVD model.

Figure 5.1 and Figure 5.2 show clearly that in order to obtain correct results it must hold that: $R_s > R_u$ and $S_s > S_u$. In particular, the following considerations can be drawn:

1. $R_s < R_u$; $S_s < S_u$: many natural frequencies with almost zero frequency are present and they are associated to non-physical modes. This effect is less prominent in configuration *FFFF*, however macroscopic errors are still present.

2. $R_s = R_u$; $S_s = S_u$: correct frequencies and modes can be obtained, but in addition to them also non-physical frequencies and modes are computed.

3. $R_s > R_u$; $S_s > S_u$: correct frequencies and modes are obtained.

Furthermore, it is sufficient to have: $R_s = R_u + 1$ and $S_s = S_u + 1$ in order to compute the correct frequencies and modes, without the presence of any non-physical response. Table 5.2 compares the relative errors for the first five natural frequencies for the simply-supported configuration. The error is defined as: $err = |f_{RMVT} - f_{PVD}|/f_{PVD} \times 100$.

Mode	err: $\Delta = +1$	err: $\Delta = +5$
1	2.4584×10^{-13}	2.0896×10^{-13}
2	1.0249×10^{-13}	1.8448×10^{-13}
3	2.0498×10^{-14}	8.1992×10^{-14}
4	4.0943×10^{-13}	3.9481×10^{-13}
5	5.2641×10^{-13}	3.3632×10^{-13}

Table 5.2: First five natural frequencies errors for a simply-supported plate between PVD and RMVT, for $\Delta = +1$ and $\Delta = +5$.

Increasing more than one the Ritz approximation orders for stress variables in each dimension, with respect to the orders for displacement variables, would not affect the results. Therefore, using much higher relative orders of approximation for stress variables would only increase the computational cost, resulting in a non-optimal selection of parameters.

5.2 Model orders

The relative orders used for the model expansion of displacements and stresses is important as it may cause numerical instabilities. The present section discusses which models result more correct, both from numerical results and from an analytical standpoint.

5.2.1 Free-vibration problem

Regarding the stability of the free-vibration problem, D'Ottavio in his work [40] highlighted the possibility of instabilities under the form of spurious modes when employing a wrong mixed model.

Correct models, in this case, are defined as models that satisfy the two following conditions:

1. There are no stress modes not conjugated to any kinematic mode.
2. Apart from the kinematic modes associated with plane stress modes, all the kinematic modes have to be associated with a transverse stress mode.

These two conditions derive from analytical requirements that need to be fulfilled by the stiffness matrix $\mathbf{K}$. First of all, it is convenient to collect the displacement variables into vector $\mathbb{U}$, and the stress variables into vector $\mathbb{S}$. It is then possible to rearrange the elements of the stiffness matrix into four sub-matrices:

$$\mathbf{Kv} = \begin{bmatrix} \mathbb{A} & \mathbb{B}^T \\ \mathbb{B} & \mathbb{C} \end{bmatrix} \begin{Bmatrix} \mathbb{U} \\ \mathbb{S} \end{Bmatrix} \tag{5.1}$$

where for a flat plate geometry the arrays have the following form:

$$\mathbb{A} = \begin{bmatrix} \mathbf{K}_{u_x u_x} & \mathbf{K}_{u_x u_y} & \mathbf{0} \\ \mathbf{K}_{u_y u_x} & \mathbf{K}_{u_y u_y} & \mathbf{0} \\ \mathbf{0} & \mathbf{0} & \mathbf{0} \end{bmatrix} \quad \mathbb{B} = \begin{bmatrix} \mathbf{K}_{s_x u_x} & \mathbf{K}_{s_x u_y} & \mathbf{K}_{s_x u_z} \\ \mathbf{K}_{s_y u_x} & \mathbf{K}_{s_y u_y} & \mathbf{K}_{s_y u_z} \\ \mathbf{K}_{s_z u_x} & \mathbf{K}_{s_z u_y} & \mathbf{K}_{s_z u_z} \end{bmatrix} \quad \mathbb{C} = \begin{bmatrix} \mathbf{K}_{s_x s_x} & \mathbf{K}_{s_x s_y} & \mathbf{0} \\ \mathbf{K}_{s_y s_x} & \mathbf{K}_{s_y s_y} & \mathbf{0} \\ \mathbf{0} & \mathbf{0} & \mathbf{K}_{s_z s_z} \end{bmatrix}$$

Furthermore, it is useful to separate the coupling matrix $\mathbb{B}$ into the contribution due to the geometric terms only ($\mathbb{B}_G$) and the contribution due to the Poisson constitutive coupling ($\mathbb{B}_C$).

$$\mathbb{B} = \mathbb{B}_G + \mathbb{B}_C = \begin{bmatrix} \mathbf{K}_{s_x u_x} & \mathbf{K}_{s_x u_y} & \mathbf{K}_{s_x u_z} \\ \mathbf{K}_{s_y u_x} & \mathbf{K}_{s_y u_y} & \mathbf{K}_{s_y u_z} \\ \mathbf{0} & \mathbf{0} & \mathbf{K}_{s_z u_z} \end{bmatrix} + \begin{bmatrix} \mathbf{0} & \mathbf{0} & \mathbf{0} \\ \mathbf{0} & \mathbf{0} & \mathbf{0} \\ \mathbf{K}_{s_z u_x} & \mathbf{K}_{s_z u_y} & \mathbf{0} \end{bmatrix} \tag{5.2}$$

Since RMVT involves only transverse strains and stresses, membrane strains do not need to be considered for the analysis of spurious modes: only the contributions of the in-plane displacements to the transverse stresses, that constitute the $\mathbb{B}_C$ array, should be examined.

Condition 1 and 2 listed above, derive from the most comprehensive treatment of the stability analysis of a numerical method discretized as in Eq.(5.1). Condition 1 follows from the *inf-sup* or LBB condition on the coupling matrix $\mathbb{B}$:

$$ker(\mathbb{B}_G^T) = \{\} \tag{5.3}$$

while condition 2 follows from the *elker* condition on the matrix $\mathbb{A}$, denoting $\mathbf{k}_B$ the kernel of $\mathbb{B}_G$:

$$rank({\mathbf{k}_B}^T \, \mathbb{A} \, \mathbf{k}_B) = N_\Omega \tag{5.4}$$

where N_Ω is the number of kinematic modes not-conjugated to any transverse stress, i.e, plane stress modes.

In an internal report D'Ottavio [40] examined the thickness modes of the fundamental mode ($m = n = 1$) by means of the Navier solution. He found that optimal models fulfill indeed $ker(\mathbb{B}_G^T) = \{\}$, and that $rank(ker(\mathbb{B}_G)^T \, \mathbb{A} \, ker(\mathbb{B}_G))) = 3$. The three plane stress modes identified in his work correspond to those of the classical laminated plate theory (CLPT). Especially, two membrane modes associated to the z-independent functions u_{x0} and u_{y0}, and one pure bending deformation mode associated to the z-independent function u_{z0}.

In the following, the same analysis as the one carried out by D'Ottavio is reported for the present numerical method, to investigate whether similar considerations still hold true. Several models are considered, and the two main algebraic indexes previously described are reported for each one of them:

$$N_{stress} = ker(\mathbb{B}_G^T)$$
$$N_{kin} = rank({\mathbf{k}_B}^T \, \mathbb{A} \, \mathbf{k}_B)$$

Furthermore, to get an insight into the influence that the Ritz orders of expansion have on these parameters, different Ritz orders of approximation were used for each model.

The same test case described in Section 5.1 is here adopted (homogeneous square plate with $a/h = 10$) but only the set of boundary conditions *SSSS* is considered. This corresponds to the configuration examined by D'Ottavio [40]. The Ritz orders of expansion for displacement variables are fixed at $R_u = S_u = 10$.

Since the models here adopted have $N_{u_x} = N_{u_y} = N_{u_\alpha}$ and $N_{\sigma_{xz}} = N_{\sigma_{yz}} = N_{\sigma_{\alpha z}}$. The following simplified notation is introduced for mixed models:

$$EM^{N_{\sigma_{\alpha z}} N_{\sigma_{zz}}}_{N_{u_\alpha} N_{u_z}} \tag{5.5}$$

$\mathbf{R_s = S_s}$	9		10		11		15	
Model	N_{stress}	N_{kin}	N_{stress}	N_{kin}	N_{stress}	N_{kin}	N_{stress}	N_{kin}
No top-bottom b.cs.								
$EM^{0,-}_{1,0}$	0	274	0	250	23	241	231	241
$EM^{1,-}_{1,0}$	162	274	200	250	265	241	681	241
$EM^{3,-}_{1,0}$	486	274	600	250	749	241	1581	241
$EM^{4,-}_{1,0}$	648	274	800	250	991	241	2031	241
$EM^{0,0}_{1,0}$	81	274	100	250	144	241	456	241
$EM^{0,1}_{1,0}$	162	274	200	250	265	241	681	241
$EM^{1,0}_{1,0}$	243	274	300	250	386	241	906	241
$EM^{1,1}_{1,0}$	324	274	400	250	507	241	1131	241
σ_{xz} and σ_{yz} top-bottom b.cs. (plane stress)								
$EM^{1,-}_{1,0}$	0	400	0	400	0	400	0	400
$EM^{2,-}_{1,0}$	0	274	0	250	23	241	231	241
$EM^{3,-}_{1,0}$	162	274	200	250	265	241	681	241
$EM^{4,-}_{1,0}$	324	274	400	250	507	241	1131	241
$EM^{5,-}_{1,0}$	486	274	600	250	749	241	1581	241
σ_{xz}, σ_{yz} and σ_{zz} top-bottom b.cs. (3D law)								
$EM^{2,1}_{1,0}$	0	274	0	250	23	241	231	241
$EM^{2,2}_{1,0}$	81	274	100	250	144	241	456	241
$EM^{2,3}_{1,0}$	162	274	200	250	265	241	681	241

Table 5.3: Algebraic parameters for the Reissner-Mindlin kinematics. $R_u = S_u = 10$.

Table 5.3 reports the number of not-conjugated stress modes and not-conjugated kinematic modes for different mixed models based on the Reissner-Mindlin kinematics and different Ritz orders of expansion. The results in red are associated with wrong results, i.e. modes at zero frequency. The results underlined are those models that present the less number of not-conjugated stress modes and not-conjugated kinematic modes. Additional results are reported in Appendix D for models of the type: $EM^{N_{\sigma\alpha z}N_{\sigma zz}}_{3,0}$ and $EM^{N_{\sigma\alpha z}N_{\sigma zz}}_{3,2}$.

It is clear that correct results can be obtained only for models and Ritz orders of expansion that minimize the number of not-conjugated kinematic modes. In the present framework, that differs from the one studied by D'Ottavio only in the in-plane approximation, the correct number of not-conjugated kinematic modes results to be dependant on the kinematic model. For the kinematic models here considered the correct number of not-conjugated kinematic modes results to be:

- $EM^{N_{\sigma\alpha z}N_{\sigma zz}}_{1,0}$: $N_{kin} = 241$ (Reissner-Mindlin kinematics).
- $EM^{N_{\sigma\alpha z}N_{\sigma zz}}_{3,0}$: $N_{kin} = 259$.
- $EM^{N_{\sigma\alpha z}N_{\sigma zz}}_{3,2}$: $N_{kin} = 221$.

Incorrect models are characterized by a higher number of N_{kin}. Similarly, Ritz orders of approximation $R_s \leq R_u$, $S_s \leq S_u$ present a higher number of not-conjugated kinematic

modes. The smaller are the Ritz orders used for the stress variables compared to those of the kinematic variables, the higher is the value of N_{kin}. This result confirms the conclusion of Section 5.1, where it is stated that correct Ritz orders satisfy the relations $R_s > R_u$ and $S_s > S_u$.

Differently from what is obtained when a Navier solution is adopted, there are no models having zero not-conjugated stress modes and minimizing the not-conjugated kinematic modes at the same time. This result may be because the in-plane Ritz orders of expansion for the stress variables have a higher base than those adopted for the displacements. Indeed, if the Ritz orders for the stress variables are further increased, compared to those used for the displacement variables, the number of not-conjugated stress modes increases as well. Nevertheless - as can be noticed from Table 5.4 where the non-dimensional eigenfrequencies for the first four modes of the Reissner-Mindlin kinematics are reported, for $R_s = S_s = 11$ and $R_s = S_s = 15$ - the increase of not-conjugated stress modes due to higher Ritz orders for the transverse stress variables does not affect the results. This result supports once more the conclusion of Section 5.1, where it is stated that $R_s = R_u + 1$ and $S_u = S_s + 1$ are the optimal Ritz orders of expansion due to computational reasons. However, in accordance with the results obtained by D'Ottavio [40], Table 5.4 shows that higher not-conjugated stress modes due to the model, may increase the rigidity. Further studies should be conducted to investigate the reason why not-conjugated stress modes due to the Ritz approximation do not affect the solution as much as not-conjugated stress modes due to the model.

Finally, it is highlighted that models associated with optimal values for both N_{stress} and N_{kin} fulfill the condition of having the DOF of the displacement variables one unit higher than the DOF of the stress variables (the imposition of the top-bottom stress boundary conditions removes two DOF per stress variable).

Model	$\bar{\omega}_1$	$\bar{\omega}_2 = \bar{\omega}_3$	$\bar{\omega}_4$
$ED_{1,0}\,(k=1)$	5.7944	13.8987	19.4833
$ED_{1,0}\,(k=5/6)$	5.7693	13.7637	19.4833

$\mathbf{R_s} = \mathbf{S_s}$	11			15		
Model	$\bar{\omega}_1$	$\bar{\omega}_2 = \bar{\omega}_3$	$\bar{\omega}_4$	$\bar{\omega}_1$	$\bar{\omega}_2 = \bar{\omega}_3$	$\bar{\omega}_4$
No top-bottom b.cs.						
$EM^{0,-}_{1,0}$	5.7944	13.8987	19.4833	5.7944	13.8987	19.4833
$EM^{1,-}_{1,0}$	5.7944	13.8987	19.4833	5.7944	13.8987	19.4833
$EM^{3,-}_{1,0}$	5.7944	13.8987	19.4833	5.7944	13.8987	19.4833
$EM^{4,-}_{1,0}$	5.7944	13.8987	19.4833	5.7944	13.8987	19.4833
$EM^{0,0}_{1,0}$	5.7944	13.8987	19.4833	5.7944	13.8987	19.4833
$EM^{0,1}_{1,0}$	*6.3820*	*15.2152*	19.4833	*6.3820*	*15.2152*	19.4833
$EM^{1,0}_{1,0}$	5.7944	13.8987	19.4833	5.7944	13.8987	19.4833
$EM^{1,1}_{1,0}$	*6.3820*	*15.2152*	19.4833	*6.3820*	*15.2152*	19.4833
σ_{xz} and σ_{yz} top-bottom b.cs. (plane stress)						
$EM^{1,-}_{1,0}$	0	0	0	0	0	0
$EM^{2,-}_{1,0}$	5.7693	13.7637	19.4833	5.7693	13.7637	19.4833
$EM^{3,-}_{1,0}$	5.7693	13.7637	19.4833	5.7693	13.7637	19.4833
$EM^{4,-}_{1,0}$	*5.7854*	*13.8500*	19.4833	*5.7854*	*13.8500*	19.4833
$EM^{5,-}_{1,0}$	*5.7854*	*13.8500*	19.4833	*5.7854*	*13.8500*	19.4833
σ_{xz}, σ_{yz} and σ_{zz} top-bottom b.cs. (3D law)						
$EM^{2,1}_{1,0}$	5.7693	13.7637	19.4833	5.7693	13.7637	19.4833
$EM^{2,2}_{1,0}$	5.7693	13.7637	19.4833	5.7693	13.7637	19.4833
$EM^{2,3}_{1,0}$	*6.1819*	*14.6744*	19.4833	*6.1819*	*14.6744*	19.4833

Table 5.4: First four non-dimensional frequencies for the Reissner-Mindlin kinematics. $R_u = S_u = 10$. $\bar{\omega} = \frac{a^2}{h}\sqrt{\frac{\rho}{E_{22}}}\,\omega$

It can be concluded that the number of not-conjugated stress modes and not-conjugated kinematic modes are deeply connected to the definition of correct mixed models. Despite the numerical differences in the parameters, the models here identified as correct coincide with those reported by D'Ottavio to have zero not-conjugated stress modes and three not-conjugated kinematic modes for the Navier solution [40]. Further studies should be conducted to investigate the physical meaning of the values here obtained.

5.2.2 Bending problem

Considerations about the model choice can be drawn considering the linear static problem. Demasi in his work [41], showed that when a LW model is adopted it may lead to oscillations, either in the displacement field or in the stress field. These oscillations depend on the relative orders used for the displacement field and the stress field. The main finding by Demasi is that these oscillations disappear when the order used for the out-of-plane displacement u_z is the same as the order used for σ_{zz}. No stress b.cs. were enforced at the

plate's top and bottom surfaces by Demasi.

Demasi's considerations were based on a strong-form solution (Navier) applied to the GUF. It is shown here that these considerations hold true even in the present framework of a weak-form solution (Ritz). In fact the very same results obtained by Demasi are recovered. The capability of the present formulation to reproduce the same results obtained by Demasi supports the hypothesis made at the beginning of this chapter stating that the in-plane and the out-of-plane approximation do not influence each other.

The test case utilized by Demasi [41] is considered:

Geometry Square plate ($a = b$). The plate is constituted of two layers. The thickness ratio is $D = a/h = 4$. The two plies have an equal thickness of h/2.

Composite stack Cross-ply laminate: [90/0].

Material properties The material properties of the top ply are:

$\mathbf{E_{11}}$ [-]	$\mathbf{E_{22}}$ [-]	$\mathbf{E_{33}}$ [-]
25	1	10
$\mathbf{G_{12}}$ [-]	$\mathbf{G_{13}}$ [-]	$\mathbf{G_{23}}$ [-]
0.5	0.5	0.2
$\boldsymbol{\nu_{12}}$ [-]	$\boldsymbol{\nu_{13}}$ [-]	$\boldsymbol{\nu_{23}}$ [-]
0.25	0.25	0.25

Table 5.5: Model orders test case by Demasi: top ply material properties. E_{11}, E_{22}, E_{33}, G_{12}, G_{13}, G_{23} are normalized over E_{22}.

The material properties of the bottom ply are:

$\mathbf{E_{11}}$ [-]	$\mathbf{E_{22}}$ [-]	$\mathbf{E_{33}}$ [-]
25	1	1
$\mathbf{G_{12}}$ [-]	$\mathbf{G_{13}}$ [-]	$\mathbf{G_{23}}$ [-]
0.5	0.5	0.2
$\boldsymbol{\nu_{12}}$ [-]	$\boldsymbol{\nu_{13}}$ [-]	$\boldsymbol{\nu_{23}}$ [-]
0.25	0.25	0.25

Table 5.6: Model orders test case by Demasi: bottom ply material properties. E_{11}, E_{22}, E_{33}, G_{12}, G_{13}, G_{23} are normalized over E_{22}.

Boundary conditions Simply-supported on all four sides: *SSSS*.

Load Bisinusoidal load applied on the top surface: $P = P_0 sin(\frac{\pi}{a}x) sin(\frac{\pi}{b}y)$.

Results The results are made non-dimensional in the following manner:

$$
\begin{aligned}
(\bar{u}_x, \bar{u}_y) &= \frac{E_{22}^{bot}}{P_0 h D^3}(u_x, u_y) \quad \bar{u}_z = \frac{100 E_{22}^{bot}}{P_0 h D^4} u_z \\
\bar{\sigma}_{xx} &= \frac{1}{P_0 D^2}\sigma_{xx} \quad \bar{\sigma}_{xz} = \frac{1}{P_0 D}\sigma_{xz} \quad \bar{\sigma}_{zz} = \frac{1}{P_0}\sigma_{zz}
\end{aligned}
\tag{5.6}
$$

where *bot* refers to the bottom ply. The following nondimensional thickness coordinate is adopted: $\xi = \frac{z}{h}$. $\bar{u}_x$ and $\bar{\sigma}_{xz}$ are calculated at $x = 0$, $y = a/2$; $\bar{u}_y$ is calculated at $x = a/2$, $y = 0$ and $\bar{u}_z$, $\bar{\sigma}_{xx}$ and $\bar{\sigma}_{zz}$ are calculated at $x = a/2$, $y = b/2$.

Computational model Seven different LW models are considered:

Model	$LM^{3,3,3}_{5,5,5}$	$LM^{3,3,3}_{5,5,3}$	$LM^{6,6,6}_{4,4,4}$	$LM^{6,6,4}_{4,4,4}$	$LM^{3,4,5}_{5,6,4}$	$LM^{3,4,4}_{5,6,4}$	$LM^{3,3,3}_{2,2,2}$

Table 5.7: Demasi model order test case: models.

No top-bottom stress boundary conditions were imposed, unless otherwise specified. Based on the results of the previous section, the Ritz orders are here set so that $R_s = R_u + 1$ and $S_s = S_u + 1$ with $R_u = S_u = 10$, $R_s = S_s = 11$

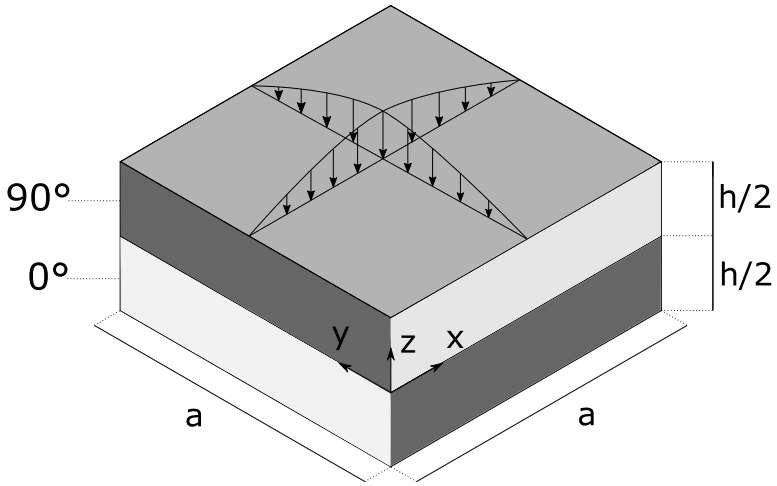

Figure 5.3: Demasi model orders test case.

Figure 5.4 reports the results comparing the class of theories in which the orders of displacement variables are lower than the orders of stress variables. It appears that oscillations in the σ_{zz} field appear if $N_{\sigma_{zz}} > N_{u_z}$. These oscillations disappear by choosing $N_{\sigma_{zz}} = N_{u_z}$.

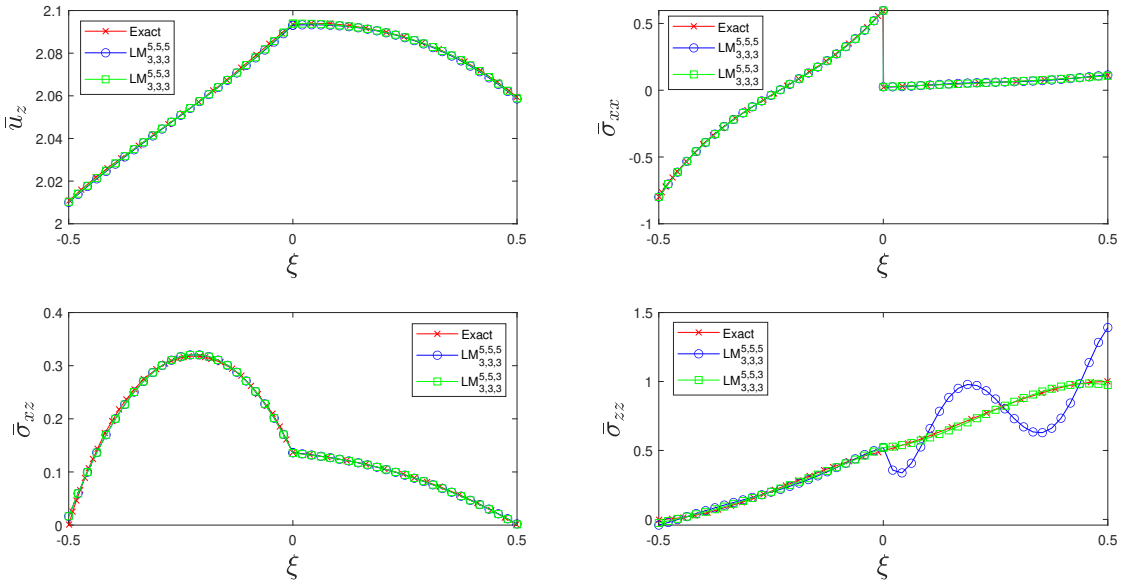

Figure 5.4: $LM^{5,5,5}_{3,3,3}$ and $LM^{5,5,3}_{3,3,3}$; $R_u = S_u = 10$, $R_s = S_s = 11$. Transverse stresses are computed *a priori*.

Figure 5.5 compares the class of theories in which the orders of displacement variables are higher than the orders of stress variables. It appears that oscillations in the σ_{zz} field appear if $N_{\sigma_{zz}} < N_{u_z}$. These oscillations disappear by choosing $N_{\sigma_{zz}} = N_{u_z}$.

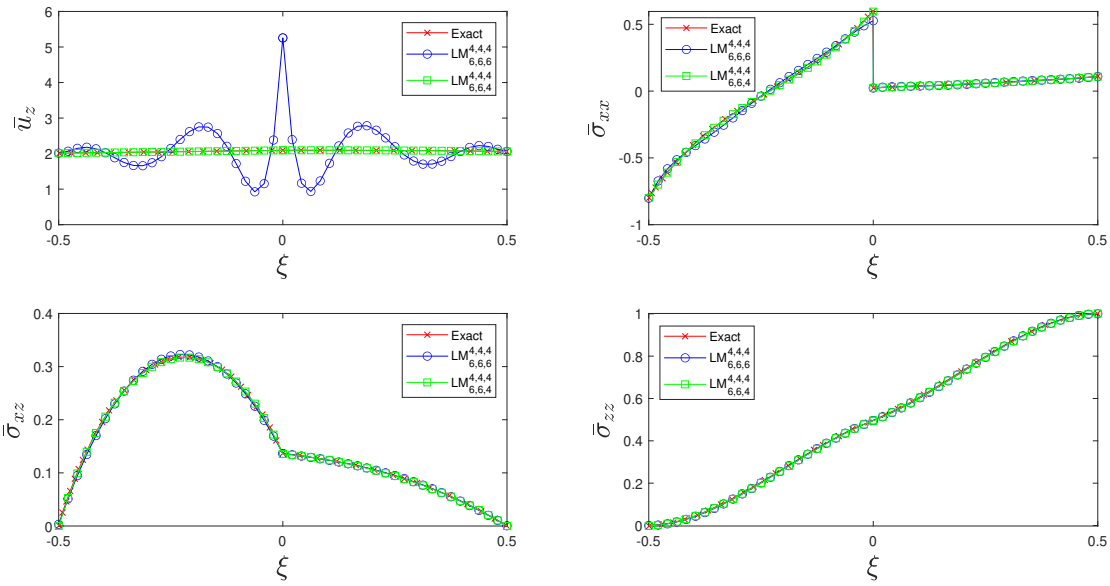

Figure 5.5: $LM^{4,4,4}_{6,6,6}$ and $LM^{4,4,4}_{6,6,4}$; $R_u = S_u = 10$, $R_s = S_s = 11$. Transverse stresses are computed *a priori*.

Even if results for u_x and u_y are not reported by Demasi [41], for sake of completeness, it is reported that these fields present oscillations only for the class of theories in which the orders of displacement variables are higher than the orders of stress variable. As shown in Figure 5.6, even for u_x and u_y the oscillations disappear if $N_{u_z} = N_{\sigma_{zz}}$ is imposed.

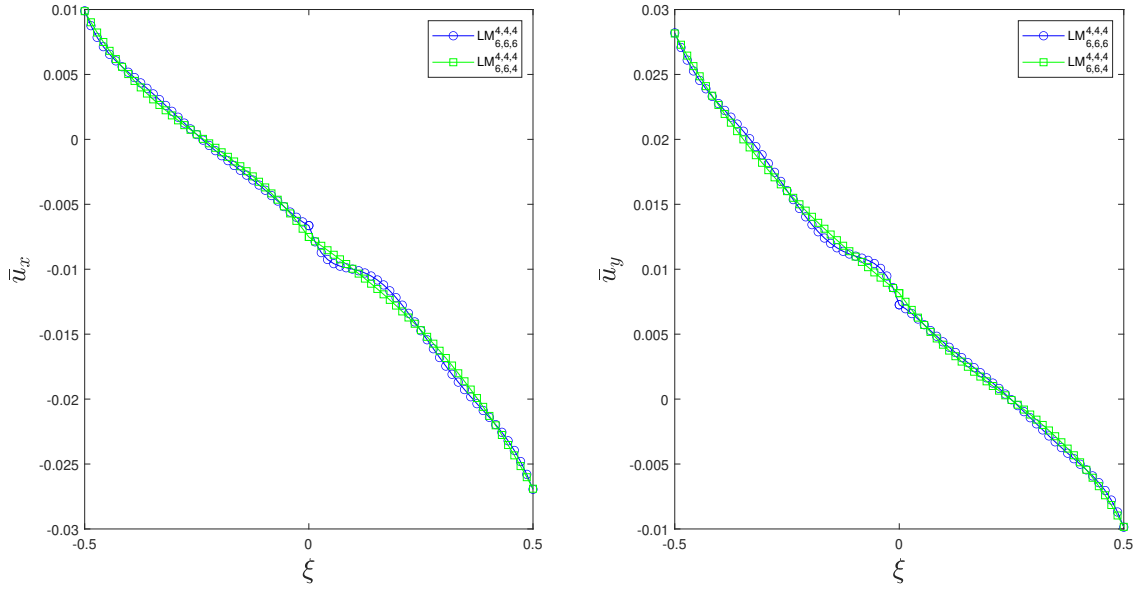

Figure 5.6: $LM^{4,4,4}_{6,6,6}$ and $LM^{4,4,4}_{6,6,4}$; $R_u = S_u = 10$, $R_s = S_s = 11$. $\bar{u}_x$ and $\bar{u}_y$ through-the-thickness field.

Finally, even when considering a class with general orders of expansion, as in Figure 5.7, oscillations may arise. Even in this last case, imposing $N_{u_z} = N_{\sigma_{zz}}$ will solve the oscillation issue.

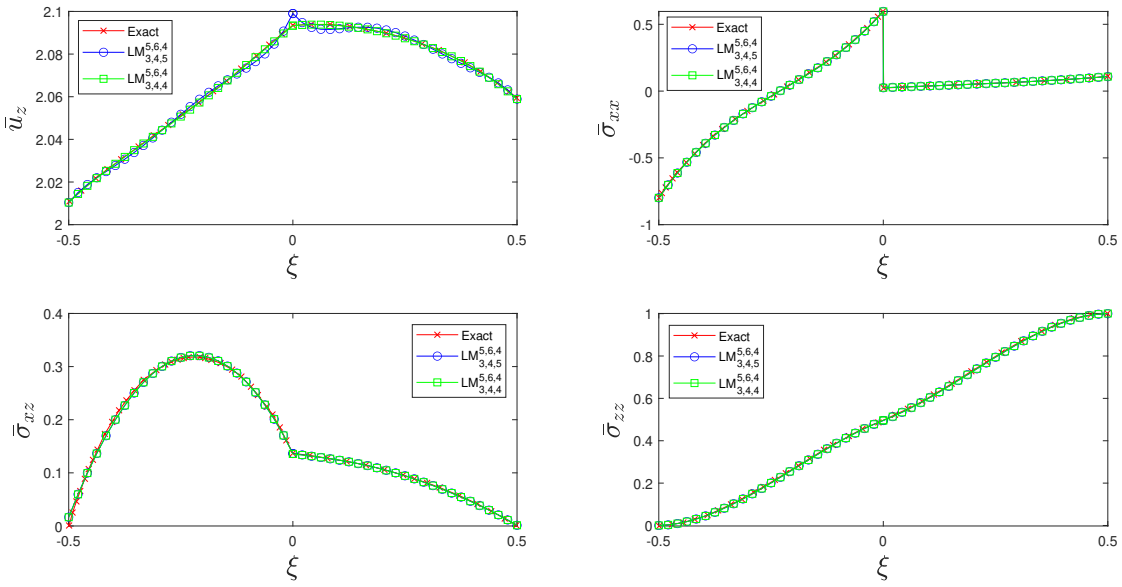

Figure 5.7: $LM^{5,6,4}_{3,4,5}$ and $LM^{5,6,4}_{3,4,4}$; $R_u = S_u = 10$, $R_s = S_s = 11$. Transverse stresses are computed *a priori*.

Even if not present in the previous models, oscillations also in the variable σ_{xz} (and σ_{yz}) may arise when computed *a priori*. For instance, as illustrated in Figure 5.8, model $LM^{3,3,3}_{2,2,2}$ presents oscillations both in the field σ_{xz} and σ_{zz}. Finally, it is shown that the imposition of top-bottom stress boundary conditions mitigates the oscillations at the boundaries. However, the results are still unacceptable overall. In Figure 5.8 theory $LM^{3,3,3}_{2,2,2}$ without top-bottom stress boundary conditions and theory $LM^{3,3,3}_{2,2,2}$ with the imposition of $\sigma_{xz}(z = h/2) = \sigma_{xz}(z = -h/2) = 0$ are compared.

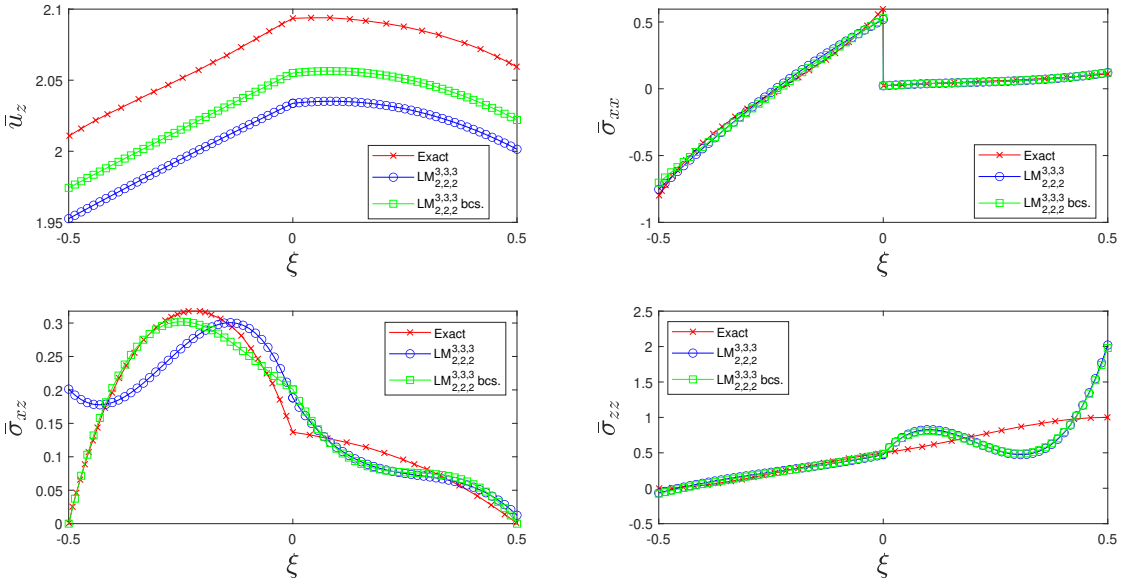

Figure 5.8: $LM^{3,3,3}_{2,2,2}$ and $LM^{3,3,3}_{2,2,2}$ with $\sigma_{xz}(z = h/2) = \sigma_{xz}(z = -h/2) = 0$; $R_u = S_u = 10$, $R_s = S_s = 11$. Transverse stresses are computed *a priori*.

Recalling the analysis made in Section 5.2.1, it is possible to compute the number of not-conjugated stress modes (N_{stress}) and not-conjugates kinematic modes (N_{kin}) also for the models presented here. It is particularly interesting to compare the values of these parameters with the results in the plots for the classes of theories $N_u > N_\sigma$ and $N_\sigma > N_u$; before and after the imposition of $N_{u_z} = N_{\sigma_{zz}}$. Table 5.8 collects the algebraic parameters for the models $LW^{4,4,4}_{6,6,6}$, $LW^{4,4,4}_{6,6,4}$, $LW^{5,5,5}_{3,3,3}$ and $LW^{5,5,3}_{3,3,3}$. The class of theories with $N_u > N_\sigma$, that shows oscillations in the displacement field, presents a higher value of both N_{kin} and N_{stress} compared to the modified model with $N_{u_z} = N_{\sigma_{zz}}$. The class of theories with $N_\sigma > N_u$, that shows oscillations in σ_{zz}, presents a higher value of N_{stress} compared to the modified model with $N_{u_z} = N_{\sigma_{zz}}$.

The correlation between the oscillations in the linear static problem and these parameters should be further studied. Different models should be considered, in order to make the conclusions general.

Model	N_{stress}	N_{kin}
$LW^{4,4,4}_{6,6,6}$	510	812
$LW^{4,4,4}_{6,6,4}$	648	672
$LW^{5,5,5}_{3,3,3}$	2174	204
$LW^{5,5,3}_{3,3,3}$	1690	204

Table 5.8: Algebraic parameters for the models adopted by Demasi.

Chapter 6

Conclusions

The present work has developed a novel numerical method based upon RMVT for the solution of the free-vibration problem and the linear static problem. The governing equations were derived applying to RMVT the *Sublaminate Generalized Unified Formulation* (S-GUF) and *the Ritz approximation*. The present method was applied to the main geometries of interest in the aerospace field: plates, cylindrical panels, and closed cylinders.

By comparing the results obtained through the present method with the results in scientific literature it was possible to assess the correctness of the results and therefore to validate both the mathematical model and the code. In particular, for each problem, all three geometries were investigated.

The results show the effectiveness of the method in particular to compute transverse stresses and to impose their continuity *a priori* at the interfaces of two plies.

The effects of different parameters relative to the present theory were investigated: the effect of the relative Ritz orders of expansion for displacements (M_u) and stresses (M_s), the orders of the model and the imposition of top-bottom stress boundary condition.

It was shown that a correct Ritz approximation must satisfy that: $R_s > R_u$ and $S_s > S_u$. Furthermore, $R_s = R_u + 1$ and $S_s = S_u + 1$ results to be the best condition to impose since an increase in the stress approximation would not improve the results, but only the computational cost.

The orders of the model must be selected carefully since oscillations may arise in the linear static problem, and non-physical frequencies and modes may be present in the free-vibration analysis. The choice of the orders can be guided by analytical parameters on the stiffness matrix, particularly, by checking that the number of not-conjugated kinematic modes is minimized.

6.1 Future developments

The present formulation can be applied to solve other different problems and expanded to other geometries. For example:

- **Generic geometry** The equations for doubly-curved shells have been derived. Although it would be possible to extend the present formulation to structures with generic curvatures such as cylinders with a non-constant radius of curvature, or elliptical cylinders.
- **Variable stiffness** The present formulation could be expanded in order to account also for functionally graded materials (FGM) [42] and variable stiffness materials (VSM), or possibly a combination of the two. FGM are materials whose physical properties vary along the thickness while VSM are materials whose physical properties vary in the plane.
- **Piezoelectric materials** The present models could be expanded so to include piezoelectric layers within the laminate. These materials deform when under a potential difference and vice-versa.
- **Thermal loads** It could be possible to include in the present framework the analysis of thermal loads.
- **Additional analyses** Additional analyses other than the free-vibration and the linear static problem could be performed, for example: forced vibrations, buckling, direct and modal frequency analysis, transient response, etc.

Appendices

Appendix A

Constitutive relation

The models described in Section 2.3 are completely general and applicable to any kind of structure. However to obtain the solution of a real problem, physical quantities describing its unique behavior must be introduced. These quantities are represented through the constitutive relation which relates strains to stresses.

Stresses (σ_{ij}) and stains (ε_{ij}) can be represented as symmetric second order tensors, which can be put in relation with each other through the forth order elasticity tensor $\mathbb{C}_{ijkl}$ by the *Classical Form of Hooke's Law* (CFHL), in case the hypotheses of elasticity and linearity are respected:

$$\sigma_{ij} = \mathbb{C}_{ijkl}\varepsilon_{kl} \tag{A.1}$$

where $i, j, k, l = 1, 2, 3$. Exploiting the symmetry of the stress and strain tensors, it is possible to rearrange the quantities according to the Voigt-Kelvin notation, and rewrite Eq.(A.2) as:

$$\boldsymbol{\sigma} = \mathbf{C}\boldsymbol{\varepsilon} \tag{A.2}$$

or explicitly as:

$$\begin{Bmatrix} \sigma_{11} \\ \sigma_{22} \\ \sigma_{33} \\ \sigma_{23} \\ \sigma_{31} \\ \sigma_{12} \end{Bmatrix} = \begin{bmatrix} C_{11} & C_{12} & C_{13} & C_{14} & C_{15} & C_{16} \\ C_{21} & C_{22} & C_{23} & C_{24} & C_{25} & C_{26} \\ C_{31} & C_{32} & C_{33} & C_{34} & C_{35} & C_{36} \\ C_{41} & C_{42} & C_{43} & C_{44} & C_{45} & C_{46} \\ C_{51} & C_{52} & C_{53} & C_{54} & C_{55} & C_{56} \\ C_{61} & C_{62} & C_{63} & C_{64} & C_{65} & C_{66} \end{bmatrix} \begin{Bmatrix} \varepsilon_{11} \\ \varepsilon_{22} \\ \varepsilon_{33} \\ \varepsilon_{23} \\ \varepsilon_{31} \\ \varepsilon_{12} \end{Bmatrix} \tag{A.3}$$

If a *strain energy density* $W = \frac{1}{2}\sigma_{ij}\varepsilon_{ij}$ exists, then the material is defined as *hyperelastic* and it follows that:

$$\boldsymbol{\sigma} = \frac{\partial W}{\partial \boldsymbol{\varepsilon}} \tag{A.4}$$

If the material is both linear and hyperelastic, then Eq.(A.2) and Eq.(A.4) both hold true and it is possible to combine them. According to *Schwarz theorem*, for a sufficiently regular function, the sequence of differentiation is arbitrary, therefore:

$$\mathbb{C}_{ijkl} = \frac{\partial W}{\partial \varepsilon_{ij}\partial \varepsilon_{kl}} = \frac{\partial W}{\partial \varepsilon_{kl}\partial \varepsilon_{ij}} \tag{A.5}$$

so indexes ij and kl can be interchanged arbitrarily. This implies that the tensor containing the elastic moduli is symmetric:

$$\begin{Bmatrix} \sigma_{11} \\ \sigma_{22} \\ \sigma_{33} \\ \sigma_{23} \\ \sigma_{31} \\ \sigma_{12} \end{Bmatrix} = \begin{bmatrix} C_{11} & C_{12} & C_{13} & C_{14} & C_{15} & C_{16} \\ & C_{22} & C_{23} & C_{24} & C_{25} & C_{26} \\ & & C_{33} & C_{34} & C_{35} & C_{36} \\ & & & C_{44} & C_{45} & C_{46} \\ & sym & & & C_{55} & C_{56} \\ & & & & & C_{66} \end{bmatrix} \begin{Bmatrix} \varepsilon_{11} \\ \varepsilon_{22} \\ \varepsilon_{33} \\ \varepsilon_{23} \\ \varepsilon_{31} \\ \varepsilon_{12} \end{Bmatrix} \tag{A.6}$$

Further simplifications of the constitutive relation may come from the physical properties of the material. The most simple case of constitutive relation is the one relative to homogeneous materials, which is defined by only three constants:

$$\begin{Bmatrix} \sigma_{11} \\ \sigma_{22} \\ \sigma_{33} \\ \tau_{23} \\ \tau_{31} \\ \tau_{12} \end{Bmatrix} = \begin{bmatrix} C_{11} & C_{12} & C_{12} & 0 & 0 & 0 \\ & C_{11} & C_{12} & 0 & 0 & 0 \\ & & C_{11} & 0 & 0 & 0 \\ & & & C_{44} & 0 & 0 \\ & sym & & & C_{44} & 0 \\ & & & & & C_{44} \end{bmatrix} \begin{Bmatrix} \varepsilon_{11} \\ \varepsilon_{22} \\ \varepsilon_{33} \\ \gamma_{23} \\ \gamma_{31} \\ \gamma_{12} \end{Bmatrix} \tag{A.7}$$

where the engineering stress and strain vectors have been adopted, i.e.: $\tau_{23} = \sigma_{23}$, $\tau_{31} = \sigma_{31}$, $\tau_{12} = \sigma_{12}$ and $\gamma_{23} = 2\varepsilon_{23}$, $\gamma_{31} = 2\varepsilon_{31}$, $\gamma_{12} = 2\varepsilon_{12}$. The three elastic constants C_{11}, C_{12} and C_{44} can be expressed by means of physical properties as follows:

$$C_{11} = \frac{E(1-\nu)}{(1+\nu)(1-2\nu)} \qquad C_{12} = \frac{E\nu}{(1+\nu)(1-2\nu)} \qquad C_{44} = G \tag{A.8}$$

where E is the Young's modulus, ν is the Poisson's ratio and $G = \frac{E}{2(1+\nu)}$ is the shear modulus.

Given that the present work has the intent to focus on composite materials whose plies are often belonging to the category of *orthotropic materials* (materials that have three mutually orthogonal planes of elastic symmetry), it is of interest to discuss their constitutive relation. When considering composite materials it is advantageous to define both a *material coordinate system* (specific to each ply) and a *laminate coordinate system* (valid for the whole laminate). The definition of a reference system for each ply makes it easier to define their own properties while a general reference system results more convenient when it comes down to describing the whole laminate and therefore summing each ply contribution. A representation of these two frames of reference and of how they relate to one another is given in Figure A.1.

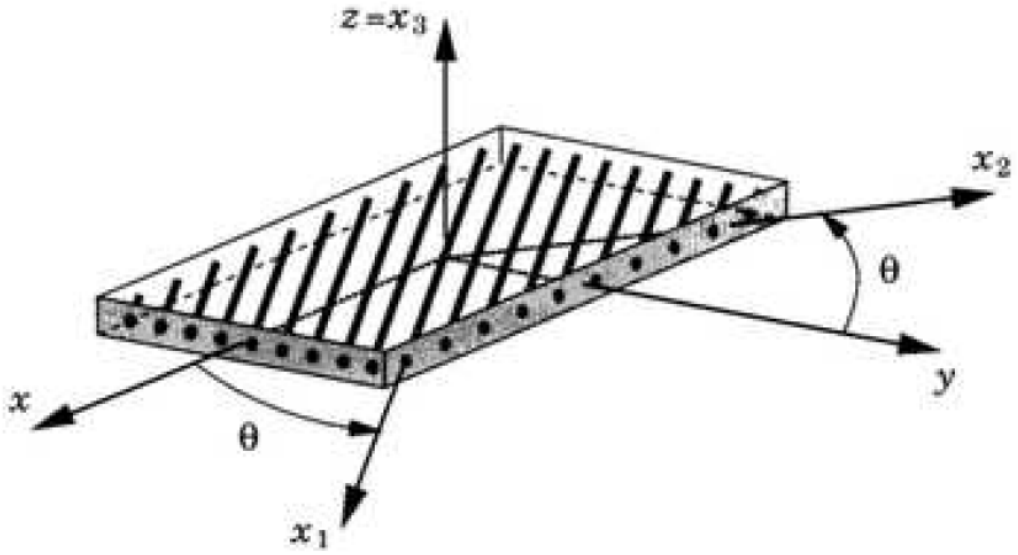

Figure A.1: Lamina with material (x_1, y_1, z_1) and laminate (x, y, z) coordinate systems (from Ref. [43]).

If we consider the material coordinate system (x_1, y_1, z_1) Hooke's law is:

$$\begin{Bmatrix} \sigma_{11} \\ \sigma_{22} \\ \sigma_{33} \\ \tau_{23} \\ \tau_{31} \\ \tau_{12} \end{Bmatrix} = \begin{bmatrix} C_{11} & C_{12} & C_{13} & 0 & 0 & 0 \\ & C_{22} & C_{23} & 0 & 0 & 0 \\ & & C_{33} & 0 & 0 & 0 \\ & & & C_{44} & 0 & 0 \\ & sym & & & C_{55} & 0 \\ & & & & & C_{66} \end{bmatrix} \begin{Bmatrix} \varepsilon_{11} \\ \varepsilon_{22} \\ \varepsilon_{33} \\ \gamma_{23} \\ \gamma_{31} \\ \gamma_{12} \end{Bmatrix} \tag{A.9}$$

or compactly:

$$\boldsymbol{\sigma_m} = \mathbf{C}\boldsymbol{\varepsilon_m} \tag{A.10}$$

In a similar manner to what was done for homogeneous materials, the nine elastic constants can be related to physical quantities as follows:

$$\begin{aligned}
C_{11} &= \frac{E_1(1-\nu_{23}\nu_{32})}{\Delta} \\
C_{12} &= \frac{E_1(\nu_{21}+\nu_{31}\nu_{23})}{\Delta} = \frac{E_2(\nu_{12}+\nu_{13}\nu_{32})}{\Delta} \\
C_{13} &= \frac{E_1(\nu_{31}+\nu_{21}\nu_{32})}{\Delta} = \frac{E_3(\nu_{13}+\nu_{12}\nu_{23})}{\Delta} \\
C_{22} &= \frac{E_2(1-\nu_{31}\nu_{13})}{\Delta} \\
C_{23} &= \frac{E_2(\nu_{32}+\nu_{31}\nu_{12})}{\Delta} = \frac{E_3(\nu_{23}+\nu_{21}\nu_{13})}{\Delta} \\
C_{33} &= \frac{E_3(1-\nu_{12}\nu_{21})}{\Delta} \\
C_{44} &= G_{23} \\
C_{55} &= G_{31} \\
C_{66} &= G_{12}
\end{aligned} \tag{A.11}$$

where

$$\Delta = 1 - \nu_{12}\nu_{21} - \nu_{23}\nu_{32} - \nu_{31}\nu_{13} - 2\nu_{12}\nu_{32}\nu_{13} \tag{A.12}$$

and

$$\frac{\nu_{ij}}{E_i} = \frac{\nu_{ji}}{E_j} \tag{A.13}$$

In the previous relations, E_i is the Young's modulus in the i direction, G_{ij} is the shear modulus in the (i, j) plane, and ν_{ij} is the Poisson's ratio of the strain in the j direction to the strain in the i direction due to an applied stress in the i direction.

By defining a laminate reference system (x, y, z) respect to which stress and strain vectors are expressed as:

$$\boldsymbol{\sigma} = [\sigma_{xx} \quad \sigma_{yy} \quad \sigma_{zz} \quad \tau_{yz} \quad \tau_{xz} \quad \tau_{xy}]^T \tag{A.14}$$

$$\boldsymbol{\varepsilon} = [\varepsilon_{xx} \quad \varepsilon_{yy} \quad \varepsilon_{zz} \quad \gamma_{yz} \quad \gamma_{xz} \quad \gamma_{xy}]^T \tag{A.15}$$

strains and stresses expressed in the two frames of reference can be easily related through the definition of a rotation matrix $\mathbf{T}$:

$$\boldsymbol{\sigma} = \mathbf{T}\boldsymbol{\varepsilon}_m \tag{A.16}$$

$$\boldsymbol{\varepsilon} = \mathbf{T}^T\boldsymbol{\varepsilon}_m \tag{A.17}$$

The rotation matrix $\mathbf{T}$ is defined in the following way:

$$\mathbf{T} = \begin{bmatrix} cos^2(\theta) & sin^2(\theta) & 0 & 0 & 0 & -2sin(\theta)cos(\theta) \\ sin^2(\theta) & cos^2(\theta) & 0 & 0 & 0 & 2sin(\theta)cos(\theta) \\ 0 & 0 & 1 & 0 & 0 & 0 \\ 0 & 0 & 0 & cos(\theta) & sin(\theta) & 0 \\ 0 & 0 & 0 & -sin(\theta) & cos(\theta) & 0 \\ sin(\theta)cos(\theta) & -sin(\theta)cos(\theta) & 0 & 0 & 0 & cos^2(\theta) - sin^2(\theta) \end{bmatrix} \tag{A.18}$$

where θ represents the angle between the two frames of reference as in Figure A.1. Substituting Eq.(A.17) into Eq.(A.19) and then using Eq.(A.16), the CFHL expressed in the laminate coordinate system results to be:

$$\boldsymbol{\sigma} = \widetilde{\mathbf{C}}\boldsymbol{\varepsilon} \tag{A.19}$$

where

$$\widetilde{\mathbf{C}} = \mathbf{T}\mathbf{C}\mathbf{T}^T = \begin{bmatrix} \widetilde{C}_{11} & \widetilde{C}_{12} & \widetilde{C}_{13} & 0 & 0 & \widetilde{C}_{16} \\ \widetilde{C}_{12} & \widetilde{C}_{22} & \widetilde{C}_{23} & 0 & 0 & \widetilde{C}_{26} \\ \widetilde{C}_{13} & \widetilde{C}_{23} & \widetilde{C}_{33} & 0 & 0 & \widetilde{C}_{36} \\ 0 & 0 & 0 & \widetilde{C}_{44} & \widetilde{C}_{45} & 0 \\ 0 & 0 & 0 & \widetilde{C}_{45} & \widetilde{C}_{55} & 0 \\ \widetilde{C}_{16} & \widetilde{C}_{26} & \widetilde{C}_{36} & 0 & 0 & \widetilde{C}_{66} \end{bmatrix} \tag{A.20}$$

Appendix B

Additional equations: Ritz S-GUF RMVT governing equations

Additional passages in the derivation of the Ritz S-GUF RMVT governing equations are here reported.

Strains and stresses matrices expansions:

$$
\begin{aligned}
&\delta\boldsymbol{\varepsilon}_{\Omega G}^{p,k^T}\boldsymbol{\sigma}_{\Omega H}^{p,k} = \\
&\frac{\partial\delta u_{x\alpha_{ux}}^{p,k}}{\partial x}\frac{C_{11}^{p,k}F_{\alpha_{ux}}F_{\beta_{ux}}}{H_x^{p,k}H_x^{p,k}}\frac{\partial u_{x\beta_{ux}}^{p,k}}{\partial x} + \frac{\partial\delta u_{x\alpha_{ux}}^{p,k}}{\partial x}\frac{C_{12}^{p,k}F_{\alpha_{ux}}F_{\beta_{uy}}}{H_x^{p,k}H_y^{p,k}}\frac{\partial u_{y\beta_{uy}}^{p,k}}{\partial y} \\
&+\frac{\partial\delta u_{x\alpha_{ux}}^{p,k}}{\partial x}\frac{C_{16}^{p,k}F_{\alpha_{ux}}F_{\beta_{ux}}}{H_x^{p,k}H_y^{p,k}}\frac{\partial u_{x\beta_{ux}}^{p,k}}{\partial y} + \frac{\partial\delta u_{x\alpha_{ux}}^{p,k}}{\partial x}\frac{C_{16}^{p,k}F_{\alpha_{ux}}F_{\beta_{uy}}}{H_x^{p,k}H_x^{p,k}}\frac{\partial u_{y\beta_{uy}}^{p,k}}{\partial x} \\
&+\frac{\partial\delta u_{y\alpha_{uy}}^{p,k}}{\partial y}\frac{C_{12}^{p,k}F_{\alpha_{uy}}F_{\beta_{ux}}}{H_y^{p,k}H_x^{p,k}}\frac{\partial u_{x\beta_{ux}}^{p,k}}{\partial x} + \frac{\partial\delta u_{y\alpha_{uy}}^{p,k}}{\partial y}\frac{C_{22}^{p,k}F_{\alpha_{uy}}F_{\beta_{uy}}}{H_y^{p,k}H_y^{p,k}}\frac{\partial u_{y\beta_{uy}}^{p,k}}{\partial y} \\
&+\frac{\partial\delta u_{y\alpha_{uy}}^{p,k}}{\partial y}\frac{C_{26}^{p,k}F_{\alpha_{uy}}F_{\beta_{ux}}}{H_y^{p,k}H_y^{p,k}}\frac{\partial u_{x\beta_{ux}}^{p,k}}{\partial y} + \frac{\partial\delta u_{y\alpha_{uy}}^{p,k}}{\partial y}\frac{C_{26}^{p,k}F_{\alpha_{uy}}F_{\beta_{uy}}}{H_y^{p,k}H_x^{p,k}}\frac{\partial u_{y\beta_{uy}}^{p,k}}{\partial x} \\
&+\frac{\partial\delta u_{x\alpha_{ux}}^{p,k}}{\partial y}\frac{C_{16}^{p,k}F_{\alpha_{ux}}F_{\beta_{ux}}}{H_y^{p,k}H_x^{p,k}}\frac{\partial u_{x\beta_{ux}}^{p,k}}{\partial x} + \frac{\partial\delta u_{x\alpha_{ux}}^{p,k}}{\partial y}\frac{C_{26}^{p,k}F_{\alpha_{ux}}F_{\beta_{uy}}}{H_y^{p,k}H_y^{p,k}}\frac{\partial u_{y\beta_{uy}}^{p,k}}{\partial y} \\
&+\frac{\partial\delta u_{x\alpha_{ux}}^{p,k}}{\partial y}\frac{C_{66}^{p,k}F_{\alpha_{ux}}F_{\beta_{ux}}}{H_y^{p,k}H_y^{p,k}}\frac{\partial u_{x\beta_{ux}}^{p,k}}{\partial y} + \frac{\partial\delta u_{x\alpha_{ux}}^{p,k}}{\partial y}\frac{C_{66}^{p,k}F_{\alpha_{ux}}F_{\beta_{uy}}}{H_y^{p,k}H_x^{p,k}}\frac{\partial u_{y\beta_{uy}}^{p,k}}{\partial x} \\
&+\frac{\partial\delta u_{y\alpha_{uy}}^{p,k}}{\partial x}\frac{C_{16}^{p,k}F_{\alpha_{uy}}F_{\beta_{ux}}}{H_x^{p,k}H_x^{p,k}}\frac{\partial u_{x\beta_{ux}}^{p,k}}{\partial x} + \frac{\partial\delta u_{y\alpha_{uy}}^{p,k}}{\partial x}\frac{C_{26}^{p,k}F_{\alpha_{uy}}F_{\beta_{uy}}}{H_x^{p,k}H_y^{p,k}}\frac{\partial u_{y\beta_{uy}}^{p,k}}{\partial y} \\
&+\frac{\partial\delta u_{y\alpha_{uy}}^{p,k}}{\partial x}\frac{C_{66}^{p,k}F_{\alpha_{uy}}F_{\beta_{ux}}}{H_x^{p,k}H_y^{p,k}}\frac{\partial u_{x\beta_{ux}}^{p,k}}{\partial y} + \frac{\partial\delta u_{y\alpha_{uy}}^{p,k}}{\partial x}\frac{C_{66}^{p,k}F_{\alpha_{uy}}F_{\beta_{uy}}}{H_x^{p,k}H_x^{p,k}}\frac{\partial u_{y\beta_{uy}}^{p,k}}{\partial x} \\
&+\frac{\partial\delta u_{x\alpha_{ux}}^{p,k}}{\partial x}\frac{C_{13}^{p,k}F_{\alpha_{ux}}F_{\beta_{sz}}}{H_x^{p,k}}s_{z\beta_{sz}}^{p,k} + \frac{\partial\delta u_{y\alpha_{uy}}^{p,k}}{\partial y}\frac{C_{23}^{p,k}F_{\alpha_{uy}}F_{\beta_{sz}}}{H_y^{p,k}}s_{z\beta_{sz}}^{p,k}
\end{aligned}
\tag{B.1}
$$

$$
\begin{aligned}
&+\frac{\partial\delta u^{p,k}_{x\alpha_{u_x}}}{\partial y}\frac{C^{p,k}_{36}F_{\alpha_{u_x}}F_{\beta_{s_z}}}{H^{p,k}_{y}}s^{p,k}_{z\beta_{s_z}}+\frac{\partial\delta u^{p,k}_{y\alpha_{u_y}}}{\partial x}\frac{C^{p,k}_{36}F_{\alpha_{u_y}}F_{\beta_{s_z}}}{H^{p,k}_{x}}s^{p,k}_{z\beta_{s_z}}\\
&+\frac{\partial\delta u^{p,k}_{x\alpha_{u_x}}}{\partial x}\frac{C^{p,k}_{11}F_{\alpha_{u_x}}F_{\beta_{u_z}}}{H^{p,k}_{x}H^{p,k}_{x}R^{p,k}_{x}}u^{p,k}_{z\beta_{u_z}}+\frac{\partial\delta u^{p,k}_{x\alpha_{u_x}}}{\partial x}\frac{C^{p,k}_{12}F_{\alpha_{u_x}}F_{\beta_{u_z}}}{H^{p,k}_{x}H^{p,k}_{y}R^{p,k}_{y}}u^{p,k}_{z\beta_{u_z}}\\
&+\frac{\partial\delta u^{p,k}_{y\alpha_{u_y}}}{\partial y}\frac{C^{p,k}_{12}F_{\alpha_{u_y}}F_{\beta_{u_z}}}{H^{p,k}_{y}H^{p,k}_{x}R^{p,k}_{x}}u^{p,k}_{z\beta_{u_z}}+\frac{\partial\delta u^{p,k}_{y\alpha_{u_y}}}{\partial y}\frac{C^{p,k}_{22}F_{\alpha_{u_y}}F_{\beta_{u_z}}}{H^{p,k}_{y}H^{p,k}_{y}R^{p,k}_{y}}u^{p,k}_{z\beta_{u_z}}\\
&+\frac{\partial\delta u^{p,k}_{x\alpha_{u_x}}}{\partial y}\frac{C^{p,k}_{16}F_{\alpha_{u_x}}F_{\beta_{u_z}}}{H^{p,k}_{y}H^{p,k}_{x}R^{p,k}_{x}}u^{p,k}_{z\beta_{u_z}}+\frac{\partial\delta u^{p,k}_{x\alpha_{u_x}}}{\partial y}\frac{C^{p,k}_{26}F_{\alpha_{u_x}}F_{\beta_{u_z}}}{H^{p,k}_{y}H^{p,k}_{y}R^{p,k}_{y}}u^{p,k}_{z\beta_{u_z}}\\
&+\frac{\partial\delta u^{p,k}_{y\alpha_{u_y}}}{\partial x}\frac{C^{p,k}_{16}F_{\alpha_{u_y}}F_{\beta_{u_z}}}{H^{p,k}_{x}H^{p,k}_{x}R^{p,k}_{x}}u^{p,k}_{z\beta_{u_z}}+\frac{\partial\delta u^{p,k}_{y\alpha_{u_y}}}{\partial x}\frac{C^{p,k}_{26}F_{\alpha_{u_y}}F_{\beta_{u_z}}}{H^{p,k}_{x}H^{p,k}_{y}R^{p,k}_{y}}u^{p,k}_{z\beta_{u_z}}\\
&+\delta u^{p,k}_{z\alpha_{u_z}}\frac{C^{p,k}_{11}F_{\alpha_{u_z}}F_{\beta_{u_x}}}{H^{p,k}_{x}H^{p,k}_{x}R^{p,k}_{x}}\frac{\partial u^{p,k}_{x\beta_{u_x}}}{\partial x}+\delta u^{p,k}_{z\alpha_{u_z}}\frac{C^{p,k}_{12}F_{\alpha_{u_z}}F_{\beta_{u_y}}}{H^{p,k}_{x}H^{p,k}_{y}R^{p,k}_{x}}\frac{\partial u^{p,k}_{y\beta_{u_y}}}{\partial y}\\
&+\delta u^{p,k}_{z\alpha_{u_z}}\frac{C^{p,k}_{16}F_{\alpha_{u_z}}F_{\beta_{u_x}}}{H^{p,k}_{x}H^{p,k}_{y}R^{p,k}_{x}}\frac{\partial u^{p,k}_{x\beta_{u_x}}}{\partial y}+\delta u^{p,k}_{z\alpha_{u_z}}\frac{C^{p,k}_{16}F_{\alpha_{u_z}}F_{\beta_{u_y}}}{H^{p,k}_{x}H^{p,k}_{x}R^{p,k}_{x}}\frac{\partial u^{p,k}_{y\beta_{u_y}}}{\partial x}\\
&+\delta u^{p,k}_{z\alpha_{u_z}}\frac{C^{p,k}_{12}F_{\alpha_{u_z}}F_{\beta_{u_x}}}{H^{p,k}_{x}H^{p,k}_{y}R^{p,k}_{y}}\frac{\partial u^{p,k}_{x\beta_{u_x}}}{\partial x}+\delta u^{p,k}_{z\alpha_{u_z}}\frac{C^{p,k}_{22}F_{\alpha_{u_z}}F_{\beta_{u_y}}}{H^{p,k}_{y}H^{p,k}_{y}R^{p,k}_{y}}\frac{\partial u^{p,k}_{y\beta_{u_y}}}{\partial y}\\
&+\delta u^{p,k}_{z\alpha_{u_z}}\frac{C^{p,k}_{26}F_{\alpha_{u_z}}F_{\beta_{u_x}}}{H^{p,k}_{y}H^{p,k}_{y}R^{p,k}_{y}}\frac{\partial u^{p,k}_{x\beta_{u_x}}}{\partial y}+\delta u^{p,k}_{z\alpha_{u_z}}\frac{C^{p,k}_{26}F_{\alpha_{u_z}}F_{\beta_{u_y}}}{H^{p,k}_{x}H^{p,k}_{y}R^{p,k}_{y}}\frac{\partial u^{p,k}_{y\beta_{u_y}}}{\partial x}\\
&+\delta u^{p,k}_{z\alpha_{u_z}}\frac{C^{p,k}_{13}F_{\alpha_{u_z}}F_{\beta_{s_z}}}{H^{p,k}_{x}R^{p,k}_{x}}s^{p,k}_{z\beta_{s_z}}+\delta u^{p,k}_{z\alpha_{u_z}}\frac{C^{p,k}_{23}F_{\alpha_{u_z}}F_{\beta_{s_z}}}{H^{p,k}_{y}R^{p,k}_{y}}s^{p,k}_{z\beta_{s_z}}\\
&+\delta u^{p,k}_{z\alpha_{u_z}}\frac{C^{p,k}_{11}F_{\alpha_{u_z}}F_{\beta_{u_z}}}{(H^{p,k}_{x}R^{p,k}_{x})^2}u^{p,k}_{z\beta_{u_z}}+\delta u^{p,k}_{z\alpha_{u_z}}\frac{C^{p,k}_{12}F_{\alpha_{u_z}}F_{\beta_{u_z}}}{H^{p,k}_{x}R^{p,k}_{x}H^{p,k}_{y}R^{p,k}_{y}}u^{p,k}_{z\beta_{u_z}}\\
&+\delta u^{p,k}_{z\alpha_{u_z}}\frac{C^{p,k}_{12}F_{\alpha_{u_z}}F_{\beta_{u_z}}}{H^{p,k}_{x}R^{p,k}_{x}H^{p,k}_{y}R^{p,k}_{y}}u^{p,k}_{z\beta_{u_z}}+\delta u^{p,k}_{z\alpha_{u_z}}\frac{C^{p,k}_{22}F_{\alpha_{u_z}}F_{\beta_{u_z}}}{(H^{p,k}_{y}R^{p,k}_{y})^2}u^{p,k}_{z\beta_{u_z}}
\end{aligned}
$$

$$
\begin{aligned}
&\delta\boldsymbol{\varepsilon}^{p,k^T}_{nG}\boldsymbol{\sigma}^{p,k}_{nM}=\\
&\frac{\partial\delta u^{p,k}_{z\alpha_{u_z}}}{\partial y}\frac{F_{\alpha_{u_z}}F_{\beta_{s_y}}}{H^{p,k}_{y}}s^{p,k}_{y\beta_{s_y}}+\frac{\partial\delta u^{p,k}_{z\alpha_{u_z}}}{\partial x}\frac{F_{\alpha_{u_z}}F_{\beta_{s_x}}}{H^{p,k}_{x}}s^{p,k}_{x\beta_{s_x}}-\delta u^{p,k}_{y\alpha_{u_y}}\frac{\lambda_D F_{\alpha_{u_y}}F_{\beta_{s_y}}}{H^{p,k}_{y}R^{p,k}_{y}}s^{p,k}_{y\beta_{s_y}}\\
&-\delta u^{p,k}_{x\alpha_{u_x}}\frac{\lambda_D F_{\alpha_{u_x}}F_{\beta_{s_x}}}{H^{p,k}_{x}R^{p,k}_{x}}s^{p,k}_{x\beta_{s_x}}+\delta u^{p,k}_{y\alpha_{u_y}}\frac{\partial F_{\alpha_{u_y}}}{\partial z}F_{\beta_{s_y}}s^{p,k}_{y\beta_{s_y}}+\delta u^{p,k}_{x\alpha_{u_x}}\frac{\partial F_{\alpha_{u_x}}}{\partial z}F_{\beta_{s_x}}s^{p,k}_{x\beta_{s_x}}\\
&+\delta u^{p,k}_{z\alpha_{u_z}}\frac{\partial F_{\alpha_{u_z}}}{\partial z}F_{\beta_{s_z}}s^{p,k}_{z\beta_{s_z}}
\end{aligned}
\tag{B.2}
$$

$$
\begin{aligned}
&\delta\boldsymbol{\sigma}_{nM}^{p,k^T}\boldsymbol{\varepsilon}_{nG}^{p,k} = \\
&\delta s_{y\alpha_{s_y}}^{p,k}\frac{F_{\alpha_{s_y}}F_{\beta_{u_z}}}{H_y^{p,k}}\frac{\partial u_{z\beta_{u_z}}^{p,k}}{\partial y} + \delta s_{x\alpha_{s_x}}^{p,k}\frac{F_{\alpha_{s_x}}F_{\beta_{u_z}}}{H_x^{p,k}}\frac{\partial u_{z\beta_{u_z}}^{p,k}}{\partial x} - \delta s_{y\alpha_{s_y}}^{p,k}\frac{\lambda_D F_{\alpha_{s_y}}F_{\beta_{u_y}}}{H_y^{p,k}R_y^{p,k}}u_{y\beta_{u_y}}^{p,k} \\
&- \delta s_{x\alpha_{s_x}}^{p,k}\frac{\lambda_D F_{\alpha_{s_x}}F_{\beta_{u_x}}}{H_x^{p,k}R_x^{p,k}}u_{x\beta_{u_x}}^{p,k} + \delta s_{y\alpha_{s_y}}^{p,k}F_{\alpha_{s_y}}\frac{\partial F_{\beta_{u_y}}}{\partial z}u_{y\beta_{u_y}}^{p,k} + \delta s_{x\alpha_{s_x}}^{p,k}F_{\alpha_{s_x}}\frac{\partial F_{\beta_{u_x}}}{\partial z}u_{x\beta_{u_x}}^{p,k} \\
&+ \delta s_{z\alpha_{s_z}}^{p,k}F_{\alpha_{s_z}}\frac{\partial F_{\beta_{u_z}}}{\partial z}u_{z\beta_{u_z}}^{p,k}
\end{aligned}
\tag{B.3}
$$

$$
\begin{aligned}
&\delta\boldsymbol{\sigma}_{nM}^{p,k^T}\boldsymbol{\varepsilon}_{nH}^{p,k} = \\
&- \delta s_{z\alpha_{s_z}}^{p,k}\frac{C_{13}^{p,k}F_{\alpha_{s_z}}F_{\beta_{u_x}}}{H_x^{p,k}}\frac{\partial u_{x\beta_{u_x}}^{p,k}}{\partial x} - \delta s_{z\alpha_{s_z}}^{p,k}\frac{C_{23}^{p,k}F_{\alpha_{s_z}}F_{\beta_{u_y}}}{H_y^{p,k}}\frac{\partial u_{y\beta_{u_y}}^{p,k}}{\partial y} - \delta s_{z\alpha_{s_z}}^{p,k}\frac{C_{36}^{p,k}F_{\alpha_{s_z}}F_{\beta_{u_x}}}{H_y^{p,k}}\frac{\partial u_{x\beta_{u_x}}^{p,k}}{\partial y} \\
&- \delta s_{z\alpha_{s_z}}^{p,k}\frac{C_{36}^{p,k}F_{\alpha_{s_z}}F_{\beta_{u_y}}}{H_x^{p,k}}\frac{\partial u_{y\beta_{u_y}}^{p,k}}{\partial x} - \delta s_{z\alpha_{s_z}}^{p,k}\frac{C_{13}^{p,k}F_{\alpha_{s_z}}F_{\beta_{u_z}}}{H_x^{p,k}R_x^{p,k}}u_{z\beta_{u_z}}^{p,k} - \delta s_{z\alpha_{s_z}}^{p,k}\frac{C_{23}^{p,k}F_{\alpha_{s_z}}F_{\beta_{u_z}}}{H_y^{p,k}R_y^{p,k}}u_{z\beta_{u_z}}^{p,k} \\
&+ \delta s_{y\alpha_{s_y}}^{p,k}C_{44}^{p,k}F_{\alpha_{s_y}}F_{\beta_{s_y}}s_{y\beta_{s_y}}^{p,k} + \delta s_{y\alpha_{s_y}}^{p,k}C_{45}^{p,k}F_{\alpha_{s_y}}F_{\beta_{s_x}}s_{x\beta_{s_x}}^{p,k} + \delta s_{x\alpha_{s_x}}^{p,k}C_{45}^{p,k}F_{\alpha_{s_x}}F_{\beta_{s_y}}s_{y\beta_{s_y}}^{p,k} \\
&+ \delta s_{x\alpha_{s_x}}^{p,k}C_{55}^{p,k}F_{\alpha_{s_x}}F_{\beta_{s_x}}s_{x\beta_{s_x}}^{p,k} + \delta s_{z\alpha_{s_z}}^{p,k}C_{33}^{p,k}F_{\alpha_{s_z}}F_{\beta_{s_z}}s_{z\beta_{s_z}}^{p,k}
\end{aligned}
\tag{B.4}
$$

Introduction of the thickness integrals:

$$
\begin{aligned}
&\sum_{k=1}^{N_k}\sum_{p=1}^{N_p^k}\int_x\int_y\Big[\delta u_{x\alpha_{u_x}}^{p,k^T}\ {}^{H_xH_y}Z_{\rho u_x u_x}^{p,k\alpha_{u_x}\beta_{u_x}}\ddot{u}_{x\beta_{u_x}}^{p,k}+\delta u_{y\alpha_{u_y}}^{p,k^T}\ {}^{H_xH_y}Z_{\rho u_y u_y}^{p,k\alpha_{u_y}\beta_{u_y}}\ddot{u}_{y\beta_{u_y}}^{p,k}\\
&+\delta u_{z\alpha_{u_z}}^{p,k^T}\ {}^{H_xH_y}Z_{\rho u_z u_z}^{p,k\alpha_{u_z}\beta_{u_z}}\ddot{u}_{z\beta_{u_z}}^{p,k}\Big]\mathrm{d}x\mathrm{d}y\\
&+\sum_{k=1}^{N_k}\sum_{p=1}^{N_p^k}\int_x\int_y\Big[\frac{\partial\delta u_{x\alpha_{u_x}}^{p,k}}{\partial x}\ {}^{H_y}_{H_x}Z_{11u_xu_x}^{p,k\alpha_{u_x}\beta_{u_x}}\frac{\partial u_{x\beta_{u_x}}^{p,k}}{\partial x}+\frac{\partial\delta u_{x\alpha_{u_x}}^{p,k}}{\partial x}Z_{12u_xu_y}^{p,k\alpha_{u_x}\beta_{u_y}}\frac{\partial u_{y\beta_{u_y}}^{p,k}}{\partial y}\\
&+\frac{\partial\delta u_{x\alpha_{u_x}}^{p,k}}{\partial x}Z_{16u_xu_x}^{p,k\alpha_{u_x}\beta_{u_x}}\frac{\partial u_{x\beta_{u_x}}^{p,k}}{\partial y}+\frac{\partial\delta u_{x\alpha_{u_x}}^{p,k}}{\partial x}\ {}^{H_y}_{H_x}Z_{16u_xu_y}^{p,k\alpha_{u_x}\beta_{u_y}}\frac{\partial u_{y\beta_{u_y}}^{p,k}}{\partial x}+\frac{\partial\delta u_{y\alpha_{u_y}}^{p,k}}{\partial y}Z_{12u_yu_x}^{p,k\alpha_{u_y}\beta_{u_x}}\frac{\partial u_{x\beta_{u_x}}^{p,k}}{\partial x}\\
&+\frac{\partial\delta u_{y\alpha_{u_y}}^{p,k}}{\partial y}\ {}^{H_x}_{H_y}Z_{22u_yu_y}^{p,k\alpha_{u_y}\beta_{u_y}}\frac{\partial u_{y\beta_{u_y}}^{p,k}}{\partial y}+\frac{\partial\delta u_{y\alpha_{u_y}}^{p,k}}{\partial y}\ {}^{H_x}_{H_y}Z_{26u_yu_x}^{p,k\alpha_{u_y}\beta_{u_x}}\frac{\partial u_{x\beta_{u_x}}^{p,k}}{\partial y}+\frac{\partial\delta u_{y\alpha_{u_y}}^{p,k}}{\partial y}Z_{26u_yu_y}^{p,k\alpha_{u_y}\beta_{u_y}}\frac{\partial u_{y\beta_{u_y}}^{p,k}}{\partial x}\\
&+\frac{\partial\delta u_{x\alpha_{u_x}}^{p,k}}{\partial y}Z_{16u_xu_x}^{p,k\alpha_{u_x}\beta_{u_x}}\frac{\partial u_{x\beta_{u_x}}^{p,k}}{\partial x}+\frac{\partial\delta u_{x\alpha_{u_x}}^{p,k}}{\partial y}\ {}^{H_x}_{H_y}Z_{26u_xu_y}^{p,k\alpha_{u_x}\beta_{u_y}}\frac{\partial u_{y\beta_{u_y}}^{p,k}}{\partial y}+\frac{\partial\delta u_{x\alpha_{u_x}}^{p,k}}{\partial y}\ {}^{H_x}_{H_y}Z_{66u_xu_x}^{p,k\alpha_{u_x}\beta_{u_x}}\frac{\partial u_{x\beta_{u_x}}^{p,k}}{\partial y}\\
&+\frac{\partial\delta u_{x\alpha_{u_x}}^{p,k}}{\partial y}Z_{66u_xu_y}^{p,k\alpha_{u_x}\beta_{u_y}}\frac{\partial u_{y\beta_{u_y}}^{p,k}}{\partial x}+\frac{\partial\delta u_{y\alpha_{u_y}}^{p,k}}{\partial x}\ {}^{H_y}_{H_x}Z_{16u_yu_x}^{p,k\alpha_{u_y}\beta_{u_x}}\frac{\partial u_{x\beta_{u_x}}^{p,k}}{\partial x}+\frac{\partial\delta u_{y\alpha_{u_y}}^{p,k}}{\partial x}Z_{26u_yu_y}^{p,k\alpha_{u_y}\beta_{u_y}}\frac{\partial u_{y\beta_{u_y}}^{p,k}}{\partial y}\\
&+\frac{\partial\delta u_{y\alpha_{u_y}}^{p,k}}{\partial x}Z_{66u_yu_x}^{p,k\alpha_{u_y}\beta_{u_x}}\frac{\partial u_{x\beta_{u_x}}^{p,k}}{\partial y}+\frac{\partial\delta u_{y\alpha_{u_y}}^{p,k}}{\partial x}\ {}^{H_y}_{H_x}Z_{66u_yu_y}^{p,k\alpha_{u_y}\beta_{u_y}}\frac{\partial u_{y\beta_{u_y}}^{p,k}}{\partial x}+\frac{\partial\delta u_{x\alpha_{u_x}}^{p,k}}{\partial x}\ {}^{H_y}Z_{13u_xs_z}^{p,k\alpha_{u_x}\beta_{s_z}}s_{z\beta_{s_z}}^{p,k}\\
&+\frac{\partial\delta u_{y\alpha_{u_y}}^{p,k}}{\partial y}\ {}^{H_x}Z_{23u_ys_z}^{p,k\alpha_{u_x}\beta_{s_z}}s_{z\beta_{s_z}}^{p,k}+\frac{\partial\delta u_{x\alpha_{u_x}}^{p,k}}{\partial y}\ {}^{H_x}Z_{36u_xs_z}^{p,k\alpha_{u_x}\beta_{s_z}}s_{z\beta_{s_z}}^{p,k}+\frac{\partial\delta u_{y\alpha_{u_y}}^{p,k}}{\partial x}\ {}^{H_y}Z_{36u_ys_z}^{p,k\alpha_{u_y}\beta_{s_z}}s_{z\beta_{s_z}}^{p,k}\\
&+\frac{\partial\delta u_{x\alpha_{u_x}}^{p,k}}{\partial x}\ {}^{H_y}_{H_xR_x}Z_{11u_xu_z}^{p,k\alpha_{u_x}\beta_{u_z}}u_{z\beta_{u_z}}^{p,k}+\frac{\partial\delta u_{x\alpha_{u_x}}^{p,k}}{\partial x}\ {}^{R_y}Z_{12u_xu_z}^{p,k\alpha_{u_x}\beta_{u_z}}u_{z\beta_{u_z}}^{p,k}+\frac{\partial\delta u_{y\alpha_{u_y}}^{p,k}}{\partial y}\ {}^{R_x}Z_{12u_yu_z}^{p,k\alpha_{u_y}\beta_{u_z}}u_{z\beta_{u_z}}^{p,k}\\
&+\frac{\partial\delta u_{y\alpha_{u_y}}^{p,k}}{\partial y}\ {}^{H_x}_{H_yR_y}Z_{22u_yu_z}^{p,k\alpha_{u_y}\beta_{u_z}}u_{z\beta_{u_z}}^{p,k}+\frac{\partial\delta u_{x\alpha_{u_x}}^{p,k}}{\partial y}\ {}^{R_x}Z_{16u_xu_z}^{p,k\alpha_{u_x}\beta_{u_z}}u_{z\beta_{u_z}}^{p,k}+\frac{\partial\delta u_{x\alpha_{u_x}}^{p,k}}{\partial y}\ {}^{H_x}_{H_yR_y}Z_{26u_xu_z}^{p,k\alpha_{u_x}\beta_{u_z}}u_{z\beta_{u_z}}^{p,k}\\
&+\frac{\partial\delta u_{y\alpha_{u_y}}^{p,k}}{\partial x}\ {}^{H_y}_{H_xR_x}Z_{16u_yu_z}^{p,k\alpha_{u_y}\beta_{u_z}}u_{z\beta_{u_z}}^{p,k}+\frac{\partial\delta u_{y\alpha_{u_y}}^{p,k}}{\partial x}\ {}^{R_y}Z_{26u_yu_z}^{p,k\alpha_{u_y}\beta_{u_z}}u_{z\beta_{u_z}}^{p,k}+\delta u_{z\alpha_{u_z}}^{p,k}\ {}^{H_y}_{H_xR_x}Z_{11u_zu_x}^{p,k\alpha_{u_z}\beta_{u_x}}\frac{\partial u_{x\beta_{u_x}}^{p,k}}{\partial x}\\
&+\delta u_{z\alpha_{u_z}}^{p,k}\ {}^{R_x}Z_{12u_zu_y}^{p,k\alpha_{u_z}\beta_{u_y}}\frac{\partial u_{y\beta_{u_y}}^{p,k}}{\partial y}+\delta u_{z\alpha_{u_z}}^{p,k}\ {}^{R_x}Z_{16u_zu_x}^{p,k\alpha_{u_z}\beta_{u_x}}\frac{\partial u_{x\beta_{u_x}}^{p,k}}{\partial y}+\delta u_{z\alpha_{u_z}}^{p,k}\ {}^{H_y}_{H_xR_x}Z_{16u_zu_y}^{p,k\alpha_{u_z}\beta_{u_y}}\frac{\partial u_{y\beta_{u_y}}^{p,k}}{\partial x}\\
&+\delta u_{z\alpha_{u_z}}^{p,k}\ {}^{R_y}Z_{12u_zu_x}^{p,k\alpha_{u_z}\beta_{u_x}}\frac{\partial u_{x\beta_{u_x}}^{p,k}}{\partial x}+\delta u_{z\alpha_{u_z}}^{p,k}\ {}^{H_x}_{H_yR_y}Z_{22u_zu_y}^{p,k\alpha_{u_z}\beta_{u_y}}\frac{\partial u_{y\beta_{u_y}}^{p,k}}{\partial y}+\delta u_{z\alpha_{u_z}}^{p,k}\ {}^{H_x}_{H_yR_y}Z_{26u_zu_x}^{p,k\alpha_{u_z}\beta_{u_x}}\frac{\partial u_{x\beta_{u_x}}^{p,k}}{\partial y}\\
&+\delta u_{z\alpha_{u_z}}^{p,k}\ {}^{R_y}Z_{26u_zu_y}^{p,k\alpha_{u_z}\beta_{u_y}}\frac{\partial u_{y\beta_{u_y}}^{p,k}}{\partial x}+\delta u_{z\alpha_{u_z}}^{p,k}\ {}^{H_y}_{R_x}Z_{13u_zs_z}^{p,k\alpha_{u_z}\beta_{s_z}}s_{z\beta_{s_z}}^{p,k}+\delta u_{z\alpha_{u_z}}^{p,k}\ {}^{H_x}_{R_y}Z_{23u_zs_z}^{p,k\alpha_{u_z}\beta_{s_z}}s_{z\beta_{s_z}}^{p,k}\\
&+\delta u_{z\alpha_{u_z}}^{p,k}\ {}^{H_y}_{H_xR_x^2}Z_{11u_zu_z}^{p,k\alpha_{u_z}\beta_{u_z}}u_{z\beta_{u_z}}^{p,k}+\delta u_{z\alpha_{u_z}}^{p,k}\ {}^{R_xR_y}Z_{12u_zu_z}^{p,k\alpha_{u_z}\beta_{u_z}}u_{z\beta_{u_z}}^{p,k}+\delta u_{z\alpha_{u_z}}^{p,k}\ {}^{R_xR_y}Z_{12u_zu_z}^{p,k\alpha_{u_z}\beta_{u_z}}u_{z\beta_{u_z}}^{p,k}\\
&+\delta u_{z\alpha_{u_z}}^{p,k}\ {}^{H_x}_{H_yR_y^2}Z_{22u_zu_z}^{p,k\alpha_{u_z}\beta_{u_z}}u_{z\beta_{u_z}}^{p,k}+\frac{\partial\delta u_{z\alpha_{u_z}}^{p,k}}{\partial y}\ {}^{H_x}Z_{u_zs_y}^{p,k\alpha_{u_z}\beta_{s_y}}s_{y\beta_{s_y}}^{p,k}+\frac{\partial\delta u_{z\alpha_{u_z}}^{p,k}}{\partial x}\ {}^{H_y}Z_{u_zs_x}^{p,k\alpha_{u_z}\beta_{s_x}}s_{x\beta_{s_x}}^{p,k}\\
&-\delta u_{y\alpha_{u_y}}^{p,k}\lambda_D\ {}^{H_x}_{R_y}Z_{u_ys_y}^{p,k\alpha_{u_y}\beta_{s_y}}s_{y\beta_{s_y}}^{p,k}-\delta u_{x\alpha_{u_x}}^{p,k}\lambda_D\ {}^{H_y}_{R_x}Z_{u_xs_x}^{p,k\alpha_{u_x}\beta_{s_x}}s_{x\beta_{s_x}}^{p,k}+\delta u_{y\alpha_{u_y}}^{p,k}\ {}^{H_xH_y}Z_{\partial u_ys_y}^{p,k\alpha_{u_y}\beta_{s_y}}s_{y\beta_{s_y}}^{p,k}\\
&+\delta u_{x\alpha_{ux}}^{p,k}\ {}^{H_xH_y}Z_{\partial u_xs_x}^{p,k\alpha_{u_x}\beta_{s_x}}s_{x\beta_{s_x}}^{p,k}+\delta u_{z\alpha_{uz}}^{p,k}\ {}^{H_xH_y}Z_{\partial u_zs_z}^{p,k\alpha_{u_z}\beta_{s_z}}s_{z\beta_{s_z}}^{p,k}+\delta s_{y\alpha_{s_y}}^{p,k}\ {}^{H_x}Z_{s_yu_z}^{p,k\alpha_{s_y}\beta_{u_z}}\frac{\partial u_{z\beta_{u_z}}^{p,k}}{\partial y}
\end{aligned}
\tag{B.5}
$$

$$
\begin{aligned}
&+\delta s^{p,k}_{x\alpha_{s_x}}\ {}^{H_y}Z^{p,k\alpha_{s_x}\beta_{u_z}}_{s_x u_z}\frac{\partial u^{p,k}_{z\beta_{u_z}}}{\partial x}-\delta s^{p,k}_{y\alpha_{s_y}}\lambda_D\ {}^{H_x}_{R_y}Z^{p,k\alpha_{s_y}\beta_{u_y}}_{s_y u_y}u^{p,k}_{y\beta_{u_y}}-\delta s^{p,k}_{x\alpha_{s_x}}\lambda_D\ {}^{H_y}_{R_x}Z^{p,k\alpha_{s_x}\beta_{u_x}}_{s_x u_x}u^{p,k}_{x\beta_{u_x}}\\
&+\delta s^{p,k}_{y\alpha_{s_y}}\ {}^{H_x H_y}Z^{p,k\alpha_{s_y}\beta_{u_y}}_{s_y\partial u_y}u^{p,k}_{y\beta_{u_y}}+\delta s^{p,k}_{x\alpha_{s_x}}\ {}^{H_x H_y}Z^{p,k\alpha_{s_x}\beta_{u_x}}_{s_x\partial u_x}u^{p,k}_{x\beta_{u_x}}+\delta s^{p,k}_{z\alpha_{s_z}}\ {}^{H_x H_y}Z^{p,k\alpha_{s_z}\beta_{u_z}}_{s_z\partial u_z}u^{p,k}_{z\beta_{u_z}}\\
&+\delta s^{p,k}_{z\alpha_{s_z}}\ {}^{H_y}Z^{p,k\alpha_{s_z}\beta_{u_x}}_{13 s_z u_x}\frac{\partial u^{p,k}_{x\beta_{u_x}}}{\partial x}+\delta s^{p,k}_{z\alpha_{s_z}}\ {}^{H_x}Z^{p,k\alpha_{s_z}\beta_{u_y}}_{23 s_z u_y}\frac{\partial u^{p,k}_{y\beta_{u_y}}}{\partial y}+\delta s^{p,k}_{z\alpha_{s_z}}\ {}^{H_x}Z^{p,k\alpha_{s_z}\beta_{u_x}}_{36 s_z u_x}\frac{\partial u^{p,k}_{x\beta_{u_x}}}{\partial y}\\
&+\delta s^{p,k}_{z\alpha_{s_z}}\ {}^{H_y}Z^{p,k\alpha_{s_z}\beta_{u_y}}_{36 s_z u_y}\frac{\partial u^{p,k}_{y\beta_{u_y}}}{\partial x}+\delta s^{p,k}_{z\alpha_{s_z}}\ {}^{H_y}_{R_x}Z^{p,k\alpha_{s_z}\beta_{u_z}}_{13 s_z u_z}u^{p,k}_{z\beta_{u_z}}+\delta s^{p,k}_{z\alpha_{s_z}}\ {}^{H_x}_{R_y}Z^{p,k\alpha_{s_z}\beta_{u_z}}_{23 s_z u_z}u^{p,k}_{z\beta_{u_z}}\\
&-\delta s^{p,k}_{y\alpha_{s_y}}\ {}^{H_x H_y}Z^{p,k\alpha_{s_y}\beta_{s_y}}_{44 s_y s_y}s^{p,k}_{y\beta_{s_y}}-\delta s^{p,k}_{y\alpha_{s_y}}\ {}^{H_x H_y}Z^{p,k\alpha_{s_y}\beta_{s_x}}_{45 s_y s_x}s^{p,k}_{x\beta_{s_x}}-\delta s^{p,k}_{x\alpha_{s_x}}\ {}^{H_x H_y}Z^{p,k\alpha_{s_x}\beta_{s_y}}_{45 s_x s_y}s^{p,k}_{y\beta_{s_y}}\\
&-\delta s^{p,k}_{x\alpha_{s_x}}\ {}^{H_x H_y}Z^{p,k\alpha_{s_x}\beta_{s_x}}_{55 s_x s_x}s^{p,k}_{x\beta_{s_x}}-\delta s^{p,k}_{z\alpha_{s_z}}\ {}^{H_x H_y}Z^{p,k\alpha_{s_z}\beta_{s_z}}_{33 s_z s_z}s^{p,k}_{z\beta_{s_z}}\Bigg]\mathrm{d}x\mathrm{d}y\\
&=\int_x\int_y\left[\delta u^{N_p^k,N_k}_{z0}f_z^{top}\left(1+\frac{h}{2R_x}\right)\left(1+\frac{h}{2R_y}\right)+\delta u^{1,1}_{z1}f_z^{bot}\left(1-\frac{h}{2R_x}\right)\left(1-\frac{h}{2R_y}\right)\right]\mathrm{d}x\mathrm{d}y
\end{aligned}
$$

Appendix C

Cylinder and plate governing equations

In the present appendix, the governing equations for shell geometries are specialized to cylinder and plate geometries.

C.1 Cylinder governing equations

The governing equations for cylindrical geometries can be easily obtained as a particular case of the equations for shells by imposing that one of the two radii of curvature is infinite.

For cylindrical geometries, which are characterized by only one radius of curvature (it is supposed, without loss of generality, that $R_x \to \infty$), the *mass matrix* ($\mathbf{M}_{ij}$) and the *stiffness matrix* ($\mathbf{K}_{ij}$) specialize to:

$$\mathbf{M}_{ij} = \begin{bmatrix} \mathbf{M}_{u_x u_x i_1 j_1} & \mathbf{0} & \mathbf{0} & \mathbf{0} & \mathbf{0} & \mathbf{0} \\ \mathbf{0} & \mathbf{M}_{u_y u_y i_1 j_1} & \mathbf{0} & \mathbf{0} & \mathbf{0} & \mathbf{0} \\ \mathbf{0} & \mathbf{0} & \mathbf{M}_{u_z u_z i_1 j_1} & \mathbf{0} & \mathbf{0} & \mathbf{0} \\ \mathbf{0} & \mathbf{0} & \mathbf{0} & \mathbf{0} & \mathbf{0} & \mathbf{0} \\ \mathbf{0} & \mathbf{0} & \mathbf{0} & \mathbf{0} & \mathbf{0} & \mathbf{0} \\ \mathbf{0} & \mathbf{0} & \mathbf{0} & \mathbf{0} & \mathbf{0} & \mathbf{0} \end{bmatrix} \tag{C.1}$$

$$\mathbf{K}_{ij} = \begin{bmatrix} \mathbf{K}_{u_x u_x i_1 j_1} & \mathbf{K}_{u_x u_y i_1 j_1} & \mathbf{K}_{u_x u_z i_1 j_1} & \mathbf{K}_{u_x s_x i_1 j_2} & \mathbf{0}_{u_x s_y i_1 j_2} & \mathbf{K}_{u_x s_z i_1 j_2} \\ \mathbf{K}_{u_y u_x i_1 j_1} & \mathbf{K}_{u_y u_y i_1 j_1} & \mathbf{K}_{u_y u_z i_1 j_1} & \mathbf{0}_{u_y s_x i_1 j_2} & \mathbf{K}_{u_y s_y i_1 j_2} & \mathbf{K}_{u_y s_z i_1 j_2} \\ \mathbf{K}_{u_z u_x i_1 j_1} & \mathbf{K}_{u_z u_y i_1 j_1} & \mathbf{K}_{u_z u_z i_1 j_1} & \mathbf{K}_{u_z s_x i_1 j_2} & \mathbf{K}_{u_z s_y i_1 j_2} & \mathbf{K}_{u_z s_z i_1 j_2} \\ \mathbf{K}_{s_x u_x i_2 j_1} & \mathbf{0}_{s_x u_y i_2 j_1} & \mathbf{K}_{s_x u_z i_2 j_1} & \mathbf{K}_{s_x s_x i_2 j_2} & \mathbf{K}_{s_x s_y i_2 j_2} & \mathbf{0}_{s_x s_z i_2 j_2} \\ \mathbf{0}_{s_y u_x i_2 j_1} & \mathbf{K}_{s_y u_y i_2 j_1} & \mathbf{K}_{s_y u_z i_2 j_1} & \mathbf{K}_{s_y s_x i_2 j_2} & \mathbf{K}_{s_y s_y i_2 j_2} & \mathbf{0}_{s_y s_z i_2 j_2} \\ \mathbf{K}_{s_z u_x i_2 j_1} & \mathbf{K}_{s_z u_y i_2 j_1} & \mathbf{K}_{s_z u_z i_2 j_1} & \mathbf{0}_{s_z s_x i_2 j_2} & \mathbf{0}_{s_z s_y i_2 j_2} & \mathbf{K}_{s_z s_z i_2 j_2} \end{bmatrix} \tag{C.2}$$

and

$$\mathbf{M}_{u_x u_x i_1 j_1} = {}^{H_y}\mathbf{Z}_{\rho u_x u_x} I^{0000}_{u_x u_x i_1 j_1} \quad \mathbf{M}_{u_y u_y i_1 j_1} = {}^{H_y}\mathbf{Z}_{\rho u_y u_y} I^{0000}_{u_y u_y i_1 j_1} \quad \mathbf{M}_{u_z u_z i_1 j_1} = {}^{H_y}\mathbf{Z}_{\rho u_z u_z} I^{0000}_{u_z u_z i_1 j_1}$$

$$
\begin{aligned}
\mathbf{K}_{u_x u_x i_1 j_1} &= {}^{H_y}\mathbf{Z}_{11 u_x u_x} I^{1010}_{u_x u_x i_1 j_1} + \mathbf{Z}_{16 u_x u_x} (I^{1001}_{u_x u_x i_1 j_1} + I^{0110}_{u_x u_x i_1 j_1}) \\
&\quad + {}_{H_y}\mathbf{Z}_{66 u_x u_x} I^{0101}_{u_x u_x i_1 j_1} \\
\mathbf{K}_{u_x u_y i_1 j_1} &= \mathbf{Z}_{12 u_x u_y} I^{1001}_{u_x u_y i_1 j_1} + {}^{H_y}\mathbf{Z}_{16 u_x u_y} I^{1010}_{u_x u_y i_1 j_1} + {}_{H_y}\mathbf{Z}_{26 u_x u_y} I^{0101}_{u_x u_y i_1 j_1} \\
&\quad + \mathbf{Z}_{66 u_x u_y} I^{0110}_{u_x u_y i_1 j_1} \\
\mathbf{K}_{u_x u_z i_1 j_1} &= {}_{R_y}\mathbf{Z}_{12 u_x u_z} I^{1000}_{u_x u_z i_1 j_1} + {}_{H_y R_y}\mathbf{Z}_{26 u_x u_z} I^{0100}_{u_x u_z i_1 j_1} \\
\mathbf{K}_{u_x s_x i_1 j_2} &= {}^{H_y}\mathbf{Z}_{\partial u_x s_x} I^{0000}_{u_x s_x i_1 j_2} \\
\mathbf{K}_{u_x s_z i_1 j_2} &= \mathbf{Z}_{36 u_x s_z} I^{0100}_{u_x s_z i_1 j_2} + {}^{H_y}\mathbf{Z}_{13 u_x s_z} I^{1000}_{u_x s_z i_1 j_2} \\
\mathbf{K}_{u_y u_x i_1 j_1} &= \mathbf{Z}_{12 u_y u_x} I^{0110}_{u_y u_x i_1 j_1} + {}_{H_y}\mathbf{Z}_{26 u_y u_x} I^{0101}_{u_y u_x i_1 j_1} + {}^{H_y}\mathbf{Z}_{16 u_y u_x} I^{1010}_{u_y u_x i_1 j_1} \\
&\quad + \mathbf{Z}_{66 u_y u_x} I^{1001}_{u_y u_x i_1 j_1} \\
\mathbf{K}_{u_y u_y i_1 j_1} &= {}_{H_y}\mathbf{Z}_{22 u_y u_y} I^{0101}_{u_y u_y i_1 j_1} + \mathbf{Z}_{26 u_y u_y} (I^{0110}_{u_y u_y i_1 j_1} + I^{1001}_{u_y u_y i_1 j_1}) \\
&\quad + {}^{H_y}\mathbf{Z}_{66 u_y u_y} I^{1010}_{u_y u_y i_1 j_1} \\
\mathbf{K}_{u_y u_z i_1 j_1} &= {}_{R_y}\mathbf{Z}_{26 u_y u_z} I^{1000}_{u_y u_z i_1 j_1} + {}_{H_y R_y}\mathbf{Z}_{22 u_y u_z} I^{0100}_{u_y u_z i_1 j_1} \\
\mathbf{K}_{u_y s_y i_1 j_2} &= -\lambda_D \, {}_{R_y}\mathbf{Z}_{u_y s_y} I^{0000}_{u_y s_y i_1 j_2} + {}^{H_y}\mathbf{Z}_{\partial u_y s_y} I^{0000}_{u_y s_y i_1 j_2} \\
\mathbf{K}_{u_y s_z i_1 j_2} &= \mathbf{Z}_{23 u_y s_z} I^{0100}_{u_y s_z i_1 j_2} + {}^{H_y}\mathbf{Z}_{36 u_y s_z} I^{1000}_{u_y s_z i_1 j_2} \\
\mathbf{K}_{u_z u_x i_1 j_1} &= {}_{R_y}\mathbf{Z}_{12 u_z u_x} I^{0010}_{u_z u_x i_1 j_1} + {}_{H_y R_y}\mathbf{Z}_{26 u_z u_x} I^{0001}_{u_z u_x i_1 j_1} \\
\mathbf{K}_{u_z u_y i_1 j_1} &= {}_{H_y R_y}\mathbf{Z}_{22 u_z u_y} I^{0001}_{u_z u_y i_1 j_1} + {}_{R_y}\mathbf{Z}_{26 u_z u_y} I^{0010}_{u_z u_y i_1 j_1} \\
\mathbf{K}_{u_z u_z i_1 j_1} &= {}_{H_y R_y^2}\mathbf{Z}_{22 u_z u_z} I^{0000}_{u_z u_z i_1 j_1} \\
\mathbf{K}_{u_z s_x i_1 j_2} &= {}^{H_y}\mathbf{Z}_{u_z s_x} I^{1000}_{u_z s_x i_1 j_2} \\
\mathbf{K}_{u_z s_y i_1 j_2} &= \mathbf{Z}_{u_z s_y} I^{0100}_{u_z s_y i_1 j_2} \\
\mathbf{K}_{u_z s_z i_1 j_2} &= {}^{H_y}\mathbf{Z}_{\partial u_z s_z} I^{0000}_{u_z s_z i_1 j_2} + {}_{R_y}\mathbf{Z}_{23 u_z s_z} I^{0000}_{u_z s_z i_1 j_2} \\
\mathbf{K}_{s_x u_x i_2 j_1} &= {}^{H_y}\mathbf{Z}_{s_x \partial u_x} I^{0000}_{s_x u_x i_2 j_1} \\
\mathbf{K}_{s_x u_z i_2 j_1} &= {}^{H_y}\mathbf{Z}_{s_x u_z} I^{0010}_{s_x u_z i_2 j_1} \\
\mathbf{K}_{s_x s_x i_2 j_2} &= -\,{}^{H_y}\mathbf{Z}_{55 s_x s_x} I^{0000}_{s_x s_x i_2 j_2} \\
\mathbf{K}_{s_x s_y i_2 j_2} &= -\,{}^{H_y}\mathbf{Z}_{45 s_x s_y} I^{0000}_{s_x s_y i_2 j_2} \\
\mathbf{K}_{s_y u_y i_2 j_1} &= -\lambda_D \, {}_{R_y}\mathbf{Z}_{s_y u_y} I^{0000}_{s_y u_y i_2 j_1} + {}^{H_y}\mathbf{Z}_{s_y \partial u_y} I^{0000}_{s_y u_y i_2 j_1} \\
\mathbf{K}_{s_y u_z i_2 j_1} &= \mathbf{Z}_{s_y u_z} I^{0001}_{s_y u_z i_2 j_1} \\
\mathbf{K}_{s_y s_x i_2 j_2} &= -\mathbf{Z}_{45 s_y s_x} I^{0000}_{s_y s_x i_2 j_2} \\
\mathbf{K}_{s_y s_y i_2 j_2} &= -\,{}^{H_y}\mathbf{Z}_{44 s_y s_y} I^{0000}_{s_y s_y i_2 j_2} \\
\mathbf{K}_{s_z u_x i_2 j_1} &= {}^{H_y}\mathbf{Z}_{13 s_z u_x} I^{0010}_{s_z u_x i_2 j_1} + \mathbf{Z}_{36 s_z u_x} I^{0001}_{s_z u_x i_2 j_1} \\
\mathbf{K}_{s_z u_y i_2 j_1} &= \mathbf{Z}_{23 s_z u_y} I^{0001}_{s_z u_y i_2 j_1} + {}^{H_y}\mathbf{Z}_{36 s_z u_y} I^{0010}_{s_z u_y i_2 j_1} \\
\mathbf{K}_{s_z u_z i_2 j_1} &= {}^{H_y}\mathbf{Z}_{s_z \partial u_z} I^{0000}_{s_z u_z i_2 j_1} + {}_{R_y}\mathbf{Z}_{23 s_z u_z} I^{0000}_{s_z u_z i_2 j_1} \\
\mathbf{K}_{s_z s_z i_2 j_2} &= -\,{}^{H_y}\mathbf{Z}_{33 s_z s_z} I^{0000}_{s_z s_z i_2 j_2}
\end{aligned}
$$

Furthermore, the load vectors for each Ritz element become:

$$\mathbf{L}_i^{top} = \begin{Bmatrix} \mathbf{0} \\ \mathbf{0} \\ \mathbf{L}_{zi_1}^{top} I_{u_z f_z i_1}^{top} \\ \mathbf{0} \\ \mathbf{0} \\ \mathbf{0} \end{Bmatrix} \qquad \mathbf{L}_i^{bot} = \begin{Bmatrix} \mathbf{0} \\ \mathbf{0} \\ \mathbf{L}_{zi_1}^{bot} I_{u_z f_z i_1}^{bot} \\ \mathbf{0} \\ \mathbf{0} \\ \mathbf{0} \end{Bmatrix} \tag{C.4}$$

where the Ritz integrals are now defined as:

$$I_{u_z f_z i_1}^{top} = \int_x \int_y N_{u_z i_1} f_z^{top}(x,y)\left(1+\frac{h}{2R_y}\right)\mathrm{d}x\mathrm{d}y \quad I_{u_z f_z i_1}^{bot} = \int_x \int_y N_{u_z i_1} f_z^{bot}(x,y)\left(1-\frac{h}{2R_y}\right)\mathrm{d}x\mathrm{d}y \tag{C.5}$$

after expanding and assembling the Ritz orders, formally, the same equation as for shell geometries is obtained:

$$\mathbf{M}\ddot{\mathbf{v}} + \mathbf{K}\mathbf{v} = \mathbf{L} \tag{C.6}$$

where

$$\mathbf{L} = \mathbf{L}^{top} f_0^{top} + \mathbf{L}^{bot} f_0^{bot} \tag{C.7}$$

C.2 Plate governing equations

The governing equations for plate geometries can be easily obtained starting from the equations for shells by imposing $R_x \to \infty$ and $R_y \to \infty$ (it implies that $H_x \to 1$ and $H_y \to 1$).

The *mass matrix* ($\mathbf{M}_{ij}$) and the *stiffness matrix* ($\mathbf{K}_{ij}$) for each Ritz element become:

$$\mathbf{M}_{ij} = \begin{bmatrix} \mathbf{M}_{u_x u_x i_1 j_1} & \mathbf{0} & \mathbf{0} & \mathbf{0} & \mathbf{0} & \mathbf{0} \\ \mathbf{0} & \mathbf{M}_{u_y u_y i_1 j_1} & \mathbf{0} & \mathbf{0} & \mathbf{0} & \mathbf{0} \\ \mathbf{0} & \mathbf{0} & \mathbf{M}_{u_z u_z i_1 j_1} & \mathbf{0} & \mathbf{0} & \mathbf{0} \\ \mathbf{0} & \mathbf{0} & \mathbf{0} & \mathbf{0} & \mathbf{0} & \mathbf{0} \\ \mathbf{0} & \mathbf{0} & \mathbf{0} & \mathbf{0} & \mathbf{0} & \mathbf{0} \\ \mathbf{0} & \mathbf{0} & \mathbf{0} & \mathbf{0} & \mathbf{0} & \mathbf{0} \end{bmatrix} \tag{C.8}$$

$$\mathbf{K}_{ij} = \begin{bmatrix} \mathbf{K}_{u_x u_x i_1 j_1} & \mathbf{K}_{u_x u_y i_1 j_1} & \mathbf{0}_{u_x u_z i_1 j_1} & \mathbf{K}_{u_x s_x i_1 j_2} & \mathbf{0}_{u_x s_y i_1 j_2} & \mathbf{K}_{u_x s_z i_1 j_2} \\ \mathbf{K}_{u_y u_x i_1 j_1} & \mathbf{K}_{u_y u_y i_1 j_1} & \mathbf{0}_{u_y u_z i_1 j_1} & \mathbf{0}_{u_y s_x i_1 j_2} & \mathbf{K}_{u_y s_y i_1 j_2} & \mathbf{K}_{u_y s_z i_1 j_2} \\ \mathbf{0}_{u_z u_x i_1 j_1} & \mathbf{0}_{u_z u_y i_1 j_1} & \mathbf{0}_{u_z u_z i_1 j_1} & \mathbf{K}_{u_z s_x i_1 j_2} & \mathbf{K}_{u_z s_y i_1 j_2} & \mathbf{K}_{u_z s_z i_1 j_2} \\ \mathbf{K}_{s_x u_x i_2 j_1} & \mathbf{0}_{s_x u_y i_2 j_1} & \mathbf{K}_{s_x u_z i_2 j_1} & \mathbf{K}_{s_x s_x i_2 j_2} & \mathbf{K}_{s_x s_y i_2 j_2} & \mathbf{0}_{s_x s_z i_2 j_2} \\ \mathbf{0}_{s_y u_x i_2 j_1} & \mathbf{K}_{s_y u_y i_2 j_1} & \mathbf{K}_{s_y u_z i_2 j_1} & \mathbf{K}_{s_y s_x i_2 j_2} & \mathbf{K}_{s_y s_y i_2 j_2} & \mathbf{0}_{s_y s_z i_2 j_2} \\ \mathbf{K}_{s_z u_x i_2 j_1} & \mathbf{K}_{s_z u_y i_2 j_1} & \mathbf{K}_{s_z u_z i_2 j_1} & \mathbf{0}_{s_z s_x i_2 j_2} & \mathbf{0}_{s_z s_y i_2 j_2} & \mathbf{K}_{s_z s_z i_2 j_2} \end{bmatrix} \tag{C.9}$$

and

$$\mathbf{M}_{u_x u_x i_1 j_1} = \mathbf{Z}_{\rho u_x u_x} I_{u_x u_x i_1 j_1}^{0000} \quad \mathbf{M}_{u_y u_y i_1 j_1} = \mathbf{Z}_{\rho u_y u_y} I_{u_y u_y i_1 j_1}^{0000} \quad \mathbf{M}_{u_z u_z i_1 j_1} = \mathbf{Z}_{\rho u_z u_z} I_{u_z u_z i_1 j_1}^{0000}$$

$$
\begin{aligned}
\mathbf{K}_{u_x u_x i_1 j_1} &= \mathbf{Z}_{11 u_x u_x} I^{1010}_{u_x u_x i_1 j_1} + \mathbf{Z}_{16 u_x u_x} (I^{1001}_{u_x u_x i_1 j_1} + I^{0110}_{u_x u_x i_1 j_1}) + \mathbf{Z}_{66 u_x u_x} I^{0101}_{u_x u_x i_1 j_1} \\
\mathbf{K}_{u_x u_y i_1 j_1} &= \mathbf{Z}_{12 u_x u_y} I^{1001}_{u_x u_y i_1 j_1} + \mathbf{Z}_{16 u_x u_y} I^{1010}_{u_x u_y i_1 j_1} + \mathbf{Z}_{26 u_x u_y} I^{0101}_{u_x u_y i_1 j_1} \\
&\quad + \mathbf{Z}_{66 u_x u_y} I^{0110}_{u_x u_y i_1 j_1} \\
\mathbf{K}_{u_x s_x i_1 j_2} &= \mathbf{Z}_{\partial u_x s_x} I^{0000}_{u_x s_x i_1 j_2} \\
\mathbf{K}_{u_x s_z i_1 j_2} &= \mathbf{Z}_{36 u_x s_z} I^{0100}_{u_x s_z i_1 j_2} + \mathbf{Z}_{13 u_x s_z} I^{1000}_{u_x s_z i_1 j_2} \\
\mathbf{K}_{u_y u_x i_1 j_1} &= \mathbf{Z}_{12 u_y u_x} I^{0110}_{u_y u_x i_1 j_1} + \mathbf{Z}_{26 u_y u_x} I^{0101}_{u_y u_x i_1 j_1} + \mathbf{Z}_{16 u_y u_x} I^{1010}_{u_y u_x i_1 j_1} \\
&\quad + \mathbf{Z}_{66 u_y u_x} I^{1001}_{u_y u_x i_1 j_1} \\
\mathbf{K}_{u_y u_y i_1 j_1} &= \mathbf{Z}_{22 u_y u_y} I^{0101}_{u_y u_y i_1 j_1} + \mathbf{Z}_{26 u_y u_y} (I^{0110}_{u_y u_y i_1 j_1} + I^{1001}_{u_y u_y i_1 j_1}) + \mathbf{Z}_{66 u_y u_y} I^{1010}_{u_y u_y i_1 j_1} \\
\mathbf{K}_{u_y s_y i_1 j_2} &= \mathbf{Z}_{\partial u_y s_y} I^{0000}_{u_y s_y i_1 j_2} \\
\mathbf{K}_{u_y s_z i_1 j_2} &= \mathbf{Z}_{23 u_y s_z} I^{0100}_{u_y s_z i_1 j_2} + \mathbf{Z}_{36 u_y s_z} I^{1000}_{u_y s_z i_1 j_2} \\
\mathbf{K}_{u_z s_x i_1 j_2} &= \mathbf{Z}_{u_z s_x} I^{1000}_{u_z s_x i_1 j_2} \\
\mathbf{K}_{u_z s_y i_1 j_2} &= \mathbf{Z}_{u_z s_y} I^{0100}_{u_z s_y i_1 j_2} \\
\mathbf{K}_{u_z s_z i_1 j_2} &= \mathbf{Z}_{\partial u_z s_z} I^{0000}_{u_z s_z i_1 j_2} \\
\mathbf{K}_{s_x u_x i_2 j_1} &= \mathbf{Z}_{s_x \partial u_x} I^{0000}_{s_x u_x i_2 j_1} \\
\mathbf{K}_{s_x u_z i_2 j_1} &= \mathbf{Z}_{s_x u_z} I^{0010}_{s_x u_z i_2 j_1} \\
\mathbf{K}_{s_x s_x i_2 j_2} &= -\mathbf{Z}_{55 s_x s_x} I^{0000}_{s_x s_x i_2 j_2} \\
\mathbf{K}_{s_x s_y i_2 j_2} &= -\mathbf{Z}_{45 s_x s_y} I^{0000}_{s_x s_y i_2 j_2} \\
\mathbf{K}_{s_y u_y i_2 j_1} &= \mathbf{Z}_{s_y \partial u_y} I^{0000}_{s_y u_y i_2 j_1} \\
\mathbf{K}_{s_y u_z i_2 j_1} &= \mathbf{Z}_{s_y u_z} I^{0001}_{s_y u_z i_2 j_1} \\
\mathbf{K}_{s_y s_x i_2 j_2} &= -\mathbf{Z}_{45 s_y s_x} I^{0000}_{s_y s_x i_2 j_2} \\
\mathbf{K}_{s_y s_y i_2 j_2} &= -\mathbf{Z}_{44 s_y s_y} I^{0000}_{s_y s_y i_2 j_2} \\
\mathbf{K}_{s_z u_x i_2 j_1} &= \mathbf{Z}_{13 s_z u_x} I^{0010}_{s_z u_x i_2 j_1} + \mathbf{Z}_{36 s_z u_x} I^{0001}_{s_z u_x i_2 j_1} \\
\mathbf{K}_{s_z u_y i_2 j_1} &= \mathbf{Z}_{23 s_z u_y} I^{0001}_{s_z u_y i_2 j_1} + \mathbf{Z}_{36 s_z u_y} I^{0010}_{s_z u_y i_2 j_1} \\
\mathbf{K}_{s_z u_z i_2 j_1} &= \mathbf{Z}_{s_z \partial u_z} I^{0000}_{s_z u_z i_2 j_1} \\
\mathbf{K}_{s_z s_z i_2 j_2} &= -\mathbf{Z}_{33 s_z s_z} I^{0000}_{s_z s_z i_2 j_2}
\end{aligned}
$$

Furthermore, the load vectors for each Ritz element become:

$$
\mathbf{L}^{top}_i = \begin{Bmatrix} \mathbf{0} \\ \mathbf{0} \\ \mathbf{L}^{top}_{z i_1} I^{top}_{u_z f_z i_1} \\ \mathbf{0} \\ \mathbf{0} \\ \mathbf{0} \end{Bmatrix} \qquad \mathbf{L}^{bot}_i = \begin{Bmatrix} \mathbf{0} \\ \mathbf{0} \\ \mathbf{L}^{bot}_{z i_1} I^{bot}_{u_z f_z i_1} \\ \mathbf{0} \\ \mathbf{0} \\ \mathbf{0} \end{Bmatrix} \tag{C.11}
$$

where the Ritz integrals are now defined as:

$$
I^{top}_{u_z f_z i_1} = \int_x \int_y N_{u_z i_1} f^{top}_z(x,y) \mathrm{d}x \mathrm{d}y \qquad I^{bot}_{u_z f_z i_1} = \int_x \int_y N_{u_z i_1} f^{bot}_z(x,y) \mathrm{d}x \mathrm{d}y \tag{C.12}
$$

after expanding and assembling the Ritz orders, formally, the same equation as for shells and cylinders is obtained:

$$\mathbf{M}\ddot{\mathbf{v}} + \mathbf{K}\mathbf{v} = \mathbf{L} \tag{C.13}$$

where

$$\mathbf{L} = \mathbf{L}^{top} f_0^{top} + \mathbf{L}^{bot} f_0^{bot} \tag{C.14}$$

Appendix D

Algebraic results for additional mixed models

In this appendix algebraic results for additional mixed models are reported. In particular, models of the type $EM_{30}^{N_{\sigma_{\alpha z}} N_{\sigma_{zz}}}$ and $EM_{32}^{N_{\sigma_{\alpha z}} N_{\sigma_{zz}}}$ are considered.

$\mathbf{R_s} = \mathbf{S_s}$	9		10		11		15	
Model	N_{stress}	N_{kin}	N_{stress}	N_{kin}	N_{stress}	N_{kin}	N_{stress}	N_{kin}
No top-bottom b.cs.								
$EM_{3,0}^{0,-}$	0	659	0	633	23	615	231	615
$EM_{3,0}^{1,-}$	0	506	0	455	65	437	481	437
$EM_{3,0}^{2,-}$	0	354	0	277	107	259	731	259
$EM_{3,0}^{3,-}$	162	354	200	277	349	259	1181	259
$EM_{3,0}^{4,-}$	324	354	400	277	591	259	1631	259
$EM_{3,0}^{2,0}$	81	354	100	277	228	259	956	259
$EM_{3,0}^{2,1}$	162	354	200	277	349	259	1181	259
$EM_{3,0}^{2,2}$	243	354	300	277	470	259	1406	259
σ_{xz} and σ_{yz} top-bottom b.cs. (plane stress)								
$EM_{3,0}^{1,-}$	0	800	0	800	0	800	0	800
$EM_{3,0}^{2,-}$	0	658	0	633	23	615	231	615
$EM_{3,0}^{3,-}$	0	506	0	455	65	437	481	437
$EM_{3,0}^{4,-}$	0	354	0	277	107	259	731	259
$EM_{3,0}^{5,-}$	162	354	200	277	349	259	1181	259
σ_{xz}, σ_{yz} and σ_{zz} top-bottom b.cs. (3D law)								
$EM_{3,0}^{4,1}$	0	354	0	277	107	259	731	259
$EM_{3,0}^{4,2}$	81	354	100	277	228	259	956	259
$EM_{3,0}^{5,2}$	243	354	300	277	470	259	1406	259
$EM_{3,0}^{4,3}$	162	354	200	277	349	259	1181	259
$EM_{3,0}^{5,3}$	324	354	400	277	591	259	1631	259

Table D.1: Algebraic parameters for models of the type: $EM_{30}^{N_{\sigma_{\alpha z}} N_{\sigma_{zz}}}$. $R_u = S_u = 10$.

$\mathbf{R_s = S_s}$	9		10		11		15	
Model	N_{stress}	N_{kin}	N_{stress}	N_{kin}	N_{stress}	N_{kin}	N_{stress}	N_{kin}
No top-bottom b.cs.								
$EM_{3,2}^{2,0}$	0	399	0	312	109	296	837	296
$EM_{3,2}^{1,1}$	0	456	0	375	107	367	731	367
$EM_{3,2}^{2,1}$	0	334	0	229	149	221	981	221
$EM_{3,2}^{3,1}$	162	334	200	229	391	221	1431	221
$EM_{3,2}^{4,1}$	324	334	400	229	633	221	1881	221
$EM_{3,2}^{2,3}$	162	334	200	229	391	221	1431	221
$EM_{3,2}^{2,4}$	244	334	300	229	512	221	1656	221
$EM_{3,2}^{3,3}$	324	334	400	229	633	221	1881	221
$EM_{3,2}^{4,3}$	486	334	600	229	875	221	2331	221
σ_{xz} and σ_{yz} top-bottom b.cs. (plane stress)								
$EM_{3,2}^{2,1}$	0	578	0	521	65	513	481	513
$EM_{3,2}^{3,1}$	0	456	0	375	107	367	731	367
$EM_{3,2}^{4,1}$	0	334	0	229	149	221	981	221
$EM_{3,2}^{5,1}$	162	334	200	229	391	221	1431	221
$EM_{3,2}^{4,-}$	0	464	0	395	69	371	693	371
$EM_{3,2}^{4,0}$	0	399	0	312	109	296	837	296
$EM_{3,2}^{4,2}$	81	334	100	229	270	221	1206	221
σ_{xz}, σ_{yz} and σ_{zz} top-bottom b.cs. (3D law)								
$EM_{3,2}^{4,1}$	0	464	0	395	69	371	693	371
$EM_{3,2}^{4,2}$	0	399	0	312	109	296	837	296
$EM_{3,2}^{4,3}$	0	334	0	229	149	221	981	221
$EM_{3,2}^{4,4}$	81	334	100	229	270	221	1206	221
σ_{zz} top-bottom b.cs.								
$EM_{3,2}^{2,1}$	0	464	0	395	69	371	693	371
$EM_{3,2}^{2,2}$	0	399	0	312	109	296	837	296
$EM_{3,2}^{2,3}$	0	334	0	229	149	221	981	221
$EM_{3,2}^{2,4}$	81	334	100	229	270	221	1206	221
$EM_{3,2}^{4,1}$	324	464	400	395	553	371	1593	371
$EM_{3,2}^{4,2}$	324	399	400	312	593	296	1737	296
$EM_{3,2}^{4,3}$	324	334	400	229	633	221	1881	221
$EM_{3,2}^{4,4}$	405	334	500	229	754	221	2106	221

Table D.2: Algebraic parameters for models of the type: $EM_{32}^{N_{\sigma_{xz}} N_{\sigma_{zz}}}$. $R_u = S_u = 10$.

Bibliography

[1] M. D'Ottavio et al. "Bending analysis of composite laminated and sandwich structures using sublaminate variable-kinematic Ritz models". In: *Composite Structures, 155* (2016).

[2] L. Dozio R. Vescovini. "Analysis of Monolithic and Sandwich Panels Subjected to Non-Uniform Thickness-Wise Boundary Conditions." In: *Curved and Layered Structures, 5* (2018).

[3] R. Vescovini L. Dozio M. D'Ottavio and O. Polit. "On the application of the Ritz method to free vibration and buckling analysis of highly anisotropic plates." In: *Composite Structures, 192* (2018).

[4] M. D'Ottavio R. Vescovini L. Dozio and O. Polit. "Buckling and Wrinkling of Anisotropic Sandwich Plates ." In: *International Journal of Engineering Science, 130* (2018).

[5] M. D'Ottavio A. Krasnobrizha E. Valot O. Polit R. Vescovini and L. Dozio. "Dynamic Response of Viscoelastic Multiple-Core Sandwich Structures ." In: *Journal of Sound and Vibration, 491* (2021).

[6] L. Dozio R. Vescovini. "Thermal Buckling Response of Laminated and Sandwich Plates Using Refined 2-D Models ." In: *Composite Structures, 176* (2017).

[7] L. Dozio R. Vescovini. "Thermal Buckling Behaviour of Thin and Thick Variable-Stiffness Panels." In: *Journal of Composites Science, 2(4)* (2018).

[8] R. Vescovini M. D'Ottavio L. Dozio and O. Polit. "The Ritz – Sublaminate Generalized Unified Formulation Approach for Piezoelectric Composite Plates." In: *International Journal of Smart and Nano Materials, 9* (2018).

[9] R. Vescovini A. Gorgeri and L. Dozio. "Analysis of multiple-core sandwich cylindrical shells using a sublaminate formulation." In: *Composite Structures, 225* (2019).

[10] R. Vescovini A. Gorgeri and L. Dozio. "Sublaminate Variable Kinematics Shell Models for Functionally Graded Sandwich Panels: Bending and Free Vibration Response." In: *Mechanics of Advanced Materials and Structures, 0* (2020).

[11] A.J.M. Ferreira C.M.C. Roque E. Carrera M. Cinefra. "Analysis of thick isotropic and cross-ply laminated plates by radial basis functions and a Unified Formulation." In: *Journal of Sound and Vibration, 330(4)* (2011).

[12] A.J.M. Ferreira C.M.C. Roque E. Carrera M. Cinefra and O. Polit. "Radial basis functions collocation and a unified formulation for bending, vibration and buckling analysis of laminated plates, according to a variation of Murakami's zig-zag theory." In: *European Journal of Mechanics, A/Solids, 30(4)* (2011).

[13] J.D. Rodrigues C.M.C. Roque A.J.M. Ferreira E.Carrera and M.Cinefra. "Radial basis functions-finite differences collocation and a unified formulation for bending, vibration and buckling analysis of laminated plates, according to Murakami's zig-zag theory." In: *Composite structures, 93(7)* (2011).

[14] O. Polit M. Cinefra M. D'Ottavio and E. Carrera. "Assessment of MITC plate elements based on CUF with respect to distorted meshes." In: *Composite structures, 238* (2020).

[15] E. Carrera M. Cinefra and P. Nali. "MITC technique extended to variable kinematic multilayered plate elements." In: *Composite Structures, 92(8)* (2010).

[16] L. Demasi. "∞^6 Mixed plate theories based on the Generalized Unified Formulation. Part: I: Governing equations". In: *Composite Structures, 87* (2008).

[17] M. D'Ottavio. "A Sublaminate Generalized Unified Formulation for the analysis of composite structures." In: *Composite Structures, 142* (2016).

[18] C. Wenzel M.D'Ottavio O. Polit and P. Vidal. "Assessment of free-edge singularities in composite laminates using higher-order plate elements." In: *Mechanics of Advanced Materials and Structures, 23* (2016).

[19] T.H.C. Le M. D'Ottavio P.Vidal and O.Polit. "A new robust quadrilateral four-node variable kinematics plate element for composite structures." In: *Finite Elements in Analysis and Design, 133* (2017).

[20] M. D'Ottavio D.Ballhause T.Wallmersperger B.Kröplin. "Considerations on high-order finite elements for multilayered plates based on Unified Formulation." In: *Composites & Structures, 84* (2006).

[21] H. Kraus. "Mechanics of laminated composite plates and shells". In: *John Wiley & Sons* (1967).

[22] E. Reissner. "On a certain mixed variational theorem and a proposed application". In: *John Wiley & Sons* (1984).

[23] E. Reissner. "On a mixed variational theorem and on shear deformable plate theory". In: *John Wiley & Sons* (1986).

[24] G. Kirchhoff. "Über das Gleichgewicht und die Bewegung einer elastischen Scheibe". In: *Journal für die reine und angewandte Mathematik* (1850).

[25] R.D. Mindlin. "Influence of rotary inertia and shear on flexural motions of isotropic elastic plates". In: *Journal of Applied Mechanics, 18* (1951).

[26] A. E. H. Love. "A treatise on the mathematical theory of elasticity". In: *volume 1* (1892).

[27] A. E. H. Love. "The Small Free Vibrations and Deformation of a Thin Elastic Shell". In: *Phil. Trans. R. Soc. Lond.,179:491-546* (1888).

[28] L. H. Donnell. "Beams, Plates, and Shells". In: *Engineering societies monographs. McGraw- Hill Inc., US, New York* (1976).

[29] E. Carrera S. Brischetto and L. Demasi. "Improved bending analysis of sandwich plates using a zig-zag function". In: *Composite Structures* (2009).

[30] A. Toledano and H. Murakami. "A Composite Plate Theory for Arbitrary Laminate Configurations". In: *Journal of Applied Mechanics* (1987).

[31] E. Carrera. "A class of two dimensional theories for multilayered plates analysis". In: *Atti Accademia delle Scienze di Torino. Memorie Scienze Fisiche* (1995).

[32] L. Demasi. "∞^3 Hierarchy plate theories for thick and thin composite plates: the generalized unified formulation". In: *Composite Structures, 84* (2008).

[33] L. Demasi. "∞^6 Mixed plate theories based on the Generalized Unified Formulation. Part: II: Layerwise theories". In: *Composite Structures, 87* (2008).

[34] N. J. Pagano. "Exact Solutions for Rectangular Bidirectional Composites and Sandwich Plates". In: *Journal of Composite Materials* (1970).

[35] L. Demasi. "Quasi-3D analysis of free vibration of anisotropic plates". In: *Composite Structures 74* (2006).

[36] J. G. Ren. "Exact Solutions for Laminated Cylindrical Shells in Cylindrical Bending". In: *Composites Science and Technology 29; 169-187* (1987).

[37] E. Asadi and M. S. Qatu. "Free vibration of thick laminated cylindrical shells with different boundary conditions using general differential quadrature". In: *Journal of Vibration and Control, 19(3) 356-366* (2012).

[38] K. Chandrashekhara and B. S. Kumar. "Static Analysis of Thick Laminated Circular Cylindrical Shells". In: *Journal of Pressure Vessel Technology* (1993).

[39] S. Brischetto. "AN EXACT 3D SOLUTION FOR FREE VIBRATIONS OF MULTI-LAYERED CROSS-PLY COMPOSITE AND SANDWICH PLATES AND SHELLS". In: *International Journal of Applied Mechanics* (2014).

[40] M. D'Ottavio. "Analysis of RMVT based plate models." In: *Internal report* (2020).

[41] L. Demasi. "∞^6 Mixed plate theories based on the Generalized Unified Formulation. Part: V: Results". In: *Composite Structures, 88* (2008).

[42] Y. Miyamoto W. A. Kaysser B. H. Rabin A. Kawasaki and R. G. Ford. *Functionally graded materials: design, processing and applications.* 1999.

[43] J.N. Reddy. "Mechanics of laminated composite plates and shells". In: *CRC Press* (2004).